Investigation of the Lymphocyte Function during Tubulointerstitial Injury in the Native Kidney

Victoria Ingham

Institute of Cellular Medicine, Newcastle University

Degree of Doctor of Medicine

April 2012

Abstract

Tubulointerstitial inflammation and fibrosis is frequently seen in patients with progressive renal failure, irrespective of the aetiology, and may represent a common pathway to renal failure. However, the role and function of tubulointerstitial lymphocytes in the pathogenesis of renal fibrosis is unknown. Using the well-characterised mouse model of unilateral ureteric obstruction (UUO) I determined the phenotype of infiltrating lymphocytes and by sequencing the complementarity-determining region 3 (CDR3) of the variable β-chain examined whether there were clonal populations of T cells within UUO and normal kidney.

There was a strong correlation between lymphocyte infiltration and tubulointerstitial expansion, α-SMA staining and collagen I deposition. A population of these infiltrating CD4+ and CD8+ lymphocytes also displayed the surface makers CD69 and CD44, and the nuclear proliferation marker Ki67. This suggests activation and proliferation of T cells in response to self-antigen recognition and the loss of immunological tolerance.

Infiltrating T cells within UUO kidney demonstrated over expression of certain TRVβ gene segments in particular TRVβ3, suggesting a clonal population of lymphocytes. In normal and sham operated kidney over expression of T cells with the TRVβ13.2, 29 and 1 gene segments suggested populations of resident NKT cells expressing an invariant T cell receptor.

On sequence analysis of the CDR3 region of infiltrating lymphocytes, large clonal populations of T cells were seen in individual UUO kidneys at 7 and 14 days after obstruction but not 28 days. These clonal populations in UUO kidney that were also in normal kidney had an identical amino acid motif within the CDR3 region. This suggests a population of T cells in normal kidney proliferate in response to injury.

These lymphocytes could be a potential target for therapeutic interventions to prevent fibrosis in renal diseases that are not characteristically believed to be immune mediated.

Table of contents

Index of Figures and Tables

Figures

Tables

Acknowledgements

I would like to thank Professor Neil Sheerin for the opportunity to carry out this project and for his support and encouragement throughout. Professor John Kirby was also a great source of knowledge and provided me with support and advice. Dr Adrain Smith, in the department of Zoology at Oxford University, offered guidance when designing the TRVβ experiments. Furthermore I owe a large debt of gratitude to all those people I worked alongside in the department and who assisted me in learning the many techniques involved in the project, especially Dr Ellen Hatch to whom I will be forever grateful.

My funding was very generously provided for 18 months by the Northern Kidney Research Fund.

The experimental work described as carried out in the Institute of Cellular Medicine at Newcastle University between April 2008 and October 2009. All the work described is my own.

Abbreviations

AID	autoimmune disease
ADN	adriamycin nephropathy
APC	antigen presenting cell
APC	allophycocyanin
APC-Cy7	combines allophycocyanin and a cyanine dye
ATG	anti-thymocyte globulin
ATP	adenosine-5'-triphosphate
BCR	B cell receptor
BSA	bovine serum albumin
CDR	complementarity-determining region
CFU	colony forming units
CIA	collagen-induced arthritis
CKD	chronic kidney disease
CLIP	class II-associated invariant chain peptide
CMI	cell mediated immunity
DAB	diaminobenzidine
DAMP	danger associated molecular pattern
DAPI	4', 6-diamidino-2-phenylindole
DC	dendritic cell
DEPC	diethylpyrocarbonate
DMEM	Dulbecco's modified eagle medium
DNA	deoxyribonucleic acid
DPX	distyrene, plasticizer and xylene resin
EAE	experimental allergic encephalitis
EDTA	ethylenediaminetetraacetic acid
ER	endoplasmic reticulum
FACS	fluorescence activated cell sorting
6FAM	6-carboxyfluorescein
FITC	fluorescein isothyanate
GFR	glomerular filtration rate
GM-CSF	granulocyte-macrophage colony-stimulating factor
HLA	human leukocyte antigen
d-H_2O	distilled water

HPF	high powered field
HRP	Horseradish peroxidise
Hsp	heat shock protein
ICAM	intercellular adhesion molecule
ICOS	inducible co-stimulator
IE	interstitial expansion
IF	immunofluorescence
IHC	immunohistochemistry
IMGT	ImMunoGeneTics
IRI	ischaemia-reperfusion injury
LB	lysogency broth
LFA-1	lymphocyte function-associated antigen-1
LICOS	ligand of inducible co-stimulator
LPS	lipopolysacchride
MBG NFQ	minor grove binding protein non-fluorescent quencher
MBP	myelin basic protein
β-ME	β-mercaptoethanol
MHC	major histocompatibilty complex
MMF	mycophenolate mofetil
M-MLV	moloney-murine leukaemic virus
MS	multiple sclerosis
NFAT	nuclear factor of activated T cells
NKT	natural killer T cell
NO	nitric oxide
NTC	non-template control
OD	optical density
ORFS	open reading frame sequence
PAMP	pathogen-associated molecular patterns
PAS	Periodic acid Schiff
PBS	phosphate buffered saline
PBST	phosphate buffered saline with tween
PCR	polymerase chain reaction
PE	R-phycoerythrin
PerCP	peridinin-chlorophyll protein
PRR	pattern recognition receptor

PTM	post translational modification
RAG-1	recombination activation gene-1
RNA	ribonucleic acid
ROI	region of interest
ROX	6-carboxyl-x-rhodamine
SCID	severe combined immunodeficiency
SEM	standard error of the mean
SLE	systemic lupus erythematosus
α-SMA	alpha-smooth muscle actin
SNP	single-nucleotide polymorphism
SOC	super optimal broth
STAT	signal transduction and activator of transcription
Strep-HRP	Streptavidin-conjugated Horseradish peroxidase
TAP	transporter associated with antigen processing
TBE	tris/borate/EDTA
TCR	T cell receptor
TEC	tubular epithelial cell
TI	tubulointerstitium
TLR	toll-like receptors
Tm	melting temperature
Treg	T regulatory cells
TRITC	tetramethyl rhodamine iso-thiocyanate
UUO	unilateral ureteric obstruction
VEGF	vascular endothelial growth factor

Chapter 1. Introduction

My thesis focuses on the function of T lymphocytes in the development of renal tubulointerstitial injury. I will describe the development of the T cell response to antigen, in particular the development of the α:β T cell and the β-chain in the mouse. I will then go on to describe the process of T cell activation and lymphocyte effector functions. Subsequently, I will demonstrate how a loss of tolerance to self can cause autoimmunity. The final part of the introduction reviews the current literature regarding tubulointerstitial kidney injury and fibrosis.

1.1 Role of lymphocytes in the adaptive immune response

Lymphocytes form part of the adaptive immune response and are critical in the host's defences against foreign antigen and thus infection. In order for lymphocytes to detect foreign pathogens they have unique receptors capable of recognising individual antigens. Immunological memory also develops after exposure to a foreign antigen such that a more rapid and effective response occurs on a second encounter with the pathogen. Ordinarily lymphocytes are tolerant to self antigens however, when tolerance mechanisms fail, autoimmunity develops.

1.2 T cell development

T cells develop and mature in the thymus by a process of positive and negative selection, which is termed central tolerance. Any autoreactive T cells not deleted in this way can also be prevented from activation in the periphery by the process of peripheral tolerance. This allows the development of T cells which are tolerant to self but are able to recognise harmful non-self, however, this is not absolute.

1.2.1. Central tolerance

Positive selection occurs first in the thymic cortex where pre-T cells, which are CD8 and CD4 double negative, are positively selected when they recognise self MHC on cortical epithelial cells which express self class I and II major histocompatability complex (MHC) molecules. This also defines which pre-T cells become CD8+ and CD4+ cells, depending upon whether they recognise class I or II MHC respectively. This generates many autoreactive T cells which have a high affinity for self MHC antigens. Therefore the process of negative selection follows in the thymic medulla, where CD8+ and CD4+ T cells are deleted if they bind to self peptide: self MHC on an antigen presenting cell (APC) with high enough affinity to allow T cell activation.

Negative selection of such activated T cells occurs by apoptosis. Many antigens present within the medullary thymus have been generated at this ectopic location due to the presence of the AIRE transcription factor which regulates the ectopic expression of peripheral tissue restricted antigens.

After the process of positive and negative central selection, single positive self MHC restricted naive T cells (CD8+ or CD4+), which are predominantly not autoreactive, egress from the thymus.

1.2.2. Peripheral tolerance

Just as central tolerance involves the positive selection/survival of T cells which recognise self MHC and negative selection/deletion of autoreactive T cells recognising self peptide: self MHC, similar mechanisms occur in the periphery. The process of negative selection in the thymus is not a perfect one, allowing some autoreactive T cells to escape the thymus, since not all autoantigens are expressed in or can reach the thymus. Therefore these emigrating autoreactive T cells require negative selection in the periphery either by elimination or inactivation. When lymphocytes do encounter and bind strongly to their cognate self antigen in the periphery for the first time, three possible mechanisms are able to induce tolerance; anergy, deletion and survival/ignorance.

Anergic T cells develop when antigen is presented to a T cell in the absence of a co-stimulation (Macian, Im et al. 2004). Co-stimulation is absent when there are no innate immune signals to the APC to activate it. Therefore when an autoreactive T cell recognises a self peptide: self MHC complex in the absence of inflammation, the T cell is rendered anergic. Anergic T cells are fully inactivated and even when they do encounter antigen in the presence of full co-stimulation they are still unable to initiate a response. They are unable to produce IL-2 due to a failure to generate nuclear factor of activated T cells (NFAT) and therefore unable to divide. They may also have the ability to inhibit/suppress/regulate other positive immune responses. The second alternative is that instead of anergy, T cells undergo activation-induced death and are deleted after a short period of activation and cell division.

Another alternative is that T regulatory cells (Tregs) can modulate the activation and proliferation of autoreactive T cells which have escaped central tolerance. The exact mechanisms by which they exert their effects are unclear. However, these suppressive effects may be mediated by direct contact between the Treg and lymphocyte (Ng,

Duggan et al. 2001) or indirectly by soluble mediators such as IL-10 and TGF-β acting at short distances from the cell or bound to the cell surface (Dieckmann, Bruett et al. 2002; Nakamura, Kitani et al. 2004).

Survival of naive T cells in the periphery occurs by positive selection. It is dependent upon covert T cell receptor signalling after weak interactions with self MHC +/- self-antigen, along with the IL-7 and IL-15 cytokines (Surh and Sprent 2008). Lymphocytes probably encounter their positively selected ligands on lymphoid dendritic cells (DCs) in T-cell zones of secondary lymphoid organs. These specific dendritic cells lack sufficient co-stimulatory potential to induce full T cell activation however contact does allow signalling to the naive T cell which promotes survival.

1.3 T cell receptor generation

The T cell receptor (TCR) on the T lymphocyte recognises antigen only when it is presented on the surface of an antigen presenting cell with self MHC. Individual T cells have numerous copies of a single TCR which has a unique antigen-binding site. This determines which antigens that lymphocyte can recognise. Billions of different T lymphocytes, each with unique TCRs, are required to produce responses to an almost unlimited range of antigens. In order to generate such a diverse TCR repertoire for the wide range of antigen specificities, the TCR is made up of two chains with both variable (V) regions and invariant constant (C) regions.

A complex mechanism has evolved for generating these highly variable TCR proteins. Each TCR variant cannot be coded in full by the genome, as this would require more genes for TCRs alone than there are genes in the whole genome. V-regions are encoded by two or three gene segments which assemble in the developing lymphocyte by somatic recombination to form the complete V-region sequence. This mechanism is called gene rearrangement. There are multiple different subtypes of each gene segment in the germ-line genome and the complete V-region is generated by a single subtype of each gene segment. The large number of different possible recombinations account for the huge diversity of TCRs that can be generated.

The majority of T cells have antigen receptor molecules on their surface made from two different polypeptide chains, alpha (α) and beta (β), which form the α:β TCR. This is the T cell population focused on during this thesis and when the term TCR is used will refer to those of the α:β subtype, unless specified. There is also a minority population of T cells which have a TCR made of a gamma (γ) and delta (δ) chain and these are named

γ:δ T cells. T cells with a γ:δ TCR are able to bind antigen directly without processing and without MHC presentation. They are specialised to bind ligands including heat shock proteins and non-peptide ligands. They also differ from α:β T cells in their pattern of expression of CD4 and CD8 co-receptors, are distributed differently in the periphery and have different functions.

1.3.1 Structure of the α:β T cell receptor

The α:β TCR is a heterodimer comprised of an α and β-chain. The β-chain (gene locus on chromosome 7) is encoded by three gene segments that make up the V-region; Vβ, Dβ, and Jβ. Gene rearrangement of these gene segments generates a functional VDJβ V-region exon that is transcribed and spliced to join to a single Cβ gene (Figure 1.1). This Cβ gene segment is comprised of four exons which encode for the constant and hinge domains as well as for the cytoplasmic and transmembrane regions. The resulting mRNA is translated to yield the TCR β-chain.

The diversity of the β-chain is generated by the combinational diversity created by there being twenty two known functional Vβ gene segments, 2 Dβ, and 13 Jβ in the mouse however, just one of each gene segment combines to form the VDJβ V-region exon as already explained (Table 1.1). Furthermore, junctional diversity is generated by non germ-line encoded contact sequences being incorporated between the V-D and D-J regions- this results in the hypervariable region or complementarity-determining region 3 (CDR3). Once the functional β-chain has been produced, it pairs with a pre-TCR α-chain (pTα) to create the pre-T cell receptor (β:pTα). Subsequently, the α-chain gene segments rearrange. The α-chain (gene locus on chromosome 14) is very similar to the β-chain but its variable domain is only encoded by two gene segments; Vα and Jα. Again rearrangement of these gene segments generates a functional VJα V-region exon that is transcribed and spliced to join to the single Cα gene segment. The resulting mRNA is translated to yield the T-cell receptor α-chain. The combinational and junctional diversity of the α-chain is created in a similar way to that of the β-chain, but there are different numbers of each functional gene segment, as listed in Table 1.1. Subsequently any one α-chain can combine with any one β-chain to further increase the α:β TCR repertoire.

The CDR3 loops of the α and β-chains are the main contact domains with the MHC presented peptide, whereas the CDR1 and 2 regions predominantly contact the residues of the MHC (Davis and Bjorkman 1988).

Figure 1.1- T cell receptor α and β-chain gene rearrangement

The α and β-chains of the TCR are formed by combining gene segments to produce the functional gene. The resulting mRNA is then translated to yield the α:β TCR.

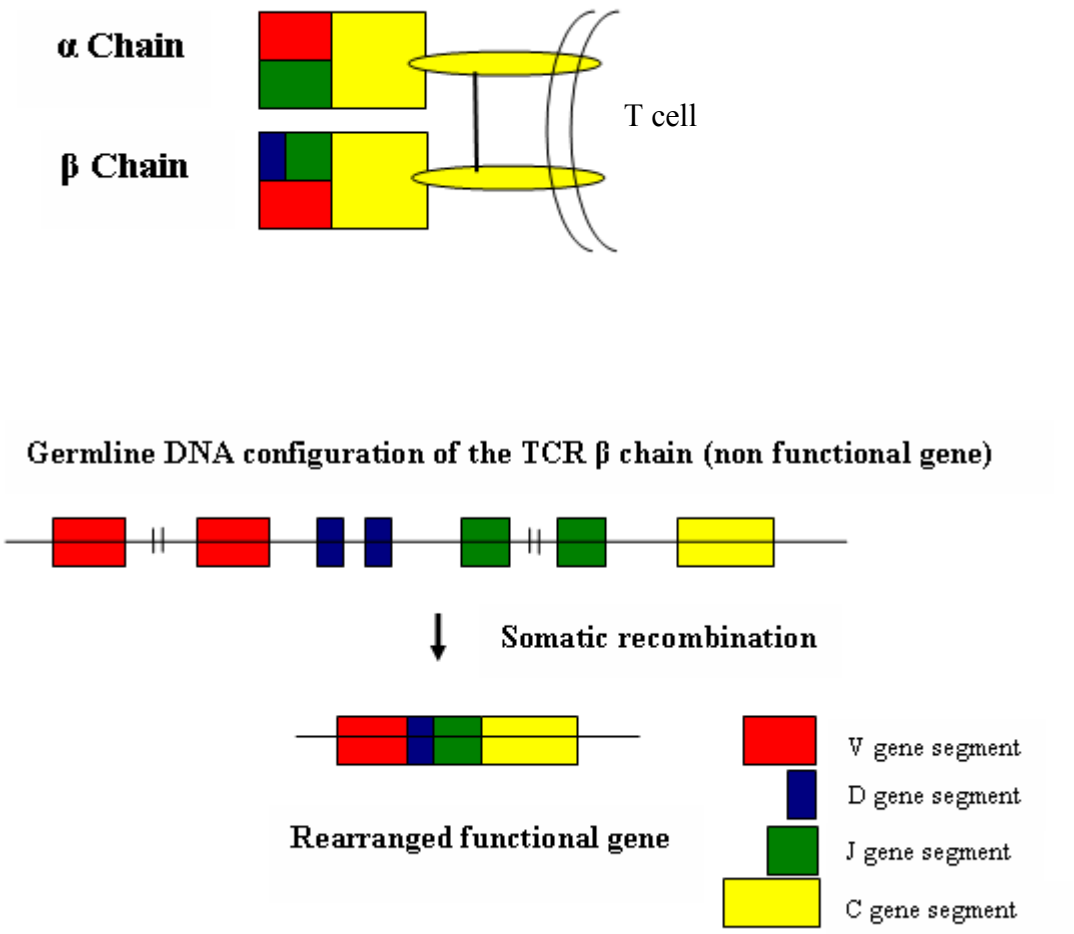

Table 1.1- Number of mouse T cell receptor functional gene segments for the α and β-chains

The TCR variable region of the α-chain is made up of the V and J gene segments, whereas the β-chain is also comprised of a D segment. There are multiple recognised functional subtypes of gene segment however, only one is ultimately expressed by an individual T cell.

Functional gene segments	Beta chain	Alpha chain
V	22	50 - 100
D	2	0
J	13	~ 50
C	2	1

1.3.2 Nomenclature for T cell receptor gene segments of the immune system

Different groups have used different names to classify the different V-region gene segments of the TCR (Table 1.2). Therefore an international committee was assigned to work out the principles of TCR nomenclature and a compilation of all available mouse (Arden, Clark et al. 1995) and human (Arden, Clark et al. 1995) TCR gene segment sequences were published by Arden et al. Subsequently the ImMunoGeneTics (IMGT) database devised nomenclature for germ line immunoglobulin and T cell receptor gene segments for human and other vertebrates (Giudicelli, Chaume et al. 2005). This has become the international reference for the immunoglobulin and T cell receptor gene nomenclature and is freely available at http://imgt.cines.fr. This is the numbering system used throughout this thesis, unless stated otherwise.

1.3.3 Structure of the γ:δ T cell receptor

A minority population of T cells have a γ:δ heterodimer TCR, which are of a distinct but similar lineage to the α:β T cells and thought to arise from a common precursor. The γ-chain is comprised of V, J and C gene segments**.** However, the δ-chain is encoded by the V, D, J and C gene segments which are found between the Vα and Jα gene segments of the TCRα locus. There are fewer V gene segments at the γ and δ loci and so less combinational diversity is created. In comparison there is increased junctional diversity of the δ-chain, with almost all the variability arising from the junctional region.

Table 1.2- Correlation between the Arden and IMGT nomenclature for the TCR β-chain V and J gene segments

The two dominant nomenclature classification systems used for the gene segments of the β-chain of the TCR were generated by Arden and IMGT however, they can be correlated as illustrated below.

Arden	= IMGT	Arden	= IMGT	Arden	= IMGT
Vβ 1.1	TRBV5	Vβ 8.3	TRBV13-1	Vβ 20.1	TRBV23
Vβ 2.1	TRBV1	Vβ 9.1	TRBV17	Vβ 21.1	TRBV25
Vβ 3.1	TRBV26	Vβ 10.1	TRBV4	Vβ 22.1	TRBV22
Vβ 4.1	TRBV2	Vβ 11.1	TRBV16	Vβ 23.1	TRBV18
Vβ 5.1	TRBV12-2	Vβ 12.1	TRBV15	Vβ 24.1	TRBV9
Vβ 5.2	TRBV12-1	Vβ 13.1	TRBV14	Vβ 25.1	TRBV10
Vβ 5.3	TRBV12-3	Vβ 14.1	TRBV31	Vβ 26.1	TRBV6
Vβ 6.1	TRBV19	Vβ 16.1	TRBV3	Vβ 28.1	TRBV8
Vβ 7.1	TRBV29	Vβ 17.1	TRBV24	Vβ 29.1	TRBV11
Vβ 8.1	TRBV13-3	Vβ 18.1	TRBV30	Vβ 30.1	TRBV27
Vβ 8.2	TRBV13-2	Vβ 19.1	TRBV21	Vβ 31.1	TRBV28

Arden	= IMGT
Jβ 1.1	TRBJ1-1
Jβ 1.2	TRBJ1-2
Jβ 1.3	TRBJ1-3
Jβ 1.4	TRBJ1-4
Jβ 1.5	TRBJ1-5
Jβ 1.6	TRBJ1-6
Jβ 2.1	TRBJ2-1
Jβ 2.2	TRBJ2-2
Jβ 2.3	TRBJ2-3
Jβ 2.4	TRBJ2-4
Jβ 2.5	TRBJ2-5
Jβ 2.6	TRBJ2-6

1.4 T cell mediated immunity and antigen processing

T cells form part of the adaptive immune defence system by recognising cells which are infected with viruses or have internalised pathogens or their products. The diverse repertoire of lymphocytes do this by being able to recognise peptide fragments of pathogen when presented to them by MHC molecules on the surface of an APC with the necessary adjunctive co-stimulatory surface protein signals. This subsequently induces the activation, proliferation and differentiation of the naive T cell into an armed effector cell which contributes to the removal of the pathogen or death of the infected cell.

1.4.1 The antigen

B cells recognised intact protein through their B cell receptor (BCR) however, T cell responses are generated after antigens have been denatured into short linear peptide sequences. Infectious agents replicate in two distinct intracellular compartments: viruses and certain bacteria replicate in the cytosol and the contiguous nuclear compartment, whereas many pathogenic bacteria replicate in endosomes and lysosomes which form part of the vesicular system.

Cells infected with viruses and bacteria living within the cytosol are eliminated by cytotoxic CD8+ T cells, whose function is to kill the infected cells. In comparison pathogens and their products in the vesicular compartment are detected by CD4+ T cells. This leads to the activation of appropriate immune effector mechanisms, which include macrophage activation resulting in the killing of intravesicle pathogens and B cell activation allowing the production of antibodies to eliminate or neutralise extracellular pathogens. Microbial antigens enter the vesicular compartment in two ways. Firstly, pathogens and their antigens/toxins can be engulfed by phagocytes (macrophages, neutrophils or dendritic cells) by the process of phagocytosis or endocytosis. Innate surface bound receptors recognise these foreign proteins and trigger phagocytosis. Pathogen derived protein can also bind to immunoglobulins on the surface of B cells, causing the protein to be internalised by endocytosis. Alternatively, immature dendritic cells can internalise pathogens by macropinocytosis, a receptor independent method. Subsequently cytosolic and intravesicle proteins are degraded and displayed on the surface of the cell as peptides.

1.4.1.1 Class I MHC presentation of peptide

In order for intracellular cytosolic proteins to be displayed on the surface of a cell with class I MHC, they are digested in the cytosol into short peptides. Proteins within all

cells are continually being degraded and replaced by newly synthesised proteins. Much of this degradation is carried out in the cytosol by large multimeric complexes called proteosomes, where large proteins are degraded and released as short peptides. The proteosome is also responsible for the production of peptides ligands for MHC class I molecules. From here these short peptide fragments are transported into the endoplasmic reticulum (ER) by an ATP dependent peptide transporter 'transporter associated with antigen processing' (TAP) where they bind class I MHC. The MHC-peptide complex then moves to the cell surface for recognition by CD8+ T cells. IFN-γ, produced by virally infected cells, is able to transform the constitutive proteosome found in all cells into the immunoproteosome, whose protease activity creates peptide fragments which are ideally suited for transport by TAP and binding to class I MHC, as well as increasing the rate at which peptides can be released.

It is not just foreign intracellular pathogens in the cytosol or nuclear compartments which are presented on the cell surface with class I MHC, but peptides from all intracellular proteins are presented to allow CD8+ T cell surveillance.

1.4.1.2 Class II MHC presentation of peptides

Components taken up into the vesicular compartment by professional antigen presenting cells are broken down within the vesicle by proteases under conditions of low intracellular pH to produce peptide fragments. Class II MHC is assembled in the ER where it is bound to an invariant chain which prevents the abundant endogenous peptide fragments present in the ER binding the class II MHC. The invariant chain also targets delivery of the MHC class II proteins to the vesicular compartment. Here the invariant chain is cleaved by the acid proteases to leave CLIP (class II-associated invariant chain peptide) bound to class II MHC. Subsequently CLIP dissociates leaving the class II MHC protein free to bind the peptide within the vesicular compartment. This class II MHC-peptide complex is then presented on the surface of the APC to CD4+ T cells.

Extracellular components from the environment, not just pathogens, can be internalised into endocytic vesicles and the peptides formed by protein degradation presented with class II MHC.

1.4.1.3 Cross presentation

Antigen presented by DCs is the most effective way to stimulate naive T cells however, pathogens which do not infect DCs can still stimulate naive CD8+ cells. DCs have the ability to engulf exogenous antigens from dying cells and present them with class I

MHC thus activating naive CD8+ cells (Bevan 1976). In order to do this the peptide fragment must be transported from the endocytic vesicle to the cytosol, whereby the peptide is taken up into the ER and bound to class I MHC (Rodriguez, Regnault et al. 1999). This is known as cross presentation.

1.4.2 Major histocompatibilty complex (MHC)

The function of MHC molecules, which are either class I or II, is to bind peptide fragments derived from pathogens and display then on the cell surface, for recognition by the appropriate T lymphocyte. This will only occur if the specific TCR recognises a complex of antigen fragment and a molecule of self MHC. This is termed MHC restriction. Class I MHC molecules are transmembrane proteins found on the surface of nearly all cells, whereas class II MHC is found only on specialised cells. The MHC is located on chromosome 6 in humans and 17 in the mouse. In humans it contains over 200 genes and these genes are called human leukocyte antigen (HLA) genes.

The class I molecule is comprised of a polymorphic α-chain encoded within the MHC complex and is associated with non-polymorphic, non MHC encoded β2 microglobulin, to form a 4 domain structure. There are three class I α-chain genes in the human called HLA-A, -B and –C and in the mouse called H2-K, -D and –L. The α1 and α2 subunits form the peptide binding cleft and are able to bind a peptide fragment 8-10 amino acids in length. MHC class I molecules are recognised by CD8+ cells.

This is in comparison to the class II MHC molecules which are made from α and β-chains which are both polymorphic and MHC encoded. There are three pairs of MHC class II α and β chain genes in the human called HLA-DR, -DP and –DQ and in the mouse two pairs called H-2A and –E. The α and β-chains create a 4 domain heterodimeric structure with the distal α1 and β1 domains forming the peptide binding cleft what is capable of binding >12-14 amino acids. MHC class II molecules are recognised by CD4+ lymphocytes.

It is difficult for pathogens to adapt such that they can escape presentation by MHC and evade immune responses. This is because MHC is polygenic: it contains several different class I and II genes, so that an individual has a set of MHC molecules with different peptide binding specificities. Also it is polymorphic: there are multiple variants of each gene within the population as a whole, therefore most individuals will be heterozygous at MHC loci.

1.4.3 The professional antigen presenting cell

There are three main cell types of professional antigen presenting cells which have the potential to express both MHC class I and II and co-stimulatory cell surface molecules for activation of lymphocytes; dendritic cells, macrophages and B cells.

Dendritic cells are the most important professional APCs and their only functions are in antigen ingestion, processing and presentation. They are the first cell type to take up antigen and present it to naive T cells. In vivo mature DCs initiate almost all naive T cell responses, with macrophages and B cells playing a larger role in antigen presentation to effector T cells. Immature dendritic cells migrate from the bone marrow to the peripheries where they survey the local environment for pathogens and peptides. They express low levels of class II MHC and co-stimulatory molecules. However, after engulfing pathogens they can be activated by the innate immune system (as described later (1.5.1.1)). This induces migration back to the regional lymph nodes and their maturation, with the upregulation of surface bound co-stimulatory and adhesion molecules such that they become highly effective at presenting antigen to naive lymphocytes.

Macrophages and B cells are professional antigen cells but differ from DCs because they are not only involved in antigen presentation but perform other immune functions, which also rely on antigen presentation. Macrophages originate in the bone marrow, circulate in blood and have few or no MHC class II or co-stimulatory molecules on their surface in the resting state. However, they differentiate and become activated in the tissues, increasing their expression of class II MHC and co-stimulatory molecules. Predominantly they are phagocytic cells, they ingest opsonised bacteria and particulate antigens by phagocytosis (rather than soluble antigens) using both Fc and complement receptors. The macrophage would then usually destroy the microorganism without T cell help in the intravesicle compartment however if these pathogens are able to avoid elimination then the adaptive immune system is required. Activated macrophages present these ingested pathogens as processed antigens with class II MHC to CD4+ T cells however, are less efficient than DCs at activating naive T cells. Once activated, T cells can provide both secreted (e.g. cytokines IFN-γ and TNF-α/β) and membrane bound signals (CD40 ligand) to macrophages to activate them further and improve their ability to act as APCs. Activated macrophages are then able to ingest foreign protein more efficiently, to kill ingested pathogens, release soluble inflammatory mediators

(e.g. TNF, IL-1, IL-12) and upregulate the expression of MHC and co-stimulatory molecules.

B cells act as professional APCs and can bind soluble pathogen components and bacterial toxins to the B cell surface immunoglobulin (i.e. the BCR), which are then internalised, processed and presented. They constitutively express MHC class II molecules but not co-stimulatory molecules. Again B cells can activate naive T cells when they express co-stimulation but are again less efficient than DCs. Generally B cells present antigen to antigen specific effector CD4+ T cells which drive B cell differentiation.

1.5 T cell activation

1.5.1 The primary response by naive T cells

Naïve T cells attach with low avidity to APCs they encounter using the T cell integrin 'lymphocyte function-associated antigen-1' (LFA-1) which binds the intercellular adhesion molecules (ICAMs) present on APCs. Other adhesion molecules are also involved which include CD2 on the T cell binding to CD58 on the APC. This provides the T cell with time to sample MHC molecules on the APC for the presence of their specific cognate peptide. Rarely the naive T cell recognises its peptide-MHC ligand and there is signalling through the TCR to produce a conformational change such that LFA-1 increases the avidity of its binding to ICAM-1 and 2 on the APC. This stabilises the interaction between the antigen-specific T cell and the APC, but the recognition by the naive T cell of this foreign peptide-MHC complex on the antigen presenting cell is insufficient on its own to stimulate T cell activation. This interaction only provides the first signal: antigen specific clonal expansion of naive T cells requires a second co-stimulatory signal. This second signal must be delivered by the same APC on which the peptide-MHC complex has been recognised. The best characterised and principle co-stimulatory molecules involved are B7.1/CD80 and B7.2/CD86 found on the APC which bind CD28 on the T cell surface allowing T cell activation and the expression of other proteins which contribute to sustaining the co-stimulatory signal (Figure 1.2) e.g. CD40 ligand (CD40L) which binds to CD40 on the APC. This binding has bidirectional effects: it transmits activating signals to the T cell and also activates the APC to express more B7 family molecules. Another pair of proteins which contribute to co-stimulation is the 4-1BB ligand on the APC and T cell 4-1BB molecule. CD28 related proteins are also induced on activated T cells. CTLA-4 closely resembles CD28 however delivers an inhibitory signal to the activated T cell reducing their proliferative response by limiting

IL-2 generation. A second CD28 related protein, inducible co-stimulator (ICOS) is induced on activated T cells and binds the ligand of ICOS (LICOS) on the activated APC and helps to drive T cell growth.

1.5.1.1 Upregulating co-stimulatory molecules on antigen presenting cells

The initial adaptive immune response by naive T cells does not occur in the tissues at the site of infection but in the draining lymphatic tissue. This presentation is aided by the innate immune system which has two roles. Firstly it directs APCs to travel from the infected tissue to the local lymphoid tissues and secondarily aids their maturation into cells which express high levels of co-stimulatory and adhesion molecules necessary for T cell activation.

At the site of infection direct microbial stimulation of non-clonal receptors on the APC takes place with the recognition of molecular patterns associated with pathogens but not with host cells. These pattern recognition receptors (PRRs), an example of which are the toll-like receptors (TLRs) (Medzhitov and Janeway 1997), recognise pathogen-associated molecular patterns (PAMPs). PAMPs can be components of the pathogen such as lipopolysaccharide. Stimulation of these innate receptors directs the DC towards the draining lymph node and induces the expression of co-stimulatory and adhesion molecules, which are required for naive T cell activation. Macrophages and B cells can also be induced by the same innate receptors to express co-stimulatory molecules and function as mature APCs.

Injured cells dying by necrosis, such as those exposed to pathogens, toxins or mechanical injury, can release danger or alarm signals in the form of molecules called danger associated molecular patterns (DAMPs). Examples of such DAMPs include heat shock proteins and fragments or components of the extracellular matrix e.g. fibronectin and heparin sulphate. DAMPs are also recognised by PRRs on APCs. The subsequent binding of the DAMPs to the PRRs has the same effect as PAMPs binding, with the development of mature APCs. They also stimulate the production of proinflammatory cytokines which contributes to the local inflammation by attracting leukocytes.

Self antigens released from injured cells, which are recognised by autoreactive T cells not deleted during negative selection in the thymus, would not ordinarily be able to activate naive T cells on their own. This is because a second signal is not generated and so the T cell becomes anergic. This is one method of peripheral negative selection as described earlier (1.2.2) to prevent autoimmunity. However, when naive T cells

recognise self antigen on mature APCs with the appropriate second signal, generated as a consequence of the DAMP-PRR interaction, then instead of inducing tolerance these T cells are activated. This is the principal behind the danger signal hypothesis proposed by Matzinger (Matzinger 2002). It allows self antigens to become immunogenic and activate autoreactive naive T cells when present in an inflammatory environment, such as when mixed with bacteria. These bacteria can be termed adjuvants. This was shown experimentally by injecting myelin basic protein with *M. tuberculosis* in susceptible animals resulting in experimental allergic encephalitis (EAE). This illustrates the importance of requiring multiple signals before T cells can be activated to ensure discrimination of self from non-self. However even this system is not perfect.

Figure 1.2- Interaction between the naive T cell and antigen presenting cell

The activation of naive T cells requires two activation signals delivered by the same antigen presenting cell. Binding of the peptide:MHC complex to the TCR provides the first signal. The second signal is transmitted by the co-stimulation and adhesion molecules on the APC which bind to their ligands on the naive T cell. This subsequently results in T cell activation.

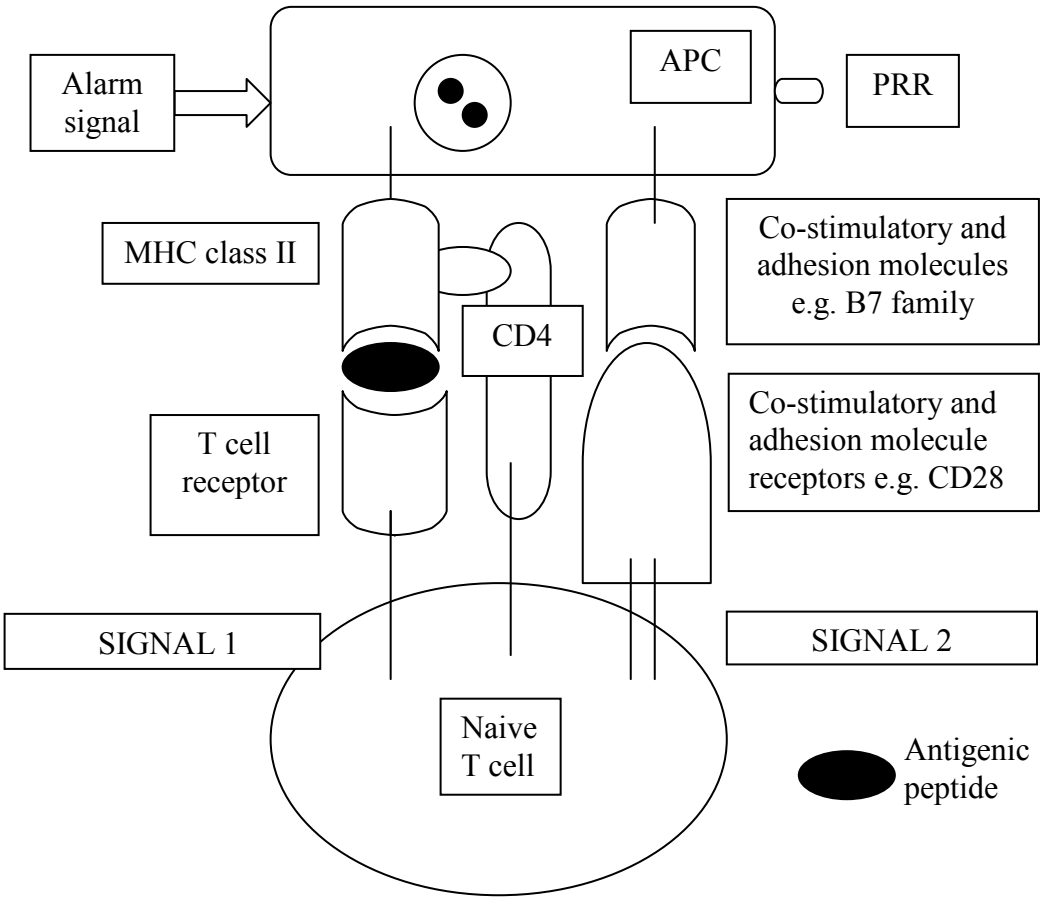

1.5.1.2 Naive CD8+ T cells

Almost all cells display surface class I MHC. This allows the surveillance of all intracellular cytosolic proteins to prevent intracellular pathogens from evading immune responses. Some intracellular viral pathogens infect professional APCs and so can be recognised by a naive CD8+ T cell and activated in a similar way to that described earlier for naive CD4+ cells. Also intracellular components released from dying infected cells can be taken up by dendritic cells and these proteins cross-presented by the DC with MHC class I antigen. These antigens are then recognised by naive CD8+ T cells, which can be activated once the DC has matured.

Naive CD8+ T cells require more co-stimulation, compared to naive CD4+ cells, to allow activation. The expression of higher levels of co-stimulatory signals can be facilitated by activated CD4+ T cells when they recognise related antigen to that recognised by a naive CD8+ T cell on the surface of the presenting cell. Signals are sent through CD40L on the activated CD4+ T cell to CD40 on the presenting cell to induce B7 family expression. Expression of the B7 family of molecules on the presenting cell generates the second signal for the naive CD8+ T cell to be activated. Other co-stimulatory molecules can be upregulated by the effector CD4+ T cell, including 4-IBB ligand.

1.5.2 Role of interleukin-2 (IL-2) in T cell activation

The cytokine IL-2 plays a role in the proliferation and differentiation of T cells. All resting T cells have a cell surface IL-2 receptor with a β and γ-chain which can bind IL-2 with moderate affinity. However, it is not until naive T cells are activated by peptide:MHC binding to the TCR that two events take place. Firstly, an α-chain is synthesised which binds with the β and γ-chain of the IL-2R to generate a high affinity IL-2 receptor, also called CD25. Secondly, IL-2 secretion is promoted by the activated T cell. The recognition by the TCR of a peptide:MHC complex induces nuclear translocation and activation of the transcription factor NFAT, which binds the IL-2 promoter gene and increases IL-2 transcription by the T cell. Not until the second signal is achieved by B7-CD28 ligation is IL-2 RNA stabilised and IL-2 synthesis increased. Binding of IL-2 to the high affinity receptor stimulates T cell proliferation, allowing activated T cells to divide 2-3 times per day and also promotes the differentiation to armed effector T cells. The immunosuppressant calcineurin inhibitors inhibit IL-2 production by disrupting signalling through the TCR whereas rapamycin disrupts signalling through the IL-2 receptor.

1.5.3 The secondary response by effector T cells

After T cell activation and clonal expansion, T cells are induced by IL-2 to differentiate into armed effector cells. Armed effector cells are able to synthesise effector molecules and perform specialised functions in cell mediated and humoral immunity. These armed effector cells undergo changes which distinguish then from naive T cells and no longer require the second co-stimulatory signal for activation when they recognise a peptide:MHC complex on an APC. This is important for CD8+ T cells since some of the cells which present antigen to them may not be professional APCs and cannot display co-stimulatory molecules. Also CD4+ cells must be able to activate both B cells and macrophages that have taken up antigen even if they are not expressing co-stimulatory molecules.

Effector T cells change their cell surface adhesion molecules to favour binding to APCs at sites of inflammation. This involves higher expression of the adhesion molecules LFA-1 and CD2 and the loss of homing L-selectin which is important to guide naive T cells from the blood to lymph nodes. Instead they express the integrin VLA-4 which facilitates binding to vascular endothelium with the surface molecule VCAM-1, expressed at sites of inflammation.

1.5.4 T cell effector functions

All effector T cells interact with their target peptide:MHC complex on a presenting cell but their functions differ depending on the membrane and secreted proteins which they express or release. This is so that the adaptive immune system can deal with different types of pathogen and cause distinct effects on the target cells. Effector T cells can be distinguished from naive and memory cells by their cell surface molecules which include CD25 and CD69. Proliferating cells can be distinguished by positive staining for Ki67. The presence of these cell surface molecules will be exploited within this thesis.

1.5.4.1 Effector CD8+ T cells

Armed effector CD8+ T cells are important in host defence against cytosolic pathogens, the commonest being viruses, which are not accessible to antibodies. They act by killing cells which harbour pathogens after recognising foreign peptide with class I MHC on their cell surface. These CD8+ T cells release cytotoxins such as perforin and granzyme from pre-stored lytic granules. Perforin forms pores in the target cell membrane lipid bi-layer allowing granzymes to enter the cell and induce apoptosis. The membrane bound

FAS ligand, a member of the TNF family, is also expressed by activated CD8+ (and some CD4+) cells and induces apoptosis of their target cells. Apoptosis occurs when a cellular protease cascade is initiated causing immunologically silent cell death. The cell remnants are rapidly taken up and destroyed by phagocytes without the induction of stimulatory molecules on the phagocyte.

CD8+ effector cells can produce the cytokine IFN-γ which blocks viral replication in the target cell and increased MHC class I peptide loading in the ER. It can also activate macrophages and recruit them as antigen presenting or effector cells. TNF-α and β are produced which act synergistically with IFN-γ.

Killing cells with effector CD8+ T cells is a precise process which minimises injury to cells not bearing the target antigen, whilst killing the infected cell target.

1.5.4.2 Differentiation of CD4+ T cells

Unlike naive CD8+ T cells which are predetermined to become cytotoxic cells and form part of cell mediated immunity (CMI), CD4+ T cells differentiate on activation into different subtypes which produce different cytokines and have different effector functions (Table 1.3). Which subtype depends upon the cytokine environment in which they are produced (Constant and Bottomly 1997), along with the type of co-stimulation used and nature of the peptide:MHC ligand. Initially this cytokine environment is generated by cells of the innate system, which act to shape the adaptive response. The most well recognised subgroups are Th1 and Th2 cells (Mosmann, Cherwinski et al. 1986).

- Th1: The presence of the cytokines IFN-γ and IL-12, signalling through signal transduction and activator of transcription 4 (STAT-4), skews the CD4 T cell population towards the Th1 phenotype. Th1 cells are important in macrophage activation, playing a role in cell mediated immunity, and induce B cells to produce opsonising IgG antibodies, part of humoral immunity. Th1 cells produce cytokines including IFN-γ and IL-2 and are characterised by the expression of the transcription factor T-bet.

- Th2: The presence of the cytokines IL-4 and IL-5, signalling through STAT-6, skews the CD4 T cell population towards the Th2 phenotype. These Th2 cells are important in activating B cells to produce neutralising antibodies such as IgM, A and E and form part of humoral immunity, as well as effecting

macrophages. Th2 cells produce IL-4 and IL-13 and are characterised by the expression of the transcription factor GATA-3.

- Th17: The more recently discovered Th17 T cells develop in the presence of IL-6 and TGF-β to produce IL-17, IL-21 and IL-23 and express the transcription factor ROR-γt (Bettelli, Carrier et al. 2006; Mangan, Harrington et al. 2006; Veldhoen, Hocking et al. 2006). IL-21 and IL-23 are responsible for maintaining the proliferation of Th17 cells. IL-17 produced by Th17 cells acts as a proinflammatory mediator and amongst other things stimulates: proinflammatory cytokines causing further local inflammation, chemoattractant molecules to recruit phagocytic cells, haematopoietic growth factors, and co-stimulatory molecules to aid T cell activation.

- Treg: T regulatory cells (discussed briefly in 1.2.2) also develop in a TGF-β cytokine environment (Bettelli, Carrier et al. 2006) but express the transcription factor FoxP3 and produce IL-10 and TGF-β. Their ability to regulate is still not absolutely defined but may include contact-dependent regulation and the release of soluble mediators to cause regulation.

Importantly, subsets of T cells can reciprocally inhibit the functions of others. Cytokines produced by Th1 cells e.g. IFN-γ can negatively regulate Th2 cells and vice versa through IL-10 (Mosmann, Cherwinski et al. 1986). Also the production of IFN-γ and IL-17 seems mutually exclusive promoting either Th1 or Th17 cells respectively (Park, Li et al. 2005), as does the formation of either Th17 or Treg cells which is dependent upon the cytokine environment (Bettelli, Carrier et al. 2006). Commitment to a particular subset of Th cell may not be stable and reprogramming to attain another phenotype may be possible. This is known as plasticity (Yang, Nurieva et al. 2008).

1.5.4.2.1 Effector Th1 cells provide help for macrophage activation

The principal function of effector Th1 cells is in classical M1 macrophage activation. This adaptive immune response is important in host defence against intra- and extracellular pathogens that have resisted death after being engulfed by macrophages. This process of macrophage activation occurs by two means: through the production of IFN-γ and by forming a sensitising contact signal through the CD40L on the T cell to the CD40 molecule on the macrophage.

Th1 cells produce a range of cytokines, chemokines and surface molecules that not only activate macrophages but recruit phagocytes to the site of injury through the production of IL-3, GM-CSF, TNF-α and β and the chemokine CCL2. They can also display the FAS ligand and induce apoptosis of cells with the FAS surface molecule, in particular macrophages. Th1 cells control and coordinate host defence against some intracellular pathogens such as *Mycobacterium* and *Pneumocystis carinii*.

Once the macrophage is activated by the Th1 cells to form potent microbial effector cells they can carry out a number of functions. These include:

- killing pathogens within the macrophage phagosomes
- synthesising and releasing peptides and proteases to attack extracellular pathogens
- increasing their cell surface class II MHC, B7 and CD40 molecules and TNF receptors to become better APCs
- producing IL-12 to direct activated CD4+ T cells towards the Th1 phenotype
- producing nitric oxide (NO)
- recruiting other cells to the site of inflammation

However macrophage activation is not specific and can cause local tissue damage.

1.5.4.2.2 Effector Th cells provide help for B cells

The extracellular space is also protected by the humoral immune response. This relies upon activation of B cells to produce antibodies which can then act to destroy extracellular pathogens or prevent the spread of intracellular infection from one cell to another. Antibodies carry out these functions either by opsonising the pathogen to facilitate phagocytosis, with or without complement, or by binding to the cell surface of the pathogen and preventing spread of infection.

The most effective B cell activation requires the help of effector Th cells, but T cell independent B cell activation can be triggered by antigens such as lipopolysaccharide or the repeated pattern of bacterial capsular polysaccharides that cross link multiple B cell receptors (BCRs) to cause activation. Ultimately Th cells act to regulate antibody production and determine the effector function of antibodies by isotype switching.

For Th cells to provide help to a naive B cell they must both recognise a linked antigen. Naive B cells recognise pathogen after it binds to the Fab end of surface bound immunoglobulin (i.e. the BCR), which provides the first signal for B cell activation.

This complex is internalised and peptide processed before presention with class II MHC on the B cell surface. Once the B cell encounters an effector Th cell which recognises that peptide, the TCR binds. The Th cell then produces cell bound and secreted proteins to activate the B cell. This B cell:Th cell interaction triggers the CD40L to bind the CD40 molecule on the B cell and is critical in providing the second signal for B cell activation. The production of IL-4 by the Th2 cell also contributes to clonal expansion. However, activation is bidirectional such that the B cell also increases expression of the B7 family of molecules, which signal to the Th cell to sustain growth and differentiation.

Signalling through the CD40 molecule on the B cell allows isotype switching. Th2 cells bound to the activated B cell can produce IL-4 and 5 stimulating the B cells to generate IgG, E and A, whereas IFN-γ production by Th1 cells triggers B cells to produce IgG2a and 3. After B cells proliferate and differentiate, they mature into either plasma or memory cells. Plasma cells produce high affinity, isotype switched antibodies and memory B cells are long lived cells but do not secrete antibody.

1.5.4.2.3 T regulatory cells

T regulatory cells have immunoregulatory capacity. They can inhibit proliferation and production of cytokines by CD4+ and CD8+ lymphocytes to polyclonal stimuli, as well as down-modulate the responses by these cells to specific antigens (Dieckmann, Plottner et al. 2001). This assists in the maintenance of tolerance to self components and allows the prevention or control of autoimmune diseases and transplant organ rejection. The transcription factor FoxP3 is expressed by Tregs and they develop in a TGF-β cytokine rich environment (Chen, Jin et al. 2003).

The mechanisms by which Tregs elicit their immunosuppressive effects are unclear but may be by contact-dependent regulation and by the release of soluble mediators to act at short distances from the Treg to cause regulation. In vitro CD4+CD25+ Tregs require specific antigens or polyclonal activators to stimulate suppressive activity through their TCRs. The subsequent suppression of effector CD25-CD4+ or CD8+ T cells is contact-dependent, requiring an association between the Treg and effector T cell, but is cytokine-independent (Takahashi, Kuniyasu et al. 1998; Thornton and Shevach 2000). Suppression of the effector T cell may occur by un-coupling of IL-2 signalling and inhibition of IL-2 production. In vivo Tregs exert their effects by both cytokine-independent and cytokine-dependent mechanisms. Tregs respond to their cognate

antigen (Romagnoli, Hudrisier et al. 2002) however, IL-10 and TGF-β are also important indirect mediators of Treg activity: these soluble cytokines act at short distances from the cell or bound to the cell surface to promote regulation (Dieckmann, Bruett et al. 2002).

Tregs can be generated both in the thymus and the periphery. Thymic or natural Tregs leave the thymus as functional MHC class II-restricted suppressor cells (Bluestone and Abbas 2003), essential for preventing autoimmunity and keeping immune responses to pathogens under control. The method of generation of peripheral/adaptive/induced Tregs may be similar to the mechanisms involved in Th1/Th2 polarisation and contribute to the development of an antigen-specific immunosuppressive response (Bluestone and Abbas 2003). At least three factors are important in their generation. The first factor involves the amount and strength of the antigen interaction on the APC with a CD4+ T cell, with low concentrations and weak stimuli resulting in more Treg generation (Thorstenson and Khoruts 2001). Secondly, the activation status of the APC is important, with immature or sub-optimally activated APCs/DCs being more likely to generate Tregs (Apostolou and von Boehmer 2004). And finally the cytokine environment in which the Tregs develop and are maintained is critical in their development, with TGF-β being instrumental in the conversion of naive T cells to Tregs (Chen, Jin et al. 2003).

Some immunosuppressive drugs have been demonstrated to augment Treg function. In particular antithymocyte globulin (ATG) depletes T cells by complement mediated lysis or activation-induced apoptosis. However, it has been demonstrated that exposure to ATG expands the Treg population and can induce development of Treg cells rather than proinflammatory T cells (Lopez, Clarkson et al. 2006). The mechanism by which this occurs is unclear. Furthermore alemtuzumab (Campath) a monoclonal antibody to CD52, found on the surface of lymphocytes, can also cause the Treg population to expand (Watanabe, Masuyama et al. 2006). These drugs are both used to treat or prevent acute rejection in transplant patients and it has been observed that these patients have increased numbers of circulating Tregs (Ciancio, Burke et al. 2005).

1.5.4.2.4 Th17 cells

The initial 1986 paradigm proposed by Mosmann and Coffman with Th1 and Th2 cells (Mosmann, Cherwinski et al. 1986) was unable to explain why mice deficient in the cytokine IFN-γ could generate a proinflammatory Th1 phenotype and remained

susceptible to inflammatory conditions such as EAE and collagen-induced arthritis (CIA) (Ferber, Brocke et al. 1996; Matthys, Vermeire et al. 1998). It was subsequently demonstrated from murine work that IL-23 stimulated the production of IL-17 by a population of mature T cells and that IL-17 was linked with the inflammation seen in CIA and EAE (Lubberts, Joosten et al. 2002; Langrish, Chen et al. 2005).

It is now known that IL-6, in combination with TGF-β induces a population of naive Th cells to differentiate into Th17 lymphocytes. ROR-γt induces the transcription of the IL-17 gene in naive Th cells. It also allows the expression of the IL-23 receptor on the Th17 cells, allowing stabilisation of the IL-17 phenotype. Three publications were produced almost simultaneously in 2006 which demonstrated that both IL-6 and TGF-β were required to generate Th17 cells from naive Th cells (Bettelli, Carrier et al. 2006; Mangan, Harrington et al. 2006; Veldhoen, Hocking et al. 2006). In humans Th17 have been generated from naive Th cells with TGF-β plus IL-21 or IL-6 and 23 (Miossec, Korn et al. 2009).

Th17 cells have multiple functions due to their production of the pleomorphic cytokine IL-17. They can initiate inflammatory reactions dominated by neutrophils in response to certain infectious agents but are also associated with generating and maintaining chronic inflammation and immunopathological diseases, such as rheumatoid arthritis, multiple sclerosis and inflammatory bowel disease.

Th17 cells and FoxP3 regulatory cells are reciprocally related to generate inflammation and autoimmunity or regulation. TGF-β induces naive T cells to express FoxP3 and develop suppressor regulatory function. However, IL-6 is able to switch the transcriptional program initiated by TGF-β in a way that induces the development of Th17 cells and the expression of the ROR-γt transcription factor.

Table 1.3- The four main types of armed effector CD4+ T cells which produce distinct effector functions

Subclass of CD4+ T cell	Cytokine responsible for skewing	Transcription factor	Cytokines and effector molecules produced	Effector function
Th1	IFN-γ IL-12	T-bet	IFN-γ TNF-α GM-CSF CD40 ligand Fas ligand	• Macrophage activation • Induce B cells to produce opsonising IgG antibodies • Provide help to activate naive CD8+ T cells
Th2	IL-4 IL-5,	GATA-3	IL-4 IL-5 IL-13 CD40 ligand	• Activate B cells and allow isotype switching • Affect macrophages • Recruit eosinophils
Treg	TGF-β	FoxP3	TGF-β IL-10	• Contact dependent regulation • Release of soluble mediators to allow regulation
Th17	IL-6 TGF-β	ROR-γt	IL-17 IL-21 IL-23	• Proinflammatory role • Autoimmune disease

1.5.5 Memory cells

The formation of memory cells is one of the most important consequences of the adaptive immune response. They provide long lasting protective immunity which allows the rapid production of antigen specific antibodies and armed effector cells on subsequent encounter with the same pathogen. Both memory T and B cells exist, which are a small persistent pool of lymphocytes which survive after initial antigen recognition independent of the original antigen but are maintained in a resting state by IL-7 and 15.

Memory B cells are formed after B cell activation when they become either terminally differentiated plasma cells secreting antibody until they die or memory B cells. The formation of a memory T cell arises after T cell activation and from effector T cells. There may be two distinct forms of memory T cell, effector and central memory cells, which are able to mature at different speeds into effector cells.

Memory cells can be distinguished from naive or effector cells by the surface markers they display. In particular the three surface proteins L-selectin, CD45 and CD44 differ between the three T cell types, with memory cells displaying high levels of CD44, low L-selectin and a different CD45 isoform.

1.5.6 NKT cells

These are lymphocytes which bridge the gap between innate and adaptive immunity. They develop in the thymus and are positively selected after CD1d-glycoprotein complexes interact with double negative thymocytes. NKT cells can be activated either by recognising endogenous and exogenous antigens or indirectly via cytokine driven mechanisms.

The NKT receptor is a semi invariant TCR which closely resembles a PRR. The Type I NKT cell receptor is formed by combining Vα14-Jα18 and Vβ8.2/7/2. This antigen specific receptor recognises glycoprotein antigen with the MHC class I-related glycoprotein CD1d on professional APCs. The prototype type I NKT cell recognises α-galactosylceramide (α-GalCer) antigen. Type II NKT cells are also CD1d restricted but have a wider repertoire of TCRs. NKT cells in mice are either CD4+ or double negative cells. Alternatively NKT cells can be activated indirectly, without cognate antigen recognition by cytokines alone. This can occur when PRRs on a DC are upregulated in response to a microbial stimulus, causing DC activation and the production of cytokines

such as IL-12, which activate NKT cells. Alternatively, a combination of both direct antigen and indirect cytokine mechanisms can activate NKT cells.

Once NKT cells are activated they produce immunoregulatory cytokines especially IL-4 and IFN-γ. Other cytokines produced include IL-2, IL-6, IL-10, IL-13, IL-17, TGF-β and TNF-α. In addition, activated NKT cells can produce haematopoietic growth factors e.g. GM-CSF and chemokines (e.g. RANTES). They are also cytolytic, expressing high levels of granzymes, perforin and FasL. Once activated NKT cells display activation markers such as CD69 and CD44 like conventional T cells however, activation is short lived and they soon become anergic. Different subtypes of NKT cells have different cytokine profiles upon activation (determined by their mode of activation) resulting in their differing effector functions.

NKT cell activation can influence both innate and adaptive immune systems: through the production of IFN-γ they influence macrophage inducing inflammatory responses, CD8+ T cell mediated cytotoxic effects against target cells and Th1 CD4+ cell responses.

1.6 Autoimmune disease

The adaptive immune system is critically important for host defences against infection, but sometimes host defences are initiated against antigens not associated with infectious agents, such as self tissue antigens. This is termed autoimmunity and can lead to tissue damage. Autoimmunity is due to loss of tolerance to self antigens and a breakdown in either central or peripheral tolerance. Autoimmune diseases (AIDs) develop when a population of self reactive, self MHC restricted T cells cause a T cell or humeral antibody mediated response resulting in injury. Once T cells are activated by self antigens they cause the same T cell effector immune responses which occur in response to pathogen. T cells can be directly cytotoxic or produce inflammatory cytokines and help B cells to produce antibodies which cause tissue damage.

1.6.1 Self perpetuating autoimmune injury

In normal immune responses against pathogen, the pathogen is destroyed and the immune response will cease but leave a population of memory lymphocytes. However, in autoimmunity the self antigen is not easily eliminated because it is either in vast excess or ubiquitous (such as chromatin in systemic lupus erythematosus (SLE)) and so the constant presence of autoantigen causes chronic inflammation and the further release of autoantigens through tissue injury. Cytokines liberated from areas of injury attract inflammatory cells such as macrophages and neutrophils which can cause further tissue injury and so a continuous and evolving self destructive process develops. Self antigens which were not the initial target of autoreactive T cells at the initiation of autoimmunity may become targets, such as DNA and other nuclear proteins in SLE. This is because self antigens are released into an environment with activated DCs and B cells that can take up and present the self antigen to autoreactive T and B cells. This process is called epitope spreading, where autoimmunity to a single epitope can spread to multiple epitopes and cause widespread autoimmunity. This has been demonstrated in the animal model of multiple sclerosis (MS), experimental allergic encephalitis, where immunisation with a single peptide of the self protein myelin basic protein (MBP) with adjuvant can ultimately lead to immune responses to other epitopes from the same protein and even to other proteins expressed in the same tissue (Lehmann, Forsthuber et al. 1992).

1.6.2 Autoimmune susceptibility

The trigger to autoimmunity is unclear but it seems that environmental factors such as drugs, infections and toxins and/or a genetic predisposition are required to elicit

autoimmune disease. These factors allow T cells to evade the mechanisms of central and/or peripheral tolerance which are fundamental to distinguishing self from non-self.

1.6.2.1 Genetic susceptibility to autoimmune disease

Many genes have been identified in which mutations or single-nucleotide polymorphisms (SNPs) are associated with increased susceptibility to autoimmunity. These include genes which are responsible for autoantigen availability and clearance, co-stimulatory molecule expression, cytokine gene expression, lymphocyte signalling and apoptosis. Well recognised examples which induce AID include mutations to the AIRE and Fas genes that encode proteins involved with thymic tolerance and apoptosis.

The most consistent genetic locus associated with increased susceptibility to AID is the MHC genotype. In human autoimmune diseases susceptibility is most strongly linked with class II MHC alleles but there are some strong associations with MHC class I alleles. Goodpasture's syndrome is an example where susceptibility to the condition is associated with the DR2 allele of class II MHC and in ankylosing spondylitis there is a very strong association with the class I MHC B27 allele.

The ability of T cells to respond to an antigen depends upon the MHC genotype to which it is bound. It may be the increased susceptibility to AID offered by certain MHC alleles is because they are better at presenting autoantigens to autoreactive T cells. Certain self MHC molecules may drive positive selection of T cells within the thymus but avoid negative selection because the MHC-self peptide complex does not bind with adequate avidity or are in low copy number. This is supported by the observations that the disease-associated MHC class II molecule I-Ag7, in non-obese diabetic (NOD) mice, binds many peptides poorly and may be less effective at driving negative selection of T cells in the thymus that bind self antigens (Carrasco-Marin, Shimizu et al. 1996).

1.6.2.2 Environmental susceptibility to autoimmune disease

Environmental factors have a strong influence on autoimmunity and AID can follow infection, inflammation, injury or toxin exposure.

1.6.2.2.1 Self antigens in an inflammatory environment

T cells which have low affinity for ubiquitous self antigen and which are unable to cause T cell activation under normal conditions may become autoreactive in an inflammatory environment. Inflammation caused by infection or injury stimulates the

release of inflammatory mediators and upregulation of co-stimulatory molecules on APCs, generating the obligate second signal required by T cells for their activation. If tissue damage increases the availability of self antigens then the autoantigen which would normally bind rarely and with low avidity to its cognate T cell may now be able to stimulate its activation (Matzinger 2002).

1.6.2.2.2 Cross reactivity with pathogenic epitopes

Certain pathogens express protein or carbohydrate antigens which resemble host self antigens, so T cells recognising these pathogenic peptides can also elicit a T cell response to self peptide from host tissue. Additionally antibodies produced against the pathogen epitope may cross react with the self protein. This concept is termed molecular mimicry and occurs in rheumatic fever where cross reactivity between streptococcal components and host tissue causes antibody and T cell mediated host tissue injury.

1.6.2.2.3 Exposing self antigen from an immunologically privileged site

There are some sites in the body including the brain and anterior chamber of the eye into which tissue grafting does not elicit rejection and these sites are termed immunologically privileged (Medawar 1948). It was originally believed that the privilege was due to passive immunological ignorance since retinal antigens were inaccessible to the immune system due to the blood:retinal barrier. However, subsequent studies have demonstrated that antigens interact with T cells at this site and do leave the eye. Therefore immune privilege must rely upon the regulation of both local and systemic immune responses to antigen. Within the aqueous humour of the eye there is local inhibition of immune responses due to a unique immunomodulatory environment which suppresses T cell activation and promotes regulation. Fas ligand is constitutively expressed in the eye and plays a major part in immune privilege by inducing apoptosis in inflammatory cells which enter the eye (Ferguson and Griffith 2006). The systemic induction of Tregs has also been demonstrated (Caspi 2010). However, if there is trauma or infection which causes the eye to rupture an autoimmune response to eye proteins can develop which attacks both eyes, termed sympathetic opthalmitis. Sequestered eye antigens can be presented to T cells in the draining lymph nodes and stimulate effector T cells to enter the healthy eye to cause injury.

A similar mechanism may occur with Dressler's syndrome, when myocardial injury releases myosin from a site previously hidden to the immune system.

1.6.2.2.4 Post translational modification in response to a physiological or inflammatory insult

Post translational modifications (PTMs) of amino acids can generate neo-epitopes from self antigens. These modifications can occur in response to cell stress, inflammation or infection. PTMs can be by the addition of new groups to the protein such as phosphorylation, methylation and glycation. This method of PTM has been demonstrated in MS (van Stipdonk, Willems et al. 1998) and CIA (Michaelsson, Malmstrom et al. 1994) where phosphorylation and glycation of peptides respectively change their immunogenicity. Alternatively amino acid conversions can be induced spontaneously or enzymatically to cause deamination and citrullination. Citrulline has provoked interest in rheumatoid arthritis as an autoantibody target (van Boekel and van Venrooij 2003). Extracellular proteolysis may also occur, generating peptide fragments prior to either form of modification. All these mechanisms will influence recognition of self by affecting MHC binding, TCR affinity and antigen processing. These mechanisms can result in increased affinity between MHC and the TCR. It may also have more subtle effects promoting or limiting epitope production by impacting on antigen processing within APCs or extracellular degradation, which could occur when a cleavage site is lost (Anderton 2004; Pedersen 2007). Self-tolerance can be lost after PTMs induced by physiological factors such as cell stretch or pressure or be secondary to inflammation.

1.6.2.2.5 Superantigens

Superantigens, which are secreted proteins of microbial origin, are able to activate a polyclonal population of T cells independent of a cognate peptide-MHC-TCR interaction. By this mechanism up to 30% of the T cell population may become activated by superantigen that binds to a specific or limited number of Vβ TCR chains and MHC class II on the APC. This interaction drives clonal proliferation of a population of T cells expressing that Vβ gene (Kappler, Wade et al. 1987). The most commonly known superantigen in mice is encoded by the mouse mammary tumour virus (MMTV) (Acha-Orbea and MacDonald 1995) and in humans the toxic shock syndrome toxin is also a superantigen.

1.6.2.3 Loss of T cell regulation

Expression of the FoxP3 transcription factor is required for Tregs to function as immunosuppressive cells (Fontenot, Gavin et al. 2003). A spontaneous mutant strain of mice, known as scurfy mice, develop a fatal lymphoproliferative disease with chronic

multi-organ inflammation. The genetic mutation in these mice disrupts the FoxP3 gene and when wild type Tregs are transferred to newborn scurfy mice the condition is prevented (Brunkow, Jeffery et al. 2001). Humans with 'immunodysregulation polyendocrinopathy enteropathy X-linked' (IPEX) have a mutation in the FoxP3 gene causing chronic inflammation and AID, treatment options include immunosuppressive therapies and bone marrow transplantation (van der Vliet and Nieuwenhuis 2007).

In AID there may be a dysregulated immune response with a loss of Treg function and a shift towards the Th1/Th17 phenotype, caused by the cytokine environment which has developed and the DC population present. Generation of proinflammatory cells may either be due to the loss of skewing towards the Treg phenotype (with the default production of proinflammatory Th1/Th17 cells) or a positive shift towards these pathways. IL-6 is the pivotal cytokine in this pathway which diverts the T cell population towards a proinflammatory rather than regulatory role, with the production of potent proinflammatory Th17 cells.

1.6.3 Classification of autoimmune disease

AID is classified as either organ specific or systemic. Mechanisms that mediate autoimmune injury are similar to those used against invading pathogens, involving both antibodies and T cells, but in autoimmunity these are autoreactive. The three dominant mechanisms of tissue injury can be classified in a similar way to hypersensitivity reactions. Autoantibodies are able to bind soluble or tissue bound self antigen and mediate injury via the Fc and complement receptor pathways. Alternatively, autoreactive T cells destroy self tissue in a similar way to destroying a virally infected cell. An important difference between the immune response against pathogens and self antigen is that in most cases self proteins are not easily eliminated.

1.6.3.1 Surface bound or matrix self antigens mediating autoimmune disease

Autoimmunity that causes damage by mechanisms analogous to type II hypersensitivity reactions occurs when IgM and IgG autoantibodies bind to cell surface or matrix antigens. Injury is caused by mechanisms involving complement activation and when the Fc component of IgG binds to Fc receptors on phagocytic cells.

Activation of the classical complement cascade can occur when either IgM or IgG autoantibodies bind cell surface or matrix antigens, leading to production of chemoattractant (C5a) and opsonizing molecules (C3b) and the membrane attack complex. Nucleated cells are relatively resistant to lysis by complement however

sublytic levels provide a powerful activating stimulus to the cell, causing cytokine release and generation of prostaglandin and leukotriene precursors that are the lipid mediators of inflammation (Hansch 1992). This occurs in Hashimoto's thyroiditis.

Secondly, the Fc portion of IgG, with self antigen bound to the Fab end, can bind to the Fc receptor on phagocytic cells such as macrophages and neutrophils and cause their activation. If the self antigen-antibody complex is of an appropriate size it may be phagocytosed: this occurs in autoimmune haemolytic anaemia when red blood cells are destroyed in phagocytic vesicles (Domen 1998). Otherwise phagocytic cells release lysosomal enzymes, cytokines and complement to cause tissue injury. This occurs in Goodpasture's disease when autoantibody binds the α3 chain of type IV collagen, a matrix protein, causing severe glomerular and often pulmonary injury (Lerner, Glassock et al. 1967).

Autoantibodies targeted at cell surface receptors can cause disease by stimulating or blocking them. In Graves' disease autoantibody binds the thyroid stimulating hormone receptor causing excessive thyroid hormone production (Bahn and Heufelder 1993) and conversely in myaesthenia gravis autoantibody binds the nicotinic acetyl choline receptor preventing neuromuscular transmission (Vincent, Lily et al. 1999).

1.6.3.2 Immune complex mediated autoimmune disease

The tissue injuries caused in immune complex mediated autoimmune disease, where soluble self antigens are bound by autoantibody, are caused by the same mechanisms as type III hypersensitivity reactions. These immune complexes can fix complement and can be bound to phagocytic cells via complement and Fc receptors. Under normal conditions these complexes would be phagocytosed causing little tissue injury. However, when normal clearance mechanisms are overwhelmed these immune complexes become pathogenic, depositing in small blood vessels and inciting an aggressive inflammatory reaction. In SLE there is IgG production to ubiquitous nuclear self antigens which are present in all nucleated cells (Kotzin 1996). On cell death these nuclear components become extracellular and large amounts of antigen are available to complex with autoantibody and deposit in small bloods vessels causing complement and phagocyte activation with subsequent tissue injury. This tissue injury releases further nuclear components and thus a further supply of self antigens and so the cycle continues.

1.6.3.3 T cell mediated autoimmune disease

Effector Th1 cells can bind their cognate self peptide:MHC complex on the surface of APCs to trigger activation. This is the same mechanism by which type IV or delayed-type hypersensitivity reactions occur, the prototypical reaction being after the intra-dermal injection of tuberculin (Facktor, Bernstein et al. 1973). Patients with previous exposure to the mycobacterium by infection or immunisation develop a localised T cell mediated inflammatory reaction within 24-72 hours, mediated by Th1 cells recognising the peptide:MHC class II complex on an APC and releasing inflammatory cytokines to establish a localised inflammatory reaction.

Activated, autoreactive Th1 cells cause local inflammation by activating macrophages and by direct damage to tissue cells. Firstly, chemokines released from the activated Th1 cell attract macrophages to the site of antigen deposition. Secondly, the release of IFN-γ induces expression of vascular adhesion molecules and activates macrophages to release inflammatory mediators. Activated macrophages can also act as APCs further amplifying the immune response. TNF-α and TNF-β increase expression of adhesion molecules on local blood vessels and increase permeability allowing inflammatory and plasma cells to enter the site. Production of IL-3 and GM-CSF stimulates further monocyte production in the bone marrow. Cumulatively these mechanisms allow infiltration of activated lymphocytes and macrophages into the tissue where the self peptide is present and cause tissue injury and cell death. Similar reactions can be caused by CD8+ T cells depending upon the pathway by which the antigen is processed. T cells are also required to sustain all autoantibody mediated responses

AIDs mediated by autoreactive T cells include diabetes mellitus, multiple sclerosis (Zamvil, Nelson et al. 1985) and SLE (Peng, Madaio et al. 1996). In type 1 diabetes mellitus, insulin peptides produced by β pancreatic islet cells are recognised by autoreactive CD8+ lymphocytes and once activated these T cells cause β cell death and reduced insulin production (Haskins and Wegmann 1996).

1.7 Tubulointerstitial kidney injury and fibrosis

1.7.1 Introduction

Chronic kidney disease (CKD) is an increasingly significant public health problem in the western world and affects approximately 10% of the adult population (Coresh, Selvin et al. 2007). Even in its mildest forms it impacts on morbidity and mortality and can also progress to renal failure, requiring dialysis or transplantation, which represents a huge health and socio-economic burden (Go, Chertow et al. 2004).

Irrespective of the cause, progressive nephron loss with leukocyte infiltration into the tubulointerstitium (TI) and fibrosis is a consistent finding in CKD (Harris and Neilson 2006). Studies have shown that, even in primary glomerular diseases, it is the degree of TI injury rather than the severity of glomerular involvement which determines renal outcome (Nath 1992; Bohle, Strutz et al. 1994). The relationship between TI inflammation and fibrosis is less well established however, the role and function of leukocytes in the pathogenesis of renal injury is becoming increasingly clear (Tapmeier, Fearn et al. 2010). Here I outline the current understanding of lymphocyte and macrophage function in the development of tubulointerstitial damage.

1.7.2 The response to kidney injury

The recognised model of fibrogenesis suggests that after an initial injury the kidney would try to repair damage and recover function. Although this repair process is initially beneficial in limiting injury and dampening down the inflammatory process, it is also pathogenic due to the production of profibrotic mediators causing a fibrotic scar to develop. Formation of this permanent scar disrupts the normal architecture of the TI and can propagate further injury, especially if the injury is either repeated or persistent as occurs in many causes of CKD.

The initial damage which mediates this injury can result from various stimuli, including autoimmune disease, infection, toxins and mechanical injury. However, both immunologically and non-immunologically mediated damage results in the infiltration of leukocytes into the TI. The interaction between these leukocytes and non-immunological factors is complex and illustrated in the transplanted kidney where a major cause of late transplant failure is caused by tubular atrophy and interstitial fibrosis. In the transplanted kidney recognition of alloantigen by the immune system is an obvious driving force for ongoing injury and fibrosis but a number of other non-allogenic factors contribute including the use of calcineurin inhibitors, ischaemia-

reperfusion, proteinuria, hyperlipidaemia and recurrent infection. Non-allogenic factors also contribute to renal injury in native kidney disease however, in the absence of an alloantigen driven response, the role and function of infiltrating leukocytes is less clear.

These initial injuries, regardless of aetiology, initiate tubular epithelial cell (TEC) activation and the production of molecules which propagate renal damage, facilitate interstitial inflammation and contribute to fibrosis. Chemokines released by TECs result in chemotactic gradients that attract inflammatory cells to the site of injury. This infiltrating leukocyte population is comprised of macrophages and lymphocytes which are predominantly T cells (Muller, Markovic-Lipkovski et al. 1992; Strutz and Neilson 1994).

1.7.3 Role of T lymphocytes in tubulointerstitial injury and fibrosis

In studies of human renal disease there is a correlation between lymphocytic infiltration into the TI and subsequent injury but causality is unproven. Two groups have demonstrated an association between the progression of IgA nephropathy and TI inflammation: In 2007 a Finnish group established that infiltration of CD3+ cells into the TI was independently associated with disease progression in all patients, both those with preserved renal function and those with renal impairment (Myllymaki, Honkanen et al. 2007). In 2008 another group retrospectively analysed a smaller population of 50 patients and showed a significant association with dual positive GMP-17 / CD8 cytotoxic T cells and progression towards renal failure in patients with normal or near normal GFR (van Es, de Heer et al. 2008). Furthermore as far back as 1975 TI inflammation was demonstrated in lupus nephritis; along with the universal presence of glomerular injury, 66% of biopsy specimens also had TI involvement (Brentjens, Sepulveda et al. 1975). Other groups demonstrated that the severity of interstitial inflammation in SLE correlated with the degree of renal insufficiency (Park, D'Agati et al. 1986; Alexopoulos, Seron et al. 1990).

In general the lymphocytic infiltrate is predominantly T cells (CD4+ > CD8+) and there are fewer B cells (Strutz and Neilson 1994). T lymphocytes probably act synergistically with macrophages to propagate injury.

In non-immunologically mediated renal disease, although lymphocyte infiltration occurs and appears to contribute to injury, it is unclear how lymphocytes become activated. As a consequence of the initial injury new antigenic epitopes may be displayed which are recognised by lymphocytes as foreign and trigger an immune response (Truong,

Farhood et al. 1992). Alternatively, autoreactive T cells which are normally anergic could recognise their cognate antigen and become activated in the proinflammatory environment of the injured kidney, thereby breaking tolerance and resulting in immune mediated injury (Matzinger 2002). The third possible explanation would be that bystander naive T cells are activated in a non-classical manner by the proinflammatory environment of the injured kidney without the need for antigen recognition (Unutmaz, Pileri et al. 1994; Rodriguez-Iturbe, Pons et al. 2001; Bangs, McMichael et al. 2006; Pedersen 2007; Bangs, Baban et al. 2009).

The exact phenotype of the T cell population may determine their contribution to fibrosis. There is strong evidence, particularly from liver disease, that Th2 CD4+ T cells promote fibrosis whilst Th1 CD4+ T cells encourage resolution and less fibrosis (Wynn 2004). Evidence for this in renal disease is limited, although treatment with IFNγ, which favours a Th1 CD4 T cell response, reduced fibrosis in an animal model of TI disease (Oldroyd, Thomas et al. 1999). In the unilateral ureteric obstruction (UUO) model Tapmeier et al demonstrated the pivotal role of CD4+ T cells in promoting renal fibrosis (Tapmeier, Fearn et al. 2010). In addition it is increasingly recognised that certain lymphocyte populations, in particular regulatory T cells, have a part to play in regulating the immune response and protecting the kidney from fibrosis (Lee, Wang et al. 2008).

In order to study the disease mechanisms involved in renal fibrosis a number of animal models of chronic kidney disease have been developed. In the case of UUO increased intra-renal pressure and stretch occurs, causing TEC injury (Chevalier 1999). In renal ischaemia-reperfusion injury the kidney becomes ischaemic, initiating cellular injury on reperfusion. In models of glomerular disease e.g. adriamycin nephropathy or the mouse model of Alport syndrome, proteinuria itself may be toxic to tubules with proteins in the filtrate initiating an inflammatory response. Lymphocytes have been manipulated in these models of CKD by using either depleting antibodies or lymphopenic animals e.g. recombination activation gene-1 (RAG-1) knockout mice or severe combined immunodeficient (SCID) mice. In the most part these studies have demonstrated that, in the absence of lymphocytes, fibrotic injury is ameliorated suggesting that T lymphocytes are playing a pathological role in promoting fibrosis.

1.7.3.1 Animal models of tubulointerstitial fibrosis

1.7.3.1.1 Unilateral Ureteric Obstruction, chemokines and chronic TI injury

The role of chemokines in the development of TI inflammatory infiltrates has been extensively described (Vielhauer, Eis et al. 2004). There is increased expression of chemokines CCL2/MCP-1 and CCL5/RANTES in the UUO kidney that correlates with the accumulation of macrophages and lymphocytes expressing the chemokine receptors CCR2 and CCR5 and also with fibrosis (Vielhauer, Anders et al. 2001). When chemokine receptor knockout animals (Eis, Luckow et al. 2004) and chemokine antagonists (Anders, Vielhauer et al. 2002) are used there is significantly less cellular infiltration into the TI compartment and less interstitial injury post obstruction. Drugs with lymphocyte specificity, including mycophenolate mofetil (MMF) and rapamycin, have been used in the UUO model. MMF, which blocks de-novo synthesis of purines by lymphocytes and confers lymphocyte specificity as an anti-proliferative agent, has been shown to reduce the TI inflammatory infiltrate in UUO animals and injury (Goncalves, Biato et al. 2004). Using rapamycin in UUO has also given similar results, with a reduction in TI injury (Wu, Wen et al. 2006). Therefore inhibition and genetic deletion of chemokine receptors and the use of immunosuppressive drugs in the UUO model have all demonstrated less mononuclear cell infiltration and a reduction in renal injury but do not distinguish between lymphocyte and macrophage function in promoting fibrosis.

However, Tapmeier et al have specifically demonstrated CD4+ T cells are pivotal to the development of fibrosis following UUO (Tapmeier, Fearn et al. 2010) and that these lymphocytes persist despite reversal of obstruction (Tapmeier, Brown et al. 2008). Niedermeier et al demonstrated in UUO that activated CD4+ cells stimulate differentiation of haematopoietic monocytes into fibroblasts that produce collagen I (Niedermeier, Reich et al. 2009). This was only seen in the appropriate cytokine environment favoured by the presence of a calcineurin inhibitor and the cytokines TGF-β and IL-13.

In contrast Shappell et al demonstrated that lymphocytes were not required for progressive TI injury in SCID mice (Shappell, Gurpinar et al. 1998). These differences may be explained by the genetic background of the mice used (Puri, Shakaib et al. 2010).

Dong et al looked at the specific phenotype of cells that were activated by DCs in the UUO model of renal injury (Dong, Bachman et al. 2008). In the presence of cytokine rich dendritic cells producing MCP-1, IL-6 and IFN-γ, IFN-γ producing CD4 Th1+ and CD8+ memory T cells, and CD4+Th17+ memory cells secreting IL-17 were thought to be responsible for renal injury.

1.7.3.1.2 Ischaemia-reperfusion injury and chronic TI injury

The role of lymphocytes both in the early and late stages after renal ischaemia-reperfusion injury (IRI) has been evaluated. It has been shown that CD4+ T cells play an important role in promoting renal injury soon after IRI. A significant attenuation of renal injury post IRI was observed in CD4-/- mice and this injury was restored when CD4+ T cells are adoptively transferred into CD4-/- animals (Rabb, Daniels et al. 2000; Burne, Daniels et al. 2001; Yokota, Daniels et al. 2002). Both athymic mice and mice treated with T cell depleting antibodies were also protected from injury. The requirement for intact co-stimulation was also evident as CD4+CD28- T cell reconstitution did not restore renal injury to that seen in the WT animals (Takada, Chandraker et al. 1997). Interestingly RAG-1 knockout mice were not protected against IRI (Burne-Taney, Yokota-Ikeda et al. 2005).

The regulatory CD4+CD25+FoxP3+ T cell population driven by the cytokine TGF-β have also been shown to reduce TI injury in IRI (Gandolfo, Jang et al. 2009; Kinsey, Sharma et al. 2009). They may act to limit immune cell activation by modulating the proinflammatory cytokine production of other T cells or macrophages, modify mononuclear cell phenotype or promote renal cell recovery (Jang, Kim et al. 2008).

After a longer follow up period of 6 weeks, renal function remained worse in animals after IRI compared to control sham operated mice and there was associated histological injury with inflammatory infiltrate, tubular atrophy and TI fibrosis (Burne-Taney, Yokota et al. 2005). The inflammatory infiltrate comprised of phagocytic cells and CD4+ lymphocytes. These infiltrating lymphocytes displayed surface markers of both activated effector and memory cells (Ascon, Ascon et al. 2009). This supports the hypothesis that lymphocytes are playing a pathogenic role in promoting chronic injury, rather than simply trafficking through the kidney, with activation occurring either by antigen dependent or independent mechanisms. This also suggests there are long term consequences of renal disease progression despite a single episode of IRI.

The mechanism of lymphocyte activation in an alloantigen or exogenous antigen-independent environment such as IRI may be explained by antigen-independent T cell activation due to high concentrations of cytokines and chemokines. RANTES is present in high levels in the IRI kidney even 6 weeks after injury (Ascon, Ascon et al. 2009). The activation of T cells by RANTES independent of antigen has been shown by Bacon et al (Bacon, Premack et al. 1995), as has T cell activation by other cytokines e.g. IL-6, IL-2 and TNF-α (Rodriguez-Iturbe, Pons et al. 2001; Bangs, McMichael et al. 2006; Pedersen 2007). The alternative and more traditional explanation for T cell activation would involve antigen recognition in the context of MHC with co-stimulation. In the settling of IRI (with no allo- or exogenous antigen) this latter explanation would suggest loss of tolerance to self antigen. This explanation is supported by two observations. Firstly, T cell deficient mice develop less injury when reconstituted with T cells with a limited T cell receptor repertoire compared to when reconstituted with normal T cells, suggesting a critical dependency on the TCR-antigen interaction (Satpute, Park et al. 2009). Secondly, renal injury is seen in normal mice after the adoptive transfer of lymphocytes from IRI mice (Burne-Taney, Liu et al. 2006). This suggests memory T cells are being transferred that have lost tolerance to renal self antigen during IRI. These T cells recognise antigenic epitopes in normal mice provoking renal injury and proteinuria. The nature of the antigen in the IRI model has not been reported.

1.7.3.1.3 Lymphocytes in secondary tubulointerstitial disease

Adriamycin nephropathy (ADN) in mice has features of human focal segmental glomerulosclerosis and is characterised by proteinuria and ensuing TI damage. Studies of lymphocyte function in this model have highlighted the importance of sub-populations of T cells. More severe glomerular and TI disease was seen after depletion of CD4+ T cells (Wang, Wang et al. 2001). In contrast, depletion of CD8+ T cells (Wang, Wang et al. 2001) resulted in significantly less injury than in the untreated animals. The increased injury seen with CD4+ T cell depletion could be due to the loss of a population of regulatory CD4+ T cells. Studies in lymphopenic SCID mice support this hypothesis. When ADN is induced in SCID mice they develop more severe disease than that seen in wild type Balb/c mice (Lee, Wang et al. 2006). Reconstituting SCID mice with polyclonal T regulatory (Tregs) cells (CD4+CD25+FoxP3+) significantly reduced interstitial injury to the level seen in wild type mice (Mahajan, Wang et al. 2006; Wang, Zhang et al. 2006). Tregs can use multiple mechanisms to suppress immune responses and TGF-β appears to be critical in the control of injury.

Alport syndrome is due to a mutation in collagen IV, a major protein of the glomerular basement membrane. A mouse model exists which has many of the features of human disease, including progressive glomerular and TI injury. When the Alport mouse is crossed with a RAG-knockout mouse to create a double knockout, the severity of the glomerular disease is unaffected as this is due to the absence of collagen IV. However, the absence of lymphocytes significantly reduces the severity of the TI disease and prevents loss of renal function (Lebleu, Sugimoto et al. 2008). This clearly demonstrates the importance of lymphocyte function in secondary TI injury. Another group demonstrated improved survival of Alport mice after irradiation, which caused depletion of bone marrow derived cells, again suggesting these cells play a role in renal injury (Katayama, Kawano et al. 2008). These results differ from those in ADN suggesting either: different mechanisms of injury occur in differing diseases, the method and timing of lymphocyte depletion may be important or that the genetic background of the mice may alter the method of injury (Puri, Shakaib et al. 2010).

Even in experimental models of hypertension, lymphocytes may be involved in renal injury. In rats with hypertension, lymphocyte proliferation has been demonstrated in response to Hsp70, an antigen whose expression is increased in the damaged kidney (Parra, Quiroz et al. 2008). Furthermore RAG-KO mice have a blunted response to induced hypertension and adoptive transfer of T cells, but not B cells, restores this (Guzik, Hoch et al. 2007). Therefore it has been proposed that in salt sensitive hypertension the intra-renal inflammation which occurs may be responsible for the subsequent renal injury. This in turn exacerbates the hypertension and accelerates the renal injury (Harrison, Vinh et al. 2010). The hypertensive models of renal injury are also ameliorated with MMF by blocking the inflammatory macrophage and lymphocyte infiltrate (Quiroz, Pons et al. 2001; Rodriguez-Iturbe, Pons et al. 2001).

1.7.3.1.4 Lymphocytes, dendritic cells and renal injury

A network of dendritic cells has been identified within the renal interstitium, close to the basolateral surface of the tubular epithelium and peritubular capillaries (Kaissling, Hegyi et al. 1996). The DCs are F4/80+ and CD11c+ and can be identified morphologically as a population distinct from macrophages (Kruger, Benke et al. 2004). Dendritic cells in their immature form are potent phagocytic cells with only weak T cell stimulatory capacity. However, a phenotypic shift can occur during inflammation with DCs maturing to develop potent T cell stimulatory capacity with upregulation of co-stimulatory and MHC class II cell surface proteins (Mellman and Steinman 2001). A

number of groups have shown that DCs are able to present peptide and activate T cells in the context of non-immune mediated renal disease.

DCs are able to sense and respond to substances reabsorbed from the tubular lumen and to changes within the interstitial compartment (Dong, Swaminathan et al. 2005). Inflammation induced by either local injury (IRI) or LPS administration induces DC trafficking to regional lymph nodes, where they have been shown to present filtered dextrans and exogenous proteins. This study also demonstrated the capacity for CD11c+ DC's to transport and present native renal antigens (Tamm Horsfall protein) in draining lymph nodes. Subsequently Edgtton et al demonstrated that injected ovalbumin could be taken up by renal DCs that then migrated to regional lymph nodes inducing activation and proliferation of CD4+ T cells in OTII transgenic mice (Edgtton, Kausman et al. 2008). These observations suggest a possible mechanism for a break in T cell tolerance to self antigen occurring when antigen is presented by DC in an inflammatory environment. This mechanism was confirmed by Macconi et al in 2009 when demonstrating that renal DC's can process the ubiquitous protein albumin in the their proteosome and present antigenic fragments with class I MHC to CD8+ T cells, causing activation and the production of IFN-γ (Macconi, Chiabrando et al. 2009).

DCs not only present antigen but may also provide signals that determine the nature of the T cell response. Using the UUO model Dong at al described the phenotype of lymphocytes that were activated by intra-renal DCs (Dong, Bachman et al. 2008). They demonstrated co-localisation of DCs and CD4+Th17+, CD4+Th1+ and CD8+ lymphocytes up to 72 hours after obstruction. After DC depletion, T cell infiltration remained but the character of this infiltrate differed: there were significantly fewer IL-17+ and IFN-γ+ T cells.

1.7.4 B cells in chronic tubulointerstitial injury

Traditionally the number of B cells within the leukocyte infiltrate in TI disease was believed to be low, accounting for <20% of the infiltrate (Hooke, Gee et al. 1987). This has been demonstrated in human subjects with primary and secondary interstitial pathologies and in diseases which are both immunologically and traditionally non-immunologically mediated for example lupus nephritis (Alexopoulos, Seron et al. 1990), interstitial nephritis (Husby, Tung et al. 1981) and diabetic nephropathy (Hooke, Gee et al. 1987). However, more recently significant populations of CD20+ B cells have been reported in membranous nephropathy (Cohen, Calvaresi et al. 2005) and within

renal allografts (Kerjaschki, Regele et al. 2004), as well as in the setting of primary and secondary (IgA) interstitial disease (Heller, Lindenmeyer et al. 2007). Interestingly these B cell infiltrates are seen in three main patterns of distribution within the TI: diffusely spread throughout the TI, as small cellular aggregates and present within larger follicle-like structures, similar to those seen in secondary lymphoid structures (Drayton, Liao et al. 2006). T cells, macrophages and DCs co-localise in these follicular structures, which may act as a localised environment for antigen presentation and the development of immune responses.

B cells can have a number of functions which include antigen presentation to T cells promoting their activation. Activated T cells can provide membrane bound (e.g. CD40L) and cytokine (e.g. IL-4) stimuli to activate B cells recognising linked peptide. These B cells can then synthesise cytokines, chemokines and antibody which may contribute to chronic interstitial injury. They may also contribute to the formation of neolymphangiogenesis which has been described in chronic TI disease (Kerjaschki, Regele et al. 2004). The presence of B cells in both primary and secondary interstitial renal disease suggests they may participate in the final common pathway which induces renal fibrosis. Little work has been performed in models of renal injury to determine the role of B cells in TI fibrosis however one published study suggested B cells may be protective in IRI (Burne-Taney, Yokota-Ikeda et al. 2005). In models of fibrosis in other tissues, the importance of B cells have been demonstrated e.g. carbon tetrachloride induced liver fibrosis (Novobrantseva, Majeau et al. 2005).

1.7.5 Macrophage function in chronic renal injury

Macrophages are functionally diverse and can synthesise several molecules which can contribute to renal injury. They can promote tissue fibrosis by the release of the fibrogenic growth factor TGF-β and matrix proteins as well as causing direct tissue injury with the release of potent inflammatory mediators for example TNF-α and reactive oxygen species. Once activated macrophages upregulate their expression of class II MHC and co-stimulatory molecules and can mediate injury via their ability to act as an APC. There is increasing evidence from proteinuric and non-proteinuric models of renal disease that macrophages play an important role in chronic renal injury. There is a clear association between the number of infiltrating macrophages in the TI and the severity of injury in both adriamycin nephropathy (Lee, Wang et al. 2006) and UUO (Diamond 1995). Several strategies have been used to confirm a pathogenic role for macrophages including macrophage depletion (Wang, Mahajan et al. 2005; Sung, Jo

et al. 2007), inhibition of chemotaxis (Watson, Zheng et al. 2009) and adoptive transfer of macrophages (Wang, Wang et al. 2008).

However, it has also become clear that there are functionally distinct populations of macrophages which play different roles in inflammation and fibrosis (Mosser and Edwards 2008). In the carbon tetrachloride induced model of hepatic fibrosis macrophage depletion during the early initiation phase causes reduced levels of injury and fibrosis. In contrast later macrophage depletion causes the resolution of fibrosis to be delayed (Duffield, Forbes et al. 2005). The classically activated M1 phenotype, induced by IFN-γ, TNF-α and TLR agonists are highly inflammatory and induce tissue injury via their production of proinflammatory mediators e.g. TNF-α, IL-6, IL-12, IFN-γ and nitric oxide and through activation of Th17 cells. The second population or 'alternatively activated macrophages' (M2) are activated by anti-inflammatory cytokines e.g. IL-4, IL-13, IL-10 and TGF-β and by the phagocytosis of apoptotic bodies (Duffield, Ware et al. 2001). These M2 macrophages promote wound healing and a fibrotic environment with the liberation of TGF-β, along with immunoregulation by stimulating Tregs. Regulatory macrophages have also been described, activated by IL-10.

The importance of macrophage phenotype can be seen in ADN. Transfer of macrophages with an M2 phenotype into SCID mice with ADN (induced by IL-4 and IL-13) reduces renal injury whereas stimulating macrophages with LPS to adopt an M1 phenotype prior to transfer worsens injury (Wang, Wang et al. 2007). This work demonstrates the phenotype of infiltrating macrophages is a critical determinant of outcome and may explain the conflicting results regarding macrophage function in UUO. Macrophage infiltration is a prominent feature of UUO and several reports demonstrate they contribute to injury. However, other reports have failed to confirm this (Nishida and Hamaoka 2008) possibly because different macrophage populations have opposing effects. In addition there may also be a regulatory population of macrophages which influence bystander macrophage function by production of IL-10. This has been demonstrated in obstructive uropathy and glomerulonephritis with genetically modified macrophages which express high levels of IL-10 (Yamagishi, Yokoo et al. 2001).

1.7.6 NKT cells and native renal injury

In the literature there is some work on the role of NKT cells in renal injury. In particular NKT cells are important in the pathogenesis of IRI (Ascon, Lopez-Briones et al. 2006;

Li, Huang et al. 2007). In Rabb's work, after 3 and 24 hours of IRI increased numbers of CD3+NK1.1+ cells were seen in the ischaemic kidney compared to normal controls. The Okusa group were able to demonstrate a significant reduction in IRI when NKT cells were depleted; either their activation was inhibited or NKT deficient mice were used. This was associated with the reduction in IFN-γ producing neutrophils suggesting that NKT cells were involved in the early injury mediated by neutrophils. To date there is no literature on the role of NKT cells in chronic tubulointerstitial injury however, work from other organ systems suggest a profound immunomodulatory role (Wu, Gabriel et al. 2009). NKT cells produce copious amounts of pro and anti-inflammatory cytokines upon activation but overall may favour immune regulation and provide a link between innate and adaptive immunity.

1.7.7 Development of fibrosis

During TI fibrosis there is an increase in the number of activated fibroblasts in the kidney. The hallmarks of fibroblast activation include expression of α-smooth muscle actin, a contractile protein usually found in perivascular smooth muscle cells (myofibroblasts) and the production of excessive ECM components including collagen type I and III and fibronectin. The increase in the activated myofibroblast population within the TI has been shown to be derived from a number of sources. The predominant source may be activated resident renal fibroblasts (Picard, Baum et al. 2008) however, epithelial derived cells (Iwano, Plieth et al. 2002), bone marrow derived CD34+ fibrocytes (Bucala, Spiegel et al. 1994; Wada, Sakai et al. 2007) and pericytes (Lin, Kisseleva et al. 2008) also contribute.

Tubular epithelial cells have been demonstrated to undergo epithelial-to-mesenchymal transition (EMT), driven by the inflammatory environment, resulting in loss of epithelial phenotype, migration through the tubular basement membrane and adoption of a myofibroblast phenotype (Robertson, Ali et al. 2004).

Fibrocytes are circulating BM-derived cells which express markers of both leukocytes and mesenchymal cells (CD45 and CD34). They have been shown to differentiate into myofibroblasts with a high potential for collagen I synthesis and thus contribute to renal fibrosis. Fibrocytes circulate in low numbers in peripheral blood and like other infiltrating cells are directed to the site of tissue injury by chemokine/chemokine receptor interactions (Anders, Vielhauer et al. 2003; Wada, Sakai et al. 2007).

Recently much interest has been shown by Duffield's group in the role of pericytes in TI fibrosis. They have shown by fate mapping that pericytes (and not cells which have undergone EMT) are responsible for the generation of myofibroblasts (Humphreys, Lin et al. 2010). Pericytes are usually adherent to endothelium but when detached after vascular injury they migrate into the interstitial space where they become myofibroblasts. Also, after pericyte detachment the capillaries become unstable causing microvascular damage by a switch in the secretion of VEGF isomers and subsequently renal ischaemia develops (Lin, Chang et al. 2011). This drives the activation of parenchymal cells that in turn recruit inflammatory cells such as macrophages and subsequently product TGF-β.

Koester's group have also lately shown that TGF-β dependent peritubular fibrosis and nephron degeneration may not involve EMT but tubular autophagy (Koesters, Kaissling et al. 2010). This is a novel method of tubular decomposition where the surrounding area becomes a dense fibrotic network derived from myofibroblasts which did not develop by EMT but from local fibroblasts or pericytes.

It is clear that lymphocytes and macrophages can influence fibroblast accumulation and activation. Th2 T cell cytokines promote the differentiation of fibrocytes whereas Th1 cytokines inhibit their differentiation (Shao, Suresh et al. 2008). In the absence of CD4+ T cell derived signals there is a reduction in the number of renal fibrocytes and collagen I deposition after UUO (Niedermeier, Reich et al. 2009). Lymphocyte and macrophage derived TGF-β can also promote EMT (Robertson, Ali et al. 2004). In renal transplantation Robertson et al demonstrated that activated CD8+ T cells were able to induce EMT and promote fibrotic injury. CD8+ T cells were induced to express the β7 integrin by TGF-β, thus enabling these CD8+CD103+ T cells to bind E-cadherin on TECs and present TGF-β to the TEC thus inducing EMT.

1.8 Hypothesis and aims

I hypothesise that T cells are recruited into the injured kidney because they are recognising and responding to autoantigens, representing a break in self tolerance.

The aims of my thesis are two fold:

1. To characterise the mononuclear infiltrate into the renal tubulointerstitium post injury, looking at the phenotype of the infiltrating cells and correlating this with levels of injury.
2. Molecular analysis of the T cell receptor to try to determine whether there is clonal proliferation of T cells in UUO kidney that would suggest antigen dependent T cell activation and loss of immunological tolerance.

Chapter 2. Materials and Methods

2.1 General materials

General chemicals were purchased from Sigma-Aldrich (Poole, UK). Histological stains, microscope slides and consumables were purchased from VWR (Lutterworth, UK), DakoCytomation (Glostrup, Denmark) and Signa-Aldrich (Poole, UK).

RNA extraction from tissue and cells was carried out using the RNAeasy Mini Kit by Quiagen (Crawley, West Sussex, UK) and TRIzol reagent purchased from Invitogen Life technologies (Paisley, Scotland). Reagents for the formation of cDNA and standard PCR were purchased from Invitogen Life technologies (Paisley, Scotland) and Promega (Southampton, UK). The custom made oligonucleotide primers were purchased from Eurofins MWG Operon (Ebersberg, Germany). Consumables, Taq polymerase and the FAM probe for real time PCR were purchased from Applied Biosystems (Warrington, UK). The TOPO TA cloning kit for sequencing used to clone and transform cells was from Invitrogen (Paisley, Scotland).

The collagenase used for kidney tissue digestion was from Sigma-Aldrich (Poole, UK) and DNAse-1 from Roche (Burgess Hill, West Sussex).

2.1.1 Buffers

Phosphate buffered saline	8g of NaCl, 0.2g of KCl, 1.44g of Na_2HPO_4, 0.24g of KH_2PO_4 in 1000ml d-H_2O, pH adjusted to 7.4
0.05% PBS-Tween	PBS containing 0.05% Tween 20
TBE	10.8g Tris base, 5.5g boric acid, 0.93g EDTA in 1000ml d-H_2O

2.2 Antibodies

The primary antibodies used throughout the thesis for immunohistochemistry (Table 2.1), imunofluorescence (Table 2.2) and flow cytometry (Table 2.3) are listed below. Primary antibodies were purchased from BD Pharmingen (Oxford, UK), Millipore (Watford, UK), Novocastra (Newcastle Upon Tyne, UK), Serotec (Oxford, UK) and Sigma-Aldrich (Poole, UK). Secondary antibodies (Table 2.4) were bought from BD Pharmingen and DakoCytomation (Glostrup, Denmark). Isotype control antibodies used in immunofluorescence and flow cytometry (Table 2.5) were purchased from BD Pharmingen.

Table 2.1- Primary antibodies used in immunohistochemistry

Antibody	Clone	Isotype	Manufacturer	Cat no
Anti-mouse CD4	H129.19	Rat IgG2a	BD Pharmingen	550278
Anti-mouse CD8	53-6.7	Rat IgG2a	BD Pharmingen	550281
Anti-mouse F4/80	A3-1	Rat IgG2b	Serotec	MCA497
Anti-mouse α-SMA	1A4	Mouse IgG2a	Sigma-Aldrich	A2547
Anti-mouse collagen I	Polyclonal	Rabbit	Millipore	AB765

Table 2.2- Primary antibodies used in immunofluorescence

Antibody	Conjugation	Clone	Isotype	Manufacturer
Anti-mouse CD4	FITC	H129.19	Rat IgG2a	BD Pharmingen
Anti-mouse CD8a	FITC	53-6.7	Rat IgG2a	BD Pharmingen
Anti-mouse CD69	PE	H1.2F3	Hamster IgG1	BD Pharmingen
Anti-mouse CD44	APC	IM7	Rat IgG2b	BD Pharmingen
Anti-human Ki67		Polyclonal	Rabbit	Novocastra

Table 2.3- Antibodies used in flow cytometry

Antibody	Conjugation	Clone	Isotype	Manufacturer
Anti-mouse CD45	APC-Cy7	30-F11	Rat IgG2b	BD Pharmingen
Anti-mouse CD4	FITC	H129.19	Rat IgG2a	BD Pharmingen
Anti-mouse CD8a	PerCP	53-6.7	Rat IgG2a	BD Pharmingen

Table 2.4- Secondary antibodies used in immunohistochemistry and fluorescence

Antibody	Conjugation	Application	Manufacturer
Goat anti-rat	Biotin	IHC: CD4, CD8 and F4/80	BD Pharminogen
Goat anti-mouse	HRP	IHC: α-SMA	DakoCytomation
Goat anti-rabbit	HRP	IHC: Collagen I	DakoCytomation
Swine anti-rabbit IgG	TRITC	IF: Ki67	DakoCytomation

Table 2.5- Isotype control antibodies used in immunofluorescence and flow cytometry

Isotype	Conjugation	Clone	Manufacturer
Rat IgG2b	APC-Cy7	A95-1	BD Pharmingen
Rat IgG2a	FITC	R35-95	BD Pharmingen
Rat IgG2a	PerCP	R35-95	BD Pharmingen
Hamster IgG1	PE	G235-2356	BD Pharmingen
Rat IgG2b	APC	A95-1	BD Pharmingen

2.3 Animal experiments

C57Bl/6 female mice between 8-10 weeks of age were used for all experiments and purchased from Charles Rivers (Watford, UK). My group had gained experience and successfully used female mice for UUO and therefore I chose this sex of mice to use. They were housed in the comparative biology centre with free access to food and water.

2.4 Animal model of chronic kidney disease

In order to investigate the role of lymphocytes in the development of renal fibrosis, the established animal model unilateral ureteric obstruction was used. Obstruction of the ureter has been shown to result in the development of fibrosis within the kidney. This process is similar the development of chronic renal damage seen in humans. All procedures were carried out according to the home office guidelines under home office licences.

2.4.1 Unilateral Ureteric Obstruction

UUO of the left kidney was performed. Anaesthesia was induced using 5% isoflurane gas in an induction chamber and mice were then given a subcutaneous injection of

500µl of buprenorphine (concentration 3µg/ml) as analgesia. Anaesthesia was then maintained using 2% isoflurane and 2l of oxygen via a mask.

Following midline laparotomy, the bowel was reflected cranially to expose the retroperitoneal area. An operating microscope was used to aid identification of the left ureter which was separated from surrounding adipose tissue. Two 7/0 silk ligatures were placed around the upper third of the ureter approximately 0.5cm apart. The ureter was cut between the ligatures, the bowel reflected back into position and the abdomen closed in 2 layers using 4/0 vicryl sutures. Sham operated controls underwent similar surgical procedures but the left ureter was only manipulated. Animals were placed in a heated chamber during recovery.

2.4.2 Sacrificing and tissue sampling

Groups of four mice were sacrificed by cervical dislocation after 3, 7 and 10 days of obstruction or sham operation when renal tissue was required for histological examination. The group size of four animals was calculated using a power calculation tool. In retrospect this group size should have been larger to increase the possibility of attaining statistically significant results. Cardiac puncture, exsanguination and subsequent perfusion with 60ml of 0.9% saline was used as the preferred method of sacrifice when animals were required for TCR analysis after 7, 14 and 28 days of obstruction or sham operation. These later time points were chosen to assess TCR clonality rather than the earlier 3, 7 and 10 days used in the histological analyses. This was because I believed that a broader range of lengths of ureteric obstruction would allow demonstration of early limited T cell clonality but also the development of a larger number of T cell clones at later time points suggestive of epitope spreading.

Obstructed and contralateral kidneys and the spleen were excised by blunt dissection. When tissue was required for histological examination the kidney was bisected cranio-caudally. One half was embedded in OCT on cork boards and snap frozen in isopentane and then liquid nitrogen and stored at -80ºC. The remaining half was fixed in 4% formalin overnight at room temperature, processed and embedded in wax for histological analysis. When tissue was required for the subsequent extraction of RNA, as described later, the organs were dissected and fragments snap frozen in liquid nitrogen and stored at -80ºC for later use.

2.5 Histology and immunohistochemical assessment

Lymphocyte and macrophage infiltration into the kidneys of UUO and normal mice were quantified and an assessment of renal injury and fibrosis was made. Subsequently, lymphocyte activation and proliferation was examined.

2.5.1 Preparation of sections

Both wax embedded and frozen sections were required for histological assessment.

2.5.1.1 Preparation of wax embedded sections

Formalin-fixed, wax embedded tissue was prepared and 2µm sections were cut using a sledge microtome (Microm HM 330, Heidelberg, Germany). Sections were floated on a 20% ethanol water bath at 42ºC, collected on glass slides and left to dry at room temperature. Slides were then dried at 37ºC overnight or alternatively 65ºC for 1 hour. Sections were de-waxed prior to use by immersion in two changes of xylene and re-hydrated through graded alcohols for approximately 1 minute each (100% and 95%) and then finally water.

2.5.1.2 Preparation of frozen sections

Frozen sections of 5µm were cut using a cryostat microtome (Leica CM1900, Nussloch, Germany), transferred to glass slides and left to air-dry overnight before staining. Alternatively these slides were stored in air-tight containers at -80ºC to use at a later date. When the stored sections were required, they were warmed to room temperature for 30 minutes prior to use.

2.5.2 Assessment of renal injury after UUO using Periodic acid Schiff (PAS) staining on wax-embedded sections

PAS staining was used to delineate tubular and glomerular basement membranes. PAS has specificity for carbohydrate residues and therefore stains the proteoglycans of these membranes. The de-waxed and re-hydrated tissue sections were incubated in 1% periodic acid for 6 minutes and then washed in distilled water. The slides were incubated with Schiff's reagent for 10 minutes, washed in running tap water for 10 minutes and counterstained with Mayer's haematoxylin for 1 minute. Finally the sections were washed in running tap water for 5 minutes before they were dehydrated through graded alcohols (70% to 100%) to xylene and mounted with DPX. Histology was examined using a Leica DMR light microscope (Leica Lasertechnik GmbH, Heidelberg, Germany).

2.5.2.1 Analysis of PAS stained sections

The volume of the interstitium in the renal cortex was used as an assessment of cortical interstitial expansion. Sections of 2 μm were cut and PAS stained. A 10 x 10 grid was superimposed on sections at x250 magnification, with 81 positive cross sections. Only the renal cortex was considered. The interstitium was defined as the area between cortical tubules and glomeruli excluding blood vessels. The number of cross sections which fell in the interstitium was expressed as a percentage of the total number of cross sections which fell within the renal cortex. This was termed the percentage interstitial expansion (% IE) and used to estimate the interstitial volume and therefore degree of renal injury. These assessments were carried out in a blinded manner on renal tissue at three time points: 3, 7 and 10 days post obstruction. Five high power fields (HPF) per animal were analysed. The mean percentage of interstitial expansion was calculated for each animal and then for the group of four animals as a whole at each time point.

2.5.3 Immunohistochemistry

2.5.3.1 CD4, CD8 and F4/80 staining of frozen sections

Frozen sections were warmed to room temperature before being fixed in ice cold acetone at -20ºC for 5 minutes and left to air dry before being washed in 1x PBS. Sections were then incubated with 0.3% hydrogen peroxide (H_2O_2) in PBS for 10 minutes to block endogenous peroxidase activity and again washed in PBS. Sections were incubated in streptavidin blocking agent for 15 minutes and then biotin blocking agent for 15 minutes (Vector Laboratories Ltd, California, USA) to block endogenous biotin, biotin receptors and streptavidin binding sites in the tissue. The slides were washed before incubation in anti-CD4 or anti-CD8 rat anti-mouse monoclonal antibodies in PBS at 1 in 20 dilution or anti-F4/80 rat anti-mouse monoclonal antibody in PBS at 1 in 50 dilution for 60 minutes. After washing, the sections were incubated with the biotinylated secondary antibody goat anti-rat polyclonal antibody in PBS at 1 in 100 dilution for 30 minutes and then washed. The sections were incubated in Streptavidin-conjugated Horseradish peroxidase (Strep-HRP) for 30 minutes. After washing, the staining was visualised with diaminobenzidine (DAB) for 5 minutes or until the desired colour intensity was reached. After DAB detection they were washed in d-H_2O for 5 minutes before counterstaining for 5 minutes in haematoxylin and ‘blued’ under running tap water for 5 minutes. The DAB waste was collected in a hazardous materials container for later appropriate disposal. Finally the slides were dehydrated

through graded alcohols (70% to 100%) to xylene and mounted with DPX before examination. Histology was then examined using a Leica DMR light microscope.

2.5.3.1.1 Analysis of CD4, CD8 and F4/80 immunohistochemical staining

The number of infiltrating cells into UUO and contralateral kidneys was quantified for four animals at 3, 7 and 10 days after ureteric obstruction. Five random non-overlapping HPFs in the renal cortex at x250 magnification were analysed for each kidney in a blinded manner. The total number of positively stained infiltrating cells was counted for each HPF and the mean number of cells per HPF calculated for each animal. Then the mean number of infiltrating cells per HPF was calculated for the group of four mice at each time point. Quantification was carried out twice and the mean score recorded.

2.5.3.2 Alpha-SMA staining of wax embedded sections

De-waxed and re-hydrated tissue sections were incubated in 0.3% H_2O_2 in PBS for 15 minutes to block endogenous peroxidise activity, after which they were washed in 0.05% PBS-Tween (PBST). Slides were then incubated with the primary antibody, monoclonal mouse anti α-SMA at 1 in 10,000 dilution in 1x PBS for 1 hour at room temperature, then washed in 0.05% PBST. Following this the Envision kit (DakoCytomation, Glostrup, Denmark) was used and the slides were incubated with a goat anti-mouse polymer conjugated with HRP for 30 minutes at room temperature, then washed in PBST. Slides were covered with DAB solution, made according to Envision kit instructions and placed in the dark for 5 to 10 minutes until a brown colouring has developed. After DAB detection they were washed in d-H_2O for 5 minutes before counterstaining for 5 minutes in haematoxylin and 'blued' under running tap water for 5 minutes. Finally the slides were dehydrated through graded alcohols (70% to 100%) to xylene and mounted with DPX before examination. Histology was examined using a Leica DMR light microscope.

2.5.3.2.1 Analysis of α-SMA stained sections

The degree of tubulointerstitial fibrosis, as determined by staining activated myofibroblasts with α-SMA was analysed using a point counting method, similar to that used to assess percentage interstitial expansion on PAS stained sections. A 10 x 10 grid was superimposed on sections at x250 magnification. The number of cross sections which fell on α-SMA stained tissue was expressed as a percentage of the total number of cross sections. These assessments were carried out on renal tissue from three time points: 3, 7 and 10 days post obstruction and five HPFs per animal were analysed in a

blinded manner. The mean percentage of α-SMA was calculated for each animal and then for the group of four animals as a whole at each time point.

2.5.3.3 Collagen I staining of frozen sections

Frozen sections were warmed to room temperature before being fixed in ice cold acetone at -20ºC for 5 minutes and then left to air dry before being washed in 1x PBS. Sections were then incubated with 0.3% H_2O_2 in PBS for 10 minutes to block endogenous peroxidase activity and again washed in 0.05% PBST. Sections were incubated in 20% goat serum for 1 hour at room temperature. Slides were then incubated with the primary antibody polyclonal rabbit anti-mouse collagen I at 1 in 200 dilution in 20% goat serum for 1 hour at room temperature, then washed in PBST. Following this, slides were incubated with a polyclonal goat anti-rabbit HRP conjugated secondary antibody at 1 in 200 dilution for 1 hour at room temperature, then washed in PBST. Staining was visualised using DAB, incubated for 5 minutes in the dark or until the desired colour intensity was reached. After DAB detection they were washed in d-H_2O for 5 minutes before counterstaining for 5 minutes in haematoxylin and 'blued' under running tap water for 5 minutes. Finally the slides were dehydrated through graded alcohols (70% to 100%) to xylene and mounted with DPX before examination. Histology was examined using a Leica DMR light microscope.

2.5.3.3.1 Analysis of collagen I stained sections

In order to analyse the area of collagen I staining per section, Q-Win software was used to capture, process and analyse the sections using the pixel intensity grading function. The mean percentage area of collagen I staining in ten non-overlapping HPFs at x250 magnification was calculated for each group of four animals at each of the three time points post obstruction in a blinded manner.

2.5.4 Immunofluorescence

UUO experiments were carried out on groups of four animals for 3, 7 and 10 days after which the animals were sacrificed and the organs harvested. Immunofluorescent staining of T lymphocytes was performed along with staining either for CD69 (a cell surface marker present on recently activated T cells), CD44 (a cell surface marker found on memory T cells) or Ki67 (the nuclear proliferation marker). Sections were assessed using a confocal laser scanning microscope and processed using Leica TCS-NT software. The numbers of single and dual positively stained cells were calculated using Photoshop software. Since the immunohistochemistry work demonstrated very little or

no cellular infiltration of lymphocytes into sham operated kidneys, the contralateral kidney of a UUO animal and normal kidneys, these tissues were not assessed by immunofluorescence.

2.5.4.1 Dual staining of CD4+ or CD8+ cells with CD69 or CD44

Frozen sections were warmed to room temperature before being fixed in ice cold acetone at -20ºC for 5 minutes and then left to air dry before being washed in 1x PBS. Slides were then incubated in 1% BSA in PBS for 1 hour at room temperature to block non-specific binding of the antibody. 200µl of diluted antibody in 1% BSA was applied to the sections in a humidified chamber for 1 hour at room temperature in the dark. All antibodies were applied individually and in appropriate combinations. The rat anti-mouse CD4 and CD8 FITC linked monoclonal antibodies were used at 1 in 20 dilution. The hamster anti-mouse CD69 PE linked monoclonal antibody was diluted 1 in 10 and the rat anti-mouse CD44 APC linked monoclonal antibody was diluted to 1 in 20. After incubation they were washed in PBS. When DAPI was used to aid cell localisation, it was used at 1 in 3000 dilution in d-H_2O applied to the sections for 5 minutes. Washed slides were mounted with a fluorescent mounting medium (DakoCryomation, Glostrup, Denmark) and placed in the dark at 4ºC.

2.5.4.2 Dual staining of CD4 or CD8 cells with Ki67

Sections were prepared as in 2.5.4.1. and incubated with 200µl of the diluted antibody in 1% BSA in PBS in a humidified chamber for 1 hour at room temperature. The rat anti-mouse CD4 and CD8 monoclonal antibodies were used at 1 in 20 dilution and primarily conjugated to the fluorochrome FITC. The rabbit anti-human polyclonal Ki67 primary antibody was used at 1 in 1000 dilution. After washing in PBS, the sections were then incubated with the secondary antibody, a TRITC linked swine anti-rabbit polyclonal antibody diluted 1 in 20 in 1% BSA and further rat anti-mouse CD4 or CD8 monoclonal antibodies were added at 1 in 20 dilution and incubated for 1 hour at room temperature in the dark. The sections were washed on PBS and if DAPI was used, incubated in a 1 in 3000 dilution solution in d-H_2O for 5 minutes in the dark. The washed slides were then mounted with fluorescent mounting medium (DakoCryomation, Glostrup, Denmark) and placed in the dark at 4ºC.

2.5.5 Confocal microscopy

All slides were assessed using the Leica TCS-SP2UV confocal laser scanning microscope (Leica Lasertechnik GmbH, Heidelberg, Germany) running under Leica

TCS-NT software (version 2.0). Images were acquired through a x63 oil immersion objective lens with a numerical aperture of 1.2. An excitation beam laser from an argon ion laser of wavelength 480nm was used for the FITC and PE fluorochromes, a wavelength of 630nm for APC, 560nm for TRITC and 360nm for DAPI. Any light emitted was collected via a pinhole aperture in front of a photomultiplier tube as a photodetection device. Light was collected from one plane of focus only and any out of focus signal was excluded. The images were collected sequentially, frame by frame, and combined to produce the final image. In order to demonstrate co-localisation of stains on the same cell, the confocal software also assembled selected images in X-Z stacks and plotted pixel colour on cytofluorograms.

2.5.5.1 Analysis of stained sections by immunofluorescence

The number of single positive FITC stained CD4+ or CD8+ cells were quantified by examining between five and ten random non-overlapping HPFs at x63 magnification for each UUO kidney using Photoshop software in a blinded manner. Subsequently the number of dual positive cells stained with CD4 or CD8 and then either CD69 or Ki67 were also counted on the above sections. The percentage of dual positive cells was calculated for each HPF and the mean percentage per HPF calculated for each animal. Then the mean percentage per HPF was calculated for each group of four mice.

2.6 RNA and DNA methodology

DNA is transcribed into single stranded RNA in the nucleus under physiological conditions using RNA polymerase. RNA can take a number of forms, which are either protein-coding such as messanger RNA (mRNA) or are non-coding like ribosomal (rRNA) and transfer RNA (tRNA). The coding sequence of the mRNA determines the amino acid sequence of the protein which is produced in the ribosome with the help of tRNA and is generated after the non-coding intron sequences are spliced out. However, mRNA is unstable and easily degraded by ubiquotous RNAses. In order to measure the amount of mRNA or examine the mRNA sequences it can be amplified by PCR but in order to do this it must be extracted and reverse transcribed to DNA.

2.6.1 Extraction of RNA and assessment of purity

RNA was extracted from the whole tissue of UUO kidney and spleen, as well as from the sorted lymphocyte populations extracted from kidney tissue. Once RNA was extracted spectrophotometry and the separation of RNA fragments using agarose gel electrophoresis were used to determine the quality of this process.

2.6.1.1 Extraction of RNA from tissue

Kidney and spleen were harvested for the sacrificed animals at 7, 14 and 28 days post UUO and snap frozen in liquid nitrogen. Samples were then stored at -80˚C until required. Whole RNA was extracted using the RNeasy Mini Kit (Quiagen, West Sussex, UK) according to the manufacturer's instructions. The kit used a selective silica-gel based membrane to bind RNA, followed by removal of contaminants with a series of buffers and centrifugation.

Initially the frozen fragments of tissue were placed in 800µl of TRIzol reagent, containing guanidinium isothiocyanate and phenol, in a 1.5ml RNAse free tube without defrosting, to lyse the cells, denature the protein but maintain RNA integrity. The tissue was then homogenised using an RNAse free pestle to fragment the genomic DNA and the suspension centrifuged at 10,000 rpm for 10 minutes at 4ºC. The supernatant was then transferred to a phase lock gel separation tube and 160µl of chloroform was added and the solution mixed with vigorous shaking. The sample was left for 2-3 minutes before centrifuging at 10,000 rpm for 15 minutes at 4ºC. This allowed separation of the upper, water soluble RNA layer from the lower, organic lipid layer containing DNA and protein fragments in chloroform and phenol. This upper aqueous layer was transferred into another RNAse free tube with an equal volume of 70% ethanol, in DEPC water.

The resulting mix was applied to the RNeasy spin column and centrifuged for 15 seconds at 10,000 rpm. The flow through was then discarded. The contaminants were then removed by using a series of different wash buffers and centrifugation. RNA was then eluted from the wash column by the addition of 30µl of RNAse free water and centrifugation. The RNA samples were stored at -20ºC until they were processed into cDNA by reverse transcription.

2.6.1.2 Extraction of RNA from cells

Lymphocytes sorted by flow cytometry were collected into Quiagen lysis buffer containing β-mercaptoethanol (β-ME), as per the Quiagen RNeasy Mini Kit instructions, in order to irreversibly denature RNases. Within this lysis buffer were approximately 5x 10^5 mouse proximal tubular epithelial cells, which acted as a carrier to prevent the sorted cells adhering to the surface of the tube. The lysate was then passed five times though a blunt 20-gauge needle fitted to an RNAse-free syringe. One volume of 70% ethanol was added and mixed by pipetting. The resulting mix was applied to the RNeasy spin column and centrifuged for 15 seconds at 10,000 rpm. The flow through was then discarded. The contaminants were then removed by using a series of different wash buffers and centrifugation. RNA was eluted from the wash column by the addition of 30µl of RNAse free water and centrifugation. The RNA samples were stored at -20ºC until they were processed into cDNA by reverse transcription.

2.6.1.3 Purity and quantification of extracted RNA

The purity and quantity of RNA was estimated by spectrophotometry. UV light of different wavelengths was shone onto the RNA specimen and the amount of UV light absorbed at the different wavelengths was calculated. The purity of the RNA was calculated by measuring the ratio of UV light absorbance at 260 and 280nm. The estimated quantity of RNA was calculated by measuring the absorbance of RNA at 260nm (one OD per cm path length being equivalent to approximately 40µg/ml of RNA).

Nucleic acids, both RNA and DNA, have a maximum UV absorbance at a wavelength of 260nm however, proteins have little absorbance at this wavelength. The minimum absorbance for nucleic acids is at the lower wavelength of 215-230nm, where buffers such as Tris and proteins can absorb the UV light. At 270nm phenol absorbs UV strongly which may contaminate nucleic acid preparations and at 280nm aromatic amino acids absorb the UV light. At the higher wavelength of 320nm neither proteins

nor nucleic acids absorb. Therefore to estimate the purity of the nucleic acid the ratio of the absorbance at 260nm and 280nm was calculated:

- A_{260}/A_{280} ratio of 2.0 is characteristic of pure RNA
- A_{260}/A_{280} ratio of 1.8 is characteristic of pure DNA
- A_{260}/A_{280} ratio of 0.6 is characteristic of pure protein

The RNA was also assessed for quality by separation into the various sized fragments by agarose gel electrophoresis. Gels were prepared with 1.2% agarose in 1x TBE. Ethidium bromide (0.5µg/ml of TBE) was added to the solution before pouring into a gel cast. Once the gel had set, 1x TBE running buffer was poured over the gel in the gel tank and the RNA samples prepared for loading into the wells. A mixture of 5µl of loading buffer and 3µl of RNAse free water was added to 2µl of RNA which was heated to 65ºC for 5 minutes to separate the strands of RNA and subsequently allowed to cool for 1 minute on ice prior to loading into the gel. The RNA ladder was prepared as above, substituting the RNA specimen for the ladder. Once the wells were loaded the gel was run at 90V for 40 minutes. The rRNA fragments of 4.8kb and 1.8kb, corresponding to ribosomal 28S and 18S RNA, should then be visualised, if RNA was intact, by fluorescence of the incorporated ethidium bromide using the alpha transilluminating system from AlphaInnotech (Sussex, UK) with the AlphaEase PC software.

2.6.2 Reverse transcription

cDNA synthesis was carried out from RNA using oligo (dt)15 primers, dNTPs and reverse transcriptase according to the method by Sambrook et al (1989). RNA has a poly-A tail sequence and so a complementary dT oligonucleotide was used as a primer for the reverse transcription. RNA samples were denatured by heating to 90ºC for 5 minutes to favour the annealing of oligo dT primers to the poly-A tails of the mRNAs, and then transferred to ice to maintain the oligo dT primers in position. A 20µl reaction mixture was prepared by adding the following reagents, in order, to an RNAse free tube on ice:

Reverse transcriptase buffer (5x)	4µl
DTT (100mM)	2µl
RNasin (40U/µl)	0.75µl
dNTP mixture (5mM)	2µl

Oligo (dt)15 (0.5µg/µl)	0.32µl
Total RNA (max 1µg/µl)	5µl
RNAse free water (DEPC)	3.93µl
M-MLV reverse transcriptase (200U/µl)	1µl

The mixture was incubated at 37ºC for 40 minutes and then a further 1µl of Moloney-murine leukaemic virus (M-MLV) reverse transcriptase was added and the mixture incubated for a further 40 minutes. The cDNA product was stored at -20ºC until it was required for PCR.

2.6.3 Standard polymerase chain reaction

In order to detect the presence of genetic message for TRVβ gene segments, standard PCR was carried out using primer sequences (Hu, Watson et al. 2008). Twenty two different TRVβ primers were designed to anneal to each of the twenty two individual TRVβ gene segments as the forward primer (Table 2.6). In contrast, the reverse primer used for all the PCR reactions investigating TRVβ gene segment expression was the same throughout and was designed to anneal to the TRC region of the β-chain (Table 2.7). Primer sequences were verified using the international ImMunoGeneTics database (IMGT) and were all found to be within exons of the genomic sequence of the respective TRVβ and TRCβ gene segments. The theoretical PCR product length, in base pairs, was calculated for each set of the twenty two primer pairs assuming each TRVβ gene segment was joined to the TRDβ1 and TRJβ1 gene segments and there was no deletion of base pairs at the junctions between these segments.

Table 2.6- Twenty two TRVβ forward primer sequences and their characteristics

Each primer sequence was designed to anneal to a specific TRVβ gene segment as listed below. The manufacturer's melting temperature (Tm) is documented along with the optimum annealing temperature for the primer pair calculated using the Tm of the forward and reverse primers. The theoretical PCR product length was determined assuming that each TRVβ gene segment was joined to the TRDβ1 and TRJβ1 gene segments and that there was no deletion of base pairs at the junctions.

TRVβ	Primer sequence	Tm (°C)	Anneal temp (°C)	PCR product (bp)
1	5'- CAACATGAGCCAAGGCAGAAC -3'	59.8	55.45	186
2	5'- TCACAGCTCTAAAGCCTGATGACT -3'	61.0	56.00	198
3	5'- CACTGGAGGACTCAGCTGTGTACT -3'	64.4	58.00	186
4	5'- CAAGTCTGTAGAGCTGGAGGACTCT -3'	64.6	58.00	192
5	5'- ATATATCTGCCGTGGATCCAGAA -3'	58.9	55.00	201
12-1	5'- TGGAACTGGAGGACTCTGCTATGTA -3'	63.0	57.05	187
12-2	5'- GAGCTAGAGGACTCTGCCGTGTA -3'	64.2	57.65	185
13-1	5'- CTCCTGCTGGAATTGGCTTCT -3'	59.8	55.45	204
13-2	5'- GCTACCCCCTCTCAGACATCA -3'	61.8	56.45	189
13-3	5'- ATTCTGGAGTTGGCTTCCCTTT -3'	58.4	54.75	201
14	5'- GCAAAGCAGGGCGACACA -3'	58.2	54.65	189
15	5'- CCACTCTGAAGATTCAACCTACAGAA -3'	61.6	56.35	210
16	5'- ACGCAACCCCAGGACTCA -3'	58.2	54.65	190
17	5'- GGCTCTGCAGGCCTAGAGTATTCT -3'	64.4	57.75	196
19	5'- CATCTGCCCAGAAGAACGAGAT -3'	60.3	55.70	194
20	5'- TGACAGTTTTAAATGCATATCTTGAAGAC-3'	59.6	55.35	201
23	5'- CAGAACGTGCGAAGCAGAAGA -3'	59.8	55.45	197
24	5'- GCTGCATCCTGGAAATCCTATC -3'	60.3	55.70	213
26	5'- CAGTCCTCTGAGGCAGGAGACT -3'	64.0	57.55	196
29	5'- AGCATTTCTCCCTGATTCTGGATT -3'	59.3	55.20	216
30	5'- CAAGGCCTGGAGACAGCAGTAT -3'	62.1	56.60	186
31	5'- CTAAGCACGGAGAAGCTGCTT -3'	59.8	55.45	202

Table 2.7- Universal reverse primer TRCβ

The universal reverse primer annealed to the constant gene segment on the β-chain and its sequence is listed below along with manufacturer's documented melting temperature (Tm).

TRCβ	Primer sequence	Tm (°C)
	5'- GGTAGCCTTTTGTTTGTTTGCAA -3'	57.1

2.6.3.1 DNA amplification by standard PCR of reverse transcribed RNA from whole kidney or spleen

The following 25µl PCR mix was used for each PCR reaction during the set-up of the experiments to ensure all 22 primer pairs annealed and allowed amplification of DNA:

GoTaq Promega Taq MM x2 (PCR buffer, $MgCl_2$ and dNTPs)	12.5µl
Forward primer, TRVβx (25µM, final concentration 500nM)	0.25µl
Reverse primer, TRCβ (25µM, final concentration 500nM)	0.25µl
RNAse free water	11µl
cDNA	1µl

The cycling conditions for the PCR thermal cycler (GStorm, Gene Technologies, Braintree, UK) for each set of primer pairs were as follows:

Stage 1: 94ºC for 5 minutes for 1 cycle
Stage 2: 94ºC for 60s denaturation, 56ºC for 60s annealing and 72ºC for 60s extending for 35 cycles
Stage 3: 72ºC for 5 mins for 1 cycle
Stage 4: Cool to 4ºC

2.6.3.2 DNA amplification by standard PCR for the cloning reactions

In order to generate DNA for the cloning reactions, the following 50µl PCR mix was used for each reaction, using a high fidelity Taq master mix from Invitrogen:

Invitrogen High Fidelity Taq MM (PCR buffer, $MgCl_2$ and dNTPs)	45µl
Forward primer, TRVβ3 (12.5µM, final concentration 250nM)	1µl
Reverse primer, TRCβ (12.5µM, final concentration 250nM)	1µl
cDNA (from the stock which was diluted 1:4)	3µl

The cycling conditions were as follows:

Stage 1: 94ºC for 5 mins for 1 cycle
Stage 2: 94ºC for 60s, 56ºC for 60s, 72ºC for 60s for 30 cycles

Stage 3: 72ºC for 7 minutes final extension step for 1 cycle. This ensured DNA was fully extended and there was an A tail at the 3' end of the PCR product to allow cloning.

Stage 4: Cool to 4ºC

When using cDNA which had been generated from sorted lymphocyte populations, stage 2 was performed for either 35 or 55 cycles.

2.6.3.3 DNA amplification by standard PCR to ensure the appropriate sized plasmid insert was generated

The following 25µl PCR mix was used for each PCR reaction using plasmid vector DNA extracted from bacteria, to ensure that an appropriate sized insert had been generated:

GoTaq Promega Taq MM x2 (PCR buffer, $MgCl_2$ and dNTPs)	12.5µl
Forward primer, TRVβ3 (12.5µM, final concentration 500nM)	1µl
Reverse primer, TRCβ (12.5µM, final concentration 500nM)	1µl
cDNA (1:100 dilution of plasmid DNA)	0.5µl
RNAse free water	10µl

The cycling conditions were as follows:

Stage 1: 94ºC for 5 mins for 1 cycle

Stage 2: 94ºC for 60s, 56ºC for 60s, 72ºC for 60s for 25 cycles

Stage 3: 72ºC for 7 mins for 1 cycle

Stage 4: Cool to 4ºC

2.6.3.4 Resolving the PCR products by agarose gel electrophoresis

The products arising from PCR amplification were resolved by electrophoresis in 2% agarose to verify that an appropriate sized product had been generated, using a similar method to that described in section 2.6.1.3.

2.6.4 Real time polymerase chain reaction

Quantitative or real time PCR can be used to quantify in relative or absolute terms the starting amount of product. Real time PCR measures fluorescent molecules which are generated with successive rounds of PCR. This technique was used to assess the relative use of the TCVβ gene segments in kidney and spleen.

Alexander's group compared the two principal techniques for real time PCR when measuring TRVβ repertoires: SYBR Green and fluorescent probes (Walters and Alexander 2004). SYBR Green is a fluorescent dye which binds to all dsDNA in a PCR reaction. Alternatively fluorescent probes can be used where fluorescently labelled specific oligonucleotides are added to the PCR reaction. These can either fluoresce upon binding the target (single labelled probe) or when degraded by Taq Polymerase on amplification of the target (dual labelled probe). Alexander found that the fluorescent probe technique was more consistent across the range of TCR signal levels and more robust in the presence of contaminating non-TCR cDNA. Therefore we used the fluorescent probe Taqman technique to detect amplification of cDNA. The 6FAM (6-carboxyfluorescein) reporter dye and minor grove binding protein non-fluorescent quencher (MGB NFQ) labelled probe annealed to the constant gene segment on the β chain (Applied Biosystems, Warrington, UK) (Table 2.8).

FAM, a fluorescent reporter dye, was at the 5' end of the Taqman probe and the quencher MGB at the 3' end. When the reporter dye and quencher were in close proximity and the probe intact, no fluorescent signal was emitted as it was absorbed by the quencher. However, as the Taq Polymerase extended the probe was cleaved from the DNA strand so the reporter and quencher were separated (Figure 2.1). Therefore the dye fluoresced and was detected by the PCR machine (Applied Biosystems ABI Prism 7000 Sequence Detection System, Warrington, UK) and the signal subsequently analysed using the ABI Prism 7000 SDS software.

Table 2.8- Nucleotide sequence of the fluorescent probe used in real time PCR

The sequence of the universal fluorescent probe which annealed to the constant gene segment on the β-chain of the TCR in all the real time PCR reactions is listed below.

TRCβ Probe	Probe sequence
	5'- 6FAM CTCCACCCAAGGTC MGB NFQ -3'

Figure 2.1- Summary of the mechanism of real time PCR using fluorescent probes

The complementary probe annealed to single stranded DNA with the reporter and quencher in close proximity. When Taq Polymerase cleaved the probe the reported dye was released and detected by the PCR machine. Successive rounds of PCR generated proportionately higher levels of fluorescence.

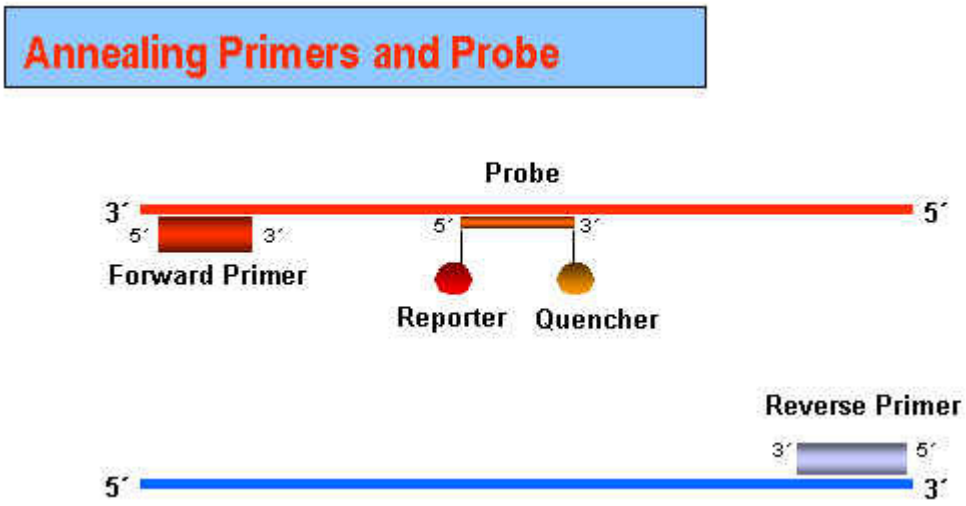

Probe: Reporter dye = FAM and Quencher = MBG

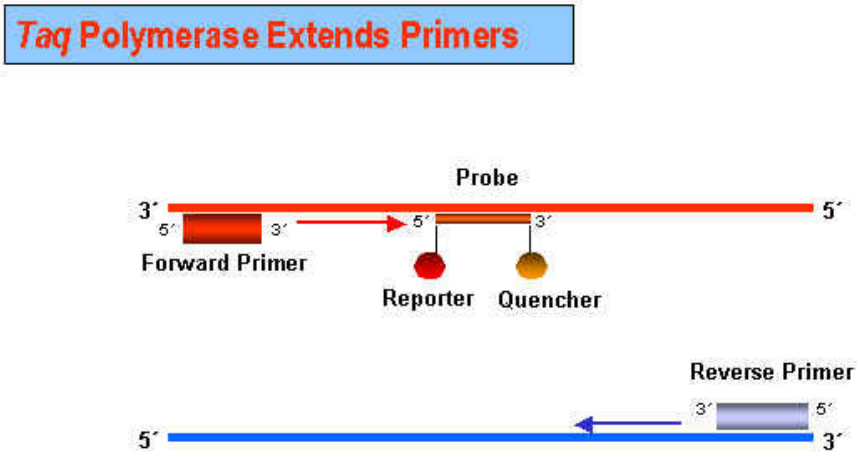

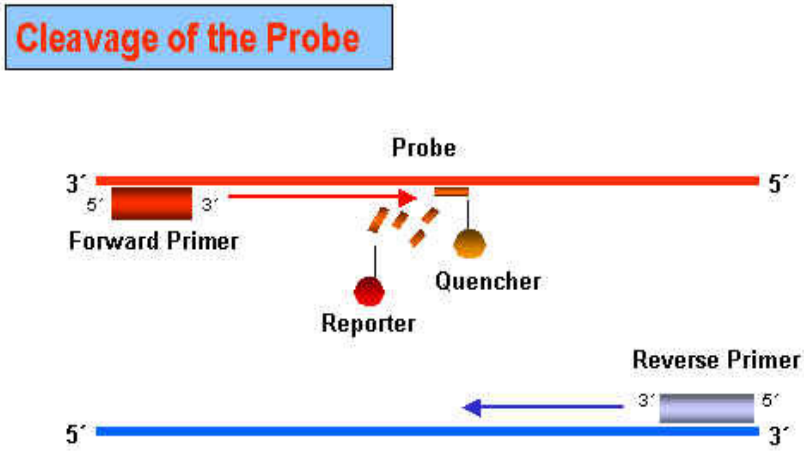

2.6.4.1 Optimising real time PCR reaction annealing temperature and primer and probe concentrations

It was clear from standard PCR reactions that the primer pairs were able to replicate the template DNA but a fluorescent probe was required to quantify the relative expression of TRVβ gene segments by T lymphocytes in UUO kidney and spleen using real time PCR. The primer and probe concentrations along with their annealing temperature had to be optimised in order to generate fluorescently labelled PCR product that could be detected by real time PCR.

Optimizing the annealing temperature of the real time PCR assay was important, as setting the annealing temperature too low may have lead to amplification of non-specific PCR products. On the other hand, setting the annealing temperature too high would reduce the yield of a desired PCR product. The optimal annealing temperature for the assays was determined using the thermal gradient feature on the real time PCR machine, setting the temperature above and below the Tm of the primers. The allowed testing of a range of temperatures simultaneously, so the annealing temperature could be optimized in a single experiment. The optimal annealing temperature was found to be 56.5ºC, at which there was the lowest Ct with no non-specific amplification.

For varying primer and probe concentrations the reactions were run in triplicate and the Ct value for each reaction documented (Table 2.9). This optimisation was performed using the primer pair annealing to TRVβ1 and TRCβ.

For a given amount of starting cDNA with the annealing temperature set at 56.5 ºC, detectable Ct values were found to be less than 40 cycles only when the probe concentration was set to greater than 300nM. Increasing concentrations of the probe made little change to the Ct value. Using a probe concentration of 300nM, increasing concentrations of the primer pair were used for a given amount of starting DNA, using an annealing temperature of 56.5ºC. There was no reduction in the Ct value when the final concentrations of the primers were increased beyond 600nM.

Using the results of these optimisation experiments, the final concentration of probe used in the PCR reaction mixture was 300nM whilst the primers were used at 600nM, with an annealing temperature of 56.5 ºC.

Table 2.9- Optimising (a) probe and (b) primer concentration for real time PCR reactions using the TRVβ1 and TRCβ primer pair

Using constant amounts of starting DNA and by setting the PCR reaction annealing temperature to 56.5 ºC, PCR product was not consistently detected below 40 cycles of PCR with probe concentrations <300nM. When the probe was used at 300nM, no reduction in Ct value was demonstrated by increasing the primer concentrations above 600nM.

(a) Probe optimisation

Probe concentration (nM)	Ct v1	Ct v2	Ct v3	Mean Ct	Primer concentration (nM)	cDNA (ng)	Annealing temp (ºC)
50	Undet	Undet	Undet		200/200	50	56.5
100	39.57	Undet	36.82		200/200	50	56.5
200	Undet	Undet	36.89		200/200	50	56.5
250	Undet	38.86	35.75		200/200	50	56.5
300	35.88	38.56	38.73	37.72	200/200	50	56.5
300	31.14	31.04	31.23	31.14	600/600	50	56.5
400	32.26	32.84	32.41	32.50	600/600	50	56.5
500	30.64	32.64	32.29	31.86	600/600	50	56.5

(b) Primer optimisation

Primer concentration (nM)	Ct v1	Ct v2	Ct v3	Mean Ct	Probe concentration (nM)	cDNA (ng)	Annealing temp (ºC)
50/50	36.13	34.96	37.52	36.20	300	50	56.5
100/100	34.57	33.36	33.30	33.74	300	50	56.5
200/200	34.04	33.20	34.20	33.81	300	50	56.5
300/300	32.60	32.68	32.69	32.66	300	50	56.5
600/600	32.71	33.00	32.46	32.72	300	50	56.5
900/900	32.38	32.19	32.74	32.44	300	50	56.5

2.6.4.2 DNA amplification by real time PCR of reverse transcribed RNA from whole kidney or spleen

To compare the relative expression of each TRVβ gene segment all twenty two different PCR reactions were run in triplicate simultaneously. The following 20µl PCR mix was used for each PCR reaction using the Applied Biosystems master mix which contained ROX as the reference dye:

Applied Biosystems master mix	10µl
Forward primer, TRVβx (5µM)	2.4µl
Reverse primer, TRCβ (5µM)	2.4µl
Taqman custom probe (5µM)	1.2µl
cDNA	4µl

The cycling conditions for the PCR thermal cycler (Applied Biosystems ABI Prism 7000 Sequence Detection System, Warrington, UK) for each set of primer pairs were as follows:

Stage 1: 50ºC for 2 mins for 1 cycle to reduce non-specific amplification
Stage 2: 95ºC for 10 mins for 1 cycle
Stage 3: 95ºC for 15s to denature and 56.5ºC for 60s to extend and anneal for 40 cycles

ABI Prism 7000 SDS software was used to generate the amplification plots and Ct values.

2.6.4.3 Calculating the Ct value of the PCR reaction

The number of PCR cycles taken to generate a threshold fluorescent intensity is termed the Ct value. This threshold fluorescent intensity is set at the start of the linear portion of the 'Log Δfluorescence (Log ΔRn) v cycle number' amplification curve during the exponential phase of the PCR reaction (Figure 2.2).

Figure 2.2- Amplification plot of Log Δfluorescence v cycle number

The number of PCR cycles required to generate a threshold fluorescent intensity is the Ct value for the PCR reaction. The change in fluorescence is determined by the PCR cycler as the ratio of the fluorescence from the reporter Taqman probe to the fluorescence from the passive reference dye ROX present in the master mix.

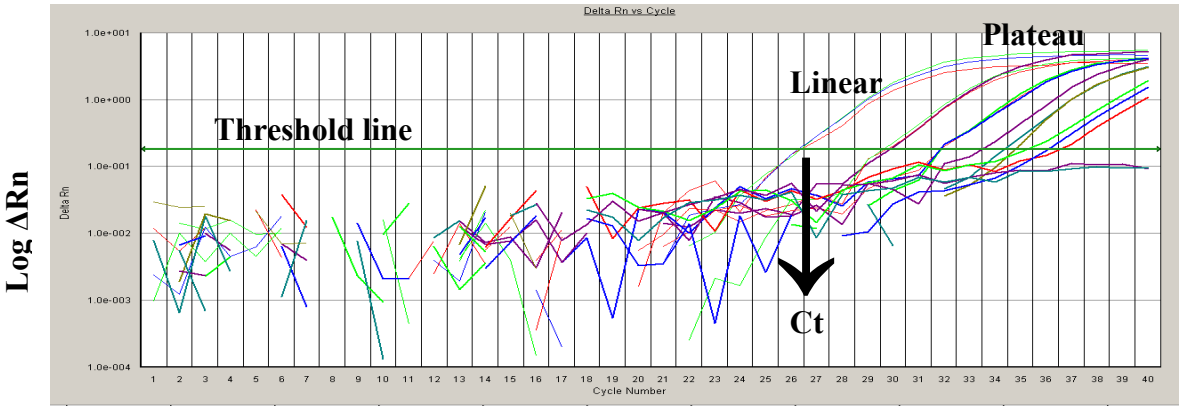

2.6.4.4 Primer efficiencies

If the amplification of product in a PCR reaction was 100% efficient then the amount of Taqman probe detected when the probe and quencher were cleaved by Taq Polymerase would double with each cycle of PCR. This would result in a linear relationship between the Ct value and log cDNA concentration for a given PCR reaction and the efficiency of that reaction would be 2. Amplification is not always this efficient. However, if the relative expressions of the twenty two TRVβ gene segments were to be compared then the individual PCR reactions needed to occur with comparable efficiency. This would then infer that any difference in the relative expression of one gene segment to another was due to the amount of starting product.

In order to calculate the efficiency of the PCR reaction the following equation was used:

$$\text{Efficiency (E)} = 10^{(-1/\text{slope})}$$

Where the slope was calculated from the standard curve of Ct v Log cDNA concentration and when the slope was -3.3 +/-10% then E = 2 or 100% +/-10%.

R^2 is statistical correlation which estimates the consistency of PCR amplification and determines how good one value is at predicting another. If $R^2=1$ then you can accurately predict the value of x (DNA concentration) given the value of y (Ct).

The efficiencies of each set of primer pairs were calculated by amplifying triplicate samples of 5 fold serial dilutions of pooled cDNA as per the method outlined in section 2.6.4.2. and the mean Ct value calculated. These values were then plotted against log cDNA concentration and the slope calculated in order to determine the efficiency of each set of primer pairs and allow comparison between them (Figure 2.3).

Figure 2.3- Calculating primer efficiency for the TRVβ1 - TRCβ primer pair

The PCR amplification plot was generated using triplicate 5-fold serial dilutions of cDNA at five concentrations (1-5) and had NTC PCR reactions (a). The mean Ct value was calculated for each cDNA concentration (ng/µl) (b) and a standard curve of mean Ct v Log cDNA concentration was generated. From this the efficiency of the PCR reaction was calculated (c), which was 97%.

(a)

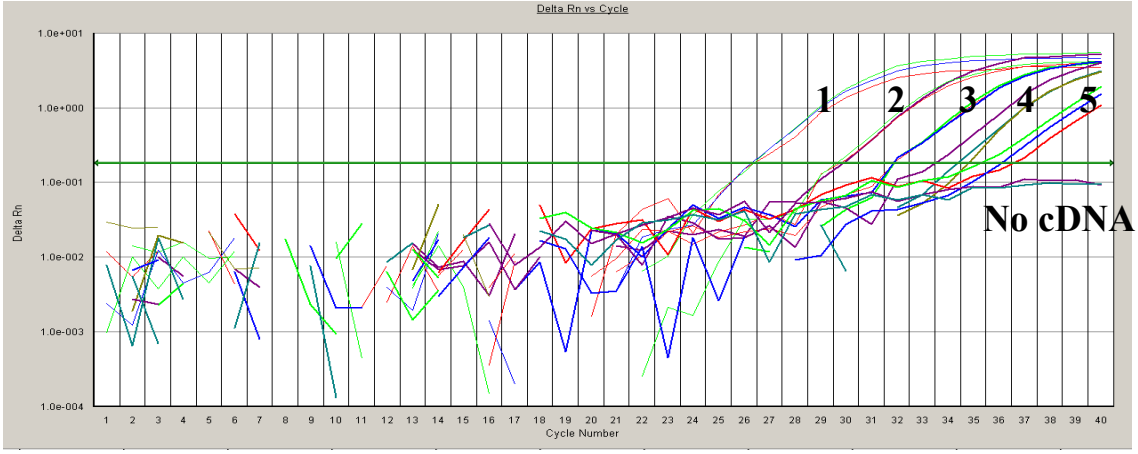

(b)

Log DNA Conc	Ct v1	Ct v2	Ct v3	Mean Ct
3.2553	26.37	26.30	26.24	26.30
2.5563	29.88	29.74	29.59	29.74
1.8573	31.84	31.80	31.77	31.80
1.1584	33.47	34.32	34.78	34.19
0.4594	36.53	35.3	36.1	35.98

(c)

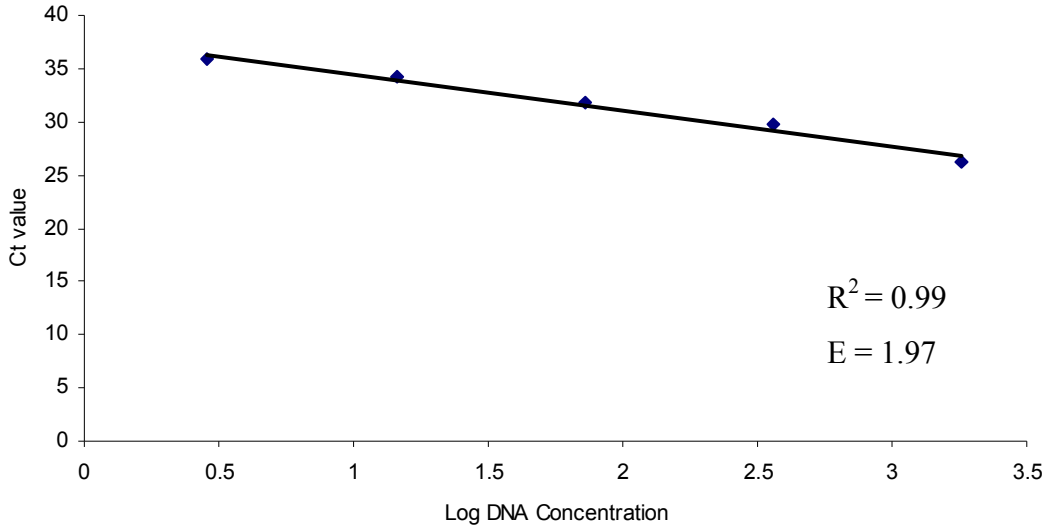

2.6.4.5 Calculating the relative use of each TRVß gene segment in kidney or spleen

The relative usage of each TRVß gene segment was calculated according to the following equation, which had been used by Pannetier's group when they were comparing the frequency of TCR transcripts in humans with rheumatoid arthritis (Lim, Baron et al. 2002).

$$U(TRV\beta y) = \sum_{x=1}^{x=22} 2^{Ct(x)-Ct(y)}$$

Where Ct(x) was the fluorescent threshold cycle number measured for TRVßx

This calculation was valid provided the efficiencies of all twenty two primer pairs were close to 100%. Multiple commercial companies suggest an acceptable range for primer efficiency which allows for comparison of reactions is 100% +/- 10%. On review of the paper by Lim et al, their mean primer pair efficiency was 87% +/- 18%, which was less strict.

2.7 Cloning methodology for sequence analysis

2.7.1 Standard PCR to generate PCR product for cloning

The high fidelity Taq polymerase, Platinum PCR SuperMix High fidelity (Invitogen, Paisley, Scotland) was used for PCR as described in 2.6.3.2. This ensured high fidelity amplification of the DNA template and minimised the errors in nucleotide addition generated by the polymerase during creation of the complementary strand. In order to achieve this, the mixture contained a *Pyrococcus* species GB-D thermostable polymerase which had proofreading ability by virtue of it's 3'-5' exonuclease activity, allowing the removal of mismatched base pairs to decrease the error rate. The mixture of the Taq DNA polymerase with a proofreading enzyme increased the fidelity of amplification approximately six times over that of a Taq DNA polymerase alone. This was important because errors generated in stand extension would ultimately lead to errors in the sequence read.

Taq polymerase is also useful when there is a limited amount of starting material as it gives higher yields and also fewer extraneous bands due to non-specific amplification at lower temperatures, due to the hotstart technology. It also has nontemplate-dependent terminal transferase activity which adds a single deoxyadenosine (A) to the 3' end of the PCR product during the final lengthened extension step. This made it possible to clone the PCR product into a linearised vector using the topoisomerase enzyme, which had a single overhanging 3' deoxythymidine (T) (Figure 2.4).

The pCR4-TOPO plasmid from Invitrogen (Paisley, Scotland) was used which contained a ccdB lethality gene, fused to the LacZα gene (Figure 2.5). The PCR product was inserted within this lethality gene to disrupt it. Therefore, if the vector re-circularised without a PCR insert and was transformed into *E. coli*, this lethality gene remained intact and the bacteria died. However, if there was a PCR insert in the plasmid vector the lethality gene was disrupted and the bacteria lived ensuring that only bacteria transformed with a plasmid vector containing a PCR insert survived. The TOPO vector also contained a kanaymcin and ampicillin resistant gene and the bacteria were grown in media containing kanamycin, selecting only bacteria transformed with a recombinant vector to survive.

Figure 2.4- Generation of a T overhang on the linearised plasmid

Topoisomerase I binds to dsDNA on the plasmid vector and cleaves the phosphodiester backbone after a 5'-CCCTT nucleotide sequence in one strand (Shuman 1994). The energy created by breaking the phosphodiester bond is conserved by the formation of a covalent bond between the 3' phosphate of the cleaved strand and the tyrosol residue (Tyr-274) of topoisomerase I. This linearises the plasmid vector. However, the phosphor-tyrosol bond between the DNA and enzyme can be attacked by the 5' hydroxyl (-OH) group of the original cleaved strand, reversing the reaction and releasing the topoisomerase enzyme, allowing the vector to re-circularise with the inserted PCR sequence.

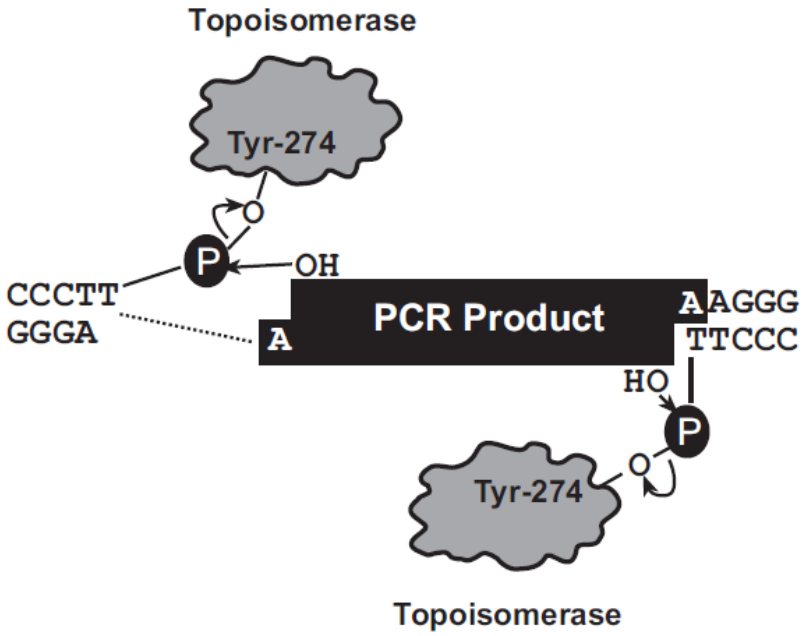

Figure 2.5- Map of the pCR4-TOPO plasmid

The LacZα-ccdB lethality gene and antibiotic resistance genes are found within the pCR4-TOPO plasmid vector.

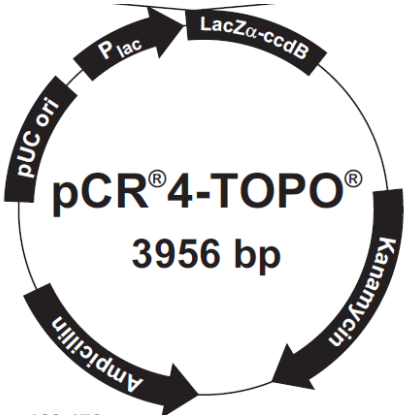

2.7.2 Cloning reaction

The TOPO TA cloning kit for sequencing (Invitrogen, Paisley, Scotland) was used to clone and transform cells. The following cloning reaction mixture was used for each cloning reaction:

PCR product	4µl
Salt solution (1.2M NaCl, 0.06M $MgCl_2$)	1µl
TOPO vector	1 µl

The reagents were mixed and incubated for 5 minutes at room temperature and the reaction placed on ice.

2.7.3 Transformation of competent bacteria

2µl of the TOPO cloning reaction was added to 1 vial of One Shot chemically competent *E. coli*, mixed and incubated on ice for 15 minutes. The *E. coli* were then heat shocked at 42°C for 30 seconds and transferred to ice. 250µl of SOC medium was added and the tube shaken horizontally at 200 rpm at 37°C for 1 hour in an orbital incubator. Aliquots of 50µl of the transformation reaction were spread onto pre-warmed LB agar plates containing kanamycin (50µg/ml) and incubated overnight at 37°C to grow individual colonies. 25-50 of these colonies were picked and individually grown overnight in LB, containing kanamycin (50µg/ml), at 37°C in the orbital incubator.

2.7.4 Plasmid extraction from competent bacteria

The PureLink quick plasmid miniprep kit (Invitrogen, Paisley, Scotland) was used to isolate plasmid DNA from *E. coli* as per the manufacturer's instructions. Cells were lysed using an alkaline/SDS buffer. The lysate was applied to a silica membrane column that selectively bound plasmid DNA. Contaminants were removed using wash buffers and the plasmid DNA was eluted into TE buffer. A sample of the extracted plasmid DNA was then used in a PCR reaction, as detailed in section 2.6.3.3, and the products resolved by agarose electrophoresis. This was performed to check there was an appropriate sized PCR cloning product insert within the plasmid vector before the extracted plasmid DNA was sent for sequencing.

2.7.5 Cloning control reactions

Control TOPO cloning reactions were performed to ensure the expected results were generated. This involved generating a control PCR product to use in the TOPO cloning reactions. Also the efficiency of transformation reactions was assessed using a pUC19 plasmid.

2.7.5.1 Control PCR product

A 750bp control PCR product was generated using the method and reagents from the TOPO TA cloning kit (Invitrogen, Paisley, Scotland) and the product resolved by agarose gel electrophoresis as a discrete band of the appropriate size.

2.7.5.2 Control TOPO cloning reaction

Two cloning reactions were performed, as outlined in section 2.7.2, one using the control 750bp PCR product and the other substituting the DNA for an equivalent volume of DEPC water. *E. coli* were transformed and colonies grown using both separate cloning reaction products, as outlined in section 2.7.3. Aliquots of both 25µl and 50µl of each transformation reaction were plated. Few colonies grew when vector only was cloned due to the intact ccbD lethality gene. In contrast, colonies grew when the control PCR product was used in the cloning reaction and there was an incremental increase in the number of colonies grown when more transformed reaction mix was plated. Colonies were then picked and grown overnight in LB with kanamycin and the plasmid DNA extracted, as outlined in section 2.7.4. The final PCR reaction using the plasmid DNA confirmed a 750bp product using agarose gel electrophoresis.

Other control studies were carried out with each set of cloning reactions to ensure:

- no growth after overnight incubation of a LB agar plate with kanamycin, demonstrating that the plates were not contaminated
- no growth on an LB agar plate with kanamycin, when unmanipulated *E. coli* were plated out because they were not resistant to kanamycin
- multiple confluent colonies grown on a LB agar plate without antibiotic added when unmanipulated *E. coli* were plated, demonstrating the bacteria could proliferate

2.7.5.3 Transformation efficiency

In order to determine how well the transformation reactions were working the transformation efficiency of the reaction was calculated using the following equation:

$$\text{Transformation efficiency} = \frac{\text{Total number of cells growing on the agar plate}}{\text{Amount of DNA spread on the agar plate in µg}}$$

50µl of One Shot competent *E.coli* were chemically transformed using the standard method, with a circular plasmid pUC19 which was equivalent to 10pg DNA. This plasmid DNA had not been cloned with a PCR product and contained an ampicillin resistance gene. One fifth of the transformation reaction was transferred onto a LB agar plate with ampicillin (100µg/ml) and after overnight incubation 60 colony forming units (cfu) developed. Therefore 30 x 10^6 cfu/µg DNA were grown, when the transformation efficiency was expected to be ~1 x 10^9 cfu/µg DNA. Therefore the efficiency of the reaction was 3%.

2.8 Sequencing

The automated sequencing service from the commercial company Macrogen (Seoul, Korea) was used to determine the nucleotide sequence of the PCR product in each plasmid vector. Macrogen use a dye-terminator method to determine nucleotide sequence, by labelling each of the four dideoxynucleotide chain terminators with different fluorescent dyes which have different wavelengths of fluorescence and emission (Sanger, Nicklen et al. 1977). They terminate DNA strand elongation because they lack the 3'-OH group required for the formation of a phosphodiester bond between two nucleotides, thus resulting in DNA fragments of varying length The sequencing reactions were conducted under BigDyeTM terminator cycling conditions and run using the Applied Biosystems automatic sequencer. Each nucleotide sequence read out from Macrogen for an individual sample of the plasmid DNA included the DNA sequence trace chromatogram (Figure 2.6). The limitations of this dye-terminator method include dye effects due to differences in the incorporation of the dye-labelled chain terminators into the DNA fragment, resulting in unequal peak heights and shapes in the electronic DNA sequence trace chromatogram after capillary electrophoresis.

Figure 2.6- Chromatogram of the sequence generated from colony 1 of the D14A9K CD4+ sorted cells

An example of a DNA sequence trace chromatogram, which accompanied each nucleotide sequence for each sample of plasmid DNA, is illustrated here.

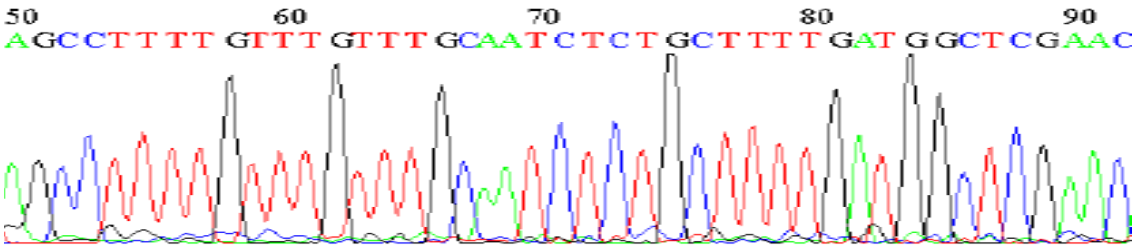

2.8.1 Sequencing analysis

The locations of each of the primer pairs and which TRJβ gene was used were first identified in each of the sequences. Subsequently the multiple sequences were aligned using the EMBL-EBI website (**www.ebi.ac.uk/Tools/clustalw2/index**). The Translate tool from the Expasy website (http://www.expasy.ch/tools/) was used for conversion of nucleotide to amino acid sequences.

2.9 Lymphocyte extraction and sorting from kidney and spleen tissue

2.9.1 Digestion of renal tissue

Mice were sacrificed, exsanguinated and perfused with 50ml of 0.9% saline until their organs became visibly pale. The UUO kidney was dissected and divided into 2 halves. One half was left whole and snap frozen in liquid isopentone and stored at -80°C along with the spleen. The other half was dissected into 1mm^3 sections and placed in DMEM (Invitrogen, Paisley, Scotland) on ice. 1.6mg/ml of collagenase (Sigma-Aldrich, Poole, UK) and 200µg/ml of DNase-1 (Roche, Burgess Hill, West Sussex) was added to the DMEM tissue suspension and incubated at 37°C for 40 minutes with agitation. The suspension was centrifuged (Heraeus Labofuge 400R, Thermofisher Scientific, Langenselbold, Germany) at 500g for 5 minutes to form a pellet. The cells were washed three times with DMEM and re-suspended in 10ml of DMEM and further digested by the addition of 200µg/ml of DNase-1 for 15 minutes at 37°C with agitation. The digest was again washed and re-suspended in FACS buffer (1% BSA) and the suspension left to settle for 20 minutes. The upper two thirds were removed for analysis and contained the low density cells of interest. The cells were counted using a haemocytometer and the ratio of live:dead cells estimated with the addition of trypan blue. The cells were then re-suspended in 1% heat inactivated mouse serum to block non-specific binding. The risk of separating immune cells from the kidney by this methodology is that the cell population may not be representative of the whole T lymphocyte pool within the UUO kidney. The very lymphocytes I am interested in, embedded within dense fibrous tissue, may be more difficult to extract. Alternatively the activated T lymphocyte population may be more liable to damage or die by this extraction procedure. This would introduce bias to the cell population retrieved and not be representative of the total kidney lymphocyte pool.

2.9.2 Flow cytometry and cell sorting

Primary fluorochrome labelled antibodies to CD45, CD4 and CD8 were added directly to the cell suspension at 0.8µg / 10^6cells and incubated at 4°C in the dark for 30 minutes in FACS tubes. Tubes were centrifuged at 350g for 5 minutes to obtain a pellet. Cells were washed three times with FACS solution and re-suspended in 200µl of FACS solution.

The intensity of the fluorescent staining on the cells was detected using the LSRII flowcytometer (Becton Dickinson, Oxford, UK) and the cells sorted into CD4+ and CD8+ populations using the FACSDIVA (Becton Dickinson, Oxford, UK). Cells were

sorted directly into plastic eppendorfs containing 1ml lysis buffer with 10µl β-mercaptoethanol (Quiagen RNA extraction kit). The lysis buffer also contained ~10^5 PTEC acting as carrier cells. These were used to discourage RNA from the sorted cells binding to the side of the tube and so improve RNA yield. RNA extraction was performed immediately using the standard Quiagen RNA extraction kit as illustrated in section 2.6.1.2. The data was analysed using the FACSDIVA software (Becton Dickinson, Oxford, UK).

2.10 Statistics

Statistics were performed using the statistical analysis function in the Prism Graph Pad program. P values were calculated to compare the means of two samples with equal variance using the student t test. ANOVA was used when making comparisons of >2 variables, when the variances of the samples were equal. The Bonferroni adjustment was made for multiple comparisons. P values using the Chi squared test were used to assess whether paired observations on two variables, expressed on a contingency table, were independent of each other. P values of less than 0.05 were regarded as significant.

Correlation coefficients (r) were calculated to determine whether there was a relationship between two factors; –1 demonstrated a perfect negative correlation, 0 no correlation and +1 a perfect positive correlation.

Chapter 3. The composition and phenotype of the cellular infiltrate post UUO injury and its correlation with renal injury and fibrosis

3.1 Introduction

Irrespective of the aetiology of chronic renal disease there are cellular infiltrates in the tubulointerstitial compartment and evidence of tubulointerstitial fibrosis, which is the morphological hallmark of chronic progressive renal disease (Harris and Neilson 2006). The rate of decline in glomerular filtration rate (GFR) strongly correlates with the extent of this tubulointerstitial damage (Nath 1992; Strutz and Neilson 1994).

An animal model which demonstrates many features of progressive renal disease seen in the clinical setting is unilateral ureteric obstruction. Within 1-2 weeks of ligation of the ureter there is consistent time-dependent leukocyte influx into the tubulointerstitial compartment and fibrosis (Schreiner, Harris et al. 1988). This has made UUO a popular rodent model for the study of renal fibrosis. I used this model to investigate the role of the inflammatory infiltrate in progressive renal disease.

The inflammatory cell recruitment into the tubulointerstitium seen both in the clinical setting and in the UUO model of kidney disease is believed to be facilitated by the up-regulation of chemokines and adhesion molecules (Vielhauer, Eis et al. 2004). Conversely if obstruction is released at an early time point in the UUO model, the amount of inflammatory infiltrate can be reversed and declines (Cochrane, Kett et al. 2005; Tapmeier, Brown et al. 2008).

My initial aim was to evaluate the time course of the inflammatory cell influx into the tubulointerstitium and to correlate this with the subsequent injury that developed. Correlating the presence of this inflammatory infiltrate with progressive renal injury does not determine that this infiltrate is playing a causal role.

On completion of lymphocyte development in the thymus, lymphocytes enter the blood stream and lymphoid organs as naive T cells. They are unable to participate in adaptive immune responses with effector function until they encounter their specific antigen with MHC and co-stimulation. Lymphocytes then proliferate and differentiate into effector cells which contribute to the removal of that antigen. Activated lymphocytes display specific cell surface antigens and nuclear markers of proliferation, which are not present when they are in their naive state. My hypothesis is that lymphocytes are playing an

active role in promoting tubulointerstitial injury in UUO. Therefore I aimed to determine whether this tubulointerstitial lymphocytic infiltrate, post UUO, was comprised of activated and proliferating T cells which could play an active role in promoting tubulointerstitial injury.

3.2 Establishing the model of UUO

UUO was performed on 8-10 week old female C57Bl/6 mice, with a parallel group of sham operated animals, and were sacrificed at 3, 7 and 10 days post obstruction. No animals died before the end of the experiment. Both the obstructed UUO kidney and the unobstructed contralateral kidney were analysed. At day 3 post obstruction, the harvested UUO kidney was not macroscopically different to a normal kidney or the contralateral kidney. By day 10, the obstructed kidney was macroscopically pale and hydronephrotic with a markedly thinned cortex (Figure 3.1). The day 7 obstructed kidneys were abnormal however the changes not as marked as that seen at the later time point.

Figure 3.1- Macroscopic appearances of the obstructed kidney at day 10 post UUO

A digital photograph of a mouse that had undergone a laparotomy and ligation of the left ureter ten days earlier. The obstructed left kidney was enlarged (arrow) due to hydronephrosis. Following removal and decompression of this kidney, marked reduction in the cortical thickness was demonstrated.

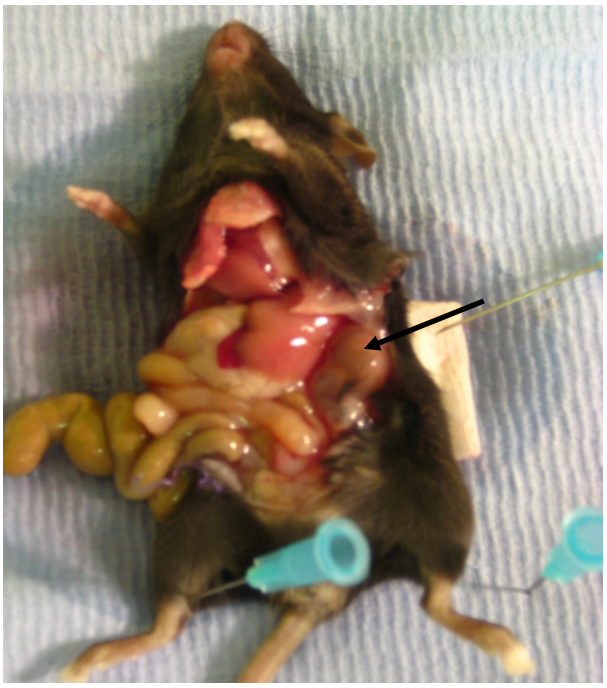

3.3 Characterising the mononuclear cell infiltrate and tubulointerstitial injury following UUO

In order to investigate the composition of the inflammatory cell infiltrate in the development of tubulointerstitial fibrosis, UUO was performed in groups of four C57Bl/6 mice. The animals were sacrificed at three time points: 3, 7 and 10 days post UUO, in parallel with sham operated animals. UUO kidneys, contralateral kidneys and renal tissue from sham operated animals were processed from the sacrificed animals. Immunohistochemical staining was carried out to identify the phenotype of the infiltrating cells and to assess the degree of injury.

3.3.1 Histological analysis of the cellular infiltration

Histological analysis of infiltrating mononuclear cells into day 3, 7 and 10 UUO kidney was performed by immunohistochemistry on frozen sections in a blinded manner (Figure 3.2). From the published literature that looked at cellular infiltration into UUO kidney, the predominant cell types were T lymphocytes and macrophages (Schreiner, Harris et al. 1988), therefore monoclonal antibodies to CD4, CD8 and F4/80 antigens were used. The F4/80 antigen is expressed on tissue macrophages and has been the predominant antibody used in the literature to detect macrophages in mice (Khazen, M'Bika J et al. 2005; van den Berg and Kraal 2005). Histological examination also demonstrated tubulitis (Figure 3.3).

A progressive increase in the mean number of CD4+ T cells infiltrating UUO kidney between 3, 7 and 10 days post obstruction was demonstrated but this did not reach statistical significance ($p=0.065$). A similar pattern of increasing F4/80+ cell infiltration with prolonged UUO was also seen and this increase in the mean number of cells between 3, 7 and 10 days post obstruction was statistically significant ($p=0.016$), although the number plateaued between day 7 and 10. The mean number of CD8+ T cells peaked after 7 days of obstruction and there were less CD8+ T cells seen at 10 days. The mean number of CD8+ T cells infiltrating the day 7 UUO kidney was significantly more than the number seen after 3 days of obstruction ($p=0.011$). Overall, the mean number of CD4+ cells predominated over the number of CD8+ cells in obstructed kidney, with a CD4:CD8 ratio of 2.5:1 and 6:1 at days 7 and 10 respectively (Figure 3.4).

Comparison was then made between the cellular infiltration seen in UUO kidney with that of sham operated kidney, the contralateral kidney from a UUO mouse and normal

kidney. These controls did not show any histological difference in cellular infiltration, where very few of the three cell types were detected (Figure 3.5). After three days of UUO there was minimal infiltration of all three cells types into the obstructed kidney and no significant difference between the mean number of infiltrating CD4+, CD8+ and F4/80+ cells compared to the controls ($p>0.05$). In comparison, after 10 days of UUO there was a significant increase in the mean number of infiltrating CD4+, CD8+ and F4/80+ cells in the day 10 UUO kidney compared to histologically normal kidneys ($p<0.05$).

Figure 3.2- Immunohistochemical staining for T cell and macrophage infiltration into the tubulointerstitium of UUO kidney at 3, 7 and 10 days post UUO

A Streptavidin-Horseradish peroxidise immunohistochemical staining technique was used on frozen sections of obstructed kidney at 3, 7 and 10 days post UUO to detect infiltrating T lymphocytes and macrophages (arrow). The number of infiltrating CD4+, CD8+ and F4/80+ cells increased with time post UUO. Magnification x250.

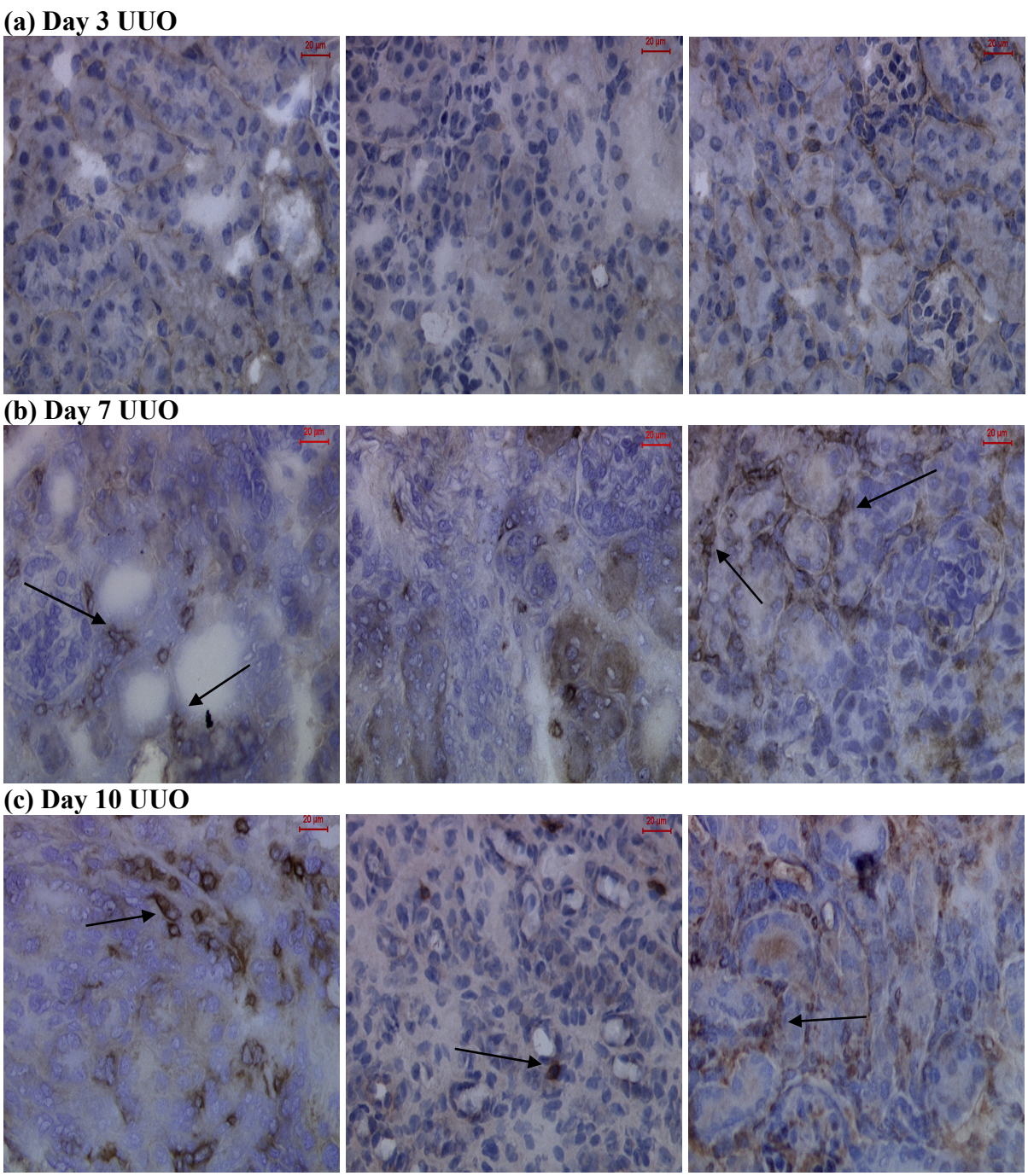

Figure 3.3- Immunohistochemical staining for CD4+ T cells in the tubulointerstitium of UUO kidney 10 days post obstruction demonstrating tubulitis

A Streptavidin-Horseradish peroxidise immunohistochemical staining technique was used on a frozen section of day 10 UUO kidney. This demonstrates CD4+ T cells (arrow) which have breached the tubular basement membrane, to cause tubulitis. Magnification x250.

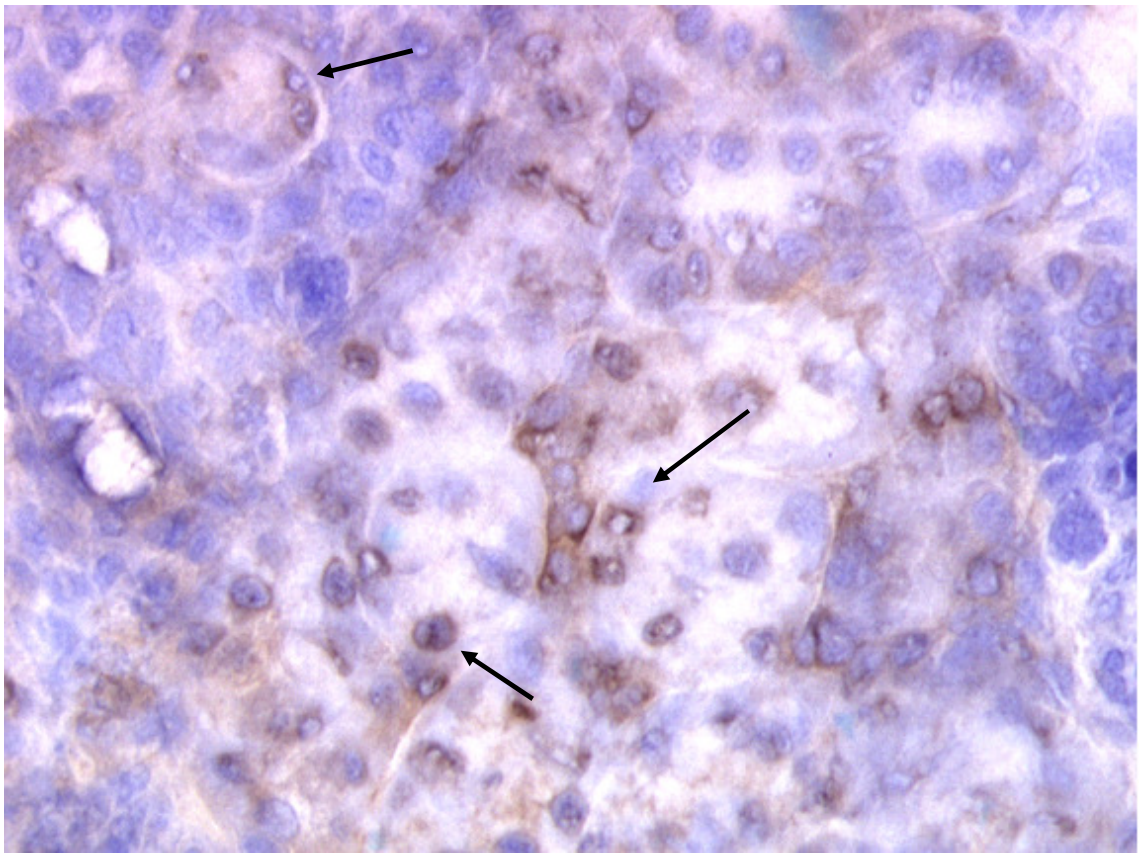

Figure 3.4- Mononuclear infiltrate into the UUO kidney at time points post UUO

The number of infiltrating cells was quantified by analysing five random non-overlapping HPF at x250 magnification for each UUO kidney. The total number of positively stained infiltrating cells was counted for each HPF and the mean number of cells per HPF calculated for each animal. Then the mean number of infiltrating cells per HPF was calculated for the group of four mice at each time point.

There was a significant change in the mean number of infiltrating F4/80+ cells (*p=0.016) and CD8+ T cells (**p=0.0008) between 3, 7 and 10 days post UUO. Although the mean number of infiltrating CD4+ T cells increased with progressive length of obstruction, this was not statistically significant (***p=0.065). There were very few infiltrating CD4+, CD8+ and F4/80+ cells in the normal, sham operated and contralateral UUO kidney sections analysed (data not shown).

Each group consisted of four mice with error bars depicting the standard error of the mean.

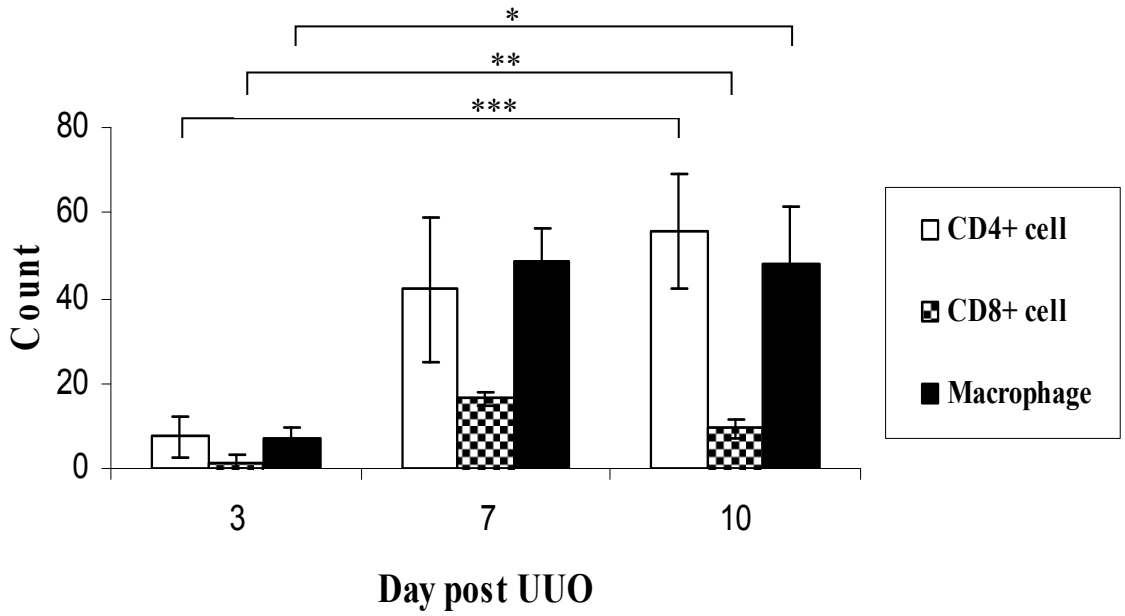

Figure 3.5- Immunohistochemical staining for T cell and macrophage infiltration into the tubulointerstitium of normal and contralateral UUO kidney and spleen

A Streptavidin-Horseradish peroxidise immunohistochemical staining technique was used on frozen sections of the contralateral kidney in a UUO animal and normal kidney and spleen to detect infiltrating T lymphocytes and macrophages. The contralateral UUO kidney and normal kidney looked identical and few cellular infiltrates were demonstrated. Identical findings were seen in sham operated kidney (data not shown). Positive staining for CD4+ and CD8+ T cells and F4/80+ macrophages was found in normal spleen, which was used as the positive control. Magnification x250.

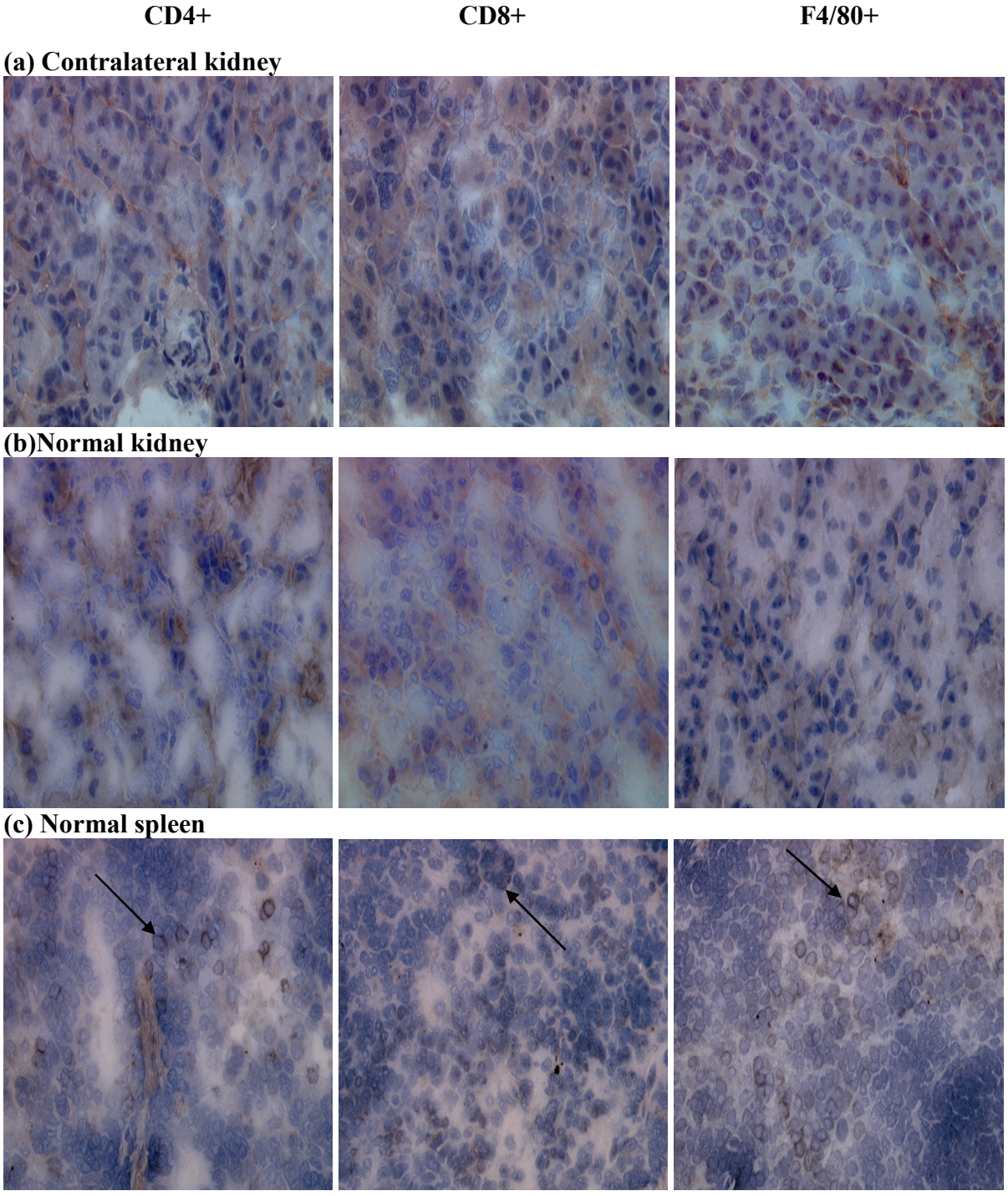

3.3.2 Histological analysis of the tubulointerstitial injury

3.3.2.1 Characterising tubulointerstitial injury with Periodic acid Schiff staining

The degree of tubulointerstitial injury can be assessed histologically in a number of ways. Initially Periodic acid Schiff (PAS) staining was performed on formalin-fixed, wax-embedded sections. Normal kidneys had a tightly packed tubulointerstitial space with back-to-back tubules and tall, tubular epithelial cells (Figure 3.6(a)). This was similar to the histology seen in both the contralateral kidney of UUO mice (Figure 3.6(b)) and the kidney of sham operated controls (not shown).

The tubulointerstitial injury demonstrated in day 3, 7 and 10 UUO kidney samples were compared (Figure 3.6(c)). In day 3 UUO kidney there was some tubulointerstitial expansion and tubular separation, as well as evidence of tubular epithelial cell flattening. More marked histological changes were seen in kidney after 7 and 10 days of obstruction, with noticeable loss of normal renal architecture, expansion of the tubulointerstitial compartment and separation of the tubules. Tubular epithelial cells lost height and became flattened and there was tubular dilatation. In some sections there was such severe injury to the tubulointerstitial compartment with prolonged obstruction that recognisable renal architecture was lost. No glomerular changes were apparent in UUO kidney confirming this to be a tubulointerstitial disease.

The percentage of cortical cross section occupied by interstitium (as a measure of interstitial expansion) was significantly greater in the obstructed compared to the contralateral kidney at day 3 ($p=0.0487$), 7 ($p=0.0024$) and 10 ($p=0.0001$) post obstruction (Figure 3.7). Similar significant increases in interstitial expansion were seen when comparing UUO and normal kidney at day 10 ($p<0.0001$) (data not shown). Furthermore, interstitial expansion increased significantly with increasing duration of obstruction in the UUO kidney ($p=0.0003$). There was also a positive correlation between the number of CD4+ cells and interstitial expansion post UUO (Figure 3.8).

These histological changes were similar to those seen in clinical biopsy specimens of patients with advanced chronic kidney disease.

Figure 3.6- PAS staining of normal kidney, contralateral kidney from a UUO animal and UUO kidney at day 3, 7 and 10 post obstruction

PAS stained, formalin fixed and wax embedded sections of normal kidney (a), day 10 contralateral kidney (b) and UUO kidney at the three time points post UUO (c) were used to assess renal injury. The contralateral kidney in figure (b) showed histologically normal renal architecture, as seen in figure (a). Figure (c) demonstrates progressive loss of normal renal architecture, with increasing expansion of the interstitial space at successive times after obstruction. There is also loss of tubular epithelial cell height and tubular dilatation (arrow). Magnification x250.

(a) Normal kidney **(b) Contralateral UUO kidney**

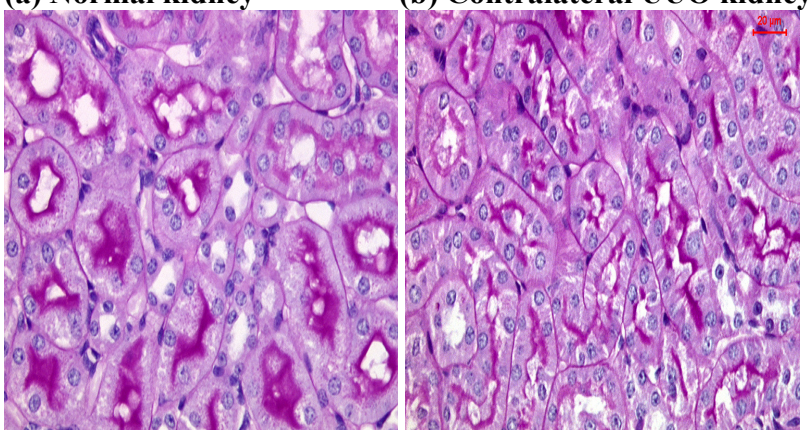

(c) Day 3 UUO **Day 7 UUO** **Day 10 UUO**

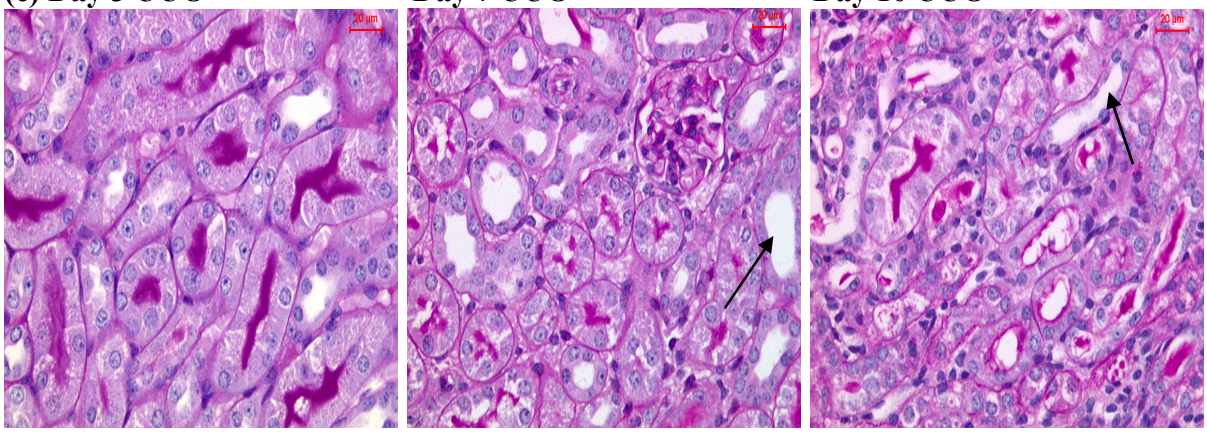

Figure 3.7- Comparison of the percentage of interstitial expansion in the UUO and contralateral kidneys at 3, 7 and 10 days post obstruction

The degree of tubular injury as assessed by PAS staining and percentage interstitial expansion was compared at three time points post UUO. To examine the degree of tubulointerstitial expansion a point counting method was used as outlined in Chapter 2. A 10 x 10 grid was superimposed over each of five HPFs per animal, with eighty one positive intersections. The number of positive intersections which lay outside the tubule and in the interstitial space were counted and used to calculate the percentage of interstitial expansion. The mean percentage of interstitial expansion was calculated for each animal and then for the group of four animals as a whole at each time point.

There was a significant difference between the mean percentage of interstitial expansion between the UUO and contralateral kidney at 3 (*p=0.0487), 7 (**p=0.0024) and 10 (***p=0.0001) days post obstruction. There was also a significant increase in interstitial expansion in the UUO kidney between 3, 7 and 10 days post obstruction (p=0.0003).

Each group consisted of four animals with error bars depicting the standard error of the mean.

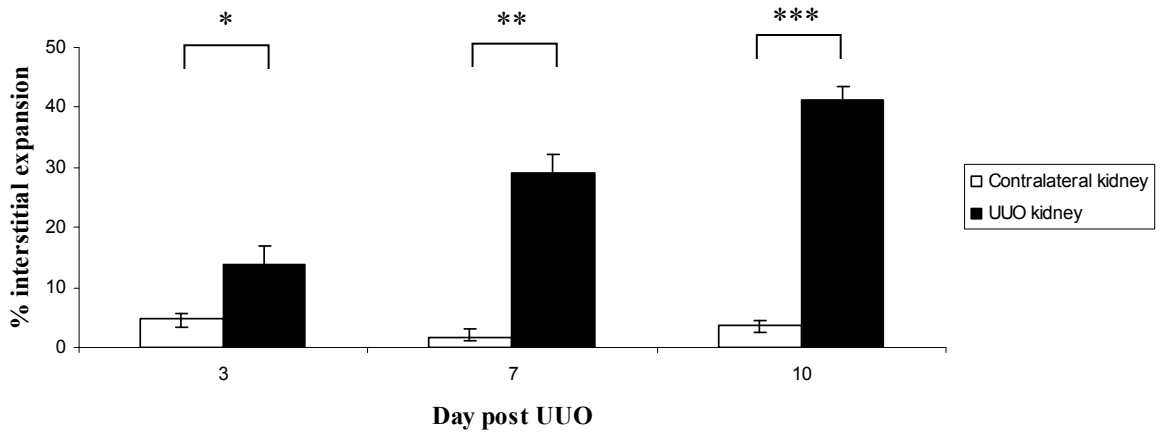

Figure 3.8- Infiltration of (a) CD4+, (b) CD8+ and (c) F4/80+ mononuclear cells correlated with interstitial expansion at 3, 7 and 10 days post UUO

The degree of tubular injury as assessed by PAS staining and percentage of interstitial expansion was correlated with the number and type of infiltrating mononuclear cells. There was a positive correlation between number of CD4+ cells and interstitial expansion with increasing length of renal obstruction (r=0.98) (a). The correlation coefficients for CD8+ and F4/80+ cells with IE were 0.59 and 0.89 respectively (b + c).

(a) CD4+

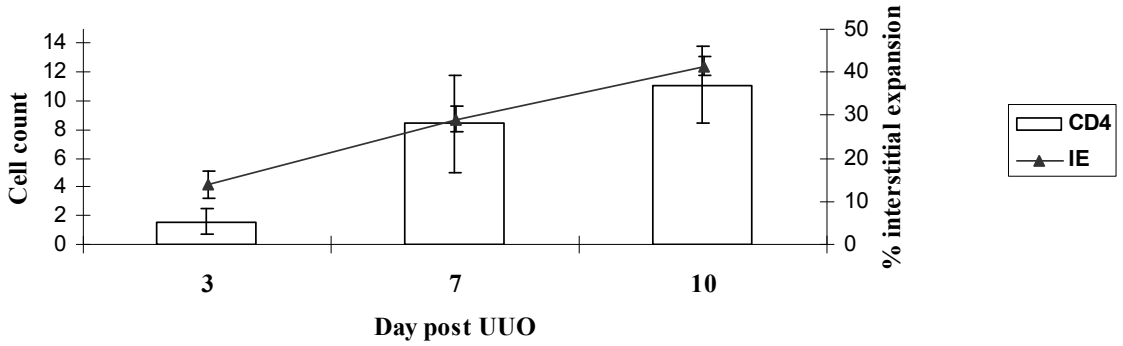

(b) CD8+

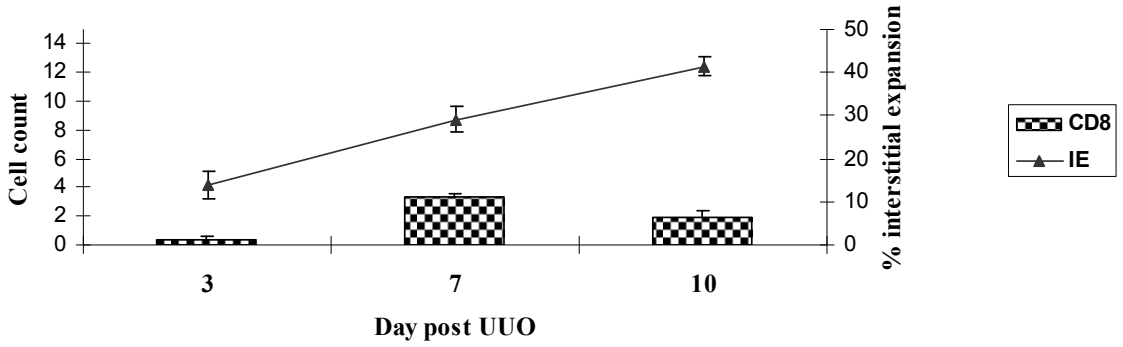

(c) F4/80+

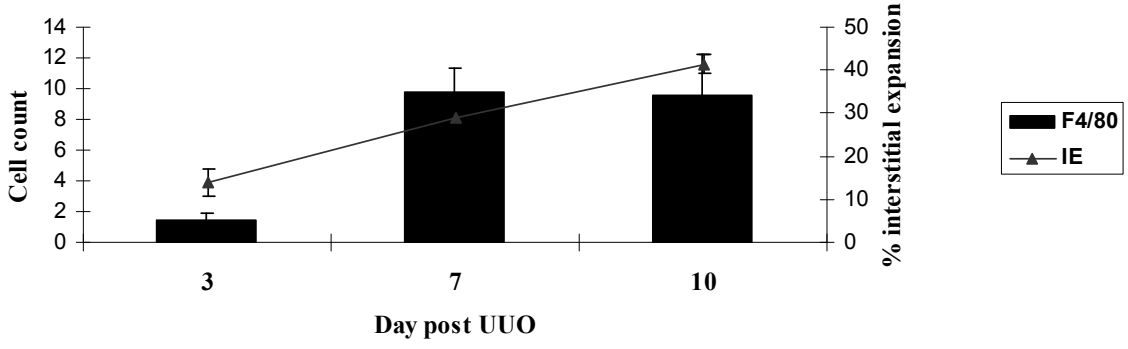

3.3.2.2 Tubulointerstitial injury and markers of fibrosis

Interstitial expansion as demonstrated by PAS staining in UUO kidney is presumed to represent the development of fibrosis and has been demonstrated in previous studies using the UUO model (Tapmeier, Brown et al. 2008). However, this expansion may represent oedema rather than fibrosis and so to characterise interstitial expansion further obstructed kidney was stained immunohistochemically for alpha-smooth muscle actin (α-SMA) and collagen I.

The key factor in renal fibrosis is the accumulation and proliferation of fibroblasts within the interstitium that are stimulated to produce large amounts of extracellular matrix. The hallmark features of fibroblast activation include expression of α-smooth muscle actin, a contractile protein usually found in perivascular smooth muscle cells, and the production of excessive extracellular matrix components including collagen type I and III and fibronectin. The origin of the expanded activated myofibroblast population within the interstitial compartment is controversial, as outlined in Chapter 1, and has been shown to be derived from a number of sources. As a consequence staining for α-SMA and collagen I are more specific methods of assessing renal fibrotic injury than calculating interstitial expansion.

Histological analysis for α-SMA and collagen I in UUO kidney 3 days after obstruction revealed low levels of positive staining (Figures 3.9(a) and 3.10(a)). In comparison there was a significant increase in staining in the UUO kidney for both markers of fibrosis between 3, 7 and 10 days of obstruction ($p<0.0001$ for α-SMA and $p=0.0003$ for collagen I). In sham operated kidney (not shown), contralateral kidney from a UUO animal (Figure 3.9(b)) and normal kidney (Figure 3.9(c) and 3.11(a)) there was little staining for the two markers of fibrotic injury. There was even significantly less α-SMA staining in the contralateral kidney of a day 3 UUO animal compared to the obstructed kidney ($p=0.0407$) (Figure 3.12) and less collagen I staining in normal kidney compared to day 3 UUO kidney ($p=0.0425$) (Figure 3.13). This data reflected the results seen with PAS stained sections when the percentage of interstitial expansion was used as a surrogate marker for fibrosis (Figure 3.7).

Overall, a clear relationship between the two markers of fibrosis, α-SMA and collagen I, the percentage of interstitial expansion and mononuclear cell infiltration has been demonstrated.

Figure 3.9- α-SMA staining of day 3, 7 and 10 UUO kidney, normal kidney and the contralateral kidney from a UUO mouse

Immunohistochemical staining of α-SMA was carried out on formalin fixed, wax embedded sections of UUO kidney from three time points post UUO (a), a day 7 UUO contralateral kidney (b) and a normal kidney (c). Figure (a) shows a progressive increase in the α-SMA staining within the expanded interstitium (brown staining). The architecture seen in the contralateral kidney (b) is similar to that in the histologically normal kidney (c) and demonstrates minimal α-SMA staining. The blood vessel in the section of normal kidney (c) has a smooth muscle wall and stains positively for α-SMA and therefore acts as a positive control. Magnification x250.

(a) Day 3 UUO kidney

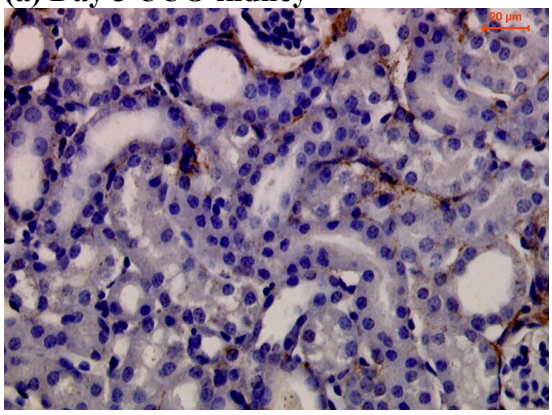

Day 7 UUO kidney

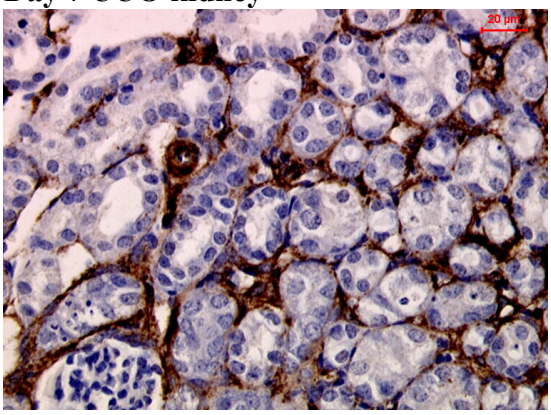

Day 10 UUO kidney

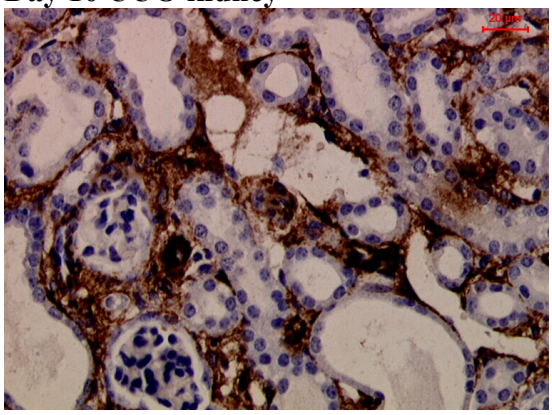

(b) Day 7 contralateral UUO kidney

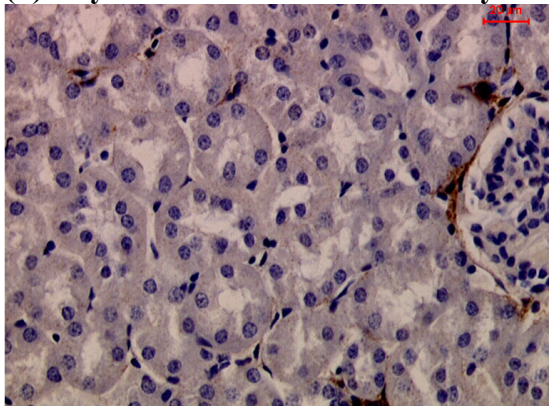

(c) Positive control: kidney vasculature

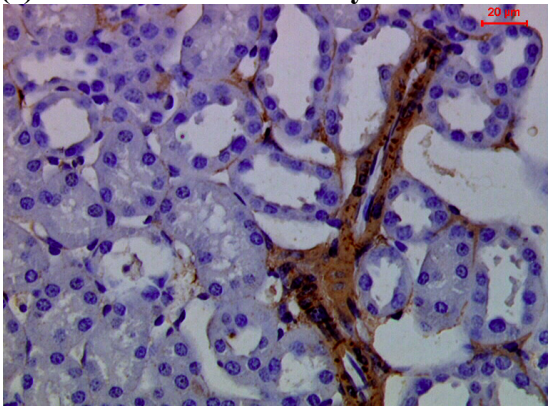

Figure 3.10- Collagen I staining of frozen tissue using pixel intensity grading to assess the percentage area of collagen I staining in UUO kidneys

Immunohistochemical staining for collagen I on frozen sections of UUO kidney was performed at 3, 7 and 10 days after ureteric obstruction (column (a)). Q-Win software was used to analyse the mean percentage area of collagen I staining (column (b)), delineated by the blue area. With increasing length of ureteric obstruction there was loss of the normal renal architecture and a progressive increase in collagen I staining along with expansion of the interstitial space. Magnification x250.

(a) Collagen I staining **(b) Percentage area of staining**

Day 3 post UUO

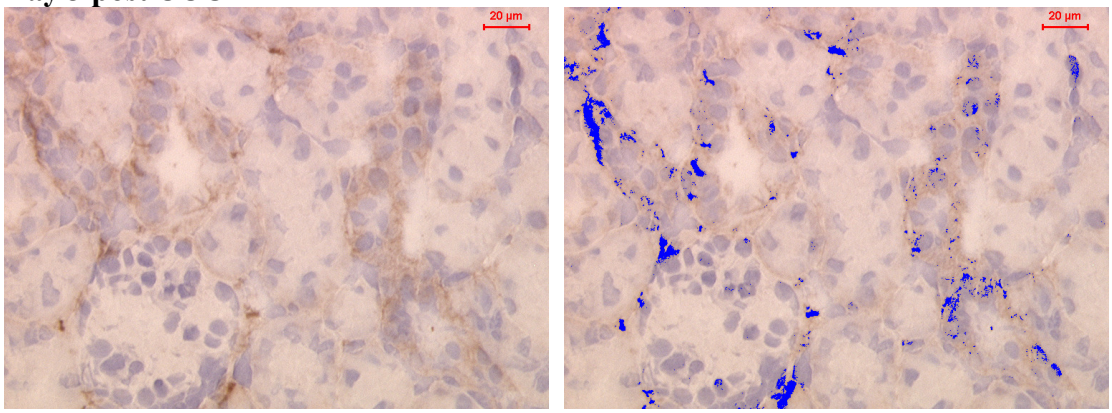

Day 7 post UUO

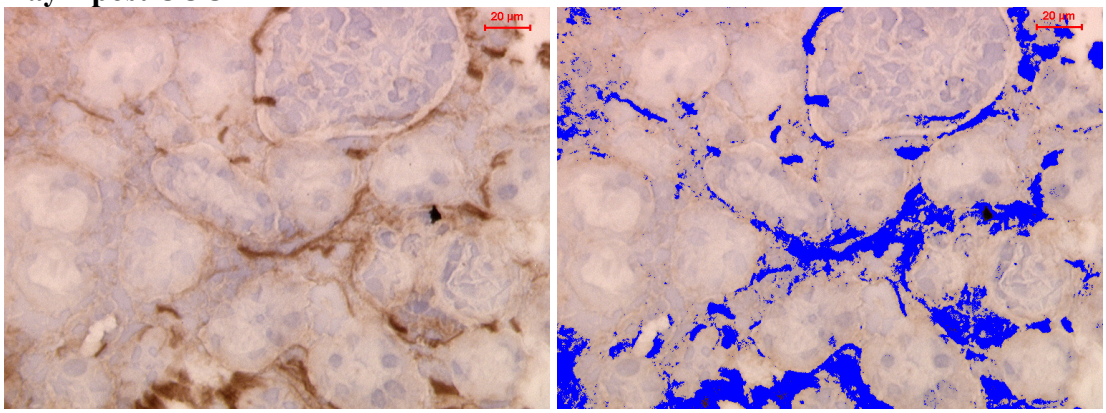

Day 10 post UUO

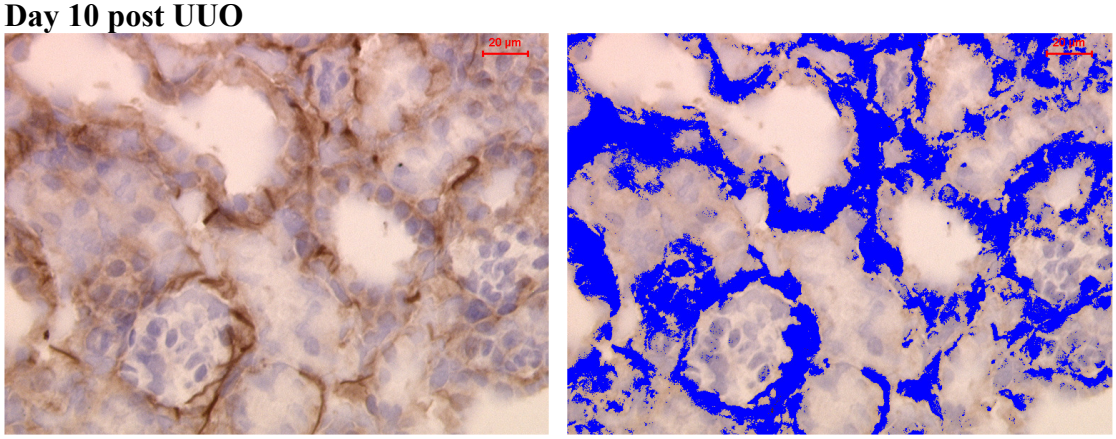

Figure 3.11- Collagen I staining of frozen kidney and liver tissue and using the pixel intensity grading to assess percentage area of collagen I staining

Frozen sections of normal kidney and liver were stained for collagen I using a horseradish peroxidise conjugated secondary antibody (a). Q-Win software determined the mean percentage area of collagen I staining using the pixel intensity grading function (b). Normal kidney acted as a negative control with little collagen I staining and normal liver a positive control because it is present in the portal fields and fibrous septa. Using the same method on UUO kidney without adding the collagen I primary antibody, there was no positive staining (c). This demonstrated that the secondary antibody and DAB bind specifically. Magnification x250.

(a) Collagen I staining **(b) Percentage area of staining**

Normal kidney

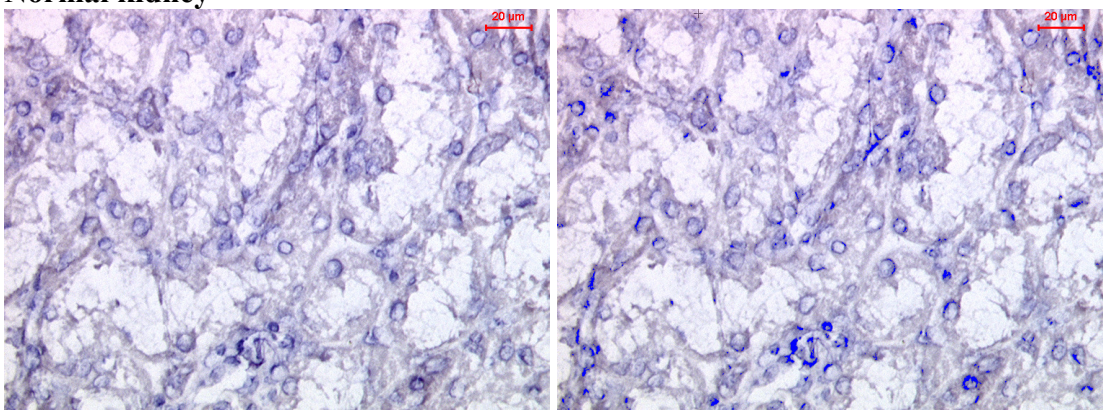

Normal Liver (positive control)

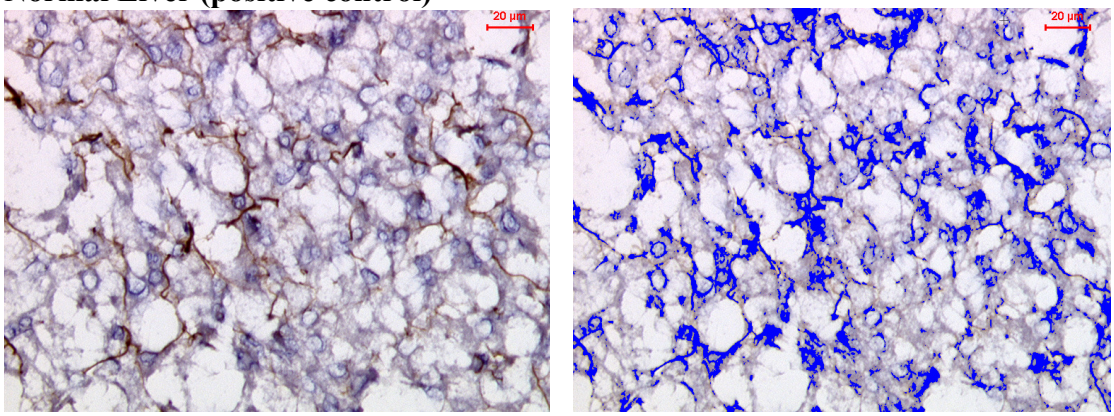

(c) No primary antibody: UUO kidney

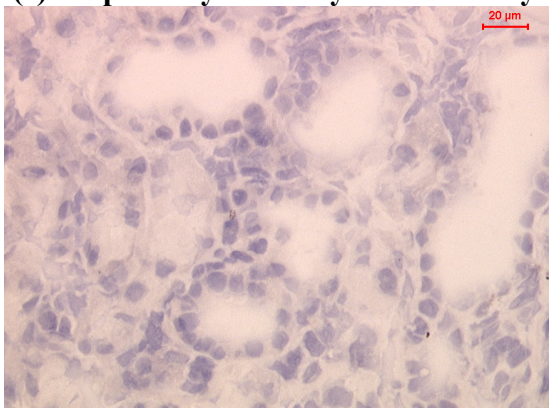

Figure 3.12- α-SMA staining of obstructed and contralateral kidney at three time points after ureteric obstruction

The degree of tubulointerstitial fibrosis, as determined by α-SMA staining of activated fibroblasts, was analysed using the point counting method illustrated in Chapter 2 and similar to that used to assess the percentage of interstitial expansion in PAS stained sections.

There was a significant difference between α-SMA staining in the obstructed compared to the contralateral kidneys in the UUO animals at all three time points (*p=0.0407, **p<0.0001 and ***p=0.0001). There was also a significant increase in the α-SMA staining of obstructed UUO kidney between 3, 7 and 10 days (p<0.0001).

Each group consisted of four mice with error bars depicting the standard error of the mean.

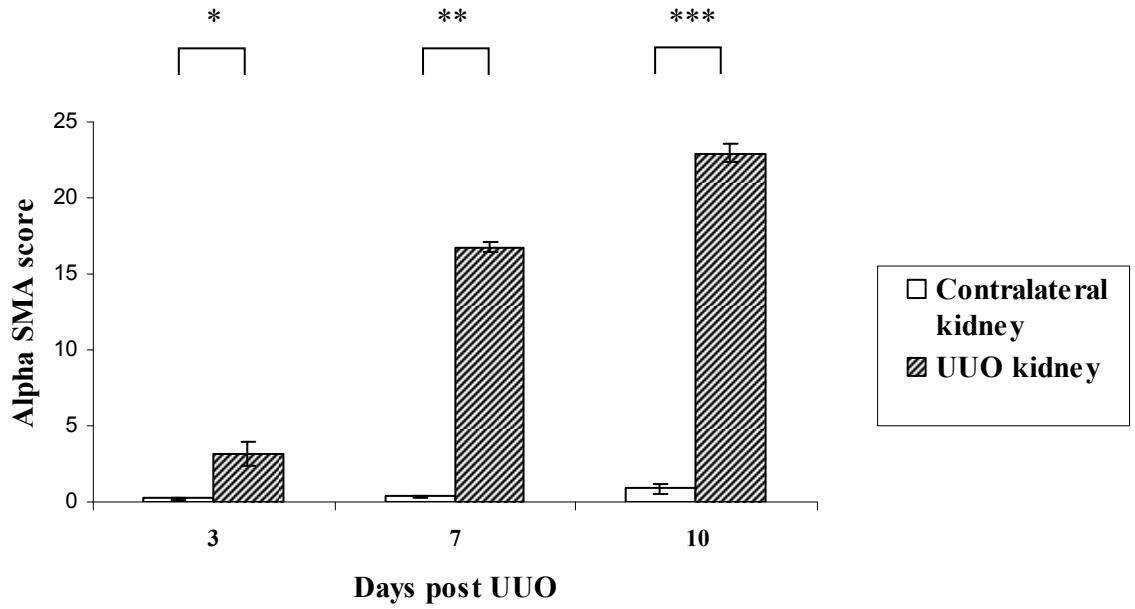

Figure 3.13- Collagen I staining of obstructed kidney 3, 7 and 10 days after UUO

The degree of tubulointerstitial fibrosis, as determined by staining the extracellular matrix protein collagen I, was assessed for normal and UUO kidney at 3, 7 and 10 days post obstruction. The percentage of the interstitial space stained by collagen I, as determined by the Q-win pixel intensity function, was calculated for ten non-overlapping HPF per mouse and the mean percentage was determined for each mouse. Finally the mean percentage of collagen I staining was calculated for the group of four mice at each time point.

The increase in Collagen I staining between normal kidney and obstructed kidney was seen as early as three days after obstruction, where a significant increase was detected (*p=0.0425). There were then significant increases in collagen I deposition in UUO kidney tissue between 3, 7 and 10 days post obstruction (p=0.0003).

Each group consisted of four mice with error bars depicting the standard error of the mean.

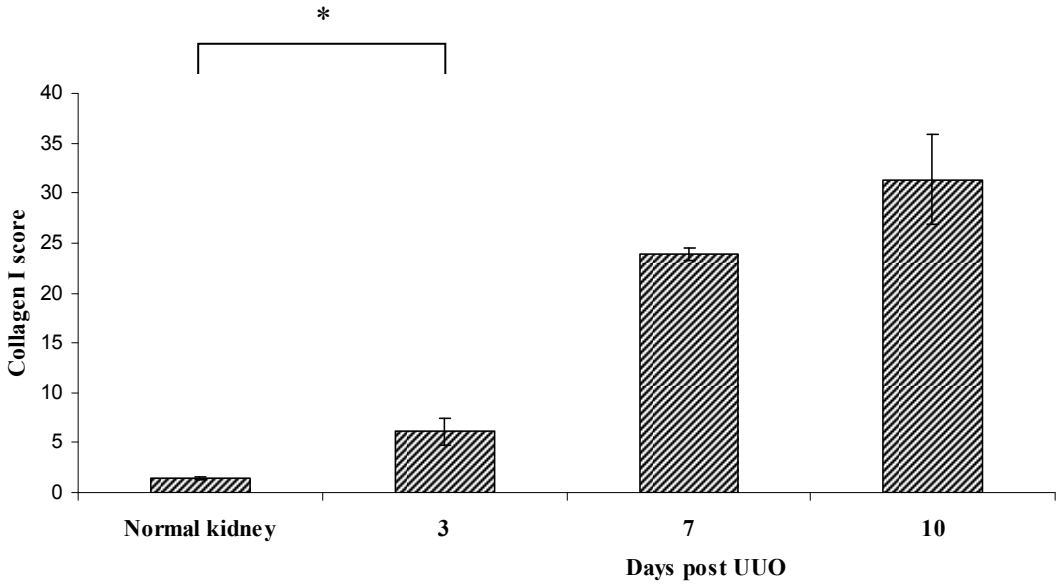

3.4 Assessing the phenotype of the infiltrating T lymphocytes

After demonstrating that the cellular infiltrate into the tubulointerstitium post UUO correlated with progressive injury and markers of fibrosis, an assessment was made to determine whether the infiltration could be actively contributing to progressive renal injury. In order to do this infiltrating T lymphocytes were examined for markers of activation and proliferation, suggesting they had effector functions. If the infiltrating T cells did not demonstrate evidence of activation or proliferation it would imply they were naive cells which had not yet recognised their cognate antigen and suggested they were trafficking through the injured tissue in response to the inflammatory chemokine gradient but not actively participating in the injury.

My hypothesis was that lymphocytes were playing an active role in promoting tubulointerstitial injury in UUO and contributing to the development of fibrosis.

3.4.1 Characteristics of activated T lymphocytes

In order to assess whether T cells within the UUO kidney were activated, well recognised surface markers of effector and memory T cell phenotype were used: CD69 and CD44. Using primary fluorochrome labelled antibodies to CD69 or CD44, immunofluorescent staining was performed on frozen sections of UUO kidney at 3, 7 and 10 days post obstruction, using groups of four mice at each time point. The sections were also dual stained with a FITC linked antibody to either CD4 or CD8. They were then assessed using the confocal laser scanning microscope and processed using Leica TCS-NT software. The images were then analysed using Photoshop software to determine the percentage of dual positive cells, which represented the activated T cell population as explained in Chapter 2. Since previous work demonstrated very little or no lymphocyte infiltration into sham operated kidney, the contralateral kidney of a UUO animal and normal kidney, these tissues were not assessed.

3.4.1.1 Activated CD69+ T cells in UUO kidney

CD69 is one of the earliest cell surface antigens expressed by T cells following activation (Cosulich, Rubartelli et al. 1987). Once expressed, CD69 acts as a co-stimulatory molecule for T cell activation. Importantly, the expression of CD69 after lymphocyte activation is transient, lasting only for a matter of hours, and therefore the subsequent lack of CD69 staining does not imply that lymphocytes were not activated (Santis, Lopez-Cabrera et al. 1995). A PE labelled antibody to the CD69 antigen was

used which was excited at a wavelength of 488nm and emitted light once activated at 578nm (Figure 3.14).

Consistent with the immunohistochemical findings presented in Figure 3.4, immunofluoresent staining demonstrated increasing numbers of CD4+ and CD8+ cellular infiltrates at successive time points post obstruction and CD4+ T cells predominated in number over CD8+ cells at all three time points. When these lymphocytes were further examined for dual staining with CD69, a group of CD4+ and CD8+ cells were shown to stain positively for CD69 at all three time points post UUO. This suggested that a proportion of the total T cell infiltrate had been recently activated (Figures 3.15 and 3.16).

There was an increase in the percentage of dual stained CD4+ cells between 3 and 7 days of obstruction, and a subsequent fall in dual staining by day 10 . In the day 7 UUO kidney the mean percentage of dual stained CD4+ T cells, implying recent activation, was approximately 44%. There was a sequential significant increase in the percentage of dual stained CD8+ cells between 3, 7 and 10 days ($p=0.0001$), with approximately 55% of all CD8+ cells being dual stained after 10 days of UUO. Interestingly the percentage of recently activated CD4+ T cells was significantly greater that the percentage of CD8+ cells 3 days after UUO ($p=0.0023$) but conversely after 10 days of obstruction there were significantly more recently activated CD8+ than CD4+ T cells ($p=0.0178$) (Figure 3.17).

In order to demonstrate co-localisation of FITC and PE staining on an individual cell the confocal software assembled the image in an X-Z stack (Figure 3.18) and plotted the pixel colour of the region of interest on a cytofluorogram (Figure 3.19). It was not possible to perform these two analyses on each dual positive cell that was counted and so a random selection was examined in this way. In all the samples reviewed this confirmed that dual positivity was due to dual staining of the same cell, rather then two single positive cells stacked on top of one another.

Isotype control antibodies labelled with FITC and PE confirmed there was no confounding non-specific antibody binding (Figure 3.20). Tubular epithelial cells demonstrated auto-fluorescence on non-stained sections. This was minimal and therefore no counter-stain was required however, it was useful for orientation within the section.

Both the FITC and PE fluorochromes were excited by the same blue argon laser at a wavelength of 488nm. The FITC labelled image was detected at around 520nm, whilst the PE labelled was detected at around 578nm. As illustrated in Figure 3.14, there was a possible area of crossover of emission between the two detection channels. It was important to minimise this to ensure only CD69 single positive cells were detected in the red 578mn channel and not also in the 520nm green channel and vice versa for FITC labelled cells. To guard against this the laser intensity and gain were adjusted and the detection range for a given fluorochrome was narrow. In order to review this, single staining of tissue sections was always performed and examined as a control. Furthermore the aim was to analyse sections that contained both single positive FITC and PE cells and dual positive cells to ensure the fluorochrome was detected in the correct channel. To maintain standardisation the detection wavelengths were constant throughout all the experiments.

Figure 3.14- Fluorescence spectrum of the fluorochromes FITC and PE

Both fluorochromes were excited by the same laser at 488nm, however the FITC labelled images were detected at around 520nm and the PE labelled images at around 578nm. The two fluorescent spectrums do overlap and therefore there was a possible area of crossover of emission between the two detection channels.

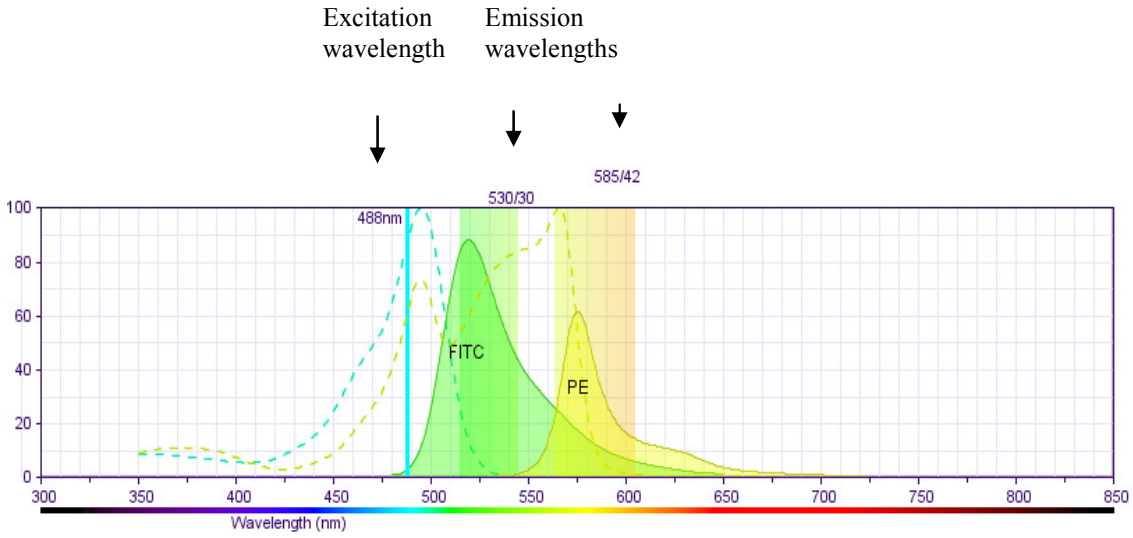

.

Figure 3.15- Immunofluorescent dual staining of FITC labelled CD4+ cells and PE labelled CD69+ cells in the interstitium of the UUO kidney at three time points

Dual staining with monoclonal antibodies conjugated to fluorochromes was carried out on UUO kidney. FITC was conjugated to the CD4 antibody (green cells) and PE to the CD69 antibody (red cells). Dual stained cells were yellow (arrow). The number of infiltrating CD4+ cells increased with time post UUO and the percentage of dual positive cells peaked at day 7. At all time points single positive CD4 cells were seen and represented naive CD4+ cells (or previously activated CD4+ cells) whilst single positive CD69 cells were activated CD4- T cells (activated CD8+ cells). Magnification x63.

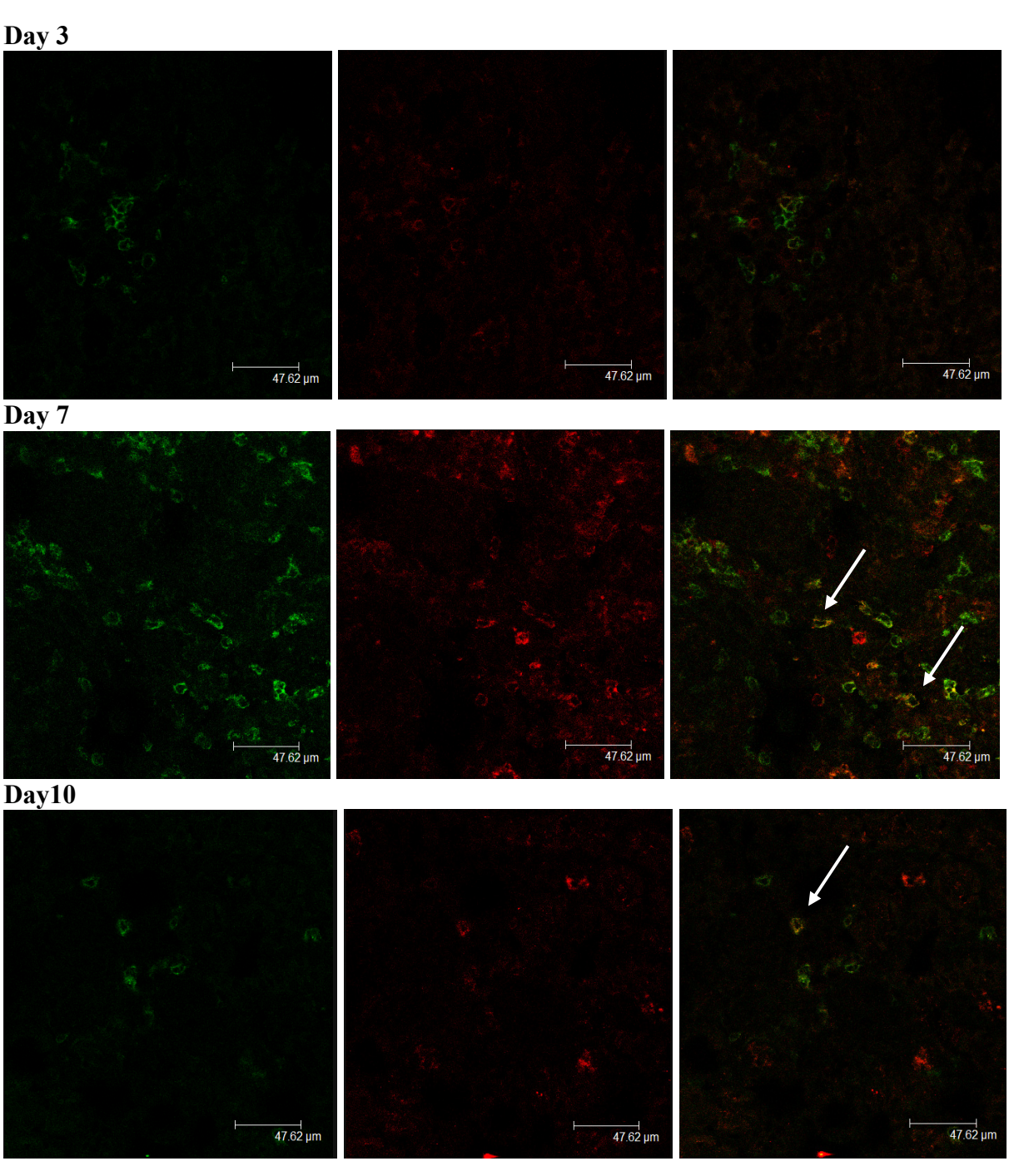

Figure 3.16- Immunofluorescent dual staining of FITC labelled CD8+ cells and PE labelled CD69+ cells in the interstitium of the day 3, 7 and 10 UUO kidney

Dual staining was performed on UUO kidney with monoclonal antibodies conjugated to fluorochromes. FITC was conjugated to the CD8 antibody (green cells) and PE to the CD69 antibody (red cells). Dual stained cells were yellow (arrow). The number of infiltrating CD8+ cells increased with time post UUO and the percentage of dual positive cells peaked at day 10. At all time points single positive CD8 cells seen represented naive CD8+ cells (or previously activated CD8+ cells) whilst single positive CD69 cells were activated CD8- T cells (activated CD4+ cells). Magnification x63.

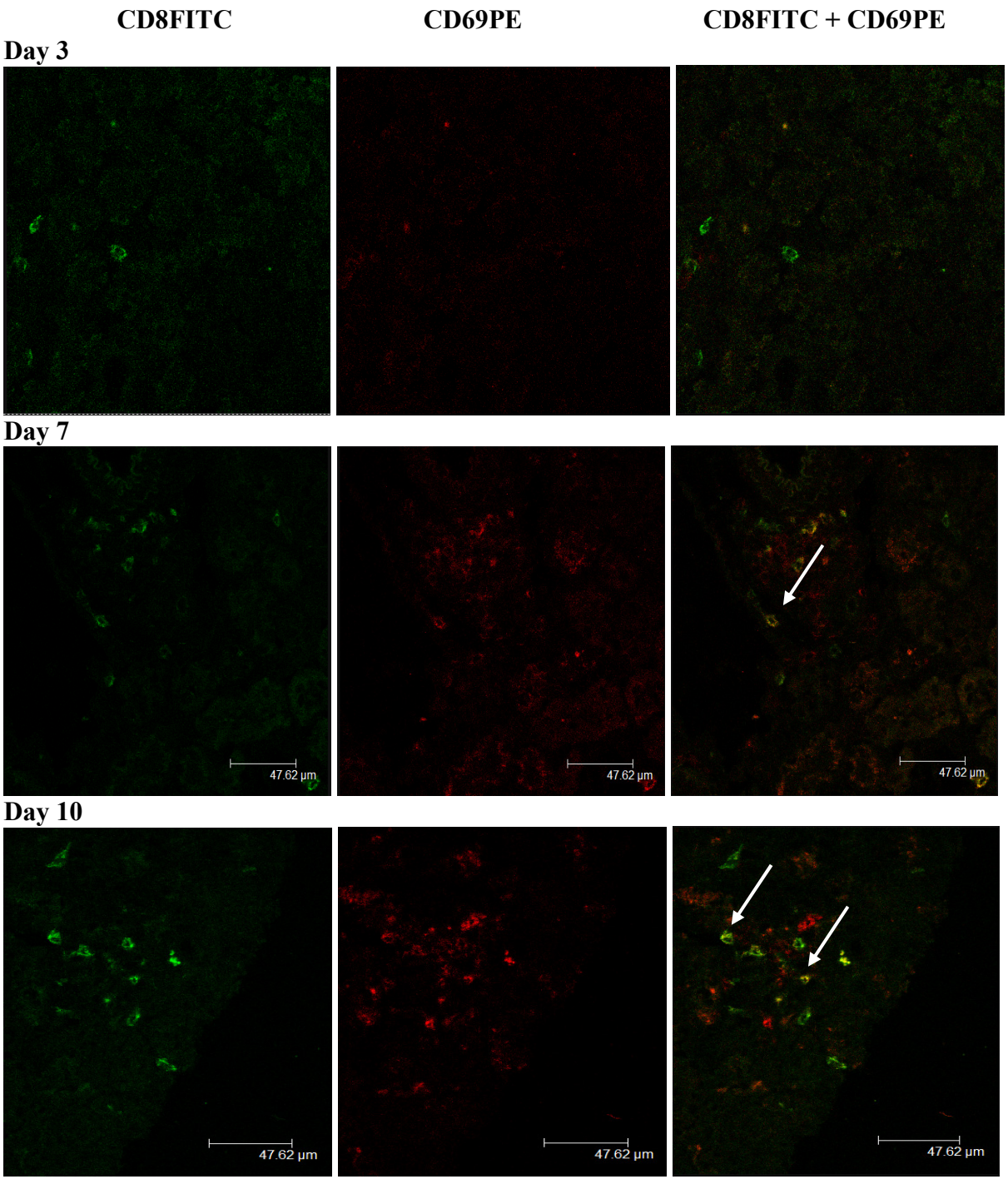

Figure 3.17- Percentage of CD69+ T lymphocytes infiltrating UUO at 3, 7 and 10 days after obstruction

The number of single and dual positive CD4+ and CD8+ cells were quantified by examining between five and ten random non-overlapping HPFs at x63 magnification for each UUO kidney. The percentage of dual positive cells was calculated for each HPF and the mean percentage per HPF calculated for each mouse. Subsequently the mean percentage per HPF was calculated for the group of four mice at each time point.

At all three time points CD4+ and CD8+ T cells were dual stained with CD69. The peak percentage of dual positive CD4+ T cells was found at day 7, when approximately 44% of CD4+ T cells were dual staining. In contrast there was a significant sequential increase in the percentage of dual stained CD8+ cells between day 3, 7 and 10 (***p=0.0001), with approximately 55% of the population being dual stained at 10 days following UUO. The percentage of recently activated CD4+ T cells was significantly greater that the percentage of CD8+ cells at day 3 (*p=0.0023) and by day 10 there was a significantly higher proportion of recently activated CD8+ cells compared to CD69+CD4+ cells (**p=0.0178).

Each group consisted of four animals with error bars depicting the standard error of the mean.

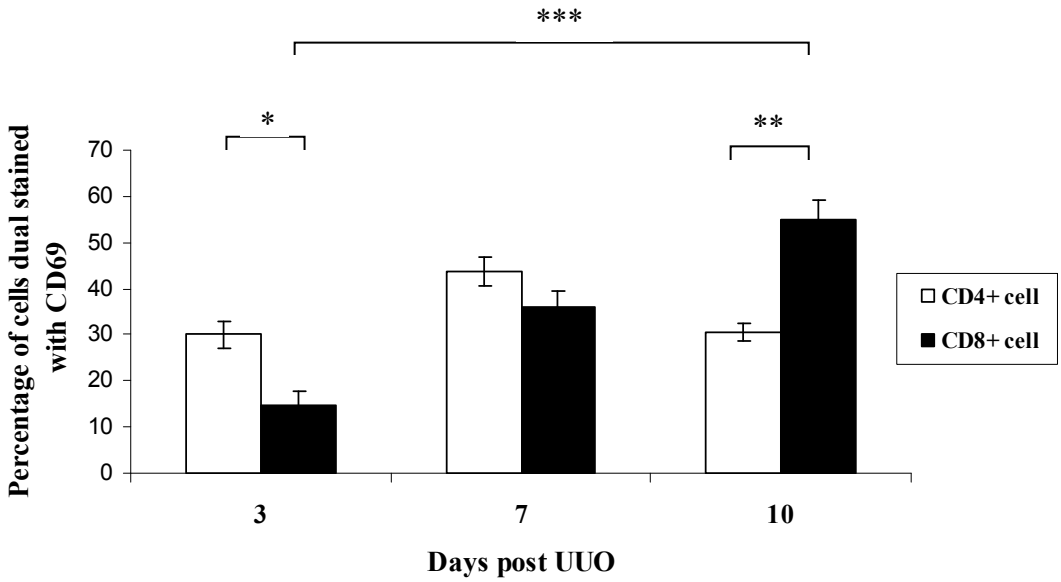

Figure 3.18- Immunofluorescent staining of FITC labelled CD8+ and PE labelled CD69+ cells in a region of interest in UUO kidney with an X-Z stack of that region

Immunofluorescent staining was performed with FITC conjugated to the CD8 antibody (green cells) and PE to the CD69 antibody (red cells). Dual stained cells were yellow. To determine whether the dual staining was due to two single positive FITC+ and PE+ cells lying in the same X-Z plane, or whether the two cell surface fluorochromes co-localised to the same cell, the confocal software assembled the image in the X-Z plane at the region of interest (ROI), the X axis shown in (a) and (b). FITC and PE staining was present at the same distance along the Z axis and overlapped on the merged image, illustrating the image was generated from a single activated CD8+ cell (c).

(a) ROI: CD8FITC

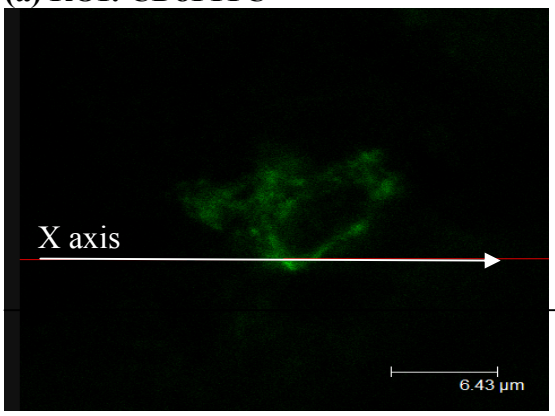

(b) ROI: CD8FITC + CD69PE

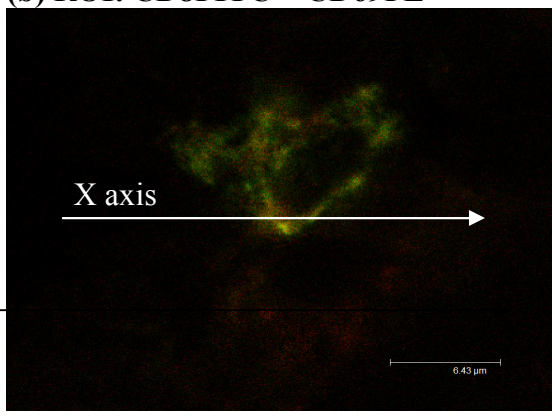

(c) X-Z stack of above ROI

CD8FITC

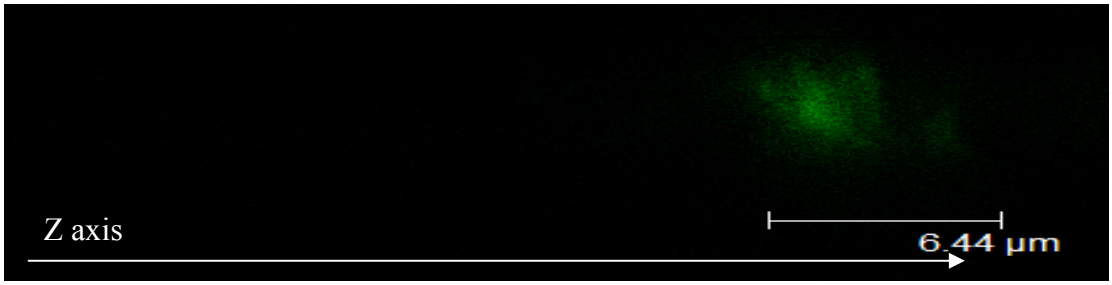

CD69PE

Merge

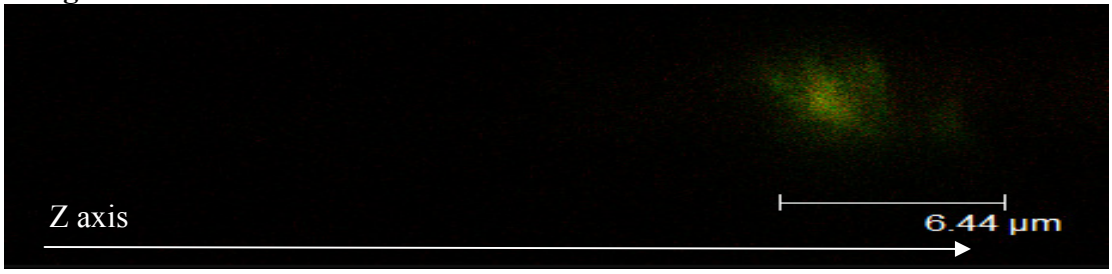

Figure 3.19- Immunofluorescent dual staining of FITC labelled CD8+ cells and PE labelled CD69+ cells in a day 7 UUO kidney with a cytofluorogram of the ROI

Immunofluorescent staining was performed using a FITC conjugated CD8 antibody (green cells) and PE conjugated CD69 antibody (red cells). When the two pictures were merged, dual staining produced yellow cells (a). The cytofluorogram is a graphical representation of the staining of each pixel in the ROI, on a plot of FITC (x axis) v PE (y axis) (b). As illustrated the predominant population of points lie equidistant between the X and Y axes, demonstrating that the majority of pixels were dual stained and co-localised. Scale as shown.

(a) ROI:CD8FITC **ROI:CD69PE** **ROI:CD8FITC+ CD69PE**

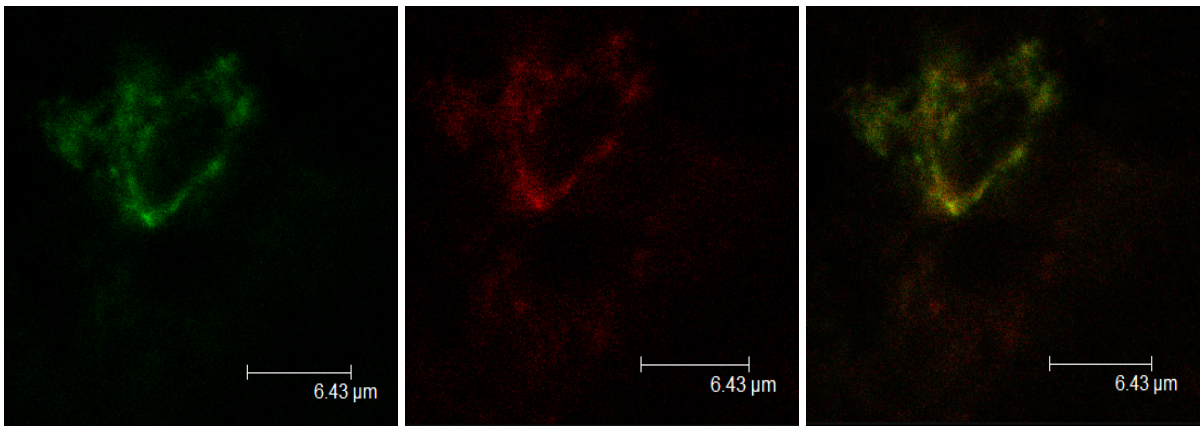

(b) Cytofluorogram

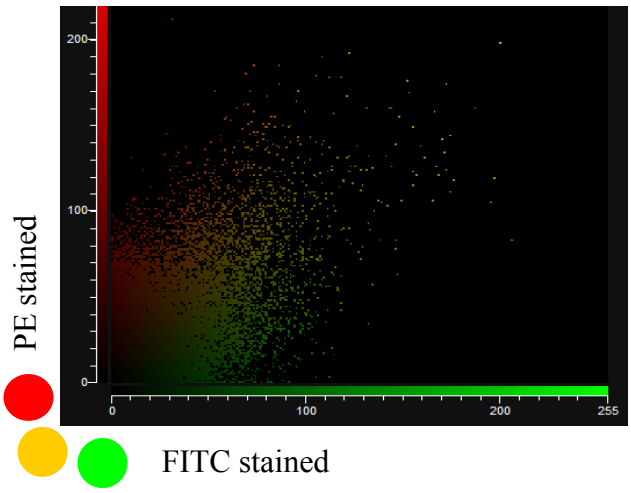

Figure 3.20- Immunofluorescent staining with FITC and PE labelled isotype control antibodies on day 7 UUO kidney and a section with no primary antibody

Immunofluorescent staining was performed with FITC and PE labelled isotype controls to look for non-specific antibody binding ((a) and (b)). This demonstrated minimal background staining of the renal tubular epithelial cells and blood vessel walls. No infiltrating cells were stained showing that the monoclonal antibodies used to detect CD4+, CD8+ and CD69+ cells were specific. An unstained UUO kidney section was assessed using the 488nm excitation laser to examine for auto-fluorescence (c). The renal tubular epithelial cells did demonstrate minimal auto-fluorescence, which was useful for orientation within the section and therefore no counter-stain was required. Magnification x63.

(a) FITC isotype control **(b) PE isotype control** **(c) No primary**

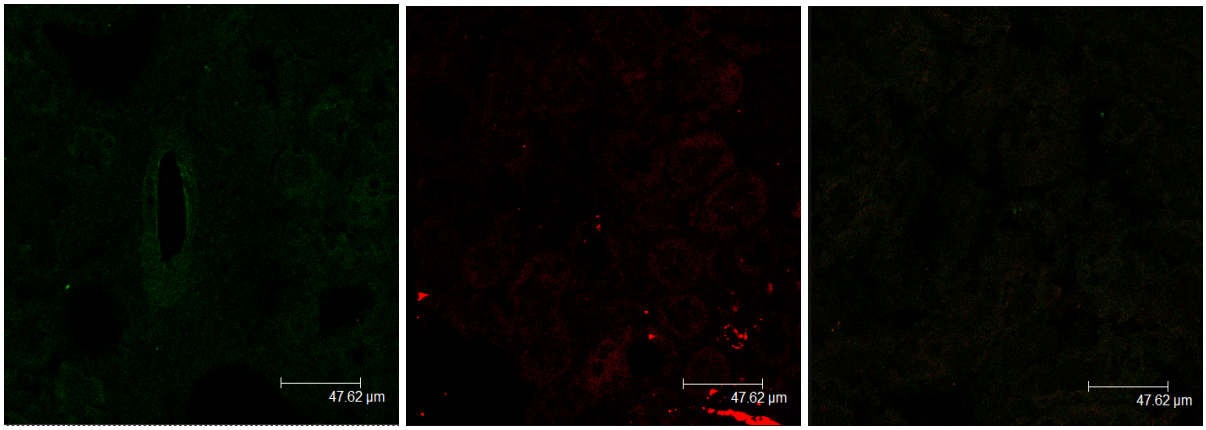

3.4.1.2 CD44+ memory T cells

CD44 is a type I transmembrane glycoprotein expressed on the surface of numerous cell types including leukocytes, fibroblasts, epithelial and endothelial cells. It is a major receptor for the ubiquitous glycosaminoglycan component of extracellular matrix, hyaluronic acid, when in an activated state but has also been shown to be a receptor for other ligands (Lesley and Hyman 1992). T cell expression of CD44 differs according to the cell's stage of differentiation and activation status. At early stages in lymphocyte development precursors in the thymus express high levels of CD44 but later during thymocyte development CD44 expression is down-regulated. Naive T cells in secondary lymphoid structures continue to be CD44 low. After T cell activation there is a rapid increase in CD44 cell surface expression, conversion of CD44 to its active form and hyaluronic acid binding. Memory T cells are typically CD44 high.

It is believed that CD44 contributes to the regulation of T cell migration in two ways. Firstly, CD44 is important in helping T cell precursors to migrate into the thymus and therefore has a role in T cell development (Wu, Kincade et al. 1993). Secondly, CD44 mediates the extravasation of mature activated T cells into areas of inflammation (DeGrendele, Estess et al. 1997). On other cell types CD44–hyaluronic interactions have been shown to mediate cell adhesion and migration (Lesley, Hyman et al. 1993).

An APC labelled antibody to the CD44 antigen was used which was excited at a wavelength of 630nm and emitted light at 660nm. Since CD44 is expressed by many cells, CD44 staining was seen widely within the renal tissue. However, differentiation between naive lymphocytes which had low levels of CD44 expression and memory lymphocytes which had high CD44 expression was possible because the cells were dual labelled with antibodies to either CD4 or CD8.

Ten days following UUO, populations of both CD4+ and CD8+ lymphocytes were found to be CD44+ (Figure 3.21) suggesting a population of activated lymphocytes with a memory phenotype. There was also a large number of cells which were only CD44+ and represented the numerous other cell types which display CD44.

Figure 3.21- Immunofluorescent dual staining of FITC labelled CD4+ or CD8+ cells and APC labelled CD44+ cells in the interstitium of day 10 UUO kidney

Dual staining with monoclonal antibodies conjugated to fluorochromes was carried out on UUO kidney tissue at 10 days following obstruction. FITC was conjugated to the CD4 (a) and CD8 (b) antibodies (green cells) and APC to the CD44 antibody (blue cells). When the two pictures were merged, dual stained cells became pale blue in colour. There were large amounts of lymphocyte negative CD44+ cell staining. However, there were populations of CD4+ and CD8+ lymphocytes which were CD44+, suggesting they were activated and had a memory phenotype (arrow). Magnification x63.

(a) CD4FITC CD44APC CD4FITC + CD44APC

Day 10 UUO kidney

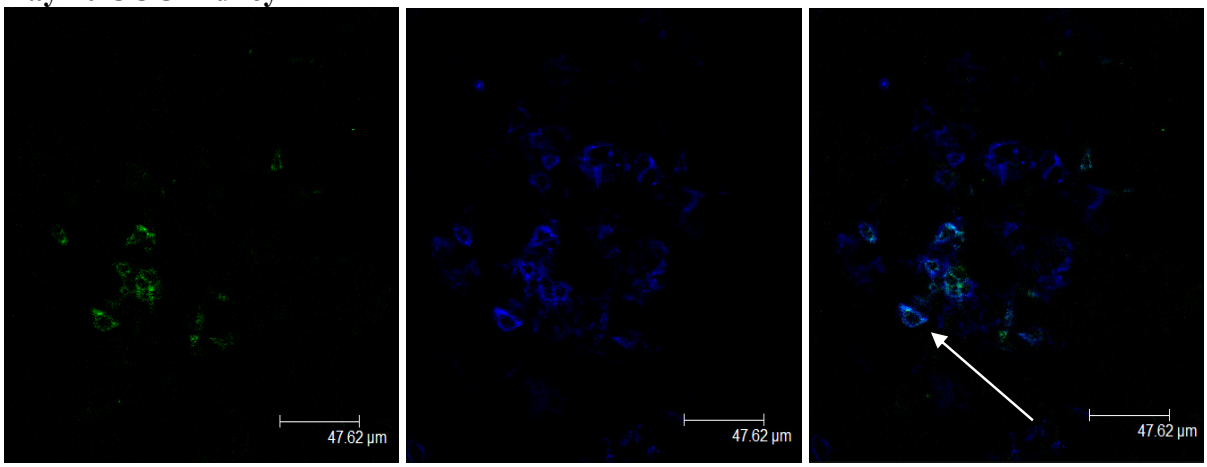

(b) CD8FITC CD44APC CD8FITC + CD44APC

Day 10 UUO kidney

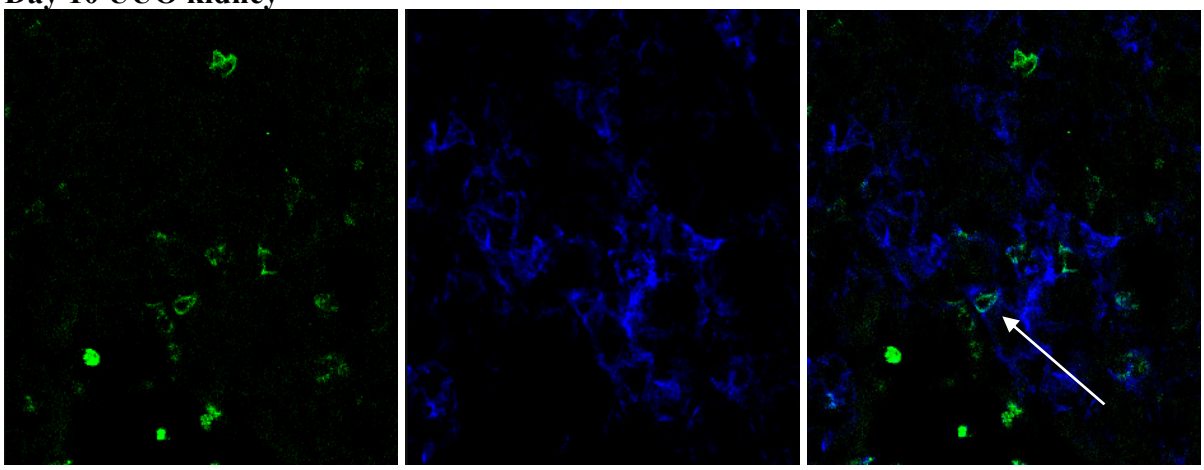

3.4.1.3 Proliferating Ki67+ T cells

Ki67 is a nuclear antigen expressed on all proliferating cells during late G_1, S, G_2 and M phases of the cell cycle and is absent from resting cells in G_0. Immunofluorescent staining was performed with a TRITC labelled antibody to the Ki67 nuclear antigen, which was excited at a wavelength of 560nm and emitted light at 578nm.

This technique demonstrated there were very few CD4+ and CD8+ proliferating cells at day 3 following UUO however, by 7 and 10 days proliferating lymphocytes were seen (Figures 3.22 and 3.23). Adding a further nuclear stain, DAPI, allowed improved localisation of the cells within the tissue architecture, especially the Ki67 negative cells (Figure 3.24). At all time points some of the Ki67+ cells identified were CD4- and CD8- when serial sections were reviewed. A number of these proliferating cells co-localised to tubular epithelial cells, identified by their auto-fluorescence (Figure 3.25). Alternative explanations for these cells may be an unconventional population of proliferating double negative T cells, of the type described by Rabb et al in normal mouse kidney (Ascon, Ascon et al. 2008), or a proliferating population of macrophages. At day 10 following UUO the mean percentage of proliferating CD4+ cells were 33% and dual positive CD8+ cells 22%, which was not significantly different ($p=0.3611$) (Figure 3.26).

As explained for the fluorochromes FITC and PE, there was a risk of detecting emission from one fluorochrome in the detection channel of the other fluorochrome due to overlapping of the two emission spectra. This was also the case for the two fluorochromes used here, FITC and TRITC therefore similar precautions were taken to minimise this as explained earlier.

Figure 3.22- Immunofluorescent dual staining of FITC labelled CD4+ and TRITC labelled Ki67+ cells in the interstitium of the UUO kidney at three time points

Dual staining with monoclonal antibodies conjugated to fluorochromes was carried out on UUO kidney tissue at 3, 7 and 10 days following obstruction. FITC was conjugated to the CD4 antibody (green cells) and TRITC to the Ki67 antibody (red nuclear staining). Dual labelled cells were seen at all three time points post obstruction, demonstrating CD4+ lymphocyte proliferation (arrow). Magnification x63.

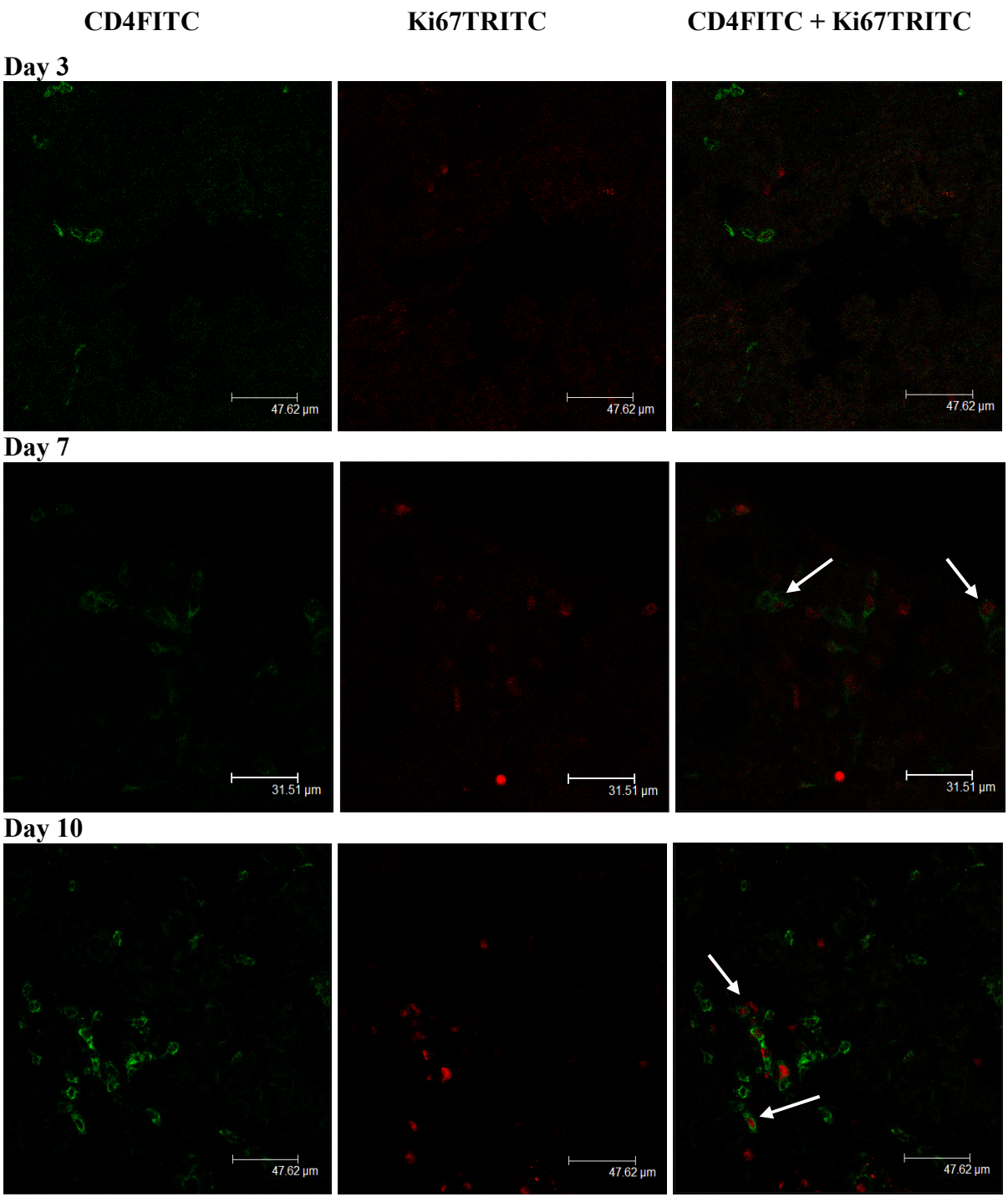

Figure 3.23- Immunofluorescent dual staining of FITC labelled CD8+ and TRITC labelled Ki67+ cells in the interstitium of day 3, 7 and 10 UUO kidney

Dual staining with monoclonal antibodies conjugated to fluorochromes was performed on UUO kidney tissue. FITC was conjugated to the CD8 antibody (green cells) and TRITC to the Ki67 antibody (red nuclear staining). The number of infiltrating CD8+ cells increased with time post obstruction however, were fewer in number that the CD4+ population. Dual labelled cells were seen at all three time points post UUO, demonstrating CD8+ cell proliferation (arrow). Magnification x63.

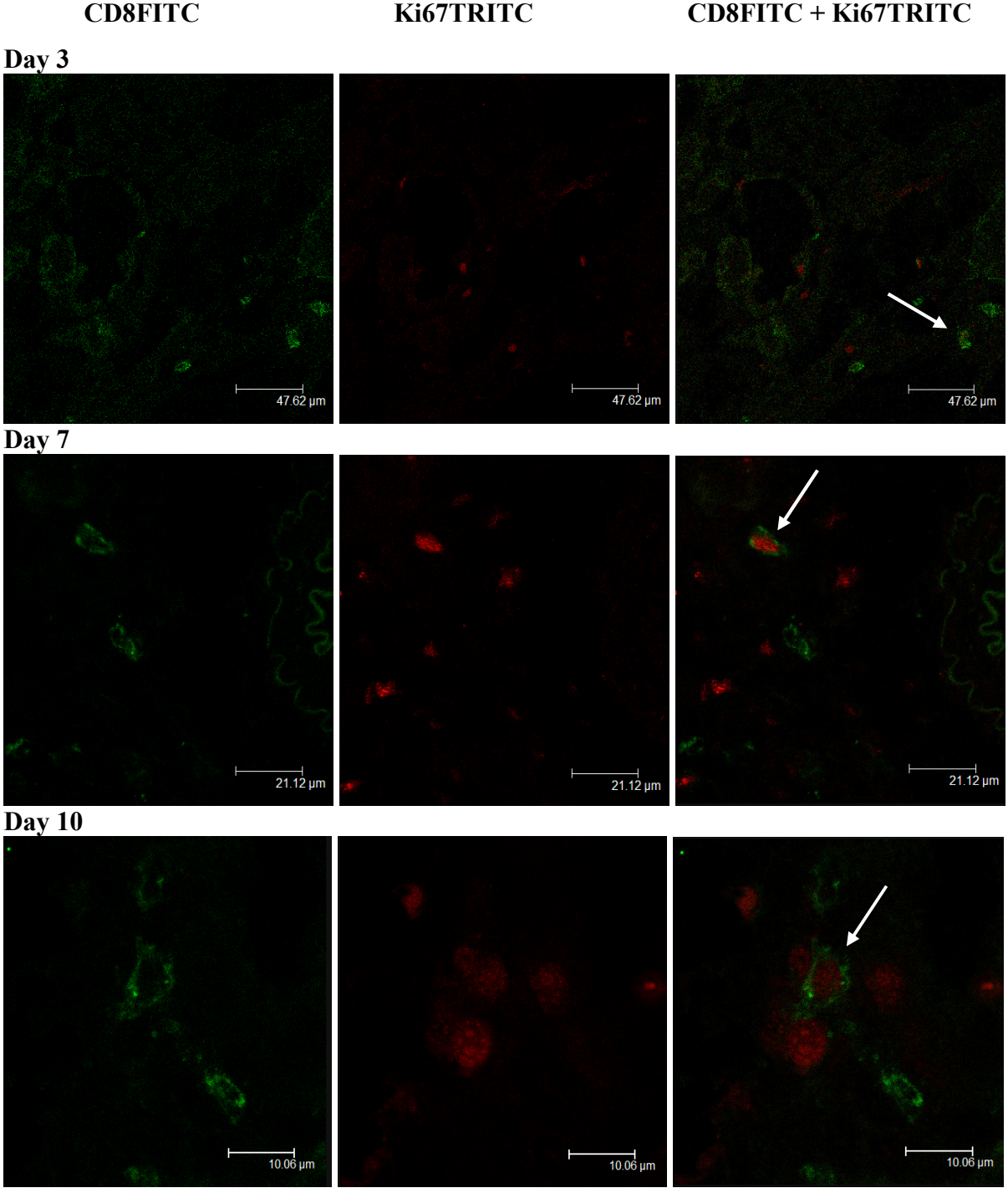

Figure 3.24- Immunofluorescent triple staining of FITC labelled CD4+ cells, TRITC labelled Ki67+ cells and DAPI in UUO kidney at 7 days post obstruction

Immunofluoresent staining of a day 7 UUO kidney using FITC labelled CD4 (green cells) and TRITC labelled Ki67 (red nuclear staining) antibodies, with DAPI (blue nuclear staining). Proliferating and non-proliferating CD4+ cells were demonstrated along with proliferating CD4- cells. DAPI staining provided better localisation of the non-proliferating CD4+ cells. Magnification x63.

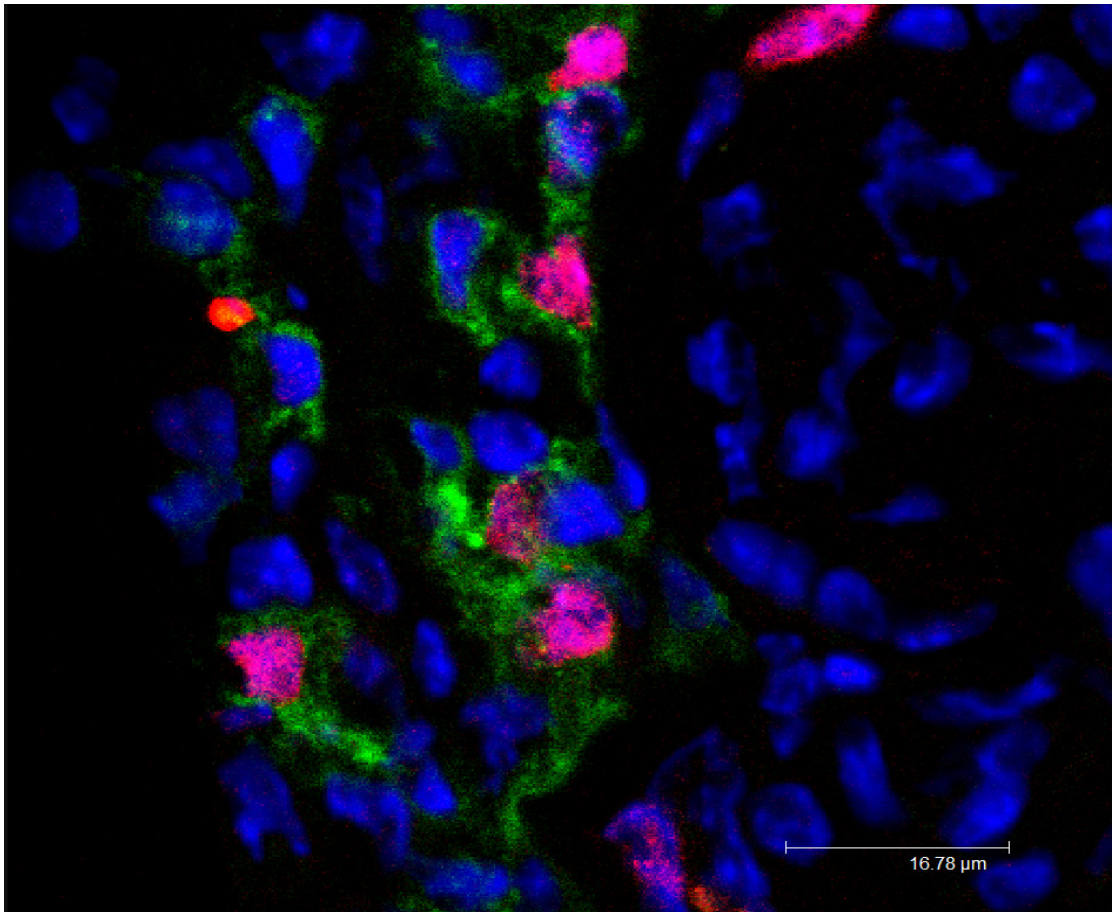

Figure 3.25- Immunofluorescent staining with a TRITC labelled antibody to Ki67 demonstrating proliferating tubular epithelial cells in the day 10 UUO kidney

Immunofluorescent staining with the nuclear Ki67 antigen conjugated to the TRITC fluorochrome was carried out alone. Auto-fluorescence allowed localisation of the tubular epithelial cells, some of which were Ki67 positive and therefore proliferating (arrow). Magnification x63.

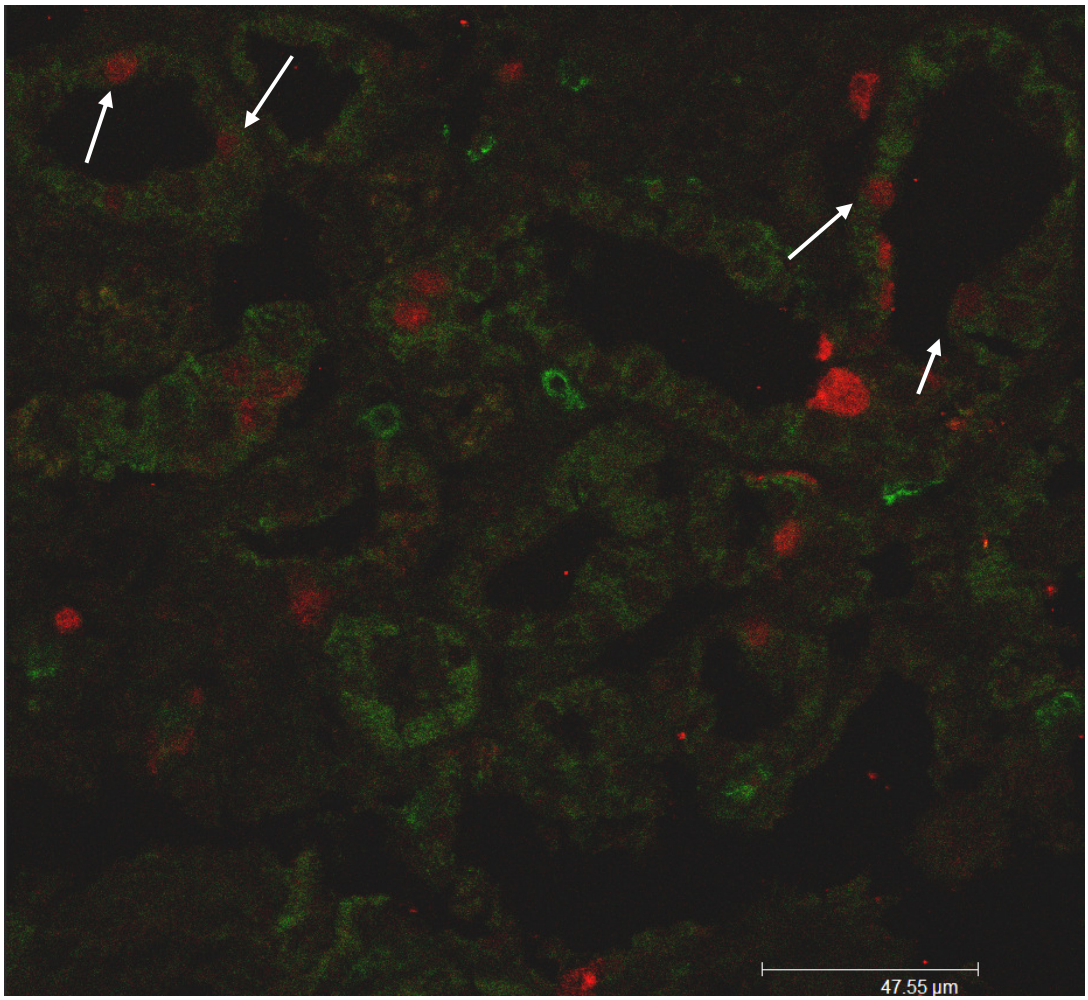

Figure 3.26- Number of proliferating CD4+ and CD8+ T cells at 10 days post UUO
The number of single and dual positive CD4+ and CD8+ cells was quantified by analysing between five and ten random non-overlapping HPFs of day 10 UUO kidney, for a group of four mice. The total numbers of single and dual positive cells were counted for each HPF and the mean number per HPF calculated for each mouse. Subsequently the mean number per HPF was calculated for the group of four mice.

There was a non-significant difference in the mean percentage of proliferating CD4+ and CD8+ cells at 10 days post obstruction, where 33% of the CD4+ cells and 22% of the CD8+ cells were Ki67+ ($p=0.3611$).

Each group consisted of four mice with error bars depicting the standard error of the mean.

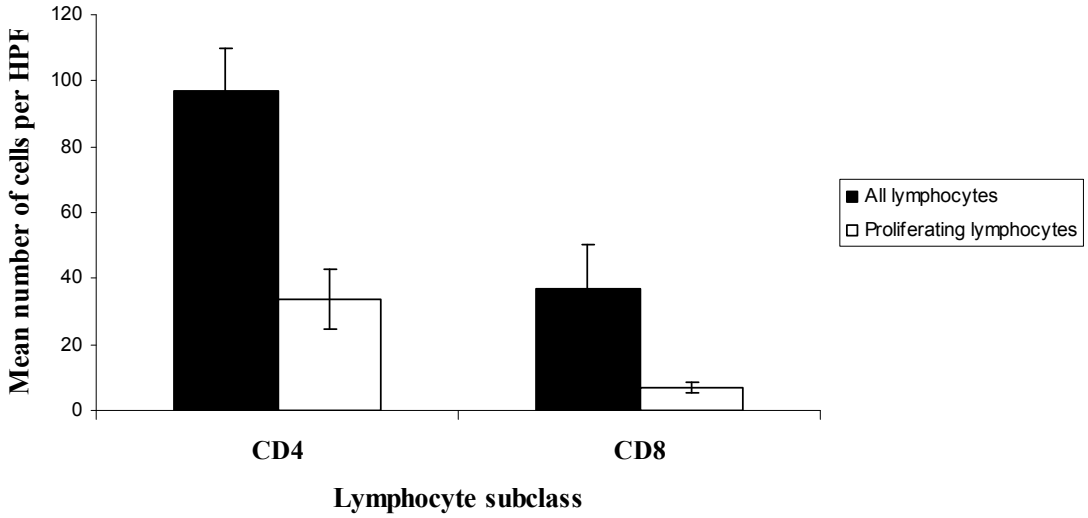

3.5 Discussion

The role of the inflammatory infiltrate into the tubulointerstitium after a non-immunologically mediated injury like UUO is unknown and therefore this chapter set out to determine whether T lymphocytes may be playing a role in propagating progressive renal injury. Work using the UUO model by Shappell et al demonstrated that in severe combined immunodeficient mice there was no difference in injury seen after UUO compared to that induced in wild-type mice also subjected to the same method of injury (Shappell, Gurpinar et al. 1998). SCID mice have no mature T and B cells due to a variety of gene defects which impair the joining of coding sequences during VDJ recombination and prevent the production of the TCR and immunoglobulin. This work suggested that lymphocytic infiltrate was not required for progressive tubular injury and development of fibrosis in the UUO model. They speculated that the prominent macrophage infiltrate into the tubulointerstitium after UUO, independent of lymphocytes, may contribute to the progressive renal injury seen. Alternatively they suggested neither mononuclear cell type were involved and that 'fibrogenic factors', produced by damaged tubular epithelial cells, may induce fibrosis.

Work by other groups, including my own, produced contradictory findings to those of Shappell. Harris et al irradiated rats which then underwent ureteric obstruction (Harris, Schreiner et al. 1989). They demonstrated that irradiation abolished leukocyte infiltration post obstruction and improved post obstruction renal function compared to non-irradiated rats. Obstruction was only maintained for 24 hours, so better post-obstruction renal function after irradiation was unlikely to be caused by the development of less renal fibrosis but due to less acute inflammation causing acute tubular injury. Infiltration of both lymphocytes and macrophages was abolished in this model and so the cell type contributing to renal dysfunction was unclear.

However, my own group carried out work on recombinant arrangement gene-I knock out mice which underwent 14 days of UUO and found significantly less renal injury in the RAG-I KO mice than in wild-type UUO controls (Tapmeier, Fearn et al. 2010). Furthermore, by reconstituting these knockout mice with lymphocytes, injury was seen at the same level as that in the wild-type mice which had undergone UUO. In a further experiment RAG-1 KO mice reconstituted with CD4+ T cells, but not CD8+ lymphocytes, had significantly greater tubulointerstitial injury than RAG-1 KO mice injected with PBS after renal obstruction. This suggested that lymphocytes do play a

role in the progressive fibrotic injury of UUO and CD4+ cells may be the predominant T lymphocyte subclass.

There is also evidence from the work on the mouse UUO model by Niedermeier et al demonstrating that the differentiation and development of fibrocytes (haematopoietic cells which produce collagen I and contribute to fibrosis) are critically dependent upon CD4+ T cells (Niedermeier, Reich et al. 2009). Importantly the context in which T cells develop determines whether fibrocyte development is supported or inhibited. In vivo depletion of CD4+ cells, either by using T cell deficient SCID mice or antibodies, resulted in less CD4+ cells and less fibrocytes in the UUO kidney. There was also a positive correlation between the number of infiltrating fibrocytes and the degree of renal fibrosis in the obstructed kidney and they demonstrated that the cytokine environment in which the T cells developed was important. In vitro the presence of calcineurin inhibitors, activated CD4+ T cells allowed fibrocyte differentiation. This was hypothesised to be because of soluble pro-fibrotic factors e.g. TGF-β that were generated and a decrease in anti-fibrocyte factors e.g. IL-2, TNF and IFN-γ mediated by the calcineurin inhibitor.

Together the results from the groups led by Harris, Tapmeier and Niedermeier directly contradict those from the work in SCID mice by Shappell, demonstrating T cell involvement is pivotal to injury. These differences may have been due to the different strains of mouse used or their genetic backgrounds (Puri, Shakaib et al. 2010).

Since the above literature suggested that T lymphocytes play a critical role in promoting renal damage by the non-immunologically mediated injury of ureteric obstruction, my initial task was to determine whether there was a definite T cell infiltrate post obstruction and to characterise the phenotype of this infiltrate. This would allow me to determine whether these lymphocytes were capable of performing effector functions which could include promoting renal fibrosis.

My initial work carried out on UUO mice demonstrated a progressive increase in the number of mononuclear cells into the tubulointerstitium with increasing time after the non-immunologically mediated obstructive injury. The T cell infiltrate consisted of more CD4+ than CD8+ cells at each of the three time points, along with macrophages. The numbers of infiltrating cells post UUO were significantly greater than in the contralateral kidney of a UUO animal or in the kidney of an unmanipulated animal. The

progressive cell infiltration correlated with fibrotic renal injury, suggesting a causal relationship.

The next series of experiments established the T lymphocyte infiltrate was not a naive T cell population but that populations of both CD4+ and CD8+ T cells demonstrated an activated effector phenotype with CD69 positivity. A population of both CD4+ and CD8+ T cells in the UUO kidney were also shown to be proliferating, as demonstrated by staining for the nuclear proliferation marker Ki67. This effector T cell population was found especially at the later time points following 7 and 10 days of obstruction and certain T lymphocytes were shown to have a memory phenotype. Chapman et al demonstrated that recruitment of primed T cells into a site of infection is antigen independent. However, for T cells to carry out effector functions they must recognise antigen and be activated and proliferating (Chapman, Castrucci et al. 2005). My work showed that infiltrating T cells had effector function and therefore if conventional immunological mechanisms were to hold true the effector T cells must have recognised antigen. They would also be theoretically capable of contributing to the fibrotic renal injury seen in these animals.

If naive T cells were activated by UUO injury then the process of T cell activation and proliferation should take some days to develop and generate significant numbers of cells within the renal tubulointerstitial space. This would be consistent with my findings of increasing numbers of activated cells between 3 and 7 days. Time is required for the numerous processes needed for classical T cell activation to occur:

- Naive T cells must be attracted to the area of inflammation by a chemokine gradient established by the UUO injury and circulate between the tissue and draining lymph node
- Dendritic cells or other APCs must be activated to become professional APCs, with a loss of their phagocytic properties and increase in co-stimulatory molecules on their surface (Dong, Swaminathan et al. 2005)
- Dendritic cell must process antigen and present it with MHC on the DC cell surface
- T cells must then recognise the peptide-MHC complex on the DC cell surface and with co-stimulation become activated

- Activated T cells must then traffic back into the injured kidney from the draining lymph node to carry out their effector functions, which may involve contributing to renal injury

It would have been interesting to look at earlier time points, before 3 days of obstruction. This would have allowed me to confirm that the development of a population of activated T cells within the UUO interstitium takes days rather than hours to develop. Certainly my experiments demonstrated very few mononuclear cells in the tubulointerstitium after 3 days of obstruction and this would suggest that the development of the effector population takes days to achieve. If significant numbers of activated T cells were found at much earlier time points, possibly even within hours of obstruction, this would suggest that they were not activated de novo by traditional immunological methods. One possible explanation for the presence of activated lymphocytes within hours of injury could be that a naive population of T cells was activated independent of antigen, which has been described (Rodriguez-Iturbe, Pons et al. 2001).

An alternative explanation for the presence of activated T cells before 3 days of renal obstruction could be that they were lymphocytes which were activated elsewhere in the body in response to an unassociated foreign antigen. Subsequently these activated lymphocytes were attracted to the area of obstructive injury by the chemokine gradient developed by renal cells in response to the increased pressure and ischaemia generated post ureteric obstruction. One possible source would be an activated lymphocyte population residing within the gut, which had been activated by recognition of gut pathogens. If this was the explanation then the infiltrating population would demonstrate an activated effector phenotype from the outset rather than the population progressively developing effector functions, as I have shown.

Resident renal α:β T cells are present within normal kidney (Ascon, Ascon et al. 2008) and Dong et al described a resident population of memory cells within normal kidney prior to UUO injury (Dong, Bachman et al. 2008). If these memory cells were re-exposed to their cognate antigen during UUO injury, they would be more rapidly activated than a population of naive T cells presented with antigen for the first time however, even this process would take some hours/days.

Interestingly, from the three time points I investigated post obstruction the peak time at which CD4+ and CD8+ cells became activated differed. There was a significantly

higher percentage of activated CD4+ cells at the earlier time points but significantly higher percentage of activated CD8+ cells at the latest time point of day 10 ($p<0.05$). In order for naive CD8+ T cells to become armed effector cells they require more co-stimulation that CD4+ T cells. This requirement can be met by either dendritic cells, activated CD4+ T cells or a combination of both. Mature dendritic cells have the highest co-stimulatory capacity of all APCs and are able to activate CD8+ T cells directly. However, some CD8+ cells still require the presence of effector CD4+ T cells during the priming of the naive CD8+ cell, which helps to activate the APC to produce higher levels of co-stimulatory activity. Once CD4+ cells are activated, the CD40 ligand on the T cell binds CD40 on the APC. This in turn induces further B7 expression on the APC and more co-stimulation, allowing CD8+ cell activation and production of IL-2. This occurs only when both the naive CD8+ cell and the activated CD4+ cell recognise related antigens on the surface of the APC. Assuming the lymphocytic infiltrate in UUO contributes to renal injury, then my data would be consistent with a mechanism by which naive CD4+ and CD8+ cells are activated in response to antigen exposure but that CD8+ T cell take longer to be activated due to the need for activated CD4+ T cell help.

My work suggests that as a consequence of the non-immunologically mediated obstructive injury to the kidney, T cells are capable of infiltrating obstructed kidney and demonstrate a phenotype which would be capable of initiating and promoting renal fibrotic injury. The postulated mechanisms by which activated T lymphocytes may propagate destructive renal fibrosis after UUO have been discussed, along with suggestions regarding which sub-groups of CD4+ lymphocyte may be involved. There was also a strong correlation between the progressive increase in macrophage number with increasing time of ureteric obstruction and destructive injury. As previously discussed macrophages have the potential to synthesise molecules which could contribute to renal injury and I postulate are most likely to work with and along side lymphocytes to cause fibrosis in the obstructed kidney. B cells and neutrophil infiltration was not assessed as previous literature had not found significant cellular infiltration by these cell types after UUO (Schreiner, Harris et al. 1988).

There are a number of technical issues that merit discussion from this chapter including the use of the monoclonal antibodies to F4/80 antigens to characterise macrophages and CD44 antigens to identify memory lymphocytes, along with the methods by which renal injury was assessed. The most widely used marker for macrophage identification in

mice in the literature is the cell surface antigen F4/80. However, there have been reports of the F4/80 antigen being present on a subpopulation of dendritic cells and so the infiltrating F4/80+ cells in the obstructed kidney in my experiments may not have been only macrophages but also dendritic cells (Kruger, Benke et al. 2004; Dong, Bachman et al. 2008). The morphology of F4/80+ cells has been used by some groups to further determine the cell type. Many investigators have also demonstrated a significant resident F4/80+ population in normal murine kidney tissue. The lack of staining in the control normal, contralateral and sham kidneys I reviewed was likely to reflect issues with the F4/80 antibody concentrations or the tissue fixation methods used. The role and function of the F4/80 antigen on the macrophage is unknown but may play a role in adaptive immunity and tolerance induction and has been characterized as a member of the epidermal growth factor (EGF)-transmembrane 7 (TM7) family (van den Berg and Kraal 2005).

In order to assess whether the infiltrating T cells demonstrated a memory phenotype, immunofluorescent staining with an antibody specific for the CD44 antigen was performed. CD44 is expressed on the surface of many cells types and therefore staining for CD44 antigen was seen widely within renal tissue. I was able to distinguish CD44+ lymphocytes from other cell types by the dual labelling technique I used. However, there is a spectrum of CD44 expression by T cells termed low, intermediate and high which was more difficult to distinguish by the immunofluorescent staining techniques I used, than when using an antibody to CD44 in flow cytometry. By immunofluorescence I should have been able to differentiate between naive lymphocytes which were CD44 low and memory lymphocytes which had high CD44 expression. I was less confident that I was able to distinguish between activated cells that were intermediately expressing effector and highly expressing memory CD44 lymphocytes. On balance, this distinction was not critical since the aim of this work, which I successfully showed, was to demonstrate the presence of a population of activated lymphocytes which had the potential to contribute to the fibrotic tissue injury seen in UUO.

In assessing renal injury both percentage interstitial expansion and immunochemical staining for α-SMA and collagen I were used. Initially interstitial expansion alone was used as a marker for renal injury but expansion may have been due to interstitial oedema caused by injury rather than the interstitial space being expanded by activated fibroblasts or extracellular matrix. Subsequently α-SMA staining and collagen I deposition correlated with the areas of interstitial expansion. Furthermore, with

increasing time after obstructive injury more fibroblasts were activated and fibrotic interstitial matrix deposited, signifying progressive fibrotic renal damage, which correlated with progressive lymphocyte infiltration.

In this chapter I have demonstrated that activated and proliferating T cells were present within the mononuclear cell infiltrate following ureteric obstruction which could potentially play an active role in promoting the fibrotic injury seen in UUO kidney.

Chapter 4. Repertoire of T cell receptor Vbeta gene segment usage in the normal and UUO kidney

4.1. Introduction

In both archetypal autoimmune diseases in humans and experimentally induced autoimmune diseases in animals, T cell clones have been demonstrated that have the same T cell receptor and therefore recognise the same antigenic epitope. In order to investigate this in the UUO model, the functional gene segments which combine to form the TCR were analysed in the population of infiltrating T cells.

In the late 1980's analysis of the TCR variable region in autoimmunity led to the 'V region hypothesis' that suggested recognition of a single epitope of an autoantigen resulted in the clonal expansion of a population of auto-reactive T cells which caused disease (Urban, Kumar et al. 1988; Kumar, Kono et al. 1989). Much of this work was carried out in the experimental allergic encephalitis model but subsequent work in both animals and humans suggested that the T cell repertoire was not as tightly restricted as was initially suggested and multiple populations of T cells developed in response to a number of antigenic epitopes. Work on immunologically mediated renal diseases such as systemic lupus erythematosus (Massengill, Goodenow et al. 1998) and Sjogrens (Murata, Kita et al. 1995) demonstrated a restricted repertoire of TRVβ gene segments expressed by infiltrating renal T cells compared to peripheral lymphocytes. Also oligoclonality was demonstrated by sequence analysis of the VDJ region, supporting the 'V region hypothesis'.

The murine model of anti-tubular basement membrane disease, which produces a T cell mediated interstitial nephritis, is induced by inoculation of renal tubular antigen in Freud's adjuvant. When Heeger's group used this model of AID they initially demonstrated TRVβ restriction in the T cell population and common amino acids when sequencing across the CDR3 region (Heeger, Smoyer et al. 1994; Heeger, Smoyer et al. 1996). This suggested that a restricted TRVβ repertoire of T cells was activated after recognition of the immunodominant epitope contained within the target antigen. However, they also found that with more advanced disease a heterogeneous population of T cells developed with a diverse TRVβ repertoire and CDR3 sequences. This suggested that after initial clonal T cell immune responses to a specific target antigen, a more heterogeneous T cell response developed with ongoing injury, where T cells recognised multiple antigenic epitopes by a process termed epitope spreading.

In this chapter I examine the T cell response during the first month of UUO injury. Using PCR I will determine whether there is over expression of a particular TRVβ gene segment in the UUO kidney compared to the spleen. If selective expansion of one TRVβ gene segment is demonstrated this would provide support for the hypothesis that antigen-dependent T cell activation may be occurring in the UUO model with the loss of immunological tolerance. However, over expression of a TRVβ gene segment in the UUO kidney would not be definitive proof for clonal proliferation since the other two gene segments and junctional diversity within the β-chain are unknown. It is also unlikely that one single clone of T cells would develop in response to UUO because of the phenomenon of epitope spreading however, by looking early in the disease process I postulate there would be restricted T cell responses to fewer antigenic epitopes.

Unmanipulated kidney and spleen in control mice and the contralateral kidney in a UUO mouse were also examined to determine the expression of the TRVβ gene segments. This allowed comparison to the normal T cell repertoire in mice.

4.2. The β-chain of the mouse T cell receptor

As outlined in Chapter 1, the β-chain of the TCR consists of a constant and variable region. The variable region consists of the V, D and J gene segments. In the mouse there are twenty two functional TRVβ gene segments however, just one is used by any T cell to create combinational diversity. More than twenty two TRVβ gene segments are recognised but the other sequences are non-functional and either pseudogenes or open reading frame sequences (orfs). The gene segments are numbered as outlined in Table 4.1 that compares the corresponding IMGT and Arden nomenclature classifications (Arden, Clark et al. 1995; Giudicelli, Chaume et al. 2005).

Table 4.1- IMGT and Arden classifications of the functional and non-functional TRVβ gene segments in the mouse

The correlation between the nomenclature of the IMGT and Arden classifications for TCR β-chain sequences in the mouse are illustrated below for functional and non-functional gene segments. Two gene segments in the IMGT classification were not recognised by Arden's group.

Functional genes		**Pseudogenes**		**Orfs**	
IMGT = Arden		IMGT = Arden		IMGT = Arden	
1	2.1	6	26.1	21	19.1
2	4.1	7	*	22	22.1
3	16.1	8	28.1		
4	10.1	9	24.1		
5	1.1	10	25.1		
12.1	5.2	11	29.1		
12.2	5.1	12.3	5.3		
13.1	8.3	18	23.1		
13.2	8.2	25	21.1		
13.3	8.1	28	31.1		
14	13.1				
15	12.1				
16	11.1				
17	9.1				
19	6.1				
20	*				
23	20.1				
24	17.1				
26	3.1				
29	7.1				
30	18.1				
31	14.1				

* Not recognised

4.3. Lymphocytes in the UUO kidney

To investigate the possibility of clonal proliferation of T cells within the UUO animal I looked at the relative expression of the twenty two TRVβ gene segments in the UUO kidney compared to spleen. If I could demonstrate relatively greater expression of a particular TRVβ gene segment in the kidney of that animal, this could suggest a clonal population of T cells had developed in the kidney expressing that particular TRVβ. This would allow me to explore the hypothesis that T cells were recruited into injured kidney because they recognised and responded to auto-antigen, representing a break in self-tolerance. Animals at different time points post UUO and controls were sacrificed and their organs perfused. The kidney and spleens were harvested and snap frozen prior to RNA extraction.

4.4. PCR optimisation

PCR was used to assess the relative expression of each TRVβ gene segment. In each reaction one of the twenty two forward primers was used, each of which annealed to one of the twenty two TRVβ gene segments on the antisense strand of DNA, with the same reverse primer annealing to the constant region on the sense strand of DNA. The conditions were optimised for standard and real time PCR to ensure accuracy of the results and exclude differences in PCR efficiency between different primer pairs.

4.4.1. RNA purity and integrity

Total RNA was extracted from mouse kidney and spleen tissue. The purity and integrity of all extracted RNA samples were tested by UV spectrophotometry and electrophoresis. These tests were carried out to ensure the RNA was not contaminated by genomic DNA or protein and had not degraded.

Figure 4.1(a) illustrates an assessment of RNA purity for one sample using the UV spectrophotometer, where an A_{260}/A_{280} ratio of 2.0 is characteristic of pure RNA. Running total RNA on an agarose gel stained with ethidium bromide demonstrated two sharp, clear ribosomal RNA bands at 28S (4.8kb) and 18S (1.8kb) confirming integrity (Figure 4.1(b)). The mRNA appears as a smear from 6kb to 0.5kb and generally makes up only between 1-5% of the total cellular RNA. Each RNA sample was assessed in this way and if the A_{260}/A_{280} ratio was <1.8 the sample was not used.

Figure 4.1- Assessment of RNA purity and integrity

An UV spectrophotometer trace is seen in panel (a) for a sample of extracted RNA, where the calculated A_{260}/A_{280} ratio for the sample was 2.07, demonstrating pure RNA which was not contaminated by genomic DNA or protein. The agarose gel (b) shows the RNA sample could be separated into two sharp, clear ribosomal RNA bands 28S (4.8kb) and 18S (1.8kb) so there was no evidence of RNA degradation.

(a) Spectrophotometer trace **(b) Agarose gel**

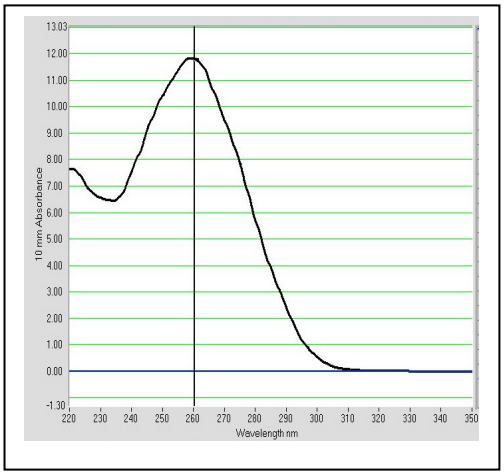

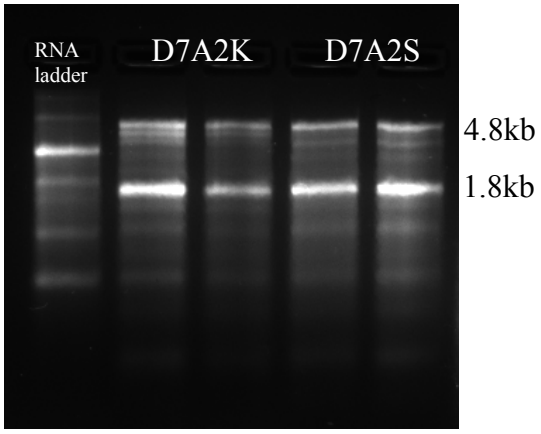

ng/ul	591.41
A260	11.828
A280	5.710
260/280	2.07
260/230	1.80

4.4.2. Polymerase chain reaction

The primer sequences used throughout this thesis to assess the TRVβ gene segment repertoire had previously been validated in experimental cardiac allograft recipients in mice (Hu, Watson et al. 2008).

4.4.2.1. Determining the presence of the primer sequences within the TRVβ gene segments and the lengths of the PCR products generated

Using the ImMunoGeneTics database (http://imgt.cines.fr/) the presence of the appropriate primer annealing sequences were confirmed in each of the twenty two functional TRVβ gene segments and TRCβ gene. The sequences for the functional TRDβ and TRJβ gene segments were also reviewed.

To establish the relative and approximate lengths of the PCR products generated by the twenty two TRVβ primer pairs, the same TRDβ1 and TRJβ1-2 gene segments were used in each theoretical sequence to allow comparison (Figure 4.2). The lengths of the twenty two PCR products varied between 185 and 216bp. These theoretical PCR product lengths do not take into account junctional diversity which is unique to each TCR. In practice when real TCR β-chain sequences were reviewed which had junctional diversity, a shorter PCR product was generated than when complete gene segments were combined theoretically.

Figure 4.2- Hypothetical section of a single strand of DNA from a TCR β-chain demonstrating the gene segments involved and annealing sites for the PCR primers

The figure illustrates a hypothetical TCR β-chain, where the TRVβ3 gene segment combines with the complete TRDβ1 (highlighted blue), TRJβ1-2 (highlighted green) and Cβ gene segments to create a nucleotide sequence without junctional diversity. The forward primers used for the PCR reactions annealed to a sequence on one of the twenty two TRVβ gene segments on the antisense strand and the reverse primer to a sequence on the sense DNA strand within the constant gene segment, which was the same for all the PCR reactions. For this sequence the locations of the primer annealing sites in either this or the complimentary strand of DNA are highlighted in bold type. The complete TRVβ3 and TRCβ gene segments are not shown. The length of PCR product generated from this reaction would be 186bp.

5'

[-TRVβ3 primer site on antisense strand-]
----------TRVβ3 gene segment----------][-TRDβ1-
CACTGGAGGACTCAGCTGTGTACTTCTGTGCCAGCAGCTTAGCGGGACA

----------][---------- TRJβ1-2----------
GGGGGCCAAACTCCGACTACACCTTCGGCTCAGGGACCAGGCTTTGGTA

-------][---------- TRCβ1----------
ATAGAGGATCTGAGAAATGTGACTCCACCCAAGGTCTCCTTGTTTGAGCC

[-TRCβ primer site on this sense chain-]

ATCAAAAGCAGAGA**TTGCAAACAAACAAAAGGCTACC** **3'**

TRVβ3 primer **5'- CACTGGAGGACTCAGCTGTGTACT -3'**
TRCβ primer **5'- GGTAGCCTTTTGTTTGTTTGCAA -3'**

4.4.2.2. Standard PCR with TRVβ primers

Standard PCR reactions were carried out using the twenty two specific Vβ primer pairs under identical conditions using reverse transcribed RNA and the PCR products were separated by agarose gel electrophoresis. This demonstrated standard PCR was able to amplify product of an appropriate size (approximately 200bp) (Figure 4.3 (a)). A GAPDH primer pair was used for comparison which generated product of the appropriate size (453bp). Control PCR reactions were performed with no template DNA to provide evidence of no contamination (Figure 4.3(b)).

Figure 4.3- PCR products separated by agarose gel electrophoresis generated using the twenty two TRVβ primers pairs (a) with and (b) without reverse transcribed RNA from whole spleen

Standard PCR reactions were carried out using each of the twenty two pairs of TRVβ primers on reverse transcribed RNA from whole spleen tissue (a) and the products separated by agarose gel electrophoresis, demonstrating a product of the appropriate size for all reactions. The gel in (b) demonstrates that no PCR products of the predicted size were generated when no cDNA was added to the reactions and excluded contamination.

(a)

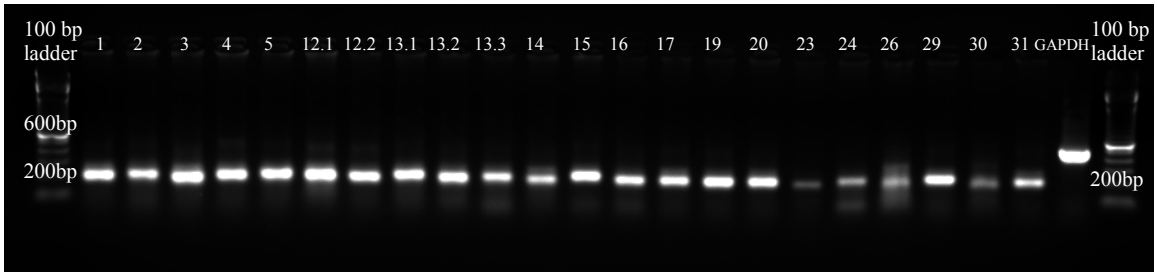

(b)

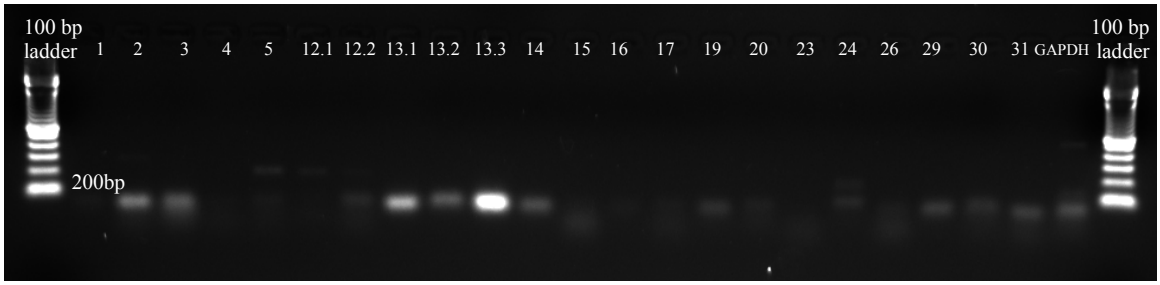

4.4.2.3. Real time PCR optimisation of primer and probe concentrations

It was clear from the standard PCR reactions that the primer pairs were able to amplify the template DNA. However a FAM labelled probe was also now required for Taqman real time PCR. Therefore the primer and probe concentrations along with the annealing temperature had to be optimised. For varying primer and probe concentrations the reactions were run in triplicate and the Ct value for each reaction derived. This optimisation was performed using the primer pair which specifically annealed to TRVβ1 and TRCβ.

For a given amount of starting cDNA with the annealing temperature set at 56.5 ºC, Ct values were calculable only when the probe concentration was set to ≥ 300nM. With increasing concentrations of probe beyond 300nM there was little change in the Ct value (Table 2.9 (a)), so a probe concentration of 300nM was used. Increasing concentrations of the primer pair were used for a given amount of starting DNA and fixed annealing temperature, with 300nM of probe. There was no change in the Ct value when the final primer concentrations were increased beyond 600nM (Table 2.9 (b)). From the results of these optimisation experiments all real time PCR experiments were preformed with a probe concentration of 300nM, primer concentration of 600nM and the annealing temperature was set to 56.5 ºC.

4.4.3. Efficiency calculations

If all the primer pairs had comparably high amplification efficiencies then any differences in the number of cycles required to generate a given fluorescent intensity (Ct value) must be related to the amount of starting template DNA. This would then allow calculation of the relative expression of each TRVβ gene segment in UUO kidney and spleen.

The amplification efficiencies for all twenty two TRVβ primer pairs were calculated to ensure they were comparable and highly efficient. This was performed using real time PCR using the method shown in section 2.6.4. The results of these methodological experiments are pivotal to all the subsequent work in this thesis so two examples from the twenty two efficiency reactions are illustrated here for the TRVβ3-TRCβ and TRVβ12.2-TRCβ primer pairs. To calculate the primer efficiencies, PCR reactions were run in triplicate with 5-fold serial dilutions in the template DNA. If a PCR reaction was 100% efficient then after completing one cycle of PCR the amount of template DNA would double and the calculated efficiency for that reaction would be 2.

4.4.3.1. Calculating the efficiency of the TRVβ3 and TRCβ primer pair

Using the primer pairs TRVβ3 and TRCβ under standard conditions the slope of the Ct v Log [DNA] graph was calculated to be -3.42 +/- 0.09 (Figure 4.4). The efficiency of the PCR reaction generated from the slope was 1.96 or 96% with an R^2 value of 0.99.

Figure 4.4- Efficiency calculation for the TRVβ3–TRCβ primer pair using the Ct slope method

The line of best fit for the scatter plot of Ct v Log [DNA] was determined by linear regression analysis. This was used to calculate the efficiency of the TRVβ3 and TRCβ primer pair, which was 96%.

(a) Mean Ct value calculated using five triplicate cDNA concentrations

TRVβ3				
Log DNA Concentration	**Ct v1**	**Ct v2**	**Ct v3**	**Mean Ct**
3.2553	26.17	26	25.97	26.05
2.5563	29.18	28.89	29.5	29.19
1.8573	30.19	31.91	31.98	31.36
1.1584	33.59	34.2	33.2	33.66
0.4594	35.93	35.97	35.37	35.76
0	0	0	0	0

slope	-3.42
1/slope	-0.29
R^2	0.99
E	1.96

(b) Standard curve of mean Ct v Log cDNA concentration (ng/µl) from which the slope of the curve and the efficiency of the reaction was calculated

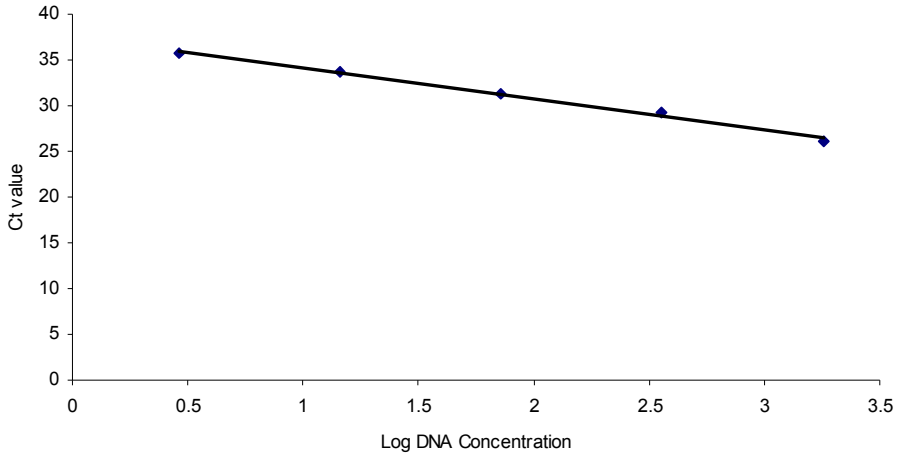

4.4.3.2. Calculating the efficiency of the TRVβ12.2 and TRCβ primer pair

Using the primer pairs TRVβ12.2 and TRCβ under standard conditions the slope of the Ct v Log [DNA] graph was calculated to be -3.50 +/- 0.06 (Figure 4.5). The efficiency of the PCR reaction generated from the slope was 1.93 or 93% with an R^2 value of 1.00.

Figure 4.5- Efficiency calculation for the TRVβ12.2–TRCβ primer pair

The line of best fit for the scatter plot of Ct v Log [DNA] was determined by linear regression analysis. This was used to calculate the efficiency of the TRVβ12.2 and TRCβ primer pair, which was 93%.

(a) Mean Ct value calculated using five triplicate cDNA concentrations

TRVβ12.2				
Log DNA Concentration	**Ct v1**	**Ct v2**	**Ct v3**	**Mean Ct**
3.2553	29.61	30.07	29.25	29.64
2.5563	32.7	32.16	32.95	32.60
1.8573		34.7	34.89	34.80
1.1584	37.43	37.49	37.11	37.34
0.4594	39.12	39.-5	39.9	39.51
0	0	0	0	0

slope	-3.50
1/slope	-0.29
R^2	1.00
E	1.93

(b) Standard curve of mean Ct v Log cDNA concentration (ng/µl) from which the slope of the curve and the efficiency of the reaction was calculated

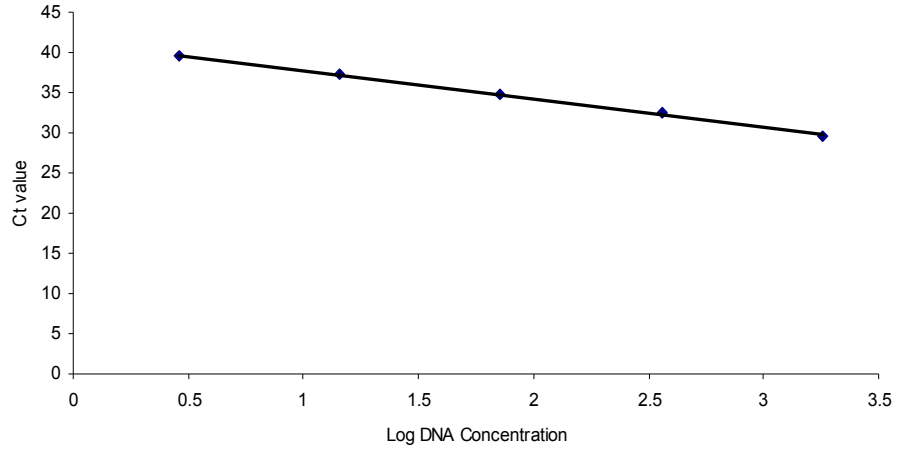

4.4.3.3. Summary of primer efficiencies

For the twenty two primer pairs the median primer efficiency was equal to 1.94 or 94%. The range of efficiencies was 1.87 - 2.07 or 87% – 107%. The median R^2 value was 0.99, with a range of 0.93 – 1.00 (Table 4.2). Both these median parameters fall within the accepted range for primer efficiency as quoted by multiple commercial technology companies including Stratagene and Applied Biosystems. They suggest the slope of the Ct v Log [DNA] plot should be -3.3 +/- 10%, generating an efficiency of 100% +/- 10%. Almost all the efficiencies of the 22 primers pairs fell within this acceptable range.

Table 4.2- Comparison of all twenty two TRVβ primer pair efficiencies

Efficiencies and R^2 values for the TRVβ primer pairs calculated from Ct v Log [DNA].

TRVβ primer	Slope	Efficiency (%)	R^2
1	-3.41	97	0.99
2	-3.24	104	0.99
3	-3.42	96	0.99
4	-3.27	102	0.98
5	-3.51	93	0.99
12.1	-3.46	95	0.93
12.2	-3.50	93	1.00
13.1	-3.60	90	0.97
13.2	-3.25	103	1.00
13.3	-3.27	102	0.98
14	-3.48	94	0.99
15	-3.16	107	0.98
16	-3.42	96	0.99
17	-3.57	91	0.98
19	-3.69	87	1.00
20	-3.24	103	0.99
23	-3.50	93	0.99
24	-3.60	89	1.00
26	-3.47	94	1.00
29	-3.43	96	1.00
30	-3.68	87	0.99
31	-3.54	92	0.98

4.5. Relative expression of TRVβ gene segments by lymphocytes in kidney and spleen of normal and UUO animals

Unmanipulated mice and mice at 7, 14 and 28 days post UUO, were sacrificed and their kidneys perfused to eliminate peripheral blood lymphocyte contamination. Extracted RNA was reverse transcribed and real time PCR was carried out on DNA from either normal, UUO or the contralateral UUO kidney and the spleen of each animal individually. All twenty two primer pairs were run in triplicate with the template DNA, along with a non-template control wells for each primer pair. All 88 PCR reactions for the tissue of interest from one animal were run simultaneously. If there was amplification of DNA in the absence of template suggesting contamination the experiment was repeated. The only control for pipetting error was that each PCR reaction was run in triplicate.

The Ct value of each PCR reaction was determined and the relative expression of each of the twenty two TRVβ gene segments was calculated for that DNA sample. This allowed me to determine the percentage of the total T cell population expressing each individual TRVβ gene segment in that tissue (Lim, Baron et al. 2002). No house-keeping gene was required for standardisation because the same quantity of template DNA was added to each reaction in a single experiment and comparisons were made between the relative expressions of the TRVβ gene segments within the one tissue.

Over expression of a particular TRVβ gene segment in the kidney compared to the spleen would suggest a clonal population of T cells had developed in the kidney due to UUO injury.

4.5.1 Relative expression of TRVβ gene segments by lymphocytes in kidney and spleen of normal animals

TRVβ gene segment usage in the kidney and spleen of three normal mice was determined. The pattern of TRVβ gene segment expression was similar in all three normal animals, reflected by the narrow SEM (Figure 4.6). For most TRVβ gene segments the proportion of T cells expressing that gene segment was consistently high or low e.g. TRVβ23, 24 and 30 were always expressed at a low level in comparison to TRVβ3 and 13.2.

However, there were differences in the expression of some TRVβ gene segments between the kidney and spleen. This was most obvious in all three animals for TRVβ13.2, where the expression of this gene segment in the kidney was up to three

times that in the spleen. TRVβ29 was also consistently over expressed in the kidney: this was most marked in animal 2 where the proportion of cells expressing TRVβ29 was three times that seen in the spleen. The gene segment TRVβ1 was over expressed in the kidney tissue of animals 1 and 3.

Of note, the Ct values for PCR reactions using normal kidney were higher than seen in the UUO kidney reflecting lower concentrations of TCR mRNA. This was expected: as demonstrated in Chapter 3 there were significantly more T cells infiltrating UUO kidney than normal controls. However, since the total amount of T cell-derived cDNA used in the PCR reactions could not be standardised between different animals, estimates of the actual differences in T cell number between UUO and normal animals and between kidney and spleen of the same animal could not be made.

Figure 4.6- Relative expression of TRVβ gene segments in the kidney and spleen of three normal mice

The bar charts in (a), (b) and (c) graphically represent the percentage of T cells in the kidney and spleen of three normal mice which express each TRVβ gene segment.

The chart in (d) illustrates the mean percentage (+/- SEM) TRVβ gene segment expression for the three normal mice. The profiles of TRVβ gene segment expression were very similar between the animals as reflected by the narrow SEM. Certain TRVβs were consistently expressed at low levels in both the kidney and spleen e.g. TRVβ23, 24 and 30 and others at higher levels e.g. TRVβ3 and 13.2. There was the over expression of the TRVβ13.2, 29 and 1 in normal kidney compared to spleen.

(a) Animal 1

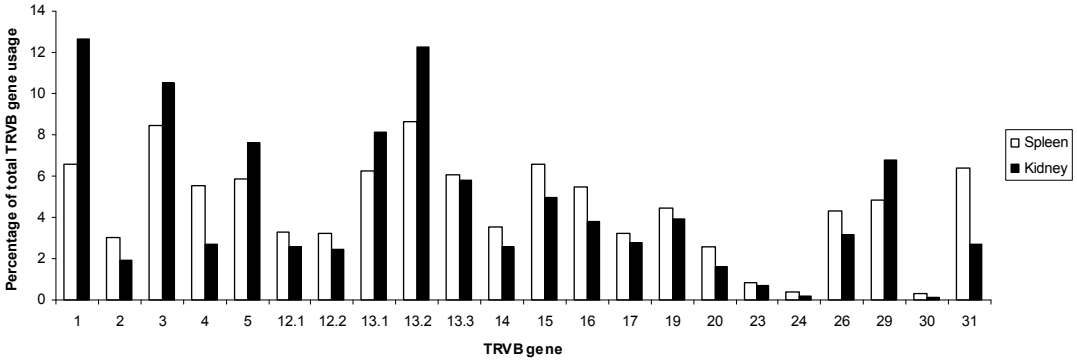

(b) Animal 2

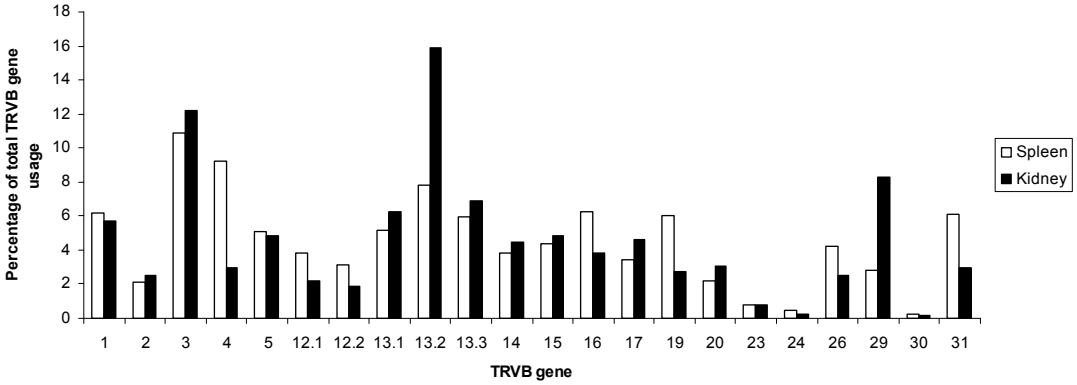

(c) Animal 3

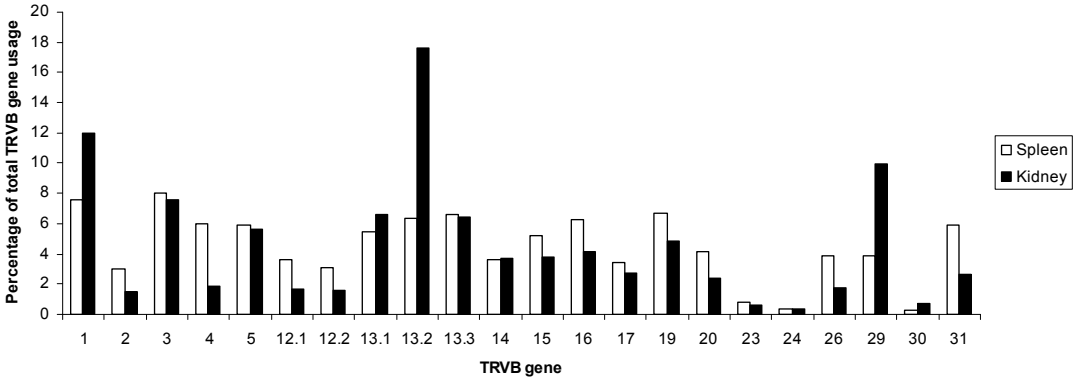

(d) Mean (+/- SEM) relative expression of the TRVβ gene segments in the kidney and spleen of three normal animals

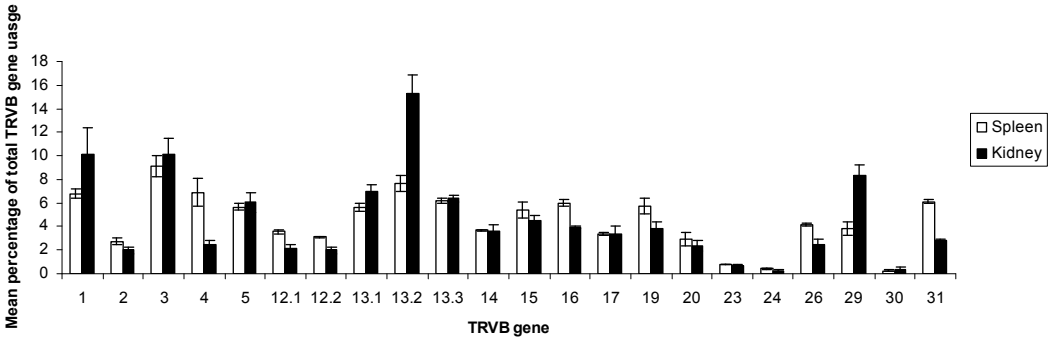

4.5.2 Relative expression of TRVβ gene segments by lymphocytes in the UUO kidney and spleen of ten UUO mice

TRVβ expression was assessed in UUO kidney and spleen from a total of ten UUO animals at 7 (n=3), 14 (n=5) and 28 (n=2) days post obstruction (Figures 4.7, 4.8 and 4.9). The number of animals used per group was small, especially at day 7 and 28, and should have been bigger to maximise the chances of achieving statistically significant results. Comparison was made between the percentage expression of the individual TRVβ gene segments in the kidney and spleen for each animal. The profile of TRVβ gene segment expression by T cells was similar between most of the mice especially at day 7 and 14 after obstruction. There was often a predominant TRVβ gene segment which was expressed by a larger percentage of T cells in the UUO kidney compared to the spleen and this was frequently the TRVβ3 gene segment (n=7/10). By day 28 the pattern of TRVβ gene segment expression was more homogenous, with no single TRVβ segment predominating as at the earlier time points. Certain TRVβ gene segments were consistently only expressed by a very small proportion of T cells in all UUO animals and at all time points e.g.TRVβ23 and 24.

Looking specifically at the day 7 animals: the predominant gene segment over expressed in the UUO kidney of two mice was TRVβ13.3 (Figure 4.7 (a) and (b)) whilst in the other mouse it was the TRVβ13.1 gene segment (Figure 4.7 (c)). Animal 2 also had relative over expression of the TRVβ3 gene segment in the UUO kidney. The percentage expression of the TRVβ13.2 and 29 gene segments were similar in the UUO kidney and spleen of all three day 7 mice.

Of the five mice that were obstructed for 14 days, four demonstrated over expression of the TRVβ3 gene segment in the UUO kidney, which was particularly pronounced in animals 3 and 6 (Figure 4.8). The proportion of the total T cell population in the kidney which expressed the TRVβ3 gene segment was between 1.3 and 2.2 times that seen in the comparator spleen: in animal 6, 10.2% of the splenic T cell population expressed TRVβ3, compared to 22.0% of the UUO kidney T cell population. Other TRVβ gene segments were over expressed in the UUO kidney of day 14 mice however, none were as pronounced as the proportion of T cells expressing the TRVβ3 segment in animal 6. Other examples include over expression of TRVβ26 in animal 2 and TRVβ13.2 in four of the animals. No day 14 UUO kidney demonstrated over expression of the TRVβ1 gene segment.

In comparison, the TRVβ profiles generated from mice obstructed for 28 days were more homogeneous (Figure 4.9). No single TRVβ gene segment accounted for >13% of the total T cell pool in that kidney: this was different to that seen in the day 7 and 14 UUO kidneys where certain TRVβ segments accounted for up to 22% of the total T cell population. There was some over expression of the TRVβ3 gene segment in the both UUO kidneys but this was less pronounced than at earlier time points.

Figure 4.7- Relative expression of TRVβ gene segments in the kidney and spleen of three day 7 UUO mice

The relative expression of the TRVβ gene segments in the UUO kidney and spleen were determined for three day 7 UUO mice.

(a) Animal 1

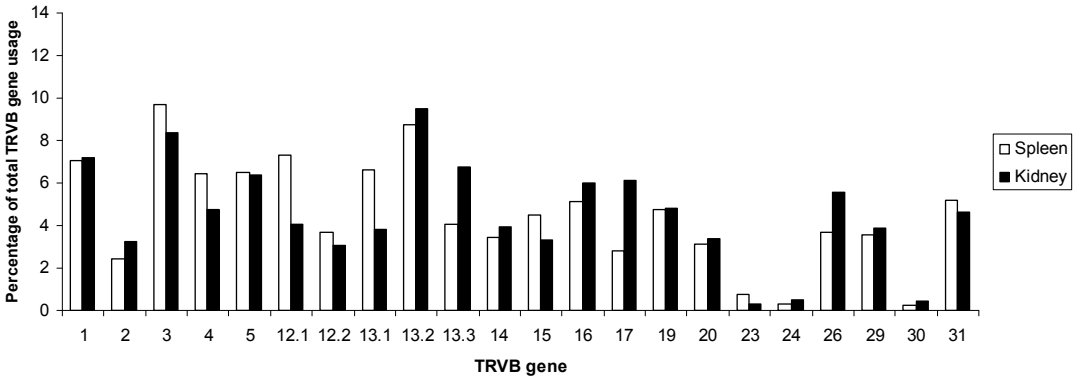

(b) Animal 2

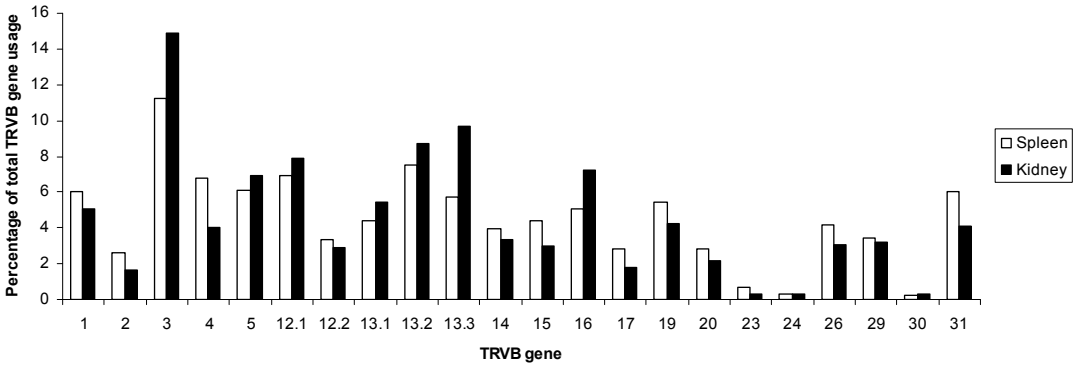

(c) Animal 3

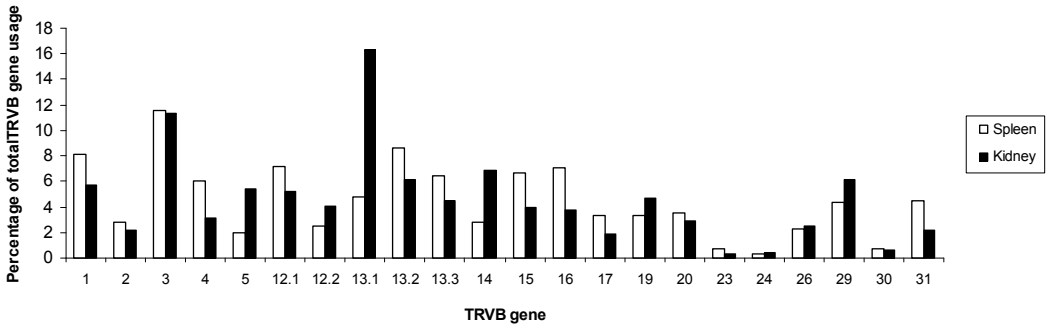

Figure 4.8- Relative expression of TRVβ gene segments in the kidney and spleen of five day 14 UUO mice

The percentage expression of TRVβ gene segments were evaluated in the UUO kidney and spleen of five mice which had 14 days of left ureteric obstruction. In all but animal 2 there was over expression of the TRVβ3 gene segment in the UUO kidney.

(a) Animal 2

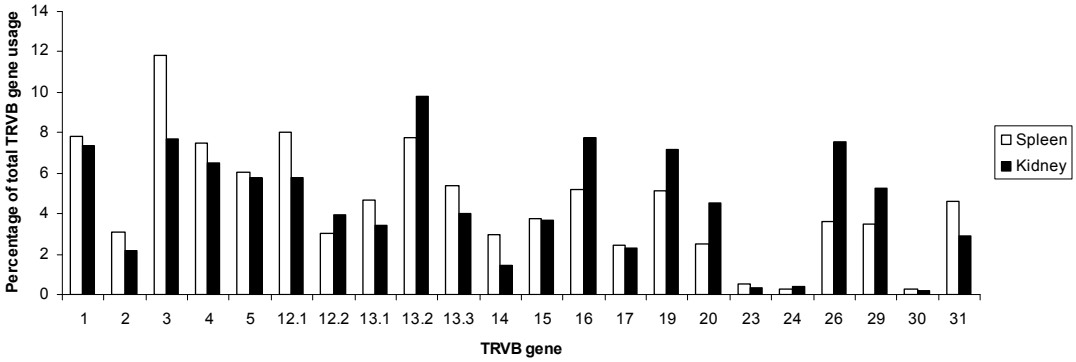

(b) Animal 3

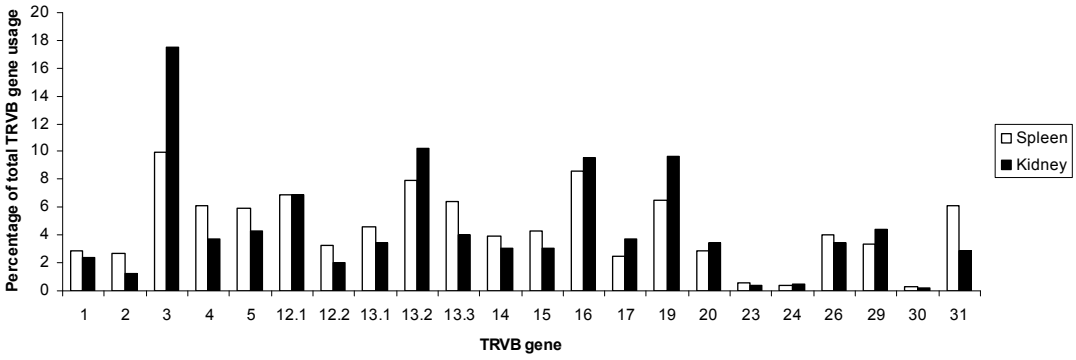

(c) Animal 6

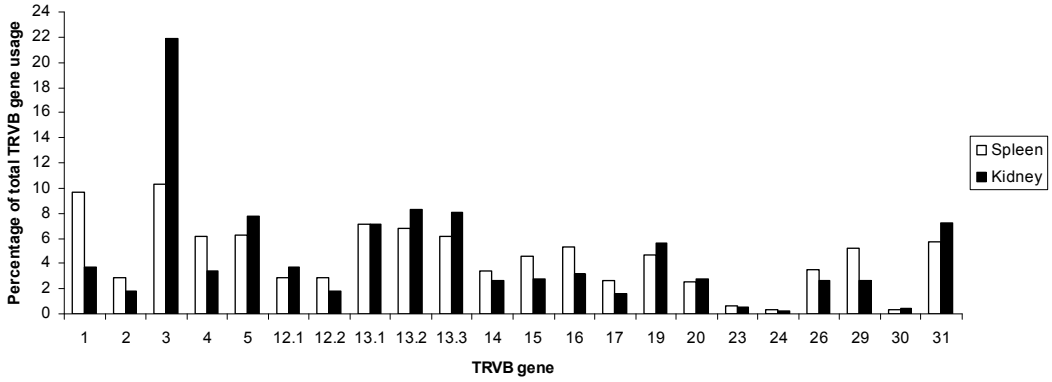

(d) Animal 7

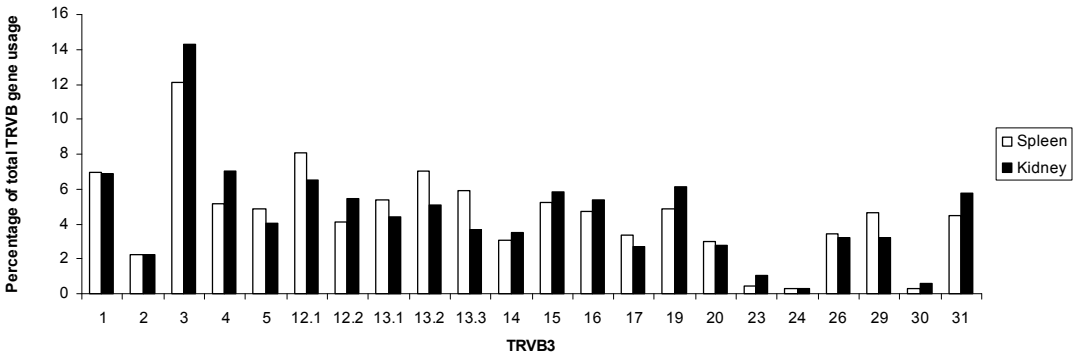

(e) Animal 9

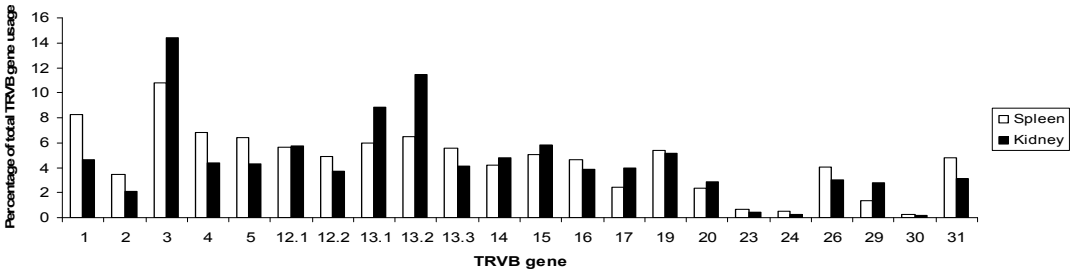

Figure 4.9- Relative expression of TRVβ gene segments in the kidney and spleen of two day 28 UUO mice

TRVβ gene segment expression was compared in the UUO kidney and spleen of two animals which had undergone 28 days of UUO. Once again there was over expression of TRVβ3 in the kidney of both animals however this was less then seen in the day 14 animals. No one TRVβ segment accounting for >13% of the total T cell pool in the kidney, which was different to the pattern seen in the day 7 and 14 UUO mice.

(a) Animal 1

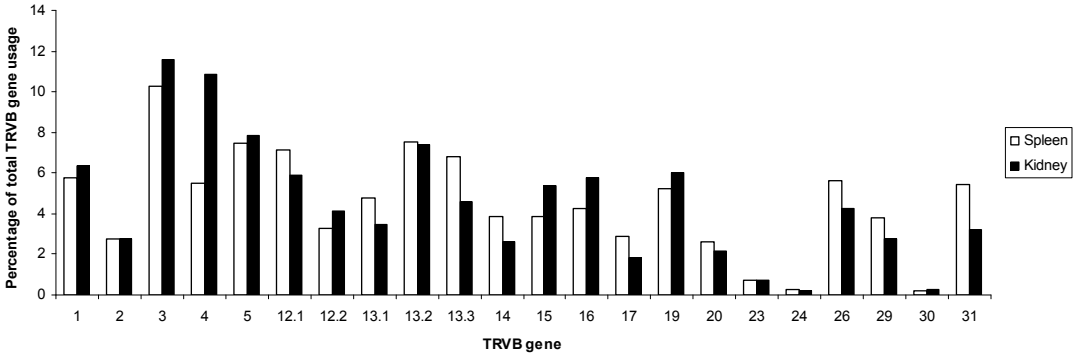

(a) Animal 2

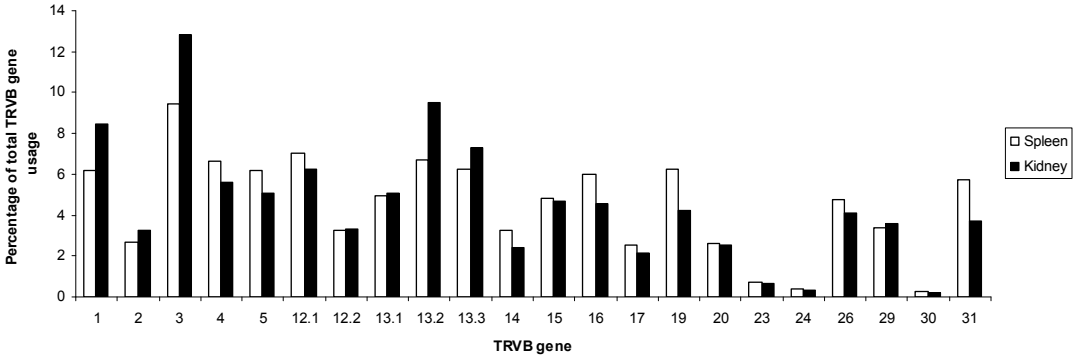

4.5.3 Relative expression of TRVβ gene segments by lymphocytes in the kidney and spleen of a sham operated day 7 animal

One animal had a sham UUO operation during which a laparotomy incision was made and the left ureter was identified and manipulated but not tied. The mouse was housed in identical conditions to the UUO mice and sacrificed after 7 days. On harvesting the sham operated left kidney there was no evidence of obstruction and the kidney was histologically normal.

Figure 4.10 graphically represents the real time data for this animal. The TRVβ gene segment expression profile was very similar to the profile in Figure 4.6 (d) which demonstrated the mean percentage TRVβ gene segment expression for three normal mice. This suggested that sham manipulation of the mouse made little difference to the renal T cell population. Consist with the findings from Chapter 3, Ct values were high, suggesting there were few TRVβ expressing cells in the sham kidney compared to the UUO kidney. Again similar to the findings in the normal kidney, the TRVβ13.2 and 29 gene segments were over expressed in the sham operated kidney.

Figure 4.10- Relative expression of TRVβ gene segments in the kidney and spleen of a sham operated day 7 UUO mouse

The expression of the TRVβ gene segments by cells in the kidney and spleen of the sham operated UUO mouse were compared. The profile was similar to that of normal mice (Figure 4.6 (d)), with the percentage expression of TRVβ13.2 predominating in the kidney.

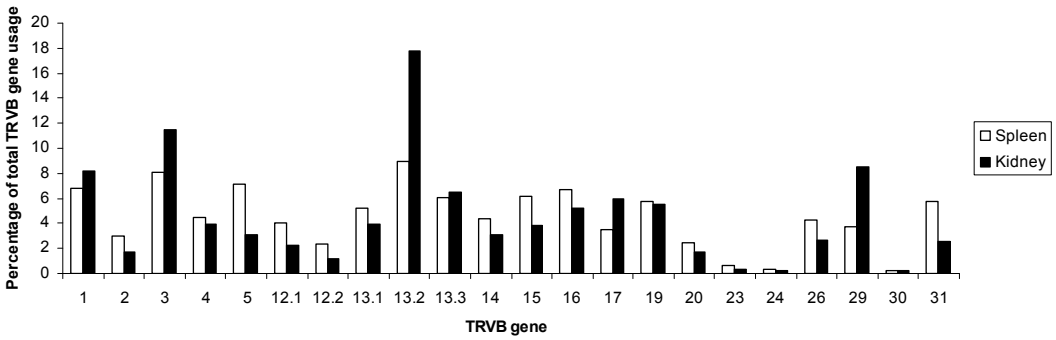

4.5.4 Mean relative expression of TRVβ gene segments by the lymphocytes in the kidney and spleen of all normal and UUO animals

The percentage expression of some TRVβ gene segments in the normal and UUO mice were similar. Certain gene segments were expressed at very low levels in both organs of both groups of mice, such as TRVβ23, 24 and 30. In comparison specific TRVβ gene segments where over expressed in kidney such as TRVβ3 in UUO animals and 1, 13.2 and 29 in normal kidneys. A variety of other TRVβ gene segments were also over expressed in the UUO kidney but not as consistently or to the extent demonstrated by TRVβ3.

4.6. Discussion

From these experiments I have demonstrated an alteration in the TRVβ expression pattern of certain TRVβ gene segments in the UUO kidney compared to the spleen, in particular in the use of TRVβ3. Such a difference was not demonstrated in the TRVβ3 T cell expression in normal mice suggesting that the results in UUO animals represent the affect of disease rather than artefact. This supports the hypothesis that antigen-dependent T cell activation may be occurring in the UUO model with the loss of immunological tolerance. Over expression of TRVβ3 at the earlier time points post UUO would be compatible with the early proliferation of a homogeneous population of T cells as shown in some AIDs. This would support the hypothesis that restricted T cell populations are responding to a limited number of auto-antigenic epitopes. Subsequent normalisation of the T cell repertoire at a later time point is in keeping with the phenomenon of epitope spreading also demonstrated in AIDs.

If antigen-dependent T cell activation had occurred in the UUO model of renal disease we must consider the theoretical mechanisms by which loss of tolerance could occur. Theoretically peripheral tolerance could be evaded by a number of mechanisms in UUO where there is a change in the interaction between a self antigen:MHC complex and TCR. Firstly, the generation of a mature population of APCs which display high levels of co-stimulatory signals could allow some autoreactive T cells to avoid peripheral tolerance. The mechanical injury caused by obstructive uropathy produces DAMP molecules which activate TLRs on APCs. This then stimulates APCs in two ways: to produce proinflammatory cytokines that trigger further leukocyte recruitment and secondly to cause upregulation of co-stimulatory molecules on the surface of the APC, such as the B7 family of surface molecules. This generates mature APCs with high levels of co-stimulatory and MHC molecules on their surface. Therefore T cells that were not deleted in the thymus by negative selection due to a weak self peptide:MHC interaction could be now be activated by the strong second co-stimulatory signal generated by inflammation. There are examples in human diseases where inflammation precipitates AID flares including SLE and MS relapses which can be triggered by infection. Injury from sunlight precipitating a SLE flare may occur by a similar mechanism.

Secondly, self antigens usually only present at immune privileged sites and sheltered from normal immune surveillance may be exposed by UUO injury. Subsequently T cells that were not negatively selected in the thymus may be exposed to these antigens

for the first time, recognise them as foreign and allow T cell activation to occur. This has been shown in the human disease sympathetic opthalmitis (Avichezer, Grajewski et al. 2003).

Thirdly, post translational modification of self antigens may occur in response to cell stress caused by the increased pressure and stretch of UUO. This can cause amino acid modifications with the addition of groups or conversion of others (Anderton 2004; Pedersen 2007). The addition of new groups to the protein may occur by phosphorylation or glycation. Amino acid conversions may occur spontaneously or enzymatically to bring about changes which include deamination or citrullination. Such modifications can increase the binding affinity of the self peptide:MHC complex to the TCR. Therefore T cells that were not negatively selected in the thymus because of a weak self peptide:MHC interaction with a TCR can now bind the TCR more strongly and cause T cell activation, pending the second co-stimulatory signal. This mechanism of post translational modification is not necessarily about generating a new antigen which is recognised as foreign, but about increasing self peptide:MHC binding affinity to T cells, that have survived negative thymic selection. However, neoantigen generation may be another mechanism by which T cell activation can occur, where the neoantigen generated as a consequence of injury is recognised by the T cell as foreign. This has been proposed as a possible mechanism for Dressler's syndrome, where there is an autoimmune response against myocardial neoantigens after myocardial injury. These reactions are usually transient and the neoantigens are subsequently removed but if the clearance mechanisms are impaired then clinical AID can result.

In the UUO model all three mechanisms may be active. Acute cell injury caused by obstruction could precipitate the upregulation of co-stimulatory molecules on APCs allowing self antigens, which wouldn't usually illicit a T cell response in a non-inflammatory environment, to do so. Also modification to self antigens by UUO injury could increase their affinity to their TCR. With ongoing obstruction further antigen modifications or neoantigen production would develop which overwhelmed clearance mechanisms resulting in an ongoing chronic inflammatory reaction. Another possibility would be the release of sequestered antigens caused by UUO injury to which tolerance had not developed.

There are examples in the literature where loss of tolerance to self antigen has been shown in models of renal injury which are not characteristically thought to be

immunologically mediated. As far back as the 1990s, Gillum's group demonstrated a change in the tubular cytoskeletal and cell membrane protein profiles in a model of renal ischemic injury associated with pronounced interstitial inflammation (Truong, Farhood et al. 1992). The atrophic tubules demonstrated neoexpression of the cytoskeletal element vimentin, which is normally only expressed by immature renal tubular cells, and subtypes of keratin not usually expressed by renal tubules. The glycoprotein profile of the tubular cells also changed with marked decrease or absolute loss of some glycoproteins. This suggests ischaemia may initiate a cell mediated immune reaction caused by alteration in the antigenic profile of tubular cells and formation of neoantigens, which are recognised by T cells not negatively selected in the thymus. Rabb's group, using the renal ischaemia-reperfusion injury model, demonstrated that when renal lymphocytes were adoptively transferred from animals which had undergone IRI into control animals, renal injury occurred (Burne-Taney, Liu et al. 2006). This suggests that adoptively transferred memory T cells, which have lost tolerance to self antigen in the inflammatory environment of IRI, are able to recognise self antigenic epitopes in the control mouse provoking proteinuria.

Other groups have looked more specifically at possible self antigens that may be involved. These antigens may be lipid, protein or carbohydrate residues that are expressed exclusively in the normal kidney and to which central tolerance had not developed (Fang, Ballet et al. 2009). Alternatively, they could be an antigen which is only expressed in damaged kidney, such as the heat shock protein 70, which has been suggested as a candidate antigen for T cell mediated injury in hypertensive kidney disease (Parra, Quiroz et al. 2008). In response to the proinflammatory stimulus LPS, Dong et al's group demonstrated dendritic cells in regional lymph nodes that were positively stained for Tamm Horsfall Protein and were able to activate T cells (Dong, Swaminathan et al. 2005). This work suggests a break in T cell tolerance could occur to the self antigen Tamm Horsfall Protein when presented by dendritic cells in an inflammatory environment. Benigni's group developed this work in their model of renal injury, showing that dendritic cells could process the self protein albumin in the dendritic cell proteosome and present antigenic fragments with class I MHC to CD8+ T cells in the draining renal LNs, causing T cell activation and the production of IFN-γ (Macconi, Chiabrando et al. 2009). Work on the reversal-UUO model demonstrates a persistent T cell inflammatory infiltrate ten weeks after re-implantation of the ureter despite there being an improvement in renal function (Tapmeier, Brown et al. 2008).

This suggests an expanded T cell population develops during the inflammatory period of ureteric obstruction which recognises self antigen and which persists despite reversal since there is ongoing recognition of self antigen.

An obvious alternative tissue to examine would be the contralateral kidney in the UUO model. If lymphocytes were activated after they had lost tolerance to an unmodified self antigen, subsequent evidence of renal injury in the contralateral kidney may have been demonstrated. However, if T cells were recognising a modified self antigen or new antigen then contralateral renal injury would not be expected. Injury to the contralateral kidney may be confounded by hyperfiltration injury in that kidney due to reduced nephron mass after the UUO kidney is no longer functional.

As illustrated by these examples, there is an expanding body of evidence to suggest that models of renal injury which are not initially immunologically mediated, such as IRI and the hypertensive and proteinuric models of renal disease, can result in the activation of a T cell population due to loss of tolerance to self antigens. In other organs similar examples of loss of tolerance to self antigen have been reported. One example is from Rose's group who demonstrated the presence of specific antibodies and CD8+ T cells to the self antigen vimentin after cardiac transplantation (Barber, Whitelegg et al. 2004). This suggests that T cells, which were not deleted during negative selection in the thymus, remained immunologically silent under non-inflammatory conditions. However, in the inflammatory environment of transplantation, there is upregulation of MHC and co-stimulatory molecules on the APC providing the second co-stimulatory signal. The self peptide:MHC complex on the APC, although weakly bound to the TCR, could then cause T cell activation due to a strong second signal.

Another explanation for loss of peripheral tolerance to self may be due to dysregulation of the regulatory T cell population. It is possible that Tregs lose their suppressive abilities during renal injury thereby permitting the expansion of autoreactive T cell populations. The inflammatory environment which develops as a consequence of renal injury, which is rich in IL-6, may skew the T cell population away from T cells with regulatory function towards a Th17 phenotype, which promotes injury.

An alternative explanation for the presence of activated T cells in the UUO kidney would be that lymphocytes were activated elsewhere in the body in response to a non-renal antigen and were subsequently attracted to the area of obstructive injury by the chemokine gradient developed by renal cells in response to ureteric obstruction. One

possible source would be an activated lymphocyte population residing within the gut, which had been activated by recognition of gut pathogens. If this was the explanation then the infiltrating population would demonstrate an activated effector phenotype from the outset rather than the population progressively developing effector functions.

Does expansion in expression of the TRVβ3 gene segment by the T cell population in the kidney really suggest clonal proliferation? The only way to explore this is by sequencing the TCRs of these T cells (see Chapter 5). However, there are other possible explanations for the expansion of particular TRVβ gene segments in UUO injury which include superantigens and T cells activated in response to non-renal antigens. Superantigens are able to cause T cell activation independent of antigen/CDR3 interactions. They bind to MHC on the APC and to specific regions on the β-chain of the TCR, encoded by the TRVβ gene segment, to trigger T cell activation. One such superantigen is coded for by the mouse mammary virus, a retrovirus able to integrate its viral genome into that of the host mouse. In the presence of superantigen a clonal proliferation of T cells using a specific TRVβ chain could be generated. Although the same TRVβ gene segment would be expressed by these T cells, the complete CDR3 region would not be identical due to differing Dβ and Jβ gene segments. If a T cell clone using a specific TRVβ gene segment had been generated by superantigen stimulation in UUO, a similarly large population of these T cells would be seen in both kidney and spleen and therefore superantigens cannot explain the differences between kidney and spleen TRVβ expression within an individual mouse. The second possible explanation for the expansion of T cells using a particular TRVβ gene segment may be because a restricted T cell population has developed in response to a foreign antigen elsewhere. A monoclonal population of T cells developed in response to a gut pathogen could be attracted along a chemokine gradient generated by inflammation within the UUO kidney. However, the consistent finding of excess TRVβ3 gene segment expression by T cells in the kidney of multiple UUO mice makes this less likely. Therefore it remains to be seen in Chapter 5 whether the over expression of TRVβ3 in the UUO kidney represents a clone of T cells.

The TRVβ expression profiles seen in the three normal and one sham mouse were very similar. This finding is consistent with other groups who have demonstrated correlation in the expression pattern of TRVβ gene segments between unrelated individuals (Melenhorst, Lay et al. 2008) but there was variability in expression of the different TRVβ gene segments. These biases or variability's in expression of gene segments have

been shown to occur at two stages: either during pre-thymic selection of TCR development or during thymic selection. Pre-thymic selection biases could occur when TRVβ, TRDβ and TRJβ gene segments combine to produce the pre-TCR or at the stage when it combines with the pTα chain to form a mature TCR. Genetic factors intrinsic to the TRVβ locus may be important such as accessibility of a particular TRVβ locus, proximity of the TRVβ gene segment to the TRDβ and TRJβ gene segments and the efficiency by which a particular β-chain can pair with an α-chain (Melenhorst, Lay et al. 2008). Others have suggested that inherent developmental genetic biases shape the repertoire prior to thymic selection (Wilson, Marechal et al. 2001). Biases in the TRVβ repertoire could also occur at the point of thymic T cell selection due to MHC interactions. The main TCR filtering process in the thymus positively selects for T cells which bind self antigen and self-MHC with low avidity, so it follows that the TRVβ repertoire is selected by MHC. Also particular TRVβ chains that recognise superantigens with Class II MHC can be negatively selected for in the thymus due to high affinity binding to the TCR, again affecting the mature TRVβ repertoire seen outside the thymus (Fairchild, Knight et al. 1991).

In normal and sham animals I demonstrated higher levels of expression of certain TRVβ gene segments in kidney compared to spleen, in particular the TRVβ13.2 and 29 segments. This was consistently seen all four animals and there are a number of explanations for this. One possibility is that it is artefact related to PCR. However, I made every effort to exclude sample contamination with a number of control checks. I always performed all PCR reactions with non-template control wells and discarded the entire experiment if template was detected in these wells. All PCR products were stored in a different laboratory to the location of the PCR reagents and all equipment was exposed to UV light to prevent DNA contamination: so this is an unlikely explanation for the over expression of TRVB13.2 and 29. Another explanation would be that circulating lymphocytes remained in the tissues despite perfusion with saline however, this technique has been an accepted strategy used by other groups performing similar experiments to eliminate circulating lymphocytes (Heeger, Smoyer et al. 1996). Since the total number of T cells within normal kidney is far fewer than in spleen or UUO kidney, a circulating clone of T cells e.g. developed in response to an infection would make more impact on the TRVβ gene segment expression profile in the normal kidney. However, it would seem unlikely that mice stored in a clean environment at different times would develop the same infection and that an identical population of T cells

would not also expand in the spleen. On balance this seems an inadequate explanation for expansion of TRVβ13.2 and 29 in the normal kidney.

I think the most likely explanation for the over expression of TRVβ13.2 and 29 are clones of T cells within the normal and sham kidney. The TRVβ13.2 and 29 gene segments as classified by IMGT are the same as the TRVβ8.2 and 7.1 gene segments as classified by Arden. Type I NKT cells display a semi-invariant TCR which is most frequently made up from TRVβ8.2, 7 and 2 gene segments (Arden classification). When translated into the IMGT nomenclature, this corresponds to the TRVβ13.2, 29 and 1 gene segments, respectively. It seems likely that I have demonstrated NKT cells in all four normal or sham kidneys expressing TRVβ13.2 (IMGT)/ 8.2 (Arden) and TRVβ29 IMGT/ 7.1 (Arden). Also in two out of three normal kidneys TRVβ1 (IMGT) was over expressed which is consistent with this also being a population of NKT cells. It is important to note that not all NKT cells have such a limited TRVβ repertoire as suggested for type I NKT cells.

Rabb's group investigated the possibility of a resident population of conventional or unconventional T lymphocytes in healthy mice kidneys and found that 23% +/- 4% of the CD3+ lymphocytes were double negative (DN) (Ascon, Ascon et al. 2008). They also found a small NKT population, as determined by CD4+NK1.1+CD1d restricted cells, accounting for 12% of the total CD3+ population. They examined the TRVβ profile of these lymphocytes in the normal kidney by flow cytometry using antibodies to the TRVβ proteins and discovered an increased percentage of CD4+ lymphocytes expressing the TRVβ2, 7, 8.1 and 8.2 chains (TRVβ1, 29, 13.3 and 13.2 respectively as classified by IMGT). They also found CD8+ cells in the normal kidney which over-expressed the TRVβ8.3 and 9 chains (TRVβ13.1 and 17 respectively, as classified by IMGT). The CD3+ DN population over expressed TRVβ2, 3, 5.5/5.2, 7, 8.3, 8.1/8.2 and 13 (TRVβ1, 26, */12.1, 29, 13.1, 13.3/13.2 and 14 respectively as classified by IMGT, where * indicates not recognised). These findings by Ascon et al are consistent with and support my findings and suggest there are resident populations of NKT cells in normal mice kidneys.

With UUO injury, there was no consistent increase in the proportion of the T cell population expressing either TRVβ13.2, 29 or 1 gene segments in the UUO kidney when compared to the expansion seen in the normal and sham kidneys. However, in the literature there are examples of NKT cells playing a role in early renal injury, with

evidence that NK and NKT cells are important in the pathogenesis of IRI (Ascon, Lopez-Briones et al. 2006; Li, Huang et al. 2007), but there is no literature on NKT cells, chronic TI injury and fibrosis. In the IRI work by Rabb, after injury increasing numbers of CD3+NK1.1+ and CD3-NK1.1+ cells were seen within the kidney after 3 hours and this correlated with an increase in serum creatinine. By 24 hours there were also increased numbers of CD4+NK1.1+ cells in the ischemic kidney compared to normal controls. NKT cells can be CD4+ and display the surface markers CD69 and CD44 therefore, despite no evidence of NKT cell involvement by other groups in chronic injury, there is a possibility that the activated T cells demonstrated in Chapter 3 may be NKT cells rather than traditional T cells. The role of NKT cells in normal kidney and disease is unclear but these cells are thought to have an immunomodulatory role (Wu, Gabriel et al. 2009). NKT cells produce copious amounts of pro and anti-inflammatory cytokines upon activation but may overall favour immune regulation and contribute to and link both innate and adaptive immunity. The groups of cytokines produced by NKT cells may determine the phenotype of the effector lymphocyte population produced and help to facilitate lymphocyte and macrophage responses.

From a technical viewpoint a number of specific decisions were made about the methods used. Taqman fluorescent probes rather than SYBR green were used for quantitative real time PCR, after reviewing published work comparing the two methods (Walters and Alexander 2004). The fluorescent probe method was found to be more consistent across a range of TCR signal levels and robust in the presence of contaminating non-TCR cDNA. Since the absolute numbers of T cells within the normal kidney were low compared to the large numbers present in the spleen, it was important that the PCR technique used were reliable across this range.

The second technical point involves primer efficiencies. Two main comparisons were made: the first between kidney and spleen using the same primer pair and second between differences in the expression of the twenty two TRVβ gene segments using different primer pairs within the same animal. Consistent and highly efficient primers pairs were required to compare the expression of the different TRVβ gene segments within a single animal, since small differences in the efficiencies of the pairs may have skewed the TRVβ gene segment profiles. The most efficient primer pair, TRVβ15-TRCβ, may have over represented the proportion of T cells expressing the TRVβ15 gene segment. Conversely, the least efficient primer pair, TRVβ19-TRCβ, may have underestimated the T cell expression of this gene segment. The efficiency of the

TRVβ3-TRCβ primer pair, when TRVβ3 was consistently one of the most highly expressed gene segments in the UUO kidney, was 1.96, when the median primer efficiency was 1.94 and the range 1.87 – 2.07. The efficiency of the TRVβ3 primer pair was not at the extremes of the range and so primer efficiency was unlikely to have accounted for the increase in TRVβ3 expression by T cells in the UUO kidney, it is more likely that this truly represented the T cell population of the UUO kidney.

Finally, one criticism for the approach taken in this chapter was that we only examined TRVβ gene segment expression within UUO kidney using real time PCR and thus transcribed TRVβ gene segments. This may not accurately represent TCR protein expression on the surface of T cells within UUO kidney. One approach would have been to use commercially available fluorochrome labelled antibodies to known TRVβ chain proteins and determine the relative protein expressions of the different TRVβ chains by flow cytometry. Other groups, including the work done by Heeger's group, showed similarity between the TRVβ protein expression by flow cytometry and TRVβ at the transcript level by real time PCR. This justifies the real time PCR method used as it has been shown to provide a reasonable approximation to the TRVβ protein expression in vivo.

In summary, the data from this chapter supports the hypothesis of antigen-dependent T cell activation in the UUO model of renal injury, with a loss of immunological tolerance. The next step was to sequence cells from UUO kidney where there was over expression of the TRVβ3 gene segment compared to the spleen, to determine whether this represented a clonal population of T cells.

Chapter 5. Evidence of T cell clonality in normal and diseased kidney

5.1 Introduction

In order to determine if antigen-dependent T cell activation occurs in UUO injury, I assessed whether T cell clones, with an identical CDR3 region, were present in obstructed kidney.

The work using real time PCR from Chapter 4 demonstrated that in seven of the ten obstructed animals there was over expression of TRVβ3 by T cells within UUO kidney compared to spleen. The expansion of this T cell population expressing TRVβ3 might suggest that a clone of T cells had developed in the UUO kidney which expressed the same CDR3 region. To determine whether this was the case, the Dβ and Jβ gene segments and intervening nucleotides expressed by these T cells were sequenced.

From the literature, groups have used a variety of methods in attempts to infer or prove the clonality of a population of T cells. Spectrotyping can be used to determine the length of the CDR3 nucleotide sequence: if a T cell population had identical CDR3 length, it would infer (but not prove) clonality of that population since the individual nucleotides may be different (Lim, Baron et al. 2002). To definitively determine whether the CDR3 region of a T cell population is identical, sequencing the region of interest is necessary.

In this chapter I present the results of T cell receptor sequencing performed on the kidney and spleen of UUO mice to establish whether a dominant sequence was present suggesting antigen-dependent T cell activation. I also sequenced the CDR3 region in lymphocytes from normal kidney and spleen to establish whether similar sequences were present without manipulation.

5.2 Cloning of CDR3 TCR sequences

Cloning techniques were used to allow the subsequent sequencing of the TCRs present in kidney and splenic tissues. Five UUO mice were examined in this way: one mouse sacrificed after 7 days of obstruction (D7 Animal 2 (A2)), three mice after 14 days (D14 Animals 3 (A3), 6 (A6) and 9(A9)) and one after 28 days (D28 Animal 2 (A2)). In all of these mice the TRVβ3 gene segment was over expressed by T cells in the UUO kidney compared to the spleen, suggesting an expanded T cell population using TRVβ3 in their CDR3 region.

Standard PCR using a Taq polymerase with proof reading capability to prevent errors in amplification and the TRVβ3-TRCβ primer pair were used to amplify the reverse transcribed mRNA extracted from kidney or splenic tissue of UUO mice. This amplified the Dβ and Jβ gene segments for each TCR along with the intervening nucleotides which provide β-chain TCR diversity.

The PCR products were then inserted into a plasmid vector and bacteria were transformed. A number of individual colonies, between 25 and 50, were selected, expanded and plasmid DNA extracted and plasmid insert sequenced. We assumed that each individual colony represented an individual T cell found in the kidney or spleen of that animal and the plasmid insert included the CDR3 β-chain region for that specific T cell. Comparison of the sequences generated from the different colonies determined whether there were identical CDR3 sequences within an individual UUO kidney and spleen and whether there were similarities between mice. Similar experiments were also performed on kidney and splenic tissue from three normal mice.

5.2.1 Determining the success of the cloning reactions

In order to determine whether the cloning reactions were successful before the plasmid inserts were sent away for sequencing, the extracted plasmid DNA from each of the chosen colonies underwent standard PCR with the TRVβ3-TRCβ primer pair and the PCR product assessed by agarose gel electrophoresis (Figure 5.1). This demonstrated that the initial PCR amplification and cloning reactions had been successful, and that the plasmids contained the TRVβ3 and TRCβ gene segments of interest in a nucleotide sequence of an appropriate size around 200bp. There was no amplification of product in the non-template control lane demonstrating no contamination of reagents with DNA.

For each of the five UUO and three normal mice examined, 25-50 colonies were chosen which had been generated from kidney tissue and 25-50 colonies from spleen. After extracting the plasmid DNA, performing standard PCR and then separating the products by agarose gel electrophoresis, it was demonstrated that 96.1% +/- 5.3% of all the plasmids contained an insert and that insert was an appropriate size. Only the plasmids with an insert of the correct size were submitted for sequencing.

Figure 5.1- PCR products separated by agarose gel electrophoresis generated using the TRVβ3-TRCβ primer pair on plasmid DNA from colonies 1-24, from the normal spleen of animal 2

Reverse transcribed RNA extracted from splenic tissue of normal animal 2 was amplified using a high fidelity Taq polymerase and the product inserted into a plasmid vector, which then transformed bacteria. Twenty four colonies were picked and grown and subsequently the plasmid DNA was extracted. Each individual colony included a unique plasmid insert which was the nucleotide sequence of the CDR3 β-chain of a TCR found in the normal spleen. Standard PCR reactions were carried out using the TRVβ3-TRCβ primer pair and the 24 different samples of extracted plasmid DNA. The products were separated by agarose gel electrophoresis to demonstrate that all 24 cloning reactions were successful with 24 similar sized PCR products being generated of around 200bp. The difference in the sizes of the products was due to the assortment of Dβ and Jβ gene segments used by each T cell and the addition and deletion of junctional nucleotides. No product was demonstrated in the NTC lane confirming no contamination of the reaction with DNA.

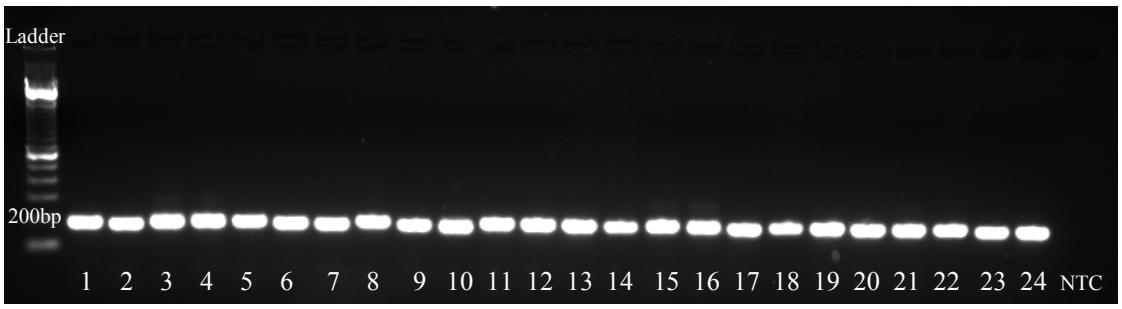

5.3 Sequencing of the TCR CDR3 region of renal and splenic lymphocytes

The TCR CDR3 sequences found in the kidney and spleen of both UUO and normal animals were assessed to investigate the presence of a dominant sequence and by inference a clonal T cell population. For each of the eight mice between 24 and 50 different samples of plasmid DNA per tissue were sent for sequencing to a commercial company (Macrogen). Between 19 and 49 successful T cell CDR3 sequences were acquired from the plasmid DNA samples. Therefore overall 91.9% +/- 8.3% of the plasmid DNA was successfully sequenced and contained a CDR3 nucleotide sequence. Comparison was then made between the CDR3 sequences generated from an individual kidney or spleen to determine which TRJβ gene segment was expressed and whether there were multiple identical sequences suggesting that this sequence was highly expressed.

5.3.1 CDR3 sequences from experimental UUO kidney

In all of the three day 14 UUO mice (A3, A6 and A9) there was one predominant TRJβ gene segment in the CDR3 region however, this TRJβ gene segment varied between the different animals. In the D14A3 mouse this was the TRJβ2.4*01 gene segment, in D14A6 TRJβ2.2*01 and in D14A9 the predominant gene segment was TRJβ2.7*01. However, not all these CDR3 sequences were the same despite containing the same TRJβ.

The CDR3 sequences were further analysed to determine how many were identical. In the single mouse examined after 7 days of UUO, the dominant identical sequence accounted for 12/39 (31%) of the total sequences examined and expressed TRJβ1.3*01 (Figure 5.2 (a)). In the day 14 UUO mice: the dominant identical sequence in the D14A3 kidney accounted for 8/39 (21%) of the total sequences and contained the TRJβ2.4*01 gene segment (Figure 5.2 (b)), in D14A6 10/45 (22%) were identical and contained TRJβ2.2*01 (Figure 5.2 (c)) and in the D14A9 kidney 14/46 (30%) were the same and expressed TRJβ2.7*01 (Figure 5.2 (d)).

A very large number of cDNA templates were available for amplification and cloning. Assuming that amplification across the CDR3 region and cloning were equally efficient for all sequences then this suggested that 21% - 31% of the initial cDNA templates expressing TRVβ3 were identical and demonstrated the presence of a clone of T cells with an identical TCR CDR3 region within the UUO kidney. In addition, as illustrated from Figures 5.2 (a-d), there were smaller numbers of identical sequences seen in the

kidney of day 7 and 14 UUO mice however, these accounted for no more than four identical sequences.

In the one day 28 UUO mouse it was not possible to demonstrate a dominant population of identical plasmid sequences from the 23 colonies examined, the largest identical number of sequences seen was a triplet (Figure 5.2 (e)).

Figure 5.2- Using UUO kidney cDNA expressing TRVβ3, TRJβ gene segment usage and the total number of identical sequences were determined in five mice (a) Day 7 A2, (b) Day 14 A3, (c) Day 14 A6, (d) Day 14 A9 and (e) Day 28 A2

TCR CDR3 gene sequences from UUO kidney at three time points were analysed: 7 days (n=1), 14 days (n=3) and 28 days (n=1). The total number of identical CDR3 β-chain sequences, categorised by the TRJβ segment they expressed, is shown. Each of the day 7 and 14 UUO kidneys demonstrated a dominant CDR3 nucleotide sequence which accounted for 21% - 31% of the plasmid inserts sequenced for that kidney. There were also smaller numbers of identical CDR3 sequences identified in these mice. By comparison the mouse sacrificed after 28 days of UUO had fewer identical sequences, the maximum being 3/23 which accounted for 13% of the total number sequenced.

(a) Day 7 Animal 2 UUO Kidney

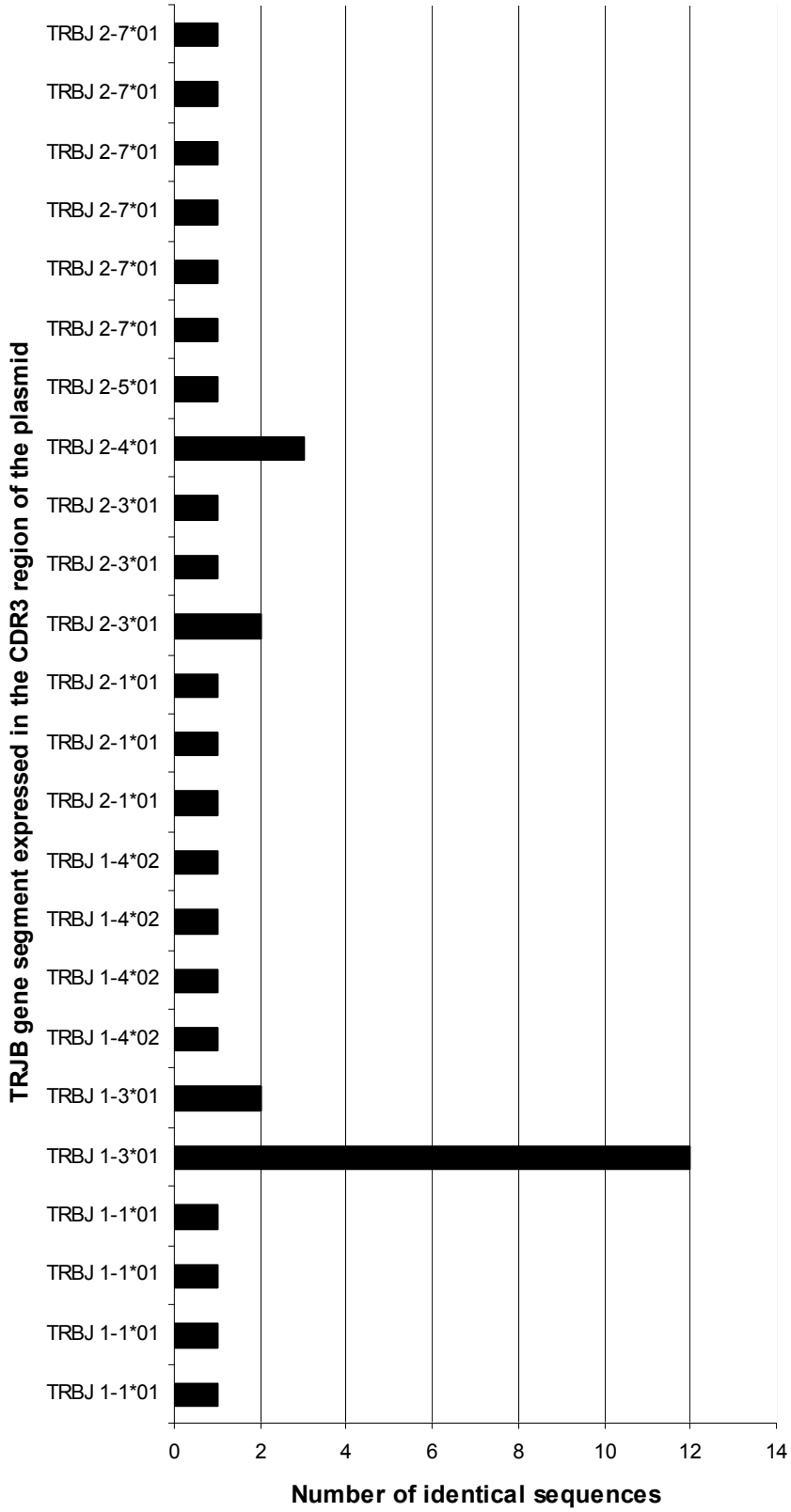

(b) Day 14 Animal 3 UUO Kidney

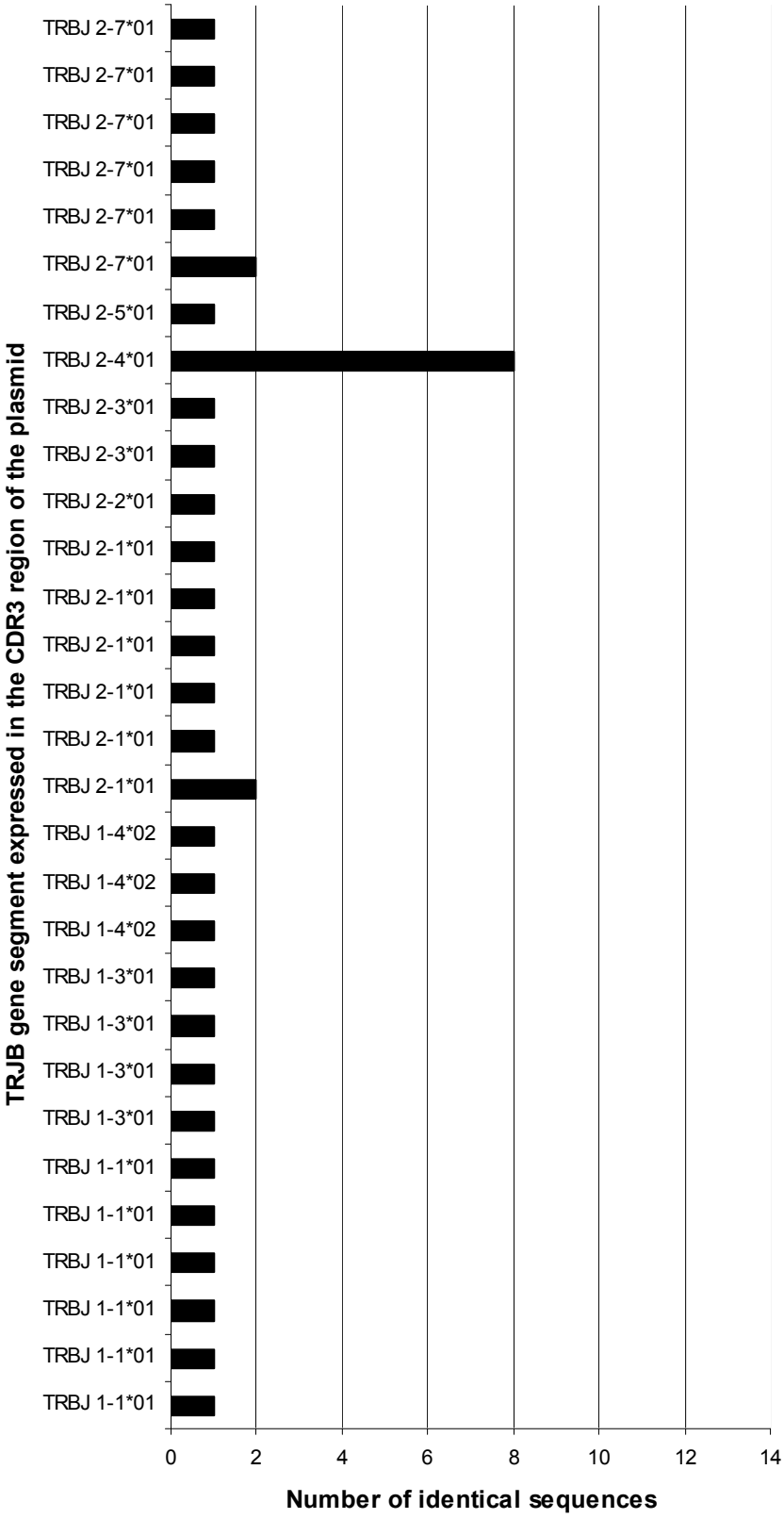

(c) Day 14 Animal 6 UUO Kidney

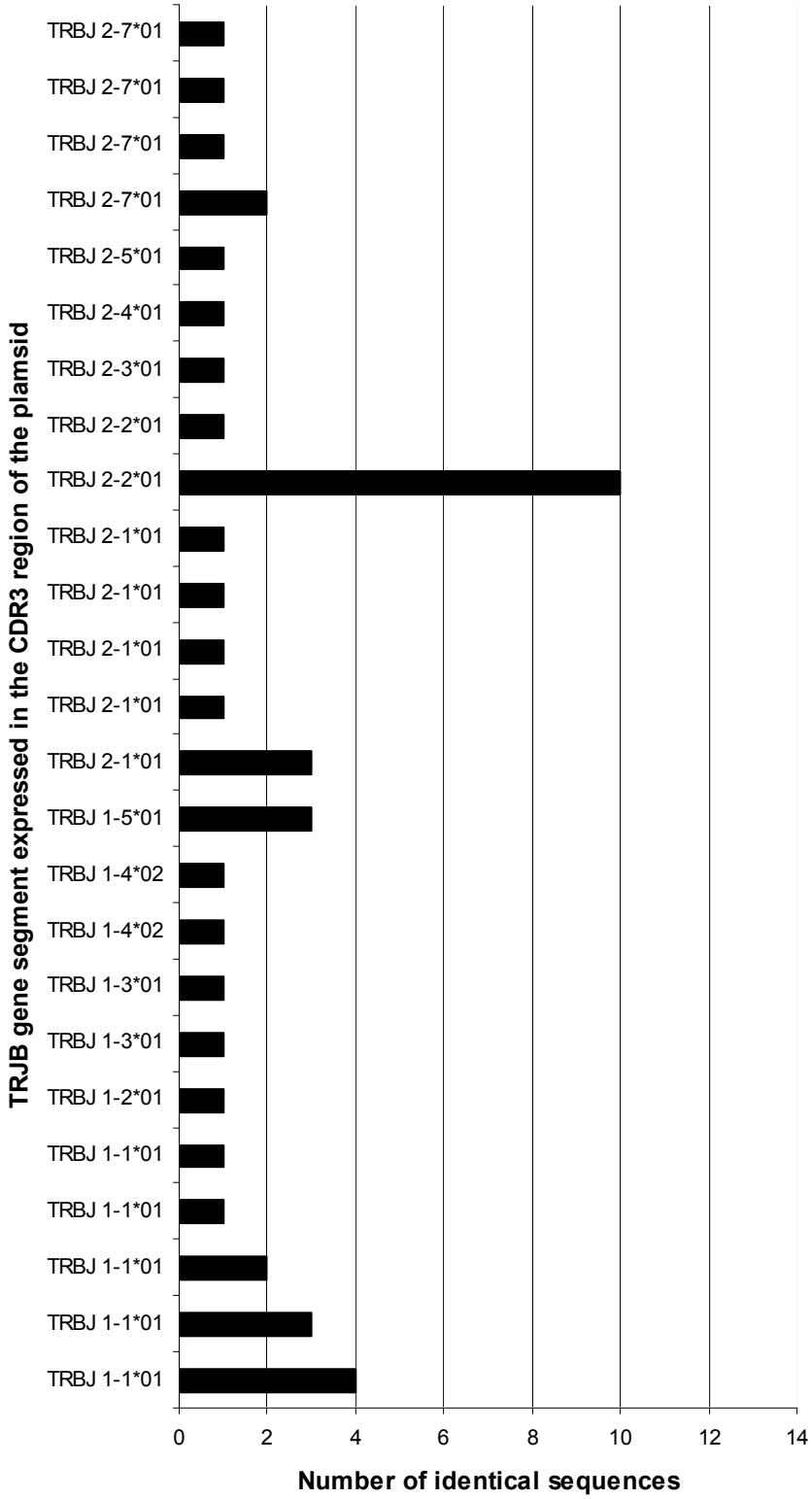

(d) Day 14 Animal 9 UUO Kidney

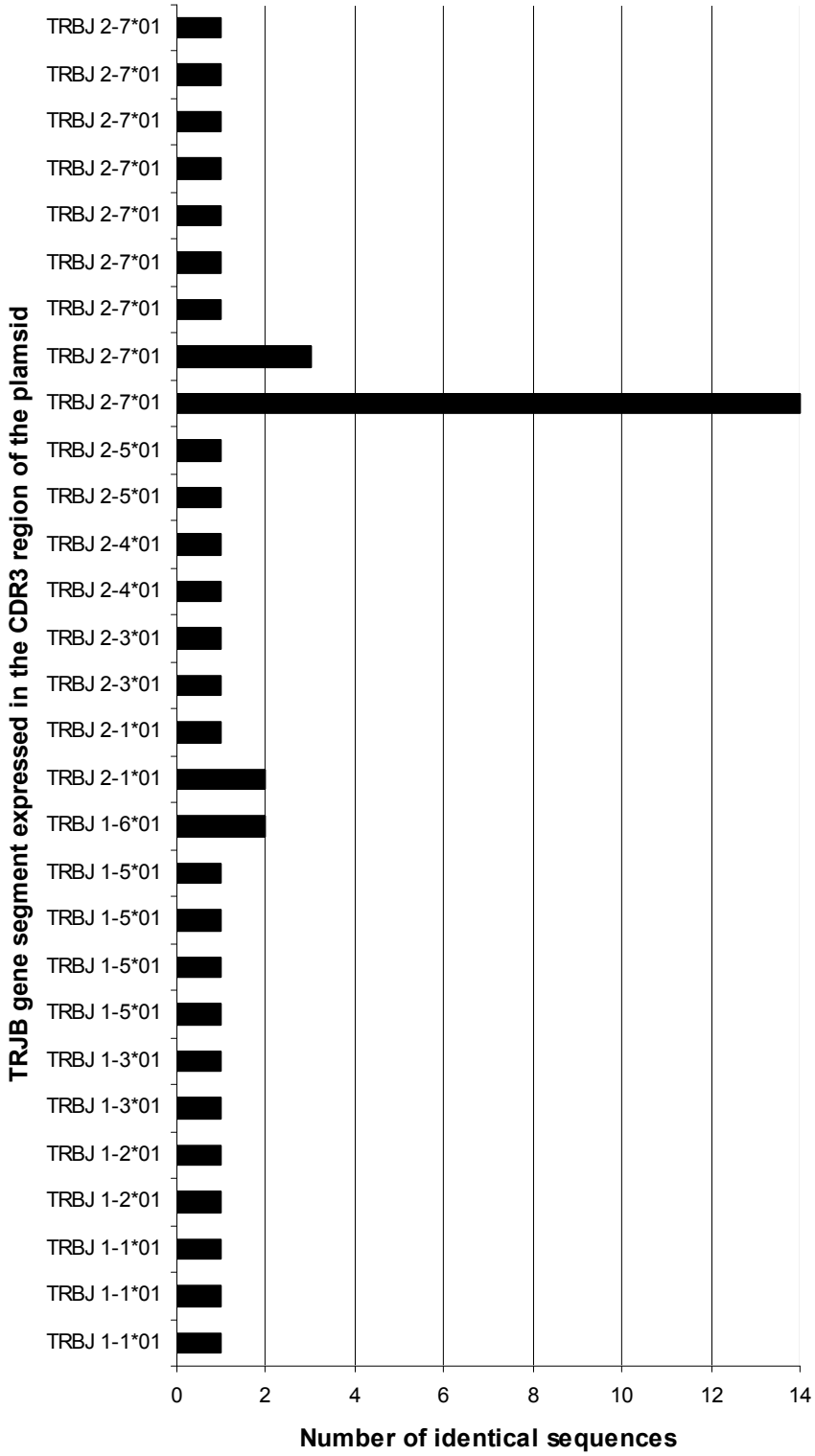

(e) Day 28 Animal 2 UUO Kidney

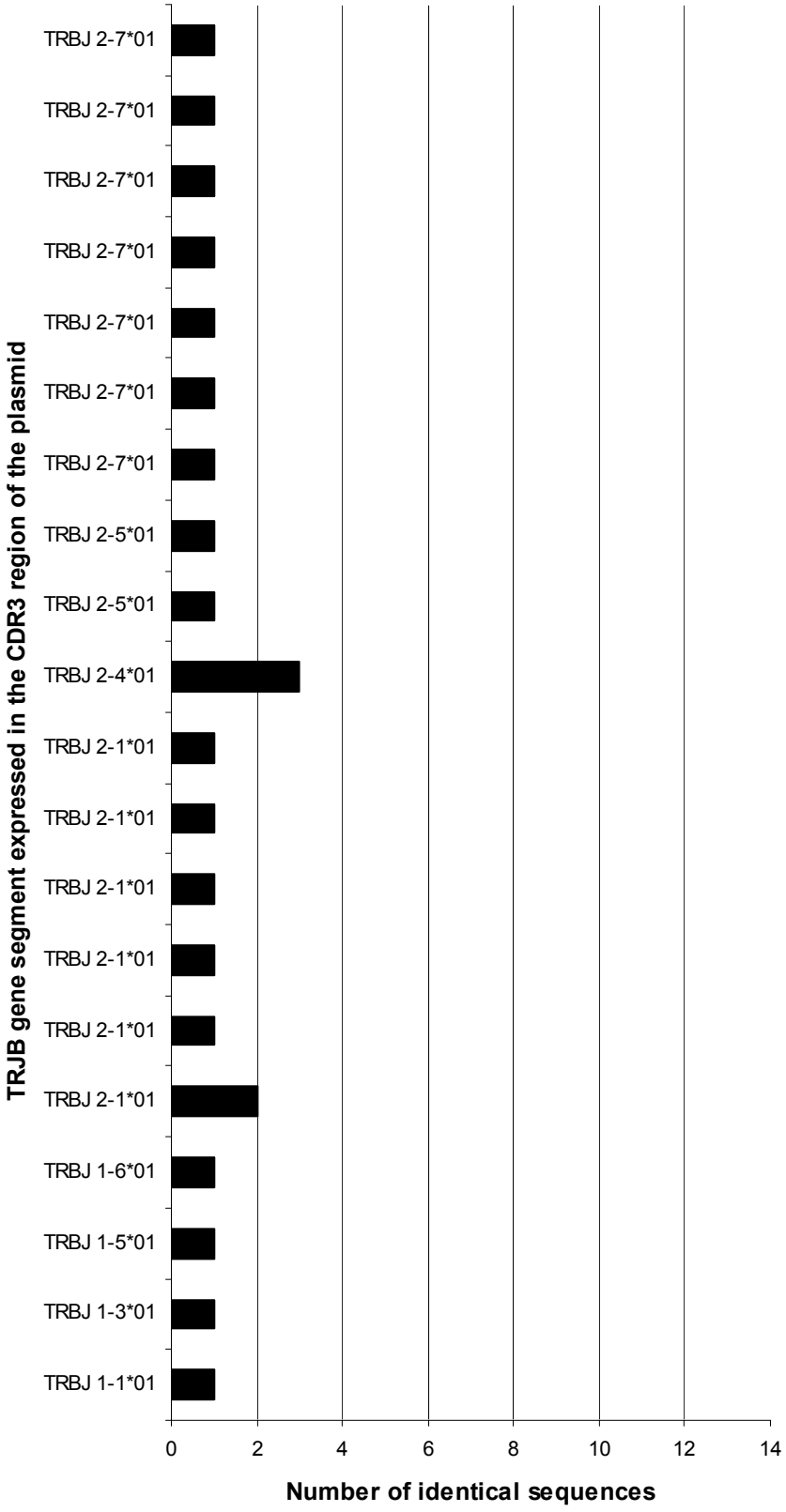

5.3.1.1 Cumulative frequency curves for UUO kidneys

An alternative method of illustrating this sequence data would be to examine the cumulative frequency of identical CDR3 sequences found in the experimental UUO kidneys (Figure 5.3). This would depend upon whether a particular sequence occurred only once, or whether there are pairs, triplets, quadruplets or >4 identical sequences found. There was a dominant CDR3 TRVβ3 sequence demonstrated in the day 7 and 14 UUO kidneys accounting for 21% – 31% of all the colonies sequenced, where there were >4 identical sequences. Furthermore, in three out of four animals <55% of the sequences were unique.

This was very different that that seen in the day 28 animal were no more that 3 identical sequences were demonstrated and 78% of the CDR3 sequences were unique single sequences. This suggested that in the mouse obstructed for 28 days there was no longer a dominant TRVβ3 CDR3 sequence.

Figure 5.3- Cumulative frequency of identical TCR sequences in experimental animals

The cumulative frequency graph illustrates the differences in the numbers of identical CDR3 sequences in the UUO kidney at the three time points.

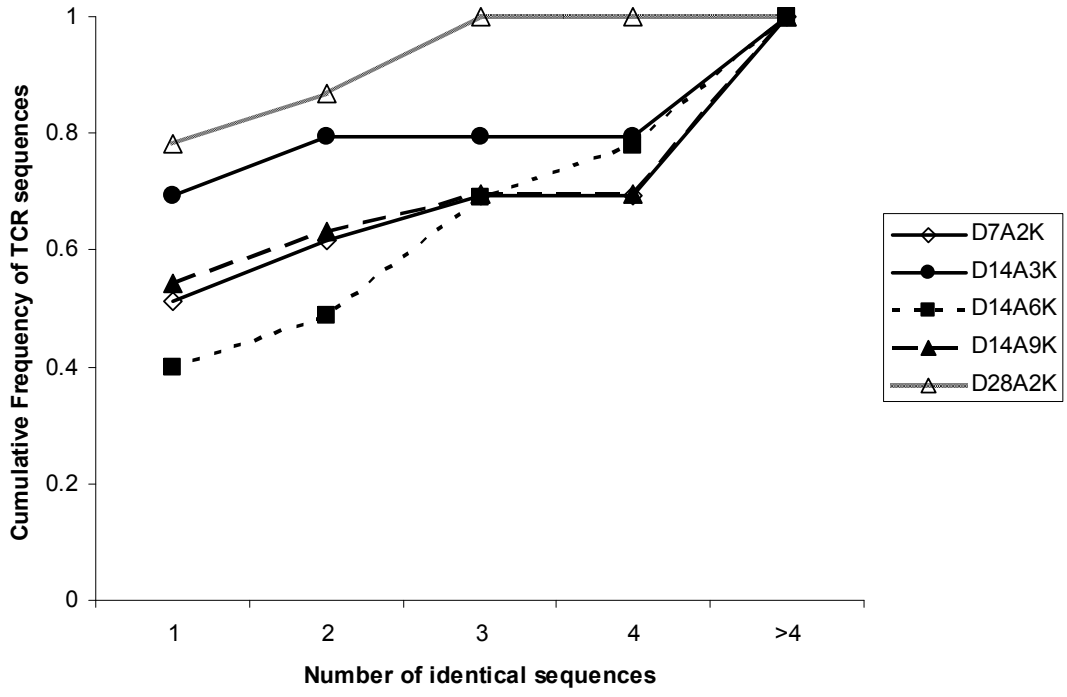

5.3.2 CDR3 sequences from experimental UUO spleen

Analysis of the TCR CDR3 sequences from the spleen of all five UUO mice demonstrated no more than one triplet of identical sequences (3/25 identical colonies sequenced from the D14A3 UUO spleen and 3/46 in the D14A9 UUO spleen) suggesting there was no dominant TCR CDR3 sequence and no T cell clone expressing TRVβ3 as illustrated in the corresponding UUO kidneys (Figure 5.4).

Figure 5.4- CDR3 sequences demonstrated in five experimental UUO spleens

The bar chart illustrates the number of identical CDR3 sequences demonstrated in the UUO spleen as a percentage of the total number of sequences. Between 64% and 92% of the CDR3 sequences in UUO spleens were unique and no more than a triplet of identical sequences were identified.

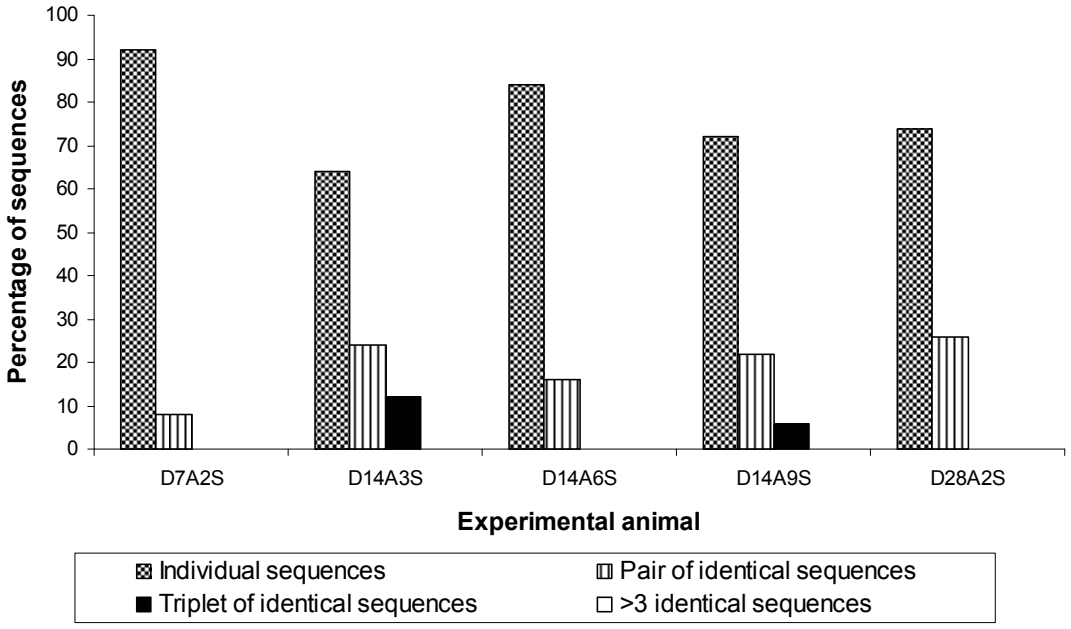

5.3.3 Comparison of the CDR3 sequences from UUO kidney and spleen

Differences between the number of identical CDR3 sequences within UUO kidney and spleen are shown in Figure 5.5. In three out of the four day 7 and 14 mice there were more individual unique CDR3 sequences within UUO spleen than obstructed kidney, as well as no dominant large identical CDR3 sequence within the UUO splenic colonies sequenced. In the day 28 UUO mouse there were no more than three repeated CDR3 sequences within kidney or spleen.

When comparing the proportion of identical sequences found in the kidney and spleen of an individual UUO mouse the Chi squared test was used (Figure 5.6). The D7A2, D14A6 and D14A9 mice showed a significantly greater proportion of ≥3 identical sequences in the kidney compared to the spleen ($p<0.05$). There were less significant differences in the proportion of ≥3 identical sequences between UUO kidney and spleen seen in the D14A3 and D28A2 animals ($p= 0.38$ and 0.07 respectively). However, for all day 7 and 14 UUO mice there was a significantly greater proportion of ≥4 identical sequences in the kidney compared to the spleen ($p<0.05$).

When comparison was made between the CDR3 nucleotide sequences identified within the UUO spleen and kidney of the same mouse, very few were identified in both organs. In the day 14 A6 mouse one pair of identical CDR3 sequences in the spleen were the same as the eight identical sequences found in that UUO kidney and one splenic sequence in the day 7 UUO mouse was the same as twelve in that UUO kidney. Three unique CDR3 sequences found in the day 14 A3 spleen were identical to three unique sequences in the UUO kidney of that mouse. Otherwise there were no similarities between the CDR3 nucleotide sequences identified in the UUO kidney and spleen of an individual mouse.

Figure 5.5- Cumulative frequency of identical TCR sequences in kidney and spleen of UUO animals expressing TRVβ3

The cumulative frequency graphs compare the differences in the numbers of identical CDR3 sequences in the UUO kidney and spleen which expressed TRVβ3 at day 7 (a), 14 (b) and 28 (c).

(a) Day 7

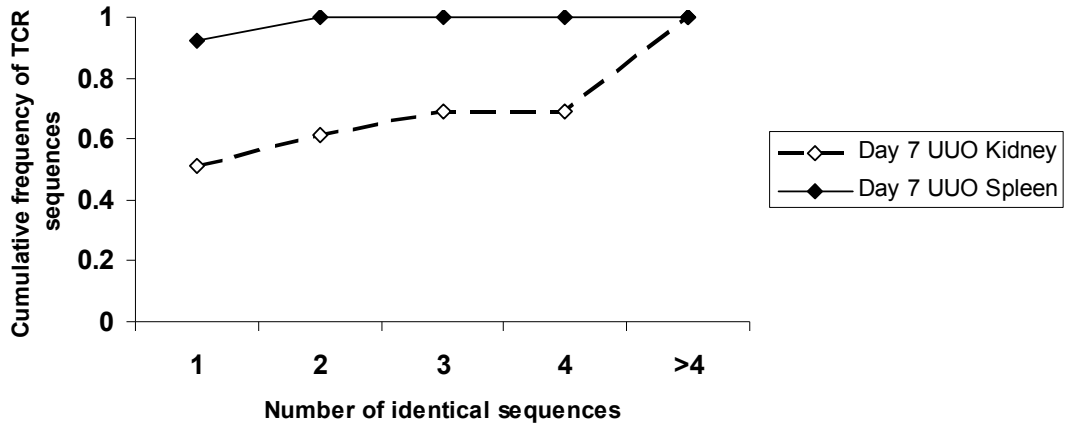

(b) Day 14

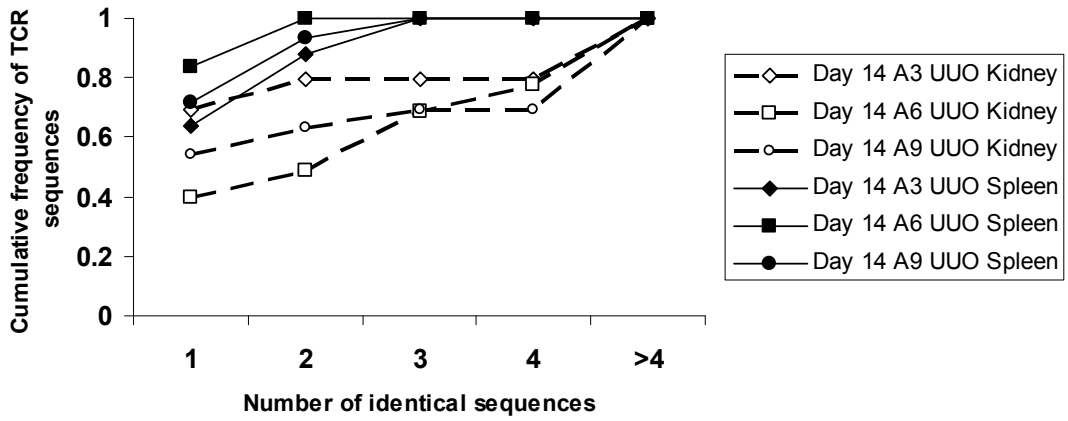

(c) Day 28

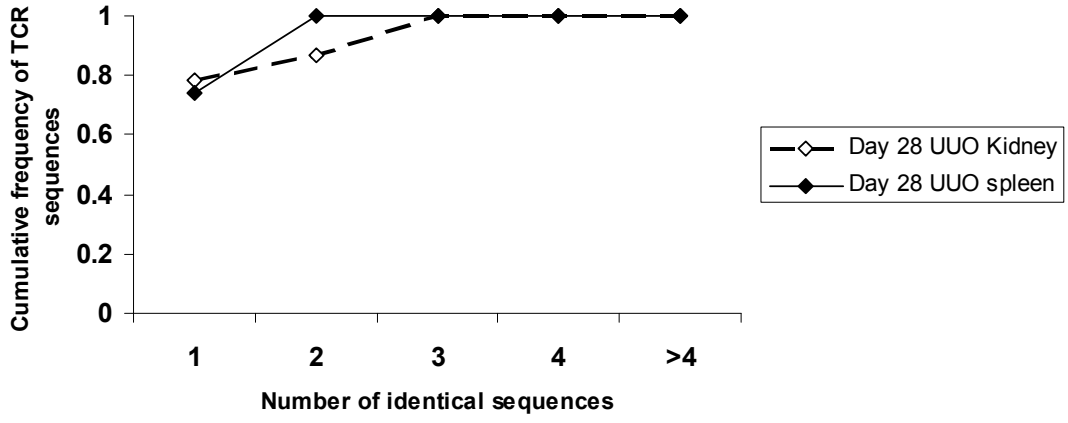

Figure 5.6- Comparison of the number of identical CDR3 sequences identified in UUO kidney and spleen

The day 7 and two of the day 14 mice (A6 and A9) showed a significantly greater proportion of ≥3 identical sequences in the UUO kidney compared to the spleen (*p<0.05). Less significant differences in the proportion of ≥3 identical sequences were found in the UUO kidney and spleen of the day 14 A3 and the day 28 mouse.

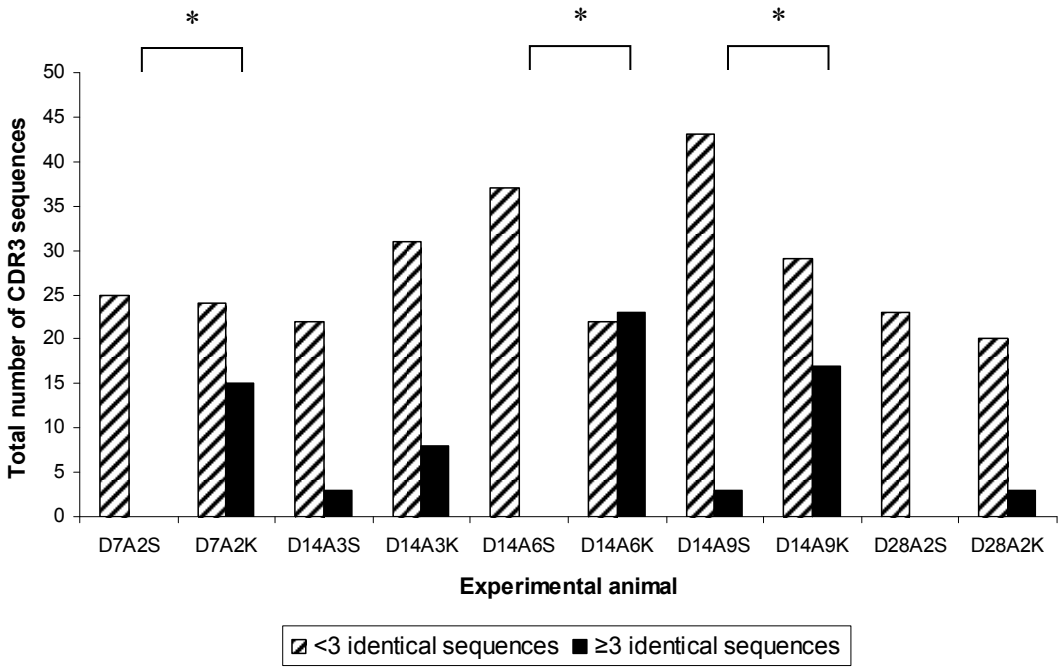

5.3.4 CDR3 sequences from normal kidney

The TCR CDR3 TRVβ3 sequences found in the kidneys of two normal C57Bl/6 mice (A2 and A3) were analysed to determine which TRJβ gene segment were expressed and if the CDR3 sequences were identical. These were the same mice whose TRVβ gene segment expression profile was examined by real time PCR in 4.5.1. The kidney from normal animal 1 (A1) was not used for cloning and sequencing as inadequate tissue was available. In both A2 and A3 kidneys there was one predominant TRJβ gene segment contained in the CDR3 region and was the same in both kidneys, TRJβ1.3*01.

In A2, the dominant identical sequence accounted for 6/20 (30%) of the total sequences and expressed TRJβ1.3*01 (Figure 5.7 (a)). There were also five other sequences that expressed TRJβ1.3*01 but had different nucleotide sequences to the dominant population and were three unique sequences and one pair of identical sequences. In A3, again there was a dominant identical sequence accounting for 7/19 (37%) of the total sequences and also expressed TRJβ1.3*01 (Figure 5.7 (b)). There were four other CDR3 sequences in the normal kidney of A3 which expressed TRJβ1.3*01 however, they all had unique nucleotide sequences. There were no other identical groups of nucleotide sequences demonstrated in the other colonies sampled from this normal kidney.

When the nucleotide sequences for the two dominant sequences were compared from A2 and A3, they were not the same. Furthermore, the dominant TCR sequences seen in the normal kidney were not seen in the spleen of these animals. This makes contamination by DNA or PCR product from the other animal unlikely. Again assuming that amplification across the CDR3 region and cloning were equally efficient for all sequences, this suggests that 30% - 37% of the initial cDNA templates expressing TRVβ3 in these two normal kidneys were identical, supporting the presence of a clone of T cells with an identical TCR CDR3 region.

Figure 5.7- Using normal kidney cDNA expressing TRVβ3, TRJβ gene segment expression and the total number of identical sequences were determined in two mice

Plasmid DNA sequences were analysed from the kidney of two normal mice. Each animal expressed a dominant TRJβ1-3*01 segment and dominant but different nucleotide sequence accounting for 30% (A2) and 37% (A3) of the total sequences. All the other CDR3 sequences examined from the two animals were unique apart from a single pair of sequences in A2, which also expressed TRJβ1-3*01.

(a) Animal 2

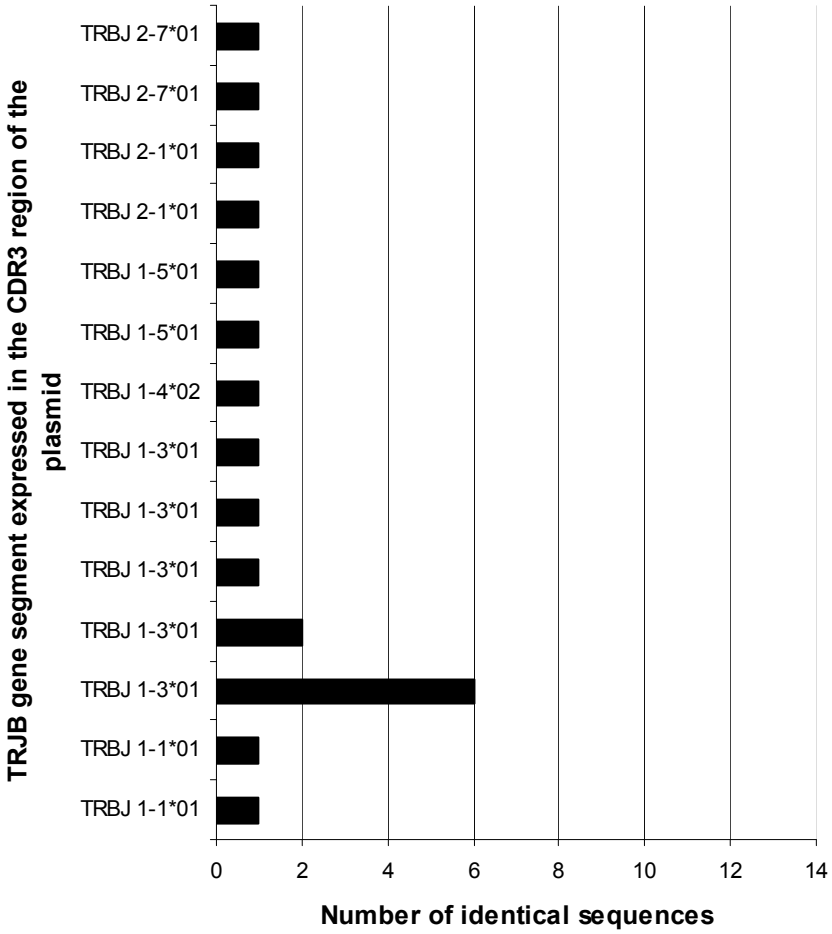

(b) Animal 3

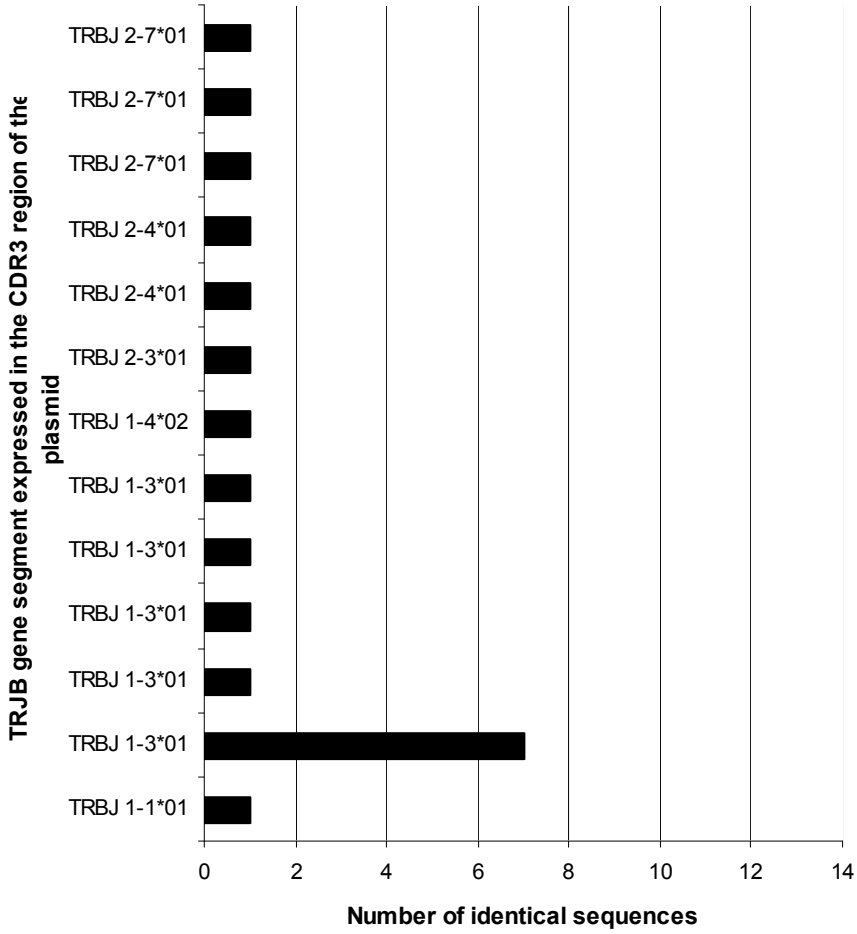
TRJB gene segment expressed in the CDR3 region of the plasmid
TRBJ 2-7*01
TRBJ 2-7*01
TRBJ 2-7*01
TRBJ 2-4*01
TRBJ 2-4*01
TRBJ 2-3*01
TRBJ 1-4*02
TRBJ 1-3*01
TRBJ 1-3*01
TRBJ 1-3*01
TRBJ 1-3*01
TRBJ 1-3*01
TRBJ 1-1*01
0
2
4
6
8
10
12
14
Number of identical sequences

5.3.4.1 Cumulative frequency curves for normal kidneys

The cumulative frequency of identical CDR3 sequences in the normal kidney of A2 and A3 demonstrated that around 60% of all the CDR3 sequences were unique in both animals (Figure 5.8). However, 30% and 37% of the sequences in the kidney of A2 and A3 respectively, which expressed TRVβ3, had an identical CDR3 region. These profiles were similar to the cumulative frequencies of identical CDR3 sequences in the day 7 and 14 UUO kidneys.

Figure 5.8- Cumulative frequency of identical TCR sequences in normal kidney

The cumulative frequency graph illustrates the differences in the numbers of identical CDR3 sequences in the kidney of two normal mice.

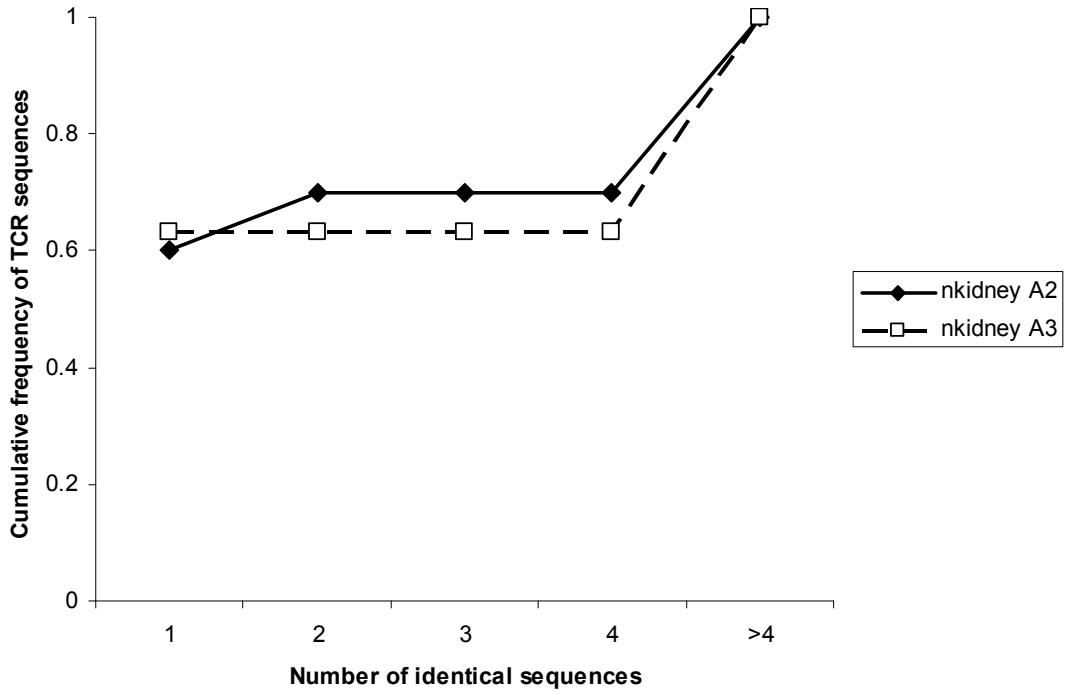

5.3.5 CDR3 sequences from normal spleen

Splenic tissue was available from all three normal animals whose TRVβ gene segment expression profile was analysed by real time PCR in Chapter 4. In all three normal spleens there was no single dominant CDR3 sequence present in contrast to the dominant sequences seen in normal kidneys, which accounted for around one third of the sequences. The cumulative frequency graph in Figure 5.9 illustrates the number of identical CDR3 sequences found in the spleens of the three normal mice. The profiles seen A1 and A2 are very similar to those seen for UUO spleens, with 80% - 94% of the sequences being unique and individual. Only pairs of identical sequences were demonstrated despite 33 and 49 different plasmid inserts being sequenced in A1 and A2 respectively. Although the CDR3 sequences from the spleen of A3 did not demonstrate a large dominant sequence of the size demonstrated in kidney, there were five identical sequences (5/45) which accounted for 11% of the total number of sequences. A pair and two triplets of identical sequences were also found in this spleen however, not one of these repeated identical sequences were seen in the kidney of that mouse or in the spleen of the other mice. When comparing all the CDR3 nucleotide sequences examined in the kidney and spleen of an individual normal mouse, none were the same.

Figure 5.9- Cumulative frequency of identical TCR sequences in normal spleen

The cumulative frequency graph illustrates the differences in the numbers of identical CDR3 sequences in the spleen of three normal mice.

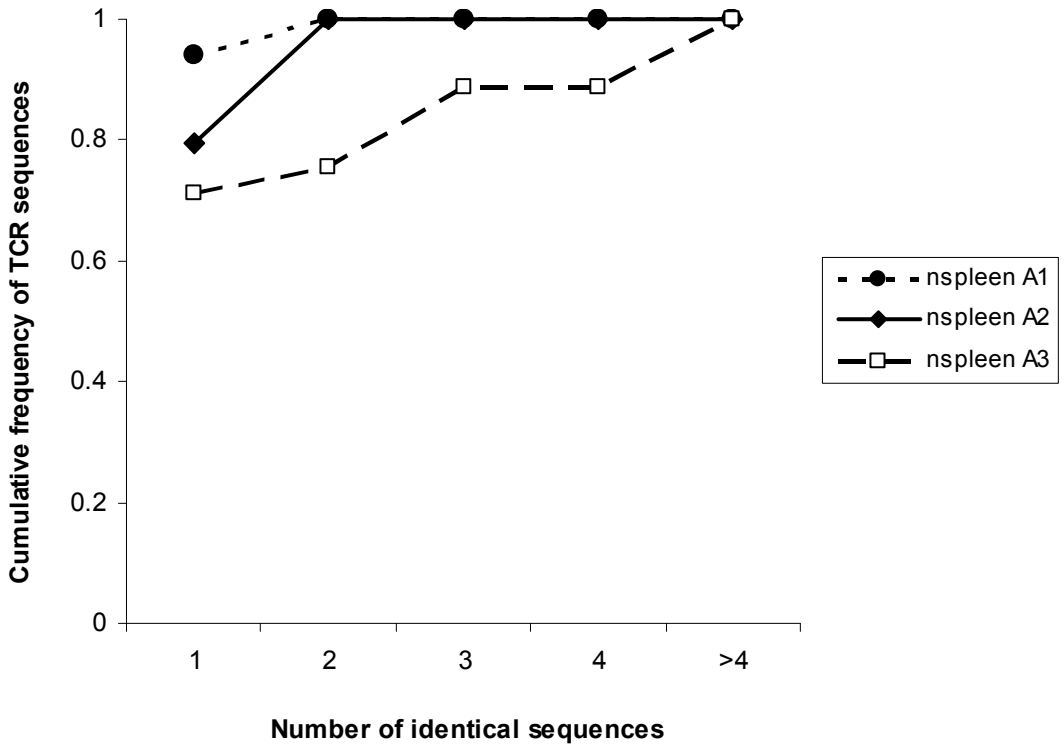

5.4 T cell populations within kidney and spleen

Using the real time PCR data from Chapter 4 which calculated the percentage of the total T cell population which expressed TRVβ3 and the maximum number of identical sequences determined using the cloning technique, an estimate could be made of the percentage of the total T cell population within the kidney or spleen of an animal which were identical and expressed TRVβ3 (Table 5.1).

In the day 7 and 14 UUO kidneys, the largest identical population of T cells expressing TRVβ3 accounted for 3.6% - 4.9% of the total T cell population in that kidney. Similarly in the normal kidneys an identical population of T cells accounted for 2.8% and 3.7% of the total population. As shown in Chapter 3, T cells were uncommon in normal kidney and large numbers were demonstrated in UUO kidney, therefore the absolute number of T cells expressing the same TCR would be far greater in the UUO kidney.

In contrast the percentage of identical T cells expressing TRVβ3 within UUO and normal spleen was between 0.4% and 1.2% of the total T cell population in that spleen. This high percentage of identical CDR3 sequences and therefore T cells within the spleen of normal and UUO animals, around 1%, would be unusual given the spleen should contain millions of different sequences/T cells. This result may be artefactual and generated because of the relatively small numbers of colonies/ TCRs sequenced out of the vast repertoire of T cells present in the spleen. The difference between the percentages of identical T cells within kidney and spleen were statistically significant ($p=0.007$).

Table 5.1- Percentage of the T cell population within kidney and spleen which expressed TRVβ3 and were identical

The table illustrates the largest percentage of the total T cell population in the kidney or spleen of normal and UUO mice that were identical and expressed TRVβ3.

	Animal	T cells expressing TRVβ3 using RT PCR data (%)	Maximum number of identical sequences / total number cloned	Identical T cell population expressing TRVβ3 (%)
UUO Kidney	Day 7 A2	14.9	12/39	4.6
	Day 14 A3	17.5	8/39	3.6
	Day 14 A6	22.0	10/45	4.9
	Day 14 A9	14.4	14/46	4.4
	Day 28 A2	12.8	3/23	1.7
UUO Spleen	Day 7 A2	11.2	2/25	0.9
	Day 14 A3	10.0	3/25	1.2
	Day 14 A6	10.3	2/37	0.8
	Day 14 A9	10.8	3/46	0.7
	Day 28 A2	9.5	2/23	0.8
Normal Kidney	A2	12.2	6/20	3.7
	A3	7.6	7/19	2.8
Normal Spleen	A1	8.5	2/33	0.5
	A2	10.8	2/49	0.4
	A3	8.0	5/45	0.9

5.5 Analysis of CDR3 amino acid sequence

The amino acid sequence of the TCR spanning the CDR3 region was determined for all the duplicate TRVβ3 sequences demonstrated in the kidney and spleen of UUO and normal mice and aligned to allow comparison (Figure 5.10). The amino acid sequences, derived from the dominant nucleotide sequence demonstrated in each animal, were grouped together (Figure 5.10 (a)), as were the amino acid sequences derived from any duplicated nucleotide sequence from the kidney and spleen of an individual mouse (Figure 5.10 (b)). This demonstrated similarities in the CDR3 region at the amino acid level between animals. Figure 5.10 illustrates a number of conserved amino acid sequences (highlighted in yellow) in identical positions within the CDR3 region. These particular amino acids were found within the TRJβ gene segment: they were likely related to the high degree of sequence homology between different TRJβ gene segments and may represent hinge regions in the CDR3 structure. They were also present in sequences from normal spleen (Figure 5.11).

A group of three amino acids RRS or arginine, arginine, serine (highlighted in red), was demonstrated within the highly variable nucleotide region found between the final section of the TRVβ gene segment and the beginning section of the TRJβ segment and which spans TRDβ. This RRS grouping was predominantly present in the multiple identical nucleotide CDR3 sequences, which included the dominant sequence in six out of the seven kidneys examined from both UUO and normal mice. This RRS amino acid motif was only found in the UUO spleen when the same sequence was identified in the UUO kidney of that mouse. This RRS motif was not identified in any of the sequences from a normal spleen (n=42).

On further examination the nucleotide sequences which coded for the arginine and serine amino acids in this RRF motif were not the same in the dominant sequence from different animals. This could be explained by redundancy in codons (Table 5.2).

Table 5.2- Nucleotide sequence coding the RRS amino acid motif

Animal	Nucleotide sequence coding for amino acid		
	R	R	S
D7A2K	CGG	CGT	TCT
D14A6K	AGA	AGG	TCC
D14A9K	CGG	CGC	TCC
D28A2K	AGG	AGG	AGT
NkidneyA2	AGG	CGT	TCT
NkidneyA3	CGG	CGT	TCT

Figure 5.10- Aligned amino acid sequences of the CDR3 region derived from the multiple identical nucleotide sequences

(a) Amino acid sequence derived from the dominant nucleotide sequence demonstrated in the kidney and spleen of an individual animal

The dominant nucleotide sequence found in the kidney and spleen of each UUO and normal animal was converted into the corresponding amino acid sequence and aligned. Within the TRJβ gene segment region there were repeated amino acid sequences in both kidney and spleen (highlighted in yellow). However in the most variable area of the CDR3 region a repeated RRS amino acid motif (highlighted in red) was seen in the dominant sequence of six out of the seven kidneys examined, but in none of the dominant splenic sequences.

Animal	TRJB		End of TRVB3																					Beginning of TRCB		
			C	A	S	S	[...TRDβ....]							[.....								TRJβ	.....]	E	D	L
UUO Kidney																										
D7A2	J1-3*01	n=12K+1S	C	A	S	S	T	G	R	R	S	G	N	T	L	Y	F	G	E	G	S	R	L	I	V	V	E	D	L
D14A3	J2-4*01	n=8K+2S	C	A	S	S	L	G	R	G	R	Q	N	T	L	Y	F	G	A	G	T	R	L	S	V	L	E	D	L
D14A6	J2-2*01	n=10K	C	A	S	S	P	Q	R	R	S	T	G	Q	L	Y	F	G	E	G	S	K	L	T	V	L	E	D	L
D14A9	J2-7*01	n=14K	C	A	S	S	P	G	-	R	R	S	Y	E	Q	Y	F	G	P	G	T	R	L	T	V	L	E	D	L
D28A2	J2-4*01	n=3K	C	A	S	S	L	G	R	R	S	Q	N	T	L	Y	F	G	A	G	T	R	L	S	V	L	E	D	L
UUO Spleen																										
D7A2	J2-7*01	n=2S	C	A	S	S	L	P	D	S	S	-	Y	E	Q	Y	F	G	P	G	T	R	L	T	V	L	E	D	L
D14A3	J2-7*01	n=3S	C	A	S	S	L	K	G	Q	G	-	Y	E	Q	Y	F	G	P	G	T	R	L	T	V	L	E	D	L
D14A6	J2-7*01	n=2S	C	A	S	S	L	-	D	W	P	-	Y	E	Q	Y	F	G	P	G	T	R	L	T	V	L	E	D	L
D14A9	J2-7*01	n=3S	C	A	S	S	Q	-	-	D	R	V	Y	E	Q	Y	F	G	P	G	T	R	L	T	V	L	E	D	L
D28A2	J2-7*01	n=2S	C	A	S	S	L	G	L	G	G	-	N	E	Q	Y	F	G	P	G	T	R	L	T	V	L	E	D	L
Normal kidney																										
nkidneyA2	J1-3*01	n=6K	C	A	S	S	L	G	R	R	S	G	N	T	L	Y	F	G	E	G	S	R	L	I	V	V	E	D	L
nkidneyA3	J1.3*01	n=7K	C	A	S	S	S	G	R	R	S	G	N	T	L	Y	F	G	E	G	S	R	L	I	V	V	E	D	L
Normal spleen																										
nspleenA1	J1-1*01	n=2S	C	A	S	S	T	G	-	A	G	-	T	E	V	F	F	G	K	G	T	R	L	T	V	V	E	D	L
nspleenA2	J2-7*01	n=2S	C	A	S	S	L	G	G	G	A	-	R	E	Q	Y	F	G	P	G	T	R	L	T	V	L	E	D	L
nspleenA3	J1-3*01	n=5S	C	A	S	S	L	E	G	T	G	G	N	T	L	Y	F	G	E	G	S	R	L	I	V	V	E	D	L

(b) Amino acid sequences derived from nucleotide sequences where there were >1 identical copy in the kidney and spleen of an individual animal

Within the TRJβ gene segment region there were repeated amino acid sequences seen in both the kidney and spleen derived from the TRJβ gene segment (highlighted in yellow). The repeated RRS amino acid motif (highlighted in red) was predominantly seen in the dominant sequence identified in the kidneys of both UUO and normal animals. However, it was seen in less commonly identified nucleotide sequences within the kidney and in a few UUO splenic sequences that were identified in the kidney of that animal. No amino acid sequence identified only in the spleen demonstrated the RRS motif.

Animal	TRJB		End of TRVB3..............CDR3........................Beginning of TRCB
			C A S S[...TRDβ....][...........TRJβ...........]E D L
nspleenA1	J1-1*01	n=2S	C A S S T G - A G - T E V F F G K G T R L T V V E D L
nspleenA2	J2-7*01	n=2S	C A S S L G L G - - F E Q Y F G P G T R L T V L E D L
nspleenA2	J2-7*01	n=2S	C A S S L G G G A - R E Q Y F G P G T R L T V L E D L
nspleenA2	J2-7*01	n=2S	C A S S L G G G - - - E Q Y F G P G T R L T V L E D L
nspleenA2	J2-7*01	n=2S	C A S S P - - G - - Y E Q Y F G P G T R L T V L E D L
nspleenA3	J1-3*01	n=5S	C A S S L E G T G G N T L Y F G E G S R L I V V E D L
nspleenA3	J2-3*01	n=3S	C A S S K G L G W A E T L Y F G S G T R L T V L E D L
nspleenA3	J2-3*01	n=3S	C A S S L G W V S A E T L Y F G S G T R L T V L E D L
nspleenA3	J2-7*01	n=2S	C A S S S D - - - S Y E Q Y F G P G T R L T V L E D L
nkidneyA2	J1-3*01	n=2K	C A S S L A R R S G N T L Y F G E G S R L I V V E D L
nkidneyA2	J1-3*01	n=6K	C A S S L G R R S G N T L Y F G E G S R L I V V E D L
nkidneyA3	J1.3*01	n=7K	C A S S S G R R S G N T L Y F G E G S R L I V V E D L
D7A2	J1-3*01	n=12K+1S	C A S S T G R R S G N T L Y F G E G S R L I V V E D L
D7A2	J1-3*01	n=2K	C A S S S D R - G G N T L Y F G E G S R L I V V E D L
D7A2	J2-3*01	n=2K	C A S S R T P S A - E T L Y F G S G T R L T V L E D L
D7A2	J2-4*01	n=3K	C A S S L G R G R Q N T L Y F G A G T R L S V L E D L
D7A2	J2-7*01	n=2S	C A S S L P D S S - Y E Q Y F G P G T R L T V L E D L
D14A3	J1-1*01	n=K+S	C A S S P G Q A N - T E V F F G K G T R L T V V E D L

D14A3	J1-3*01	n=K+S	C A S S T G R R S G N T L Y F G E G S R L I V V E D L
D14A3	J1-4*02	n=K+S	C A S S R S N E - - - R L F F G H G T K L S V L E D L
D14A3	J2-1*01	n=2K	C A S S Y V T D - - A E Q F F G P G T R L T V L E D L
D14A3	J2-4*01	n=8K+2S	C A S S L G R G R Q N T L Y F G A G T R L S V L E D L
D14A3	J2-5*01	n=2S	C A S S L D W G G H G T Q Y F G P G T R L L V L E D L
D14A3	J2-7*01	n=2S	C A S S L A D R G - L E Q Y F G P G T R L T V L E D L
D14A3	J2-7*01	n=2K	C A S S L V P G G S Y E Q Y F G P G T R L T V L E D L
D14A3	J2-7*01	n=3S	C A S S L K G Q G - Y E Q Y F G P G T R L T V L E D L
D14A6	J1-1*01	n=3K	C A S S L R R A - - - E V F F G K G T R L T V V E D L
D14A6	J1-1*01	n=4K	C A S S L T G A N - T E V F F G K G T R L T V V E D L
D14A6	J1-5*01	n=3K	C A S S L G R R N Q A P L - F G E G T R L S V L E D L
D14A6	J2-1*01	n=2S	C A S L Y - - - - - A E Q F L G P G T R L T V L E D L
D14A6	J2-1*01	n=3K	C A S R G G R H - - A E Q F F G P G T R L T V L E D L
D14A6	J2-2*01	n=10K	C A S S P Q R R S T G Q L Y F G E G S K L T V L E D L
D14A6	J2-7*01	n=2K	C A S S N - - R G - R E Q Y F G P G T R L T V L E D L
D14A6	J2-7*01	n=2S	C A S S L - D W P - Y E Q Y F G P G T R L T V L E D L
D14A9	J1-3*01	n=2S	C A S S P Q - V S G N T L Y F G E G S R L I V V E D L
D14A9	J1-6*01	n=2K	C A S S R - - Q D N S P L Y F A A G T R L T V T E D L
D14A9	J2-1*01	n=2S	C A S S L - - R G A A E Q F F G P G T R L T V L E D L
D14A9	J2-1*01	n=2S	C A S S E - - T N Y A E Q F F G P G T R L T V L E D L
D14A9	J2-1*01	n=2K	C A S S L G - E N Y A E Q F F G P G T R L T V L E D L
D14A9	J2-7*01	n=2S	C A S S T - - D R G R E Q Y F G P G T R L T V L E D L
D14A9	J2-7*01	n=3S	C A S S Q - - D R V Y E Q Y F G P G T R L T V L E D L
D14A9	J2-7*01	n=3K	C A S S L G - L G S Y E Q Y F G P G T R L T V L E D L
D14A9	J2-7*01	n=14k	C A S S P G - R R S Y E Q Y F G P G T R L T V L E D L
D28A2	J1-1*01	n=2S	C A S S S G - V N - T E V F F G K G T R L T V V E D L
D28A2	J2-1*01	n=2K	C A S S L D W G G - A E Q F F G P G T R L T V L E D L
D28A2	J2-4*01	n=3K	C A S S L G R R S Q N T L Y F G A G T R L S V L E D L
D28A2	J2-7*01	n=2S	C A S S L G L G G - N E Q Y F G P G T R L T V L E D L
D28A2	J2-7*01	n=2S	C A S S L - - G P - Y E Q Y F G P G T R L T V L E D L

Figure 5.11- Amino acid sequences derived from the CDR3 nucleotide sequences identified in the spleen of normal animal 2

Within the TRJβ gene segment region, a proportion of the repeated amino acid sequences identified earlier in the UUO animals were also seen in the sequences examined from this normal spleen (highlighted in yellow). The repeated RRS amino acid motif predominantly seen in the dominant nucleotide sequences identified in kidney was not evident in any of the sequences examined from normal spleen.

TRJB gene	Sequence	End of TRVB3..............CDR3........................Beginning of TRCB C A S S[...TRDβ....][...........TRJβ...........]E D L
TRBJ1-1*01	Sequence4	C A S S - S W - D N T E V F F G K G T R L T V V E D L
TRBJ1-1*01	Sequence11	C A S S L H R - G N T E V F F G K G T R L T V V E D L
TRBJ1-2*01	Sequence6	C A S S L D - - N S D Y T - F G S G T R L L V I E D L
TRBJ1-2*01	Sequence26	C A S S L G G - D S D Y T - F G S G T R L L V I E D L
TRBJ1-2*01	Sequence43	C A S S F G - A N Y D L S - F G S G T R L L V L E D L
TRBJ1-3*01	Sequence1	C A S S L G N - S G N T L Y F G E G S R L I V V E D L
TRBJ1-4*02	Sequence29	C A S S L G R G G N E R L F F G H G T K L S V L E D L
TRBJ1-5*01	Sequence13	C A S S L G - V N N Q A P L F G E G T R L S V L E D L
TRBJ1-6*01	Sequence9	C A S S P P - - - - - - P L Y F A A G T R L T V T E D L
TRBJ2-1*01	Sequence10	C A S S P - - - - - - - - G V F G P G T R L T V L E D L
TRBJ2-1*01	Sequence22	C A S S L T G V N Y A E Q F F G P G T R L T V L E D L
TRBJ2-1*01	Sequence32	C A S S L G — — N Y A E Q F F G P G T R L T V L E D L
TRBJ2-1*01	Sequence50	C A S S R D G D A — — E Q F F G P G T R L T V L E D L
TRBJ2-2*01	Sequence47	C A S S E T P - N T G Q L Y F G E G S K L T V L E D L
TRBJ2-3*01	Sequence12	C A S S L G - S S A E T L Y F G S G T R L T V L E D L
TRBJ2-3*01	Sequence20	C A S S P P Q - G T E T L Y F G S G T R L T V L E D L
TRBJ2-3*01	Sequence24	C A S S H R G S A - E T L Y F G S G T R L T V L E D L
TRBJ2-3*01	Sequence41	C A S S L G T T S A E T L Y F G S G T R L T V L E D L
TRBJ2-4*01	Sequence3	C A S S L A G - - G D T L Y F G A G T R L S V L E D L
TRBJ2-4*01	Sequence27	C A S S L S G - - G D T L Y F G A G T R L S V L E D L
TRBJ2-4*01	Sequence30	C A S S L Q G L - Q N T L Y F G A G T R L S V L E D L

TRBJ2-5*01	Sequence19	C A S S L G W G V Q D T Q Y F G P G T R L L V L E D L
TRBJ2-5*01	Sequence21	C T S S L A P - Q D T Q Y - F G P G T R L L V L E D L
TRBJ2-7*01	Sequence2	C A S S L - - - A Y - E Q Y F G P G T R L T V L E D L
TRBJ2-7*01	Sequence5	C A S S H R G L S - Y E Q Y F G P G T R L T V L E D L
TRBJ2-7*01	Sequence7	C A S S H D G - - - - R V F F G K G T R L T V L E D L
TRBJ2-7*01	Sequence8	C A S S L G - G G A R E Q Y F G P G T R L T V L E D L
TRBJ2-7*01	Sequence16	C A S S L G - - L G F E Q Y F G P G T R L T V L E D L
TRBJ2-7*01	Sequence17	C A S S S D R - - - N E Q Y F G P G T R L T V L E D L
TRBJ2-7*01	Sequence18	C A S S L G - G G A R E Q Y F G P G T R L T V L E D L
TRBJ2-7*01	Sequence23	C A S S L - - K Q G L E Q Y F G P G T R L T V L E D L
TRBJ2-7*01	Sequence33	C A S S L G - - L G F E Q Y F G P G T R L T V L E D L
TRBJ2-7*01	Sequence35	C A S S P - - - - G Y E Q Y F G P G T R L T V L E D L
TRBJ2-7*01	Sequence36	C A S S P - - - - G Y E Q Y F G P G T R L T V L E D L
TRBJ2-7*01	Sequence37	C A S S P T - - - G D E Q Y F G P G T R L T V L E D L
TRBJ2-7*01	Sequence39	C A S S L G - G G - - E Q Y F G P G T R L T V L E D L
TRBJ2-7*01	Sequence40	C A S S L L G - - - - E R Y F G P G T R L T V L E D L
TRBJ2-7*01	Sequence42	C A S S L G - G G - - E Q Y F G P G T R L T V L E D L
TRBJ2-7*01	Sequence44	C A S S L - - - D S - E Q Y F G P G T R L T V L E D L
TRBJ2-1*01	Sequence45	C A S S L D R V D Y A E Q F F G P G T R L T V L E D L
TRBJ2-7*01	Sequence46	C A S S L E - - V Y - E Q Y F G P G T R L T V L E D L
TRBJ2-7*01	Sequence48	C A S S L - - E G G - E Q Y F G P G T R L T V L E D L

5.6 Determining whether T cell clonality in the UUO kidney was in a CD4+ or CD8+ population

In order to determine whether the multiple identical CDR3 TRVβ3 sequences in the cDNA from whole kidney were derived from a CD4+ or CD8+ T cell population, lymphocytes were FACS sorted into two populations. However, due to the recovery of limited numbers of T cells there was an inadequate amount of mRNA to perform real time PCR on the individual CD4+ and CD8+ populations with all twenty two TRVβ primer pairs, so the whole UUO kidney was divided into halves. One half was processed, as explained in Chapter 4, using real time PCR to define the TRVβ gene segment that was over expressed in the kidney compared to the spleen. CDR3 sequences containing this over expressed TRVβ gene segment were then determined using whole tissue. The other half of the kidney was digested and T cells sorted into CD4+ and CD8+ populations by FACS before the CDR3 sequences containing the over expressed TRVβ gene segment were ascertained.

5.6.1 Determining which TRVβ gene was over expressed in the UUO kidney

The D14A9 UUO kidney demonstrated TRVβ3 gene segment over expression (Figure 5.12). Therefore, cDNA from whole UUO kidney was amplified using the TRVβ3-TRCβ primer pair and the products cloned into plasmid vectors and sequenced. Of the colonies, or CDR3 sequences, 14 out of the total 46 nucleotide sequences were identical (30%). They expressed the TRJβ2.7*01 gene segment and had the sequence shown in Figure 5.13.

Figure 5.12- Relative use of TRVβ gene segments from the Day 14 A9 UUO mouse

Over expression of the TRVβ3 gene segment was demonstrated in the day 14 A9 UUO kidney.

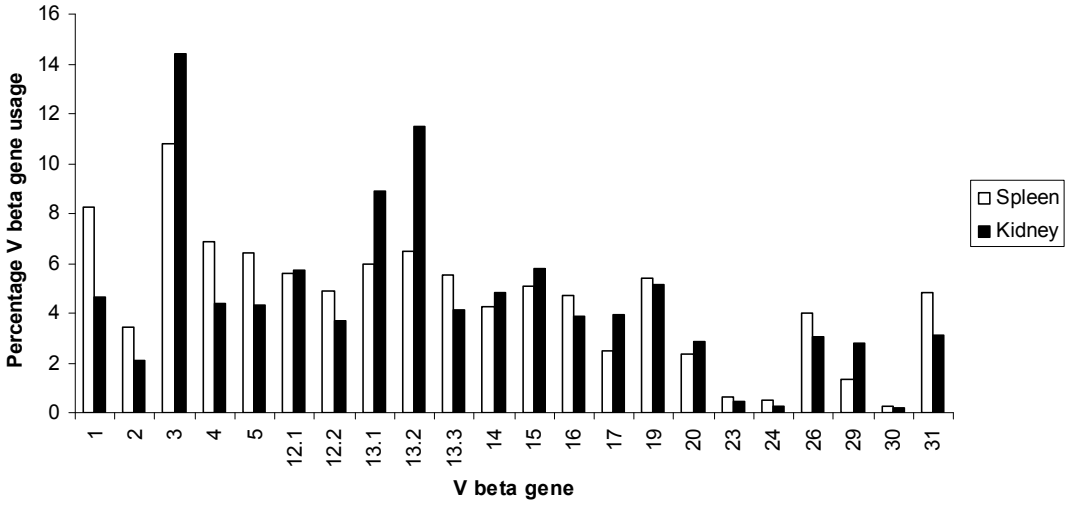

Figure 5.13- Dominant TCR CDR3 nucleotide sequence identified from whole UUO kidney tissue of the D14 A9 UUO mouse

The nucleotide sequence is outlined with the position of the primer annealing sites and position of the TRJβ2.7*01 gene segment.

Vb3 primer site on antisense strand]
----------Vb3 gene segment----------] [----------
CACTGGAGGACTCAGCTGTGTACTTCTGTGCCAGCAGCCCTGGACGGCGCTCCTATG

----------J2.7*01 gene segment----------][-------Cb gene segment-----
AACAGTACTTCGGTCCCGGCACCAGGCTCACGGTTTTAGAGGATCTGAGAAATGTGACT

[-----Cb primer site---------
---------- Cb gene segment----------
CCACCCAAGGTCTCCTTGTTTGAGCCATCAAAAGCAGAGA**TTGCAAACAAACAAAAGG**

-------]

CTACC

5.6.2 Sorting the CD4+ and CD8+ populations from the Day14 A9 UUO kidney

The other half of the D14A9 kidney was digested with collagenase and deoxyribonuclease. An estimated total of 4.8 x 10^6 cells were acquired by the digestion process, with >50% of the cells being viable as assessed by Trypan blue staining. The CD45+, CD4+ and CD8+ cells were stained with fluorochrome linked antibodies to APC-Cy7, FITC and PerCP respectively. This allowed the CD4+ and CD8+ populations of cells to be sorted using flow cytometry as shown in Figure 5.14. Figure 5.15 demonstrates the isotype controls used for the fluorochrome labelled antibodies, demonstrating no significant non-specific fluorochrome binding.

Figure 5.14- FACS sorting CD4+ and CD8+ lymphocytes from digested D14A9 kidney tissue

CD45+, CD4+ and CD8+ populations of cells, fluorochrome stained with APC-Cy7, FITC and PerCP respectively, were sorted by FACS. Approximately 1,300 CD4+ (P2) and CD8+ (P4) lymphocytes were obtained from the kidney.

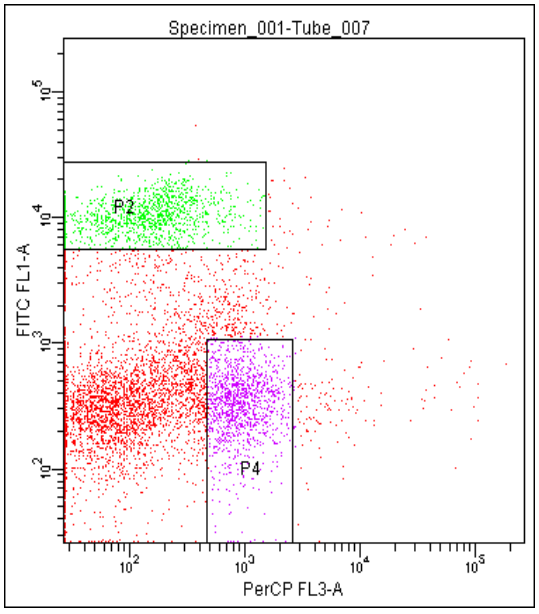

Figure 5.15- Flow cytometry performed on naive splenocytes using both a labelled antibody and its isotype control

These three histograms show overlapping populations of naive splenocytes with the same fluorescent intensity when flow cytometry was performed on cells alone and with cells labelled with the fluorochrome isotype-control antibody demonstrating there was no non-specific fluorochrome binding.

(a) APC-Cy7 label for CD45+ cells

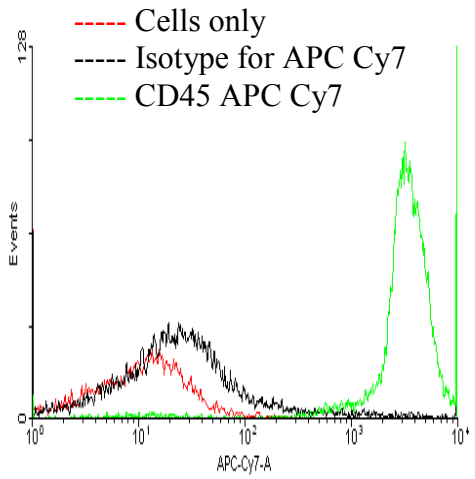

(b) PerCp label for CD8+ cells

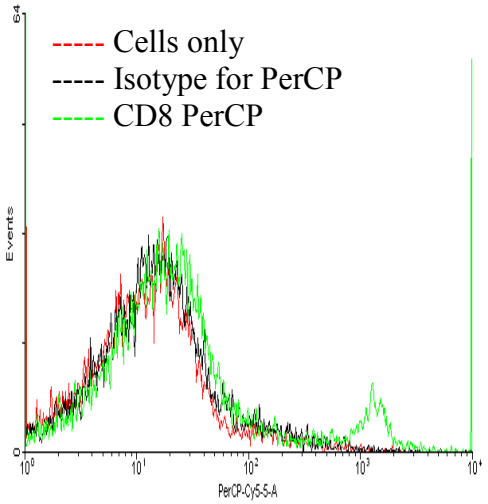

(c) FITC label for CD4+ cells

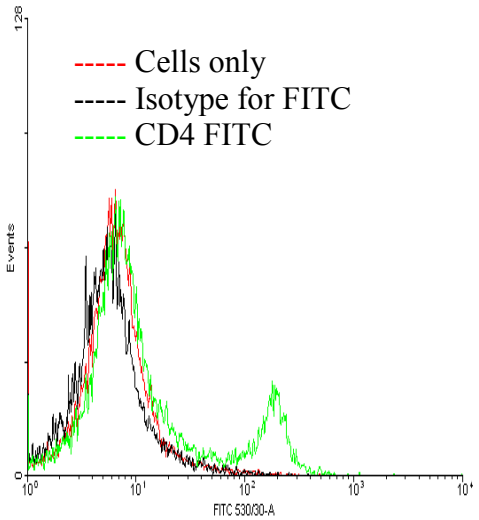

5.6.3 Sequencing the CD4+ or CD8+ lymphocyte populations from UUO kidney

In order to determine whether the dominant population of T cells found in the UUO kidney were CD4+ or CD8+, their CDR3 regions were sequenced.

5.6.3.1 Generating sufficient cDNA to use in the cloning reactions

To perform the cloning reactions using the cDNA from the sorted CD4+ and CD8+ cell populations, adequate PCR product must be generated. This was confirmed by separating the products using agarose gel electrophoresis generated after 35 cycles of PCR under standard conditions using the TRVβ3-TRCβ primer pair. An appropriately sized band of around 200bp was demonstrated (Figure 5.16).

Despite using the majority of the cDNA generated from the sorted CD4+ and CD8+ cells and 35 cycles of PCR, the bands on the gel were weak. The amount of amplicon was limited by the total number of cells that could be extracted and sorted. In addition to using the PCR product demonstrated on the gel in Figure 5.16 for the cloning reactions, it was used in a further round of PCR reactions performed using the same primer pair for a further 20 cycles. This PCR product was separated by electrophoresis on the agarose gel shown in Figure 5.17 and was of the appropriate size and therefore also used in the cloning reactions to sequence the CDR3 region of the sorted CD4 and CD8+ lymphocyte populations.

Figure 5.16- PCR product separated by agarose gel electrophoresis using cDNA from the sorted CD4+ and CD8+ populations of cells

Faint bands of amplicon were separated by agarose gel electrophoresis after high fidelity Taq polymerase and the TRVβ3-TRCβ primer pair was used for 35 cycles of PCR with cDNA from the sorted CD4+ and CD8+ cell populations.

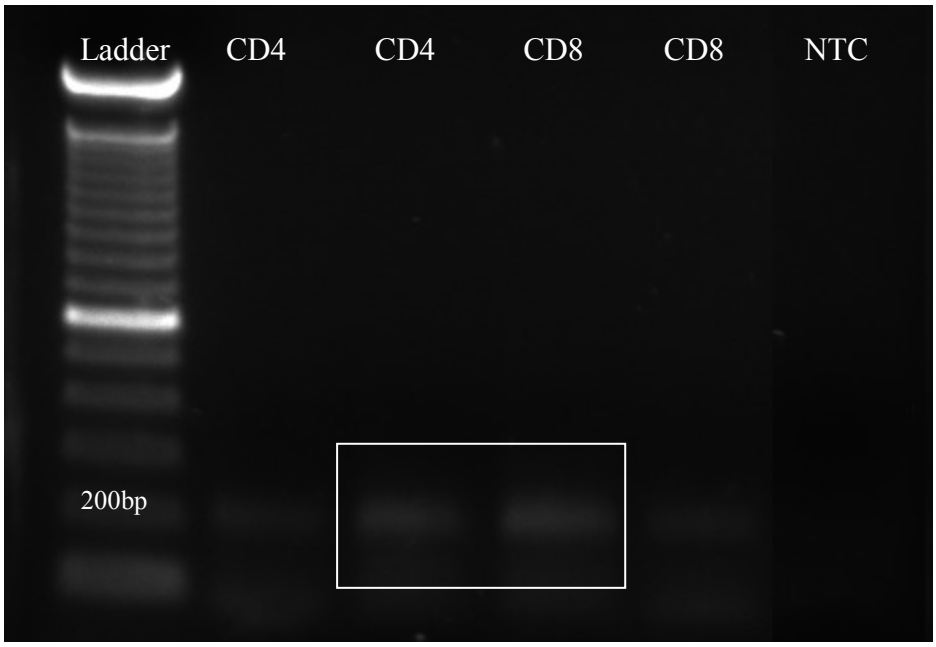

Figure 5.17- PCR product separated by agarose gel electrophoresis using cDNA that had already undergone 35 cycles of PCR

PCR products were separated by agarose gel electrophoresis after 20 cycles of PCR. The starting cDNA was that illustrated in Figure 5.16, which had been generated after 35 cycles of PCR and originated from the sorted CD4+ and CD8+ populations.

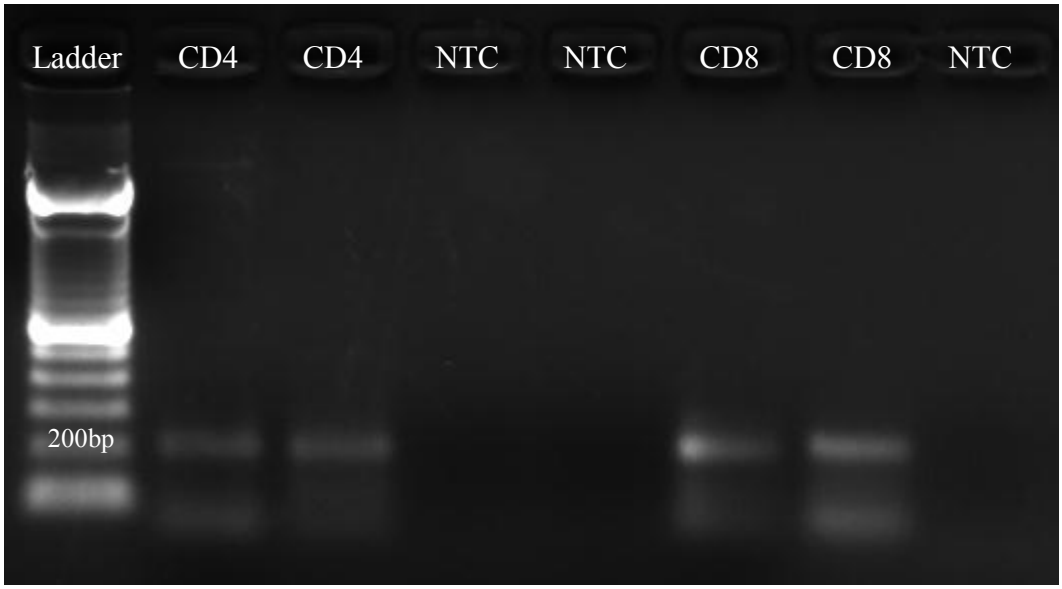

5.6.3.2 Cloning and sequencing reactions using cDNA originating from the sorted CD4+ and CD8+ populations

Cloning reactions were performed using the standard method with the PCR products shown in Figures 5.16 and 5.17. Upon completion of the cloning reactions standard PCR reactions were performed using the plasmid DNA from all the different colonies to confirm an appropriate sized insert. Both the plasmid DNA generated from the DNA that had just one round of PCR (35 cycles) and that which had two rounds of PCR (35 cycles followed by a further 20) seemed equally successful at generating an appropriate sized insert. Overall the success rate for generating an insert was less than when cDNA extracted from whole tissue was used for the cloning reactions. Therefore <50% of the plasmid DNA was sent for sequencing, which totalled 27/50 CD4+ colonies and 15/50 CD8+ colonies. The sequencing was successful in 14/27 of the sorted CD4+ TCR sequences and 11/15 of the sorted CD8+ TCR sequences.

Of the four sequences generated from the CD4+ cells which expressed TRJβ2.7*01, none were identical to the dominant sequence from whole kidney however, four out of the eight CD8+ CDR3 sequences which contained TRJβ2.7*01were identical to those 14 identical TCR sequences from whole kidney seen in that mouse. This suggested that approximately 30% of the T cell population from whole tissue which expressed TRVβ3 and 36% of the sorted CD8+ T cell population expressing TRVβ3 were identical. The dominant TRVβ3 sequence identified in whole kidney was exclusively found in the CD8+ population. In addition this sequence also contained the CDR3 RRS amino acid motif seen in other UUO mice and illustrated in Figure 5.10.

5.7 Discussion

This aim of this chapter was to determine whether there were identical T cell populations within UUO kidney. The experimental data from the last chapter demonstrated a disproportionate increase in TRVβ3 expressing T cells within the kidney compared to the spleen in UUO mice. This was not seen in normal mice where the expression of TRVβ3 in kidney and spleen was similar. The literature has demonstrated consistent expression of TRVβ gene segments in unrelated normal mice and so our results should be representative for all mice (Heeger, Smoyer et al. 1996). Therefore, the difference in TRVβ3 gene segment expression in the UUO animal must be due to the effects of obstructive injury and imply a population of T cells had expanded in the obstructed kidney: by sequencing these T cells the clonality of the infiltrate could be determined. If a dominant population of identical sequences was discovered, which would be dependent upon T cells recognising a single antigenic epitope, this would suggest a T cell population had expanded in response to a renal autoantigen or neoantigen generated by the obstructive injury. However, if the expanded UUO kidney T cell population expressing TRVβ3 was found to be a varied population of T cells with unique TCR sequences, this would imply either: a population of bystander T cells with different TCRs had expanded in the kidney activated by the inflammation generated by UUO or the T cell infiltrate was attracted to the kidney in an antigen-independent manner by chemokine mediated attraction from the circulating pool.

In order to investigate the possibility of a clonal population of T cells the TCR CDR3 TRVβ3 sequences from UUO kidney were examined. DNA from UUO kidney was amplified by PCR using the TRVβ3-TRCβ primer pair and the amplicon cloned into plasmid vectors, which then transformed bacteria. Each colony of bacteria that developed was assumed to contain a plasmid with an individual PCR product and therefore the CDR3 β-chain sequence for an individual T cell.

From the results of the UUO experiments conducted on mice obstructed for 7 and 14 days one single dominant CDR3 nucleotide sequence was seen in each kidney, this was different in each individual mouse, and accounted for 21% - 31% of the CDR3 TRVβ3 sequences examined. This would be consistent with 21% - 31% of all the TRVβ3 T cells within the UUO kidney utilising the same TCR CDR3 β-chain. This equated to an identical T cell population within the UUO kidney (assuming the α-chain was the same) which accounted for between 3.6% and 4.9% of the total T cell population. The dominant CDR3 sequence identified within the UUO kidney was rarely seen in UUO

spleen. This would suggest that this population of T cells expanded in response to obstructive injury and the recognition of either renal autoantigen or neoantigen. For this to occur there must have been a break in self-tolerance since there is no alloantigen in UUO.

The presence of a dominant identical clone implies there was proliferation of this population, which follows antigen recognition and accompanies activation to an effector phenotype. This implies this clone of T cells had effector function but does not prove it actively contributed to injury. This activated population may have either a destructive or regulatory role or, despite activation, be passive in the process of renal injury. There may be other identical clones of T cells within the kidney, since we only looked at T cells expressing TRVβ3, which have different effector functions or recognise other antigenic epitopes. As demonstrated in the literature, in traditional AIDs it is likely that tolerance is lost to multiple antigenic epitopes as the disease process develops.

In the day 28 mouse the sequencing results were different to the earlier time points and there were single individual sequences or a low frequency of repeated sequences, without a large dominant sequence. This would support the phenomenon of epitope spreading, as described by Heeger and explained in Chapter 4, which develops after progressive injury where there is no dominant clone (Heeger, Smoyer et al. 1996). Alternatively, there could have been chemokine mediated recruitment of polyclonal T cells into the area of injury, on a background of earlier antigen-dependent T cell proliferation, as shown at day 7 and 14. The third possible explanation would be the generation of a population of regulatory T cells which suppressed the immune response within the UUO kidney. All three mechanisms are not mutually exclusive.

When TRVβ3 T cells from a UUO kidney were extracted and sorted the dominant sequence was exclusively found within the CD8+ population and was identical to the dominant sequence identified from the whole kidney of that animal. This demonstrated that this clone was CD8+ but does not imply that all T cell clones within the kidney would be. This could be investigated further by looking at other CDR3 TRVβ sequences within UUO kidney where the TRVβ gene segment was over expressed in the UUO kidney, such as TRVβ26 in the D14A2 mouse, and performing similar sequencing and cell sorting experiments to those illustrated in this chapter. From the literature, two groups using the UUO model have shown fibrosis was dependent upon the presence of a CD4+ T cell population (Tapmeier, Fearn et al. 2010; Niedermeier, Reich et al. 2009).

However it is possible that the CD8+ T cells identified in the UUO kidney were acting in a similar way to those demonstrated in transplantation by Robertson et al, in adhering to TEC, presenting TGFβ, inducing EMT and causing interstitial fibrosis (Robertson, Ali et al. 2004). Most likely multiple T cell subtypes play a role in UUO injury, some of which are profibrotic whilst others are protective.

For comparison purposes CDR3 TRVβ3 sequences were analysed for normal mice, with unexpected results: a dominant CDR3 sequence and thus large proportion of identical T cells, was demonstrated in the kidney of two normal mice similar to that seen in UUO kidneys. This accounted for 30% and 37% of the CDR3 TRVβ3 sequences and for 2.8% and 3.7% of the total T cell population within those normal kidneys. A dominant sequence was not seen in normal spleen. Other groups have demonstrated resident αβ T cells within normal kidney tissue although there is no definite evidence in the literature to suggest a clonal population of resident T cells (Ascon, Ascon et al. 2008). The function of these lymphocytes is unclear but they may be involved in immune surveillance and homeostasis in the normal kidney. Griffin's group showed that within three days of UUO injury activated memory T cells were present within the kidney in association with dendritic cells (Dong, Bachman et al. 2008). This suggests that these T cells differentiated into their memory phenotype prior to the induction of UUO injury due to the rapidity of their appearance and the inflammatory environment generated by injury allowed swift activation of these memory cells to perform effector functions. This work would complement our findings, since the T cell clone within our normal kidneys may be the resting memory population seen in Rabb's work. An alternative explanation for identical populations of T cells within normal mouse may have been pyelonephritis or inadequate removal of a circulating clone of T cells. However, with both these explanations similar populations would be expected in the spleen.

When the amino acid sequences of the dominant CDR3 sequences from UUO kidney were examined, there were recurrent amino acid motifs demonstrated within the CDR3 region despite containing different TRJβ gene segments. Some of these identical amino acid sequences lay within the TRJβ gene segment and were most likely due to the high degree of homology between these J gene segments at the amino acid level despite having different nucleotide sequences. This suggestion is supported by the finding that a proportion of these sequences were also seen in the CDR3 sequences examined from a normal spleen.

However, a recurrent arginine, arginine, serine (RRS) motif was identified in the most variable region of the CDR3 sequence where multiple nucleotide additions and deletions occur outside the TRJβ gene segment. This motif was identified in the dominant sequence seen in four out of five UUO kidneys and only in UUO spleen when the same sequence was identified in the UUO kidney of that mouse. It was also demonstrated in the dominant population of CD8+ sorted T cells and seen in both dominant CDR3 TRVβ3 sequences found in the two normal kidneys. This demonstrated that groups of T cells with identical amino acid CDR3 β-chain regions were present within the kidney of different UUO and normal mice and suggested they recognised the same antigenic epitope. Assuming these clones of T cells developed in response to renal antigen and since they were found in both normal and UUO kidney, they must recognise native renal antigens, rather than antigens modified by injury. This would support the work showing Tamm-Horsfall proteins and albumin can be presented by DCs to T cells. It also refutes the other possible explanations for identical T cell populations in normal kidney, since all the UUO and normal mice cannot have had pyelonephritis or an identical circulating lymphocyte population.

The results from the CDR3 TRVβ3 sequence analyses from normal and UUO spleens were similar: no dominant sequence was identified. Diversity of the CDR3 region allows the TCR to recognise a wide range of structurally different antigenic epitopes. It has been estimated that there are 5-8 x 10^5 different β-chain nucleotide sequences which make up the TCRs of lymphocytes in naive spleen (Casrouge, Beaudoing et al. 2000). The naive mouse spleen harbours around 2 x 10^6 clones of T cells of about 19 cells each. Therefore it is unlikely that any one single sequence would be repeated in this polyclonal T cell repertoire that I sampled in UUO or normal spleen. This was generally the case with the UUO and normal spleen sequences sampled, where single unique sequences were found and only occasionally were repeated sequences described and this was very different to the sequences generated from the normal and UUO kidneys. Even though there were few duplicate sequences in the colonies I sampled, there was an apparently high percentage of identical CDR3 β-chain sequences within the spleen of normal and UUO mice which accounted for around 1% of the total T cell population. This result may be artefactual and could be due to the method used. Relatively small numbers of colonies/ T cells were sequenced out of the vast repertoire of T cells present in the spleen. Although the assumption remains that only one CDR3 sequence was found in each colony and represented a single T cell, cDNA from one original T cell

had been amplified through successive PCR reactions. It could have been possible that two identical PCR products originating from the same initial DNA sample were cloned, and subsequently two colonies had the same CDR3 insert.

An alternative explanation for identifying identical CDR3 sequences in the spleens of normal and UUO mice may be due to accidental or aerosolised contamination of DNA. Great efforts were made to try to prevent cross contamination between samples throughout all the experiments. Different areas and rooms were used for RNA extraction and reverse transcription, PCR set-up, cloning, PCR product analysis and plate preparation for sequencing. The samples and reagents were all stored in different locations to minimise cross contamination. UV irradiation hoods were used prior to setting up all PCR experiments. When comparing all the duplicate sequences seen in the spleens of the seven mice, only one pair of CDR3 sequences seen in the day 14 A3 UUO spleen was also seen in that UUO kidney and none of the duplicate sequences demonstrated in the spleens were seen in any other mouse. This suggested that the presence of identical sequences within the spleen was not due to DNA contamination.

Another technical issue important to discuss was the process of digesting UUO kidney. Extracting adequate numbers of lymphocytes from the network of fibrosed tissue in the UUO kidney proved difficult and the yield was low, despite multiple attempts to modify and improve the method. Although some T cells were successfully extracted, they may not have been representative of the whole T cell population infiltrating the kidney. T cells within areas of fibrotic injury would have been the most difficult to access as they were bound by the dense collagen network and activated and proliferating T cells may have been more liable to damage during the long digestion process. Therefore the population of sorted T cells whose TCR CDR3 I sequenced may have been a skewed population of T cells and may not be representative of the total T cell population or the population contributing to injury. I had hoped to look at the CD4+ and CD8+ populations in more detail by flow cytometry to study markers of proliferation and activation but the low cell numbers prevented this. I attempted to improve the yield by collecting the sorted cell populations into plastic tubes, rather than glass, which tend to encourage cells to adhere to their surface and prevent maximal RNA extraction. They were also collected directly into lysis buffer containing carrier cells to discourage RNA binding to the side of the tube. Despite this I was unable to increase the yield beyond ~2,000 CD4+ or CD8+ cells from half a UUO kidney.

Overall I believe this work provides evidence of a clonal proliferation of T cells within UUO kidney consistent with antigen recognition and these T cells may have existed within the normal kidney prior to the induction of injury, albeit at a much lower frequency. This would reflect a break in peripheral self-tolerance within the injured kidney, which may be to unmodified renal antigen since T cells in both normal and UUO kidney were recognising the same epitope. Just how this activated T cell infiltrate goes on to propagate or modify fibrosis and tubular cell death is unclear. I predict that there is an interaction between the T lymphocyte population and dendritic cell network, along with macrophages, which act to promote or regulate injury.

Chapter 6. Conclusions and Summary

The body of work from the literature suggests that T lymphocytes play a pathological role in the tubulointerstitial injury seen in chronic kidney disease. Therefore, using the well recognised unilateral ureteric obstruction model of tubulointerstitial injury and fibrosis I set out to examine the role of T lymphocytes within the UUO kidney.

Infiltration with both CD4+ and CD8+ lymphocytes, as well as macrophages, correlated with markers of renal injury including expansion of the interstitial compartment, α-SMA staining and collagen I deposition. Also, CD4+ and CD8+ lymphocytes within the UUO kidney demonstrated an activated and memory phenotype and showed evidence of proliferation. Traditionally activation and proliferation only occurs when T cells have recognised their cognate antigen, suggesting loss of tolerance to self antigen in UUO.

When analysing the TRVβ gene segment profile of infiltrating T cells there was over expression of the TRVβ3 segment in seven out of the ten UUO kidneys compared to their respective spleens. This was not seen in normal mice, suggesting this variation was related to UUO injury. The diversity of expression between gene segments could not be explained by differences in the efficiencies of the primer pairs.

In the day 7 and 14 UUO kidneys one single dominant CDR3 TRVβ3 sequence was demonstrated suggesting that an identical population of T cells was present within that kidney, dominant clones were not seen in UUO spleen. These populations accounted for between 3.6% and 4.9% of the total T cell population within the UUO kidney. Identical CDR3 sequences were also demonstrated in normal kidney, but not spleen, suggesting there were also identical populations of T cells within normal kidney and these accounted for 2.8% and 3.7% of the total T cell population within that kidney. Other groups have described T cells within normal kidney but none previously shown clones of T cells. No dominant clone was identified at the later time point of 28 days post obstruction, suggesting an expanded T cell repertoire due to multiple antigenic epitopes.

When the amino acid sequences of the CDR3 TRVβ3 region were determined for the infiltrating T cells, a common arginine, arginine, serine (RRS) motif was demonstrated in the dominant sequence identified in both UUO and normal kidney. The RRS motif was only found in UUO spleen when the same sequence was identified in the UUO kidney of that mouse. This suggested that the dominant populations of T cells in the UUO and normal kidney recognised a common antigenic epitope. In response to UUO

injury the resident population of T cells may proliferate and this would explain why the T cells in UUO and normal kidney have the same RRS motif and potentially recognise the same antigenic epitope.

This thesis supports the hypothesis that T cells play an active role in renal injury in the UUO model. Lymphocyte infiltration correlated with markers of renal fibrosis and T cells were activated and proliferating, which typically occurs in response to antigen recognition. Since there is no alloantigen in the UUO model, antigen recognition must occur due to a break in self-tolerance. Clones of T cells were demonstrated in UUO kidney implying they had recognised antigen and developed effector function.

Questions still need to be answered about the antigen/s to which T cells lose tolerance in this model. Since the UUO lymphocyte population may be derived from a population of resident T cells within normal kidney, it would follow that T cells lost tolerance to a native unmodified renal antigen. To investigate this further, proliferation assays could be performed using UUO lymphocytes and APCs with homogenised normal kidney, UUO kidney or specific renal antigens. T cell proliferation, as demonstrated by the uptake of tritiated thymidine into DNA, would determine whether modified or unmodified renal antigens drive loss of T cell tolerance.

From my own work I was unable to determine the role these particular clonal populations of T lymphocytes were playing in UUO kidney. Clonal populations suggest the presence of effector T cells however, whether they had a pathological role in promoting tubulointerstitial injury and fibrosis or whether they were regulatory in nature was not clear. A single dominant TRVβ3 expressing clone was seen in the UUO kidneys examined. From the results of Chapter 4, multiple TRVβ gene segments were over expressed in UUO kidney, which suggests that sequencing T cells with other over expressed TRVβ gene segments may reveal further clonal T cells populations. Most likely there were multiple clones of T cell in UUO kidney, which may have different effector functions.

An additional discovery was the presumed populations of NKT cells within normal kidney, as identified by the invariant TCR β-chains; TRVβ13.2, 29 and 1 (IMGT classification) or 8.2, 7.1 and 2 (Arden classification). They may have a role in producing cytokines, which shape the lymphocyte response depending upon the particular combination of cytokines produced and form a link between innate and adaptive immunity.

There are a number of limitations in the methods used and possible pitfalls. The UUO model itself does not perfectly replicate the multiple aetiologies of CKD seen in man, which most commonly cause a progressive decline in renal function. In men with chronic outflow obstruction once the obstruction is relieved there is often a stabilisation in renal function which can last for many years and thus the progressive decline associated with CKD is not seen. Therefore this model may not be the most translatable model of human CKD.

From the IHC and IF work from Chapter 3, only an association between activated lymphocyte infiltration and renal injury can be made. Small groups of animals were also used which may have prevented statistically significant results. The size of the groups used for TRVβ gene segment assessment in Chapter 4 were also small, which only allowed observations to be made rather than a statistical assessment. In Chapter 5 the assumption was made that each CDR3 nucleotide sequence inserted into a plasmid vector represented a TCR on an individual T cell and that the sequences generated were representative of the lymphocyte population within the kidney. This may not be true due to biases in lymphocyte extraction and preferential cloning of specific sequences into the plasmid.

There are many different directions in which this work could be developed with more time. Assuming that T cells are activated in response to antigen, studies which track the movement of T lymphocytes into and out of the kidney would be very informative. This would allow us to gain a better understanding of where antigen recognition takes place: either in the draining lymph node or perhaps in areas of lymphangiogenesis within the kidney itself. Tracking experiments could be performed by labelling lymphocytes with fluorescent dyes. Also adoptive transfer of lymphocytes from congenic B6 Thy1.1 UUO mice into either UUO or naive C57bl/6 mice would identify whether lymphocytes homed to both normal and injured or only injured kidney. This would help to determine whether UUO lymphocytes recognise renal self antigens and home even to normal kidney where there is no inflammation.

In order to explore the possibility that bystander T cells are activation due to the inflammatory environment created by UUO rather than antigen recognition, OTII mice with a transgenic TCR specific for ovalbumin peptide could be crossed with RAG-1 KO mice. T cells from the OTII-RAG-1 KO mice are unable to respond to antigen other than ovalbumin. If UUO is performed in these mice, and T cell responses are antigen

dependent, you would expect a reduction in injury. However, if similar levels of injury are seen to WT mice this would suggest that antigen independent T cell activation occurs.

Further work to look in more detail at the subtypes of CD4+ T cells which are involved in UUO injury would be very interesting. This would only be possible by flow cytometery if more T cells could be extracted from UUO kidney. One possible method to increase yield may be to use a magnetic bead separation kit. The beads are coated with antibody e.g. CD90.2, which bind T cells and allow their separation. IHC could also be performed to identify the different subtypes. The alternative approach to looking at the specific CD4 subtype would be to examine the cytokines produced in the obstructed kidney. An interesting experiment would be to evaluate the IL-6 and TGFβ cytokine profiles in the UUO kidney at successive time points post UUO. One might expect high early levels of IL-6 and high later levels of TGFβ. This would suggest the early involvement of proinflammatory Th17 cells and later the presence of CD4+CD25+ T regulatory cells with both anti-inflammatory and pro-fibrotic properties. Very early time points, including the first few days, should be examined to investigate whether very rapid activation of T cells occurs post UUO injury. This would support the hypothesis that populations of activated T cells are present within the normal kidney that are able to respond very quickly after injury.

Therapeutic agents that target this T cell inflammatory infiltrate could lead to advances in retarding the progression of most chronic renal diseases. This includes using immunomodulatory treatments for renal diseases which are not traditionally thought to be immunologically mediated such as diabetic nephropathy or obstructive uropathy. If we were able to slow the rate of decline in renal function by only a few years for common renal diseases such as diabetic nephropathy this might delay or even prevent the need for renal replacement therapy and its associated treatment burden in the large number of patients.

The rationale for using agents already in common use for modulating the immune system e.g. mycophenolate mofetil in these chronic renal diseases is becoming apparent with the increasing body of evidence supporting the pathological role of T lymphocytes in tubulointerstitial injury. Also more novel agents which provide chemokine blockade, alter the pro-fibrotic cytokine profile, promote the development of a regulatory T cell population or prevent the co-stimulatory signals from APCs to T cells are all possible

methods by which this inflammatory infiltrate could be manipulated. A clear understanding of the role of the different subpopulations of T lymphocytes during different stages of the fibrotic disease process is fundamental to ensuring that agents are used only in the appropriate context and at an appropriate time to ensure favourable and not deleterious effects on the fibrotic process to improve outcomes for patients with chronic renal insufficiency.

Reference list

Acha-Orbea, H. and H. R. MacDonald (1995). "Superantigens of mouse mammary tumor virus." Annu Rev Immunol **13**: 459-86.

Alexopoulos, E., D. Seron, et al. (1990). "Lupus nephritis: correlation of interstitial cells with glomerular function." Kidney Int **37**(1): 100-9.

Anders, H. J., V. Vielhauer, et al. (2002). "A chemokine receptor CCR-1 antagonist reduces renal fibrosis after unilateral ureter ligation." J Clin Invest **109**(2): 251-9.

Anders, H. J., V. Vielhauer, et al. (2003). "Chemokines and chemokine receptors are involved in the resolution or progression of renal disease." Kidney Int **63**(2): 401-15.

Anderton, S. M. (2004). "Post-translational modifications of self antigens: implications for autoimmunity." Curr Opin Immunol **16**(6): 753-8.

Apostolou, I. and H. von Boehmer (2004). "In vivo instruction of suppressor commitment in naive T cells." J Exp Med **199**(10): 1401-8.

Arden, B., S. P. Clark, et al. (1995). "Human T-cell receptor variable gene segment families." Immunogenetics **42**(6): 455-500.

Arden, B., S. P. Clark, et al. (1995). "Mouse T-cell receptor variable gene segment families." Immunogenetics **42**(6): 501-30.

Ascon, D. B., M. Ascon, et al. (2008). "Normal mouse kidneys contain activated and CD3+CD4- CD8- double-negative T lymphocytes with a distinct TCR repertoire." J Leukoc Biol **84**(6): 1400-9.

Ascon, D. B., S. Lopez-Briones, et al. (2006). "Phenotypic and functional characterization of kidney-infiltrating lymphocytes in renal ischemia reperfusion injury." J Immunol **177**(5): 3380-7.

Ascon, M., D. B. Ascon, et al. (2009). "Renal ischemia-reperfusion leads to long term infiltration of activated and effector-memory T lymphocytes." Kidney Int **75**(5): 526-35.

Avichezer, D., R. S. Grajewski, et al. (2003). "An immunologically privileged retinal antigen elicits tolerance: major role for central selection mechanisms." J Exp Med **198**(11): 1665-76.

Bacon, K. B., B. A. Premack, et al. (1995). "Activation of dual T cell signaling pathways by the chemokine RANTES." Science **269**(5231): 1727-30.

Bahn, R. S. and A. E. Heufelder (1993). "Pathogenesis of Graves' ophthalmopathy." N Engl J Med **329**(20): 1468-75.

Bangs, S. C., D. Baban, et al. (2009). "Human CD4+ memory T cells are preferential targets for bystander activation and apoptosis." J Immunol **182**(4): 1962-71.

Bangs, S. C., A. J. McMichael, et al. (2006). "Bystander T cell activation--implications for HIV infection and other diseases." Trends Immunol **27**(11): 518-24.

Barber, L. D., A. Whitelegg, et al. (2004). "Detection of vimentin-specific autoreactive CD8+ T cells in cardiac transplant patients." Transplantation **77**(10): 1604-9.

Bettelli, E., Y. Carrier, et al. (2006). "Reciprocal developmental pathways for the generation of pathogenic effector TH17 and regulatory T cells." Nature **441**(7090): 235-8.

Bevan, M. J. (1976). "Cross-priming for a secondary cytotoxic response to minor H antigens with H-2 congenic cells which do not cross-react in the cytotoxic assay." J Exp Med **143**(5): 1283-8.

Bluestone, J. A. and A. K. Abbas (2003). "Natural versus adaptive regulatory T cells." Nat Rev Immunol **3**(3): 253-7.

Bohle, A., F. Strutz, et al. (1994). "On the pathogenesis of chronic renal failure in primary glomerulopathies: a view from the interstitium." Exp Nephrol **2**(4): 205-10.

Brentjens, J. R., M. Sepulveda, et al. (1975). "Interstitial immune complex nephritis in patients with systemic lupus erythematosus." Kidney Int **7**(5): 342-50.

Brunkow, M. E., E. W. Jeffery, et al. (2001). "Disruption of a new forkhead/winged-helix protein, scurfin, results in the fatal lymphoproliferative disorder of the scurfy mouse." Nat Genet **27**(1): 68-73.

Bucala, R., L. A. Spiegel, et al. (1994). "Circulating fibrocytes define a new leukocyte subpopulation that mediates tissue repair." Mol Med **1**(1): 71-81.

Burne-Taney, M. J., M. Liu, et al. (2006). "Transfer of lymphocytes from mice with renal ischemia can induce albuminuria in naive mice: a possible mechanism linking early injury and progressive renal disease?" Am J Physiol Renal Physiol **291**(5): F981-6.

Burne-Taney, M. J., N. Yokota-Ikeda, et al. (2005). "Effects of combined T- and B-cell deficiency on murine ischemia reperfusion injury." Am J Transplant **5**(6): 1186-93.

Burne-Taney, M. J., N. Yokota, et al. (2005). "Persistent renal and extrarenal immune changes after severe ischemic injury." Kidney Int **67**(3): 1002-9.

Burne, M. J., F. Daniels, et al. (2001). "Identification of the CD4(+) T cell as a major pathogenic factor in ischemic acute renal failure." J Clin Invest **108**(9): 1283-90.

Carrasco-Marin, E., J. Shimizu, et al. (1996). "The class II MHC I-Ag7 molecules from non-obese diabetic mice are poor peptide binders." J Immunol **156**(2): 450-8.

Caspi, R. R. (2010). "A look at autoimmunity and inflammation in the eye." J Clin Invest **120**(9): 3073-83.

Casrouge, A., E. Beaudoing, et al. (2000). "Size estimate of the alpha beta TCR repertoire of naive mouse splenocytes." J Immunol **164**(11): 5782-7.

Chapman, T. J., M. R. Castrucci, et al. (2005). "Antigen-specific and non-specific CD4+ T cell recruitment and proliferation during influenza infection." Virology **340**(2): 296-306.

Chen, W., W. Jin, et al. (2003). "Conversion of peripheral CD4+CD25- naive T cells to CD4+CD25+ regulatory T cells by TGF-beta induction of transcription factor Foxp3." J Exp Med **198**(12): 1875-86.

Chevalier, R. L. (1999). "Molecular and cellular pathophysiology of obstructive nephropathy." Pediatr Nephrol **13**(7): 612-9.

Ciancio, G., G. W. Burke, et al. (2005). "A randomized trial of three renal transplant induction antibodies: early comparison of tacrolimus, mycophenolate mofetil,

and steroid dosing, and newer immune-monitoring." Transplantation **80**(4): 457-65.

Cochrane, A. L., M. M. Kett, et al. (2005). "Renal structural and functional repair in a mouse model of reversal of ureteral obstruction." J Am Soc Nephrol **16**(12): 3623-30.

Cohen, C. D., N. Calvaresi, et al. (2005). "CD20-positive infiltrates in human membranous glomerulonephritis." J Nephrol **18**(3): 328-33.

Constant, S. L. and K. Bottomly (1997). "Induction of Th1 and Th2 CD4+ T cell responses: the alternative approaches." Annu Rev Immunol **15**: 297-322.

Coresh, J., E. Selvin, et al. (2007). "Prevalence of chronic kidney disease in the United States." Jama **298**(17): 2038-47.

Cosulich, M. E., A. Rubartelli, et al. (1987). "Functional characterization of an antigen involved in an early step of T-cell activation." Proc Natl Acad Sci U S A **84**(12): 4205-9.

Davis, M. M. and P. J. Bjorkman (1988). "T-cell antigen receptor genes and T-cell recognition." Nature **334**(6181): 395-402.

DeGrendele, H. C., P. Estess, et al. (1997). "Requirement for CD44 in activated T cell extravasation into an inflammatory site." Science **278**(5338): 672-5.

Diamond, J. R. (1995). "Macrophages and progressive renal disease in experimental hydronephrosis." Am J Kidney Dis **26**(1): 133-40.

Dieckmann, D., C. H. Bruett, et al. (2002). "Human CD4(+)CD25(+) regulatory, contact-dependent T cells induce interleukin 10-producing, contact-independent type 1-like regulatory T cells [corrected]." J Exp Med **196**(2): 247-53.

Dieckmann, D., H. Plottner, et al. (2001). "Ex vivo isolation and characterization of CD4(+)CD25(+) T cells with regulatory properties from human blood." J Exp Med **193**(11): 1303-10.

Domen, R. E. (1998). "An overview of immune hemolytic anemias." Cleve Clin J Med **65**(2): 89-99.

Dong, X., L. A. Bachman, et al. (2008). "Dendritic cells facilitate accumulation of IL-17 T cells in the kidney following acute renal obstruction." Kidney Int **74**(10): 1294-309.

Dong, X., S. Swaminathan, et al. (2005). "Antigen presentation by dendritic cells in renal lymph nodes is linked to systemic and local injury to the kidney." Kidney Int **68**(3): 1096-108.

Drayton, D. L., S. Liao, et al. (2006). "Lymphoid organ development: from ontogeny to neogenesis." Nat Immunol **7**(4): 344-53.

Duffield, J. S., S. J. Forbes, et al. (2005). "Selective depletion of macrophages reveals distinct, opposing roles during liver injury and repair." J Clin Invest **115**(1): 56-65.

Duffield, J. S., C. F. Ware, et al. (2001). "Suppression by apoptotic cells defines tumor necrosis factor-mediated induction of glomerular mesangial cell apoptosis by activated macrophages." Am J Pathol **159**(4): 1397-404.

Edgtton, K. L., J. Y. Kausman, et al. (2008). "Intrarenal antigens activate CD4+ cells via co-stimulatory signals from dendritic cells." J Am Soc Nephrol **19**(3): 515-26.

Eis, V., B. Luckow, et al. (2004). "Chemokine receptor CCR1 but not CCR5 mediates leukocyte recruitment and subsequent renal fibrosis after unilateral ureteral obstruction." J Am Soc Nephrol **15**(2): 337-47.

Facktor, M. A., R. A. Bernstein, et al. (1973). "Hypersensitivity to tetanus toxoid." J Allergy Clin Immunol **52**(1): 1-12.

Fairchild, S., A. M. Knight, et al. (1991). "Co-segregation of a gene encoding a deletion ligand for Tcrb-V3+ T cells with Mtv-3." Immunogenetics **34**(4): 227-30.

Fang, C., C. Ballet, et al. (2009). "Autoimmune responses against renal tissue proteins in long-term surviving allograft recipients." Transpl Int **22**(11): 1091-9.

Ferber, I. A., S. Brocke, et al. (1996). "Mice with a disrupted IFN-gamma gene are susceptible to the induction of experimental autoimmune encephalomyelitis (EAE)." J Immunol **156**(1): 5-7.

Ferguson, T. A. and T. S. Griffith (2006). "A vision of cell death: Fas ligand and immune privilege 10 years later." Immunol Rev **213**: 228-38.

Fontenot, J. D., M. A. Gavin, et al. (2003). "Foxp3 programs the development and function of CD4+CD25+ regulatory T cells." Nat Immunol **4**(4): 330-6.

Gandolfo, M. T., H. R. Jang, et al. (2009). "Foxp3+ regulatory T cells participate in repair of ischemic acute kidney injury." Kidney Int **76**(7): 717-29.

Giudicelli, V., D. Chaume, et al. (2005). "IMGT/GENE-DB: a comprehensive database for human and mouse immunoglobulin and T cell receptor genes." Nucleic Acids Res **33**(Database issue): D256-61.

Go, A. S., G. M. Chertow, et al. (2004). "Chronic kidney disease and the risks of death, cardiovascular events, and hospitalization." N Engl J Med **351**(13): 1296-305.

Goncalves, R. G., M. A. Biato, et al. (2004). "Effects of mycophenolate mofetil and lisinopril on collagen deposition in unilateral ureteral obstruction in rats." Am J Nephrol **24**(5): 527-36.

Guzik, T. J., N. E. Hoch, et al. (2007). "Role of the T cell in the genesis of angiotensin II induced hypertension and vascular dysfunction." J Exp Med **204**(10): 2449-60.

Hansch, G. M. (1992). "The complement attack phase: control of lysis and non-lethal effects of C5b-9." Immunopharmacology **24**(2): 107-17.

Harris, K. P., G. F. Schreiner, et al. (1989). "Effect of leukocyte depletion on the function of the postobstructed kidney in the rat." Kidney Int **36**(2): 210-5.

Harris, R. C. and E. G. Neilson (2006). "Toward a unified theory of renal progression." Annu Rev Med **57**: 365-80.

Harrison, D. G., A. Vinh, et al. (2010). "Role of the adaptive immune system in hypertension." Curr Opin Pharmacol **10**(2): 203-7.

Haskins, K. and D. Wegmann (1996). "Diabetogenic T-cell clones." Diabetes **45**(10): 1299-305.

Heeger, P. S., W. E. Smoyer, et al. (1996). "Heterogeneous T cell receptor V beta gene repertoire in murine interstitial nephritis." Kidney Int **49**(5): 1222-30.

Heeger, P. S., W. E. Smoyer, et al. (1994). "Molecular analysis of the helper T cell response in murine interstitial nephritis. T cells recognizing an immunodominant

epitope use multiple T cell receptor V beta genes with similarities across CDR3." J Clin Invest **94**(5): 2084-92.

Heller, F., M. T. Lindenmeyer, et al. (2007). "The contribution of B cells to renal interstitial inflammation." Am J Pathol **170**(2): 457-68.

Hooke, D. H., D. C. Gee, et al. (1987). "Leukocyte analysis using monoclonal antibodies in human glomerulonephritis." Kidney Int **31**(4): 964-72.

Hu, M., D. Watson, et al. (2008). "Long-term cardiac allograft survival across an MHC mismatch after "pruning" of alloreactive CD4 T cells." J Immunol **180**(10): 6593-603.

Humphreys, B. D., S. L. Lin, et al. (2010). "Fate tracing reveals the pericyte and not epithelial origin of myofibroblasts in kidney fibrosis." Am J Pathol **176**(1): 85-97.

Husby, G., K. S. Tung, et al. (1981). "Characterization of renal tissue lymphocytes in patients with interstitial nephritis." Am J Med **70**(1): 31-8.

Iwano, M., D. Plieth, et al. (2002). "Evidence that fibroblasts derive from epithelium during tissue fibrosis." J Clin Invest **110**(3): 341-50.

Jang, H. S., J. Kim, et al. (2008). "Infiltrated macrophages contribute to recovery after ischemic injury but not to ischemic preconditioning in kidneys." Transplantation **85**(3): 447-55.

Kaissling, B., I. Hegyi, et al. (1996). "Morphology of interstitial cells in the healthy kidney." Anat Embryol (Berl) **193**(4): 303-18.

Kappler, J. W., T. Wade, et al. (1987). "A T cell receptor V beta segment that imparts reactivity to a class II major histocompatibility complex product." Cell **49**(2): 263-71.

Katayama, K., M. Kawano, et al. (2008). "Irradiation prolongs survival of Alport mice." J Am Soc Nephrol **19**(9): 1692-700.

Kerjaschki, D., H. M. Regele, et al. (2004). "Lymphatic neoangiogenesis in human kidney transplants is associated with immunologically active lymphocytic infiltrates." J Am Soc Nephrol **15**(3): 603-12.

Khazen, W., P. M'Bika J, et al. (2005). "Expression of macrophage-selective markers in human and rodent adipocytes." FEBS Lett **579**(25): 5631-4.

Kinsey, G. R., R. Sharma, et al. (2009). "Regulatory T cells suppress innate immunity in kidney ischemia-reperfusion injury." J Am Soc Nephrol **20**(8): 1744-53.

Koesters, R., B. Kaissling, et al. (2010). "Tubular overexpression of transforming growth factor-beta1 induces autophagy and fibrosis but not mesenchymal transition of renal epithelial cells." Am J Pathol **177**(2): 632-43.

Kotzin, B. L. (1996). "Systemic lupus erythematosus." Cell **85**(3): 303-6.

Kruger, T., D. Benke, et al. (2004). "Identification and functional characterization of dendritic cells in the healthy murine kidney and in experimental glomerulonephritis." J Am Soc Nephrol **15**(3): 613-21.

Kumar, V., D. H. Kono, et al. (1989). "The T-cell receptor repertoire and autoimmune diseases." Annu Rev Immunol **7**: 657-82.

Langrish, C. L., Y. Chen, et al. (2005). "IL-23 drives a pathogenic T cell population that induces autoimmune inflammation." J Exp Med **201**(2): 233-40.

Lebleu, V. S., H. Sugimoto, et al. (2008). "Lymphocytes are dispensable for glomerulonephritis but required for renal interstitial fibrosis in matrix defect-induced Alport renal disease." Lab Invest **88**(3): 284-92.

Lee, V. W., Y. Wang, et al. (2006). "Adriamycin nephropathy in severe combined immunodeficient (SCID) mice." Nephrol Dial Transplant **21**(11): 3293-8.

Lee, V. W., Y. M. Wang, et al. (2008). "Regulatory immune cells in kidney disease." Am J Physiol Renal Physiol **295**(2): F335-42.

Lehmann, P. V., T. Forsthuber, et al. (1992). "Spreading of T-cell autoimmunity to cryptic determinants of an autoantigen." Nature **358**(6382): 155-7.

Lerner, R. A., R. J. Glassock, et al. (1967). "The role of anti-glomerular basement membrane antibody in the pathogenesis of human glomerulonephritis." J Exp Med **126**(6): 989-1004.

Lesley, J. and R. Hyman (1992). "CD44 can be activated to function as an hyaluronic acid receptor in normal murine T cells." Eur J Immunol **22**(10): 2719-23.

Lesley, J., R. Hyman, et al. (1993). "CD44 and its interaction with extracellular matrix." Adv Immunol **54**: 271-335.

Li, L., L. Huang, et al. (2007). "NKT cell activation mediates neutrophil IFN-gamma production and renal ischemia-reperfusion injury." J Immunol **178**(9): 5899-911.

Lim, A., V. Baron, et al. (2002). "Combination of MHC-peptide multimer-based T cell sorting with the Immunoscope permits sensitive ex vivo quantitation and follow-up of human CD8+ T cell immune responses." J Immunol Methods **261**(1-2): 177-94.

Lin, S. L., F. C. Chang, et al. (2011). "Targeting endothelium-pericyte cross talk by inhibiting VEGF receptor signaling attenuates kidney microvascular rarefaction and fibrosis." Am J Pathol **178**(2): 911-23.

Lin, S. L., T. Kisseleva, et al. (2008). "Pericytes and perivascular fibroblasts are the primary source of collagen-producing cells in obstructive fibrosis of the kidney." Am J Pathol **173**(6): 1617-27.

Lopez, M., M. R. Clarkson, et al. (2006). "A novel mechanism of action for anti-thymocyte globulin: induction of CD4+CD25+Foxp3+ regulatory T cells." J Am Soc Nephrol **17**(10): 2844-53.

Lubberts, E., L. A. Joosten, et al. (2002). "Overexpression of IL-17 in the knee joint of collagen type II immunized mice promotes collagen arthritis and aggravates joint destruction." Inflamm Res **51**(2): 102-4.

Macconi, D., C. Chiabrando, et al. (2009). "Proteasomal processing of albumin by renal dendritic cells generates antigenic peptides." J Am Soc Nephrol **20**(1): 123-30.

Macian, F., S. H. Im, et al. (2004). "T-cell anergy." Curr Opin Immunol **16**(2): 209-16.

Mahajan, D., Y. Wang, et al. (2006). "CD4+CD25+ regulatory T cells protect against injury in an innate murine model of chronic kidney disease." J Am Soc Nephrol **17**(10): 2731-41.

Mangan, P. R., L. E. Harrington, et al. (2006). "Transforming growth factor-beta induces development of the T(H)17 lineage." Nature **441**(7090): 231-4.

Massengill, S. F., M. M. Goodenow, et al. (1998). "SLE nephritis is associated with an oligoclonal expansion of intrarenal T cells." Am J Kidney Dis **31**(3): 418-26.

Matthys, P., K. Vermeire, et al. (1998). "Anti-IL-12 antibody prevents the development and progression of collagen-induced arthritis in IFN-gamma receptor-deficient mice." Eur J Immunol **28**(7): 2143-51.

Matzinger, P. (2002). "The danger model: a renewed sense of self." Science **296**(5566): 301-5.

Medawar, P. B. (1948). "Immunity to homologous grafted skin; the fate of skin homografts transplanted to the brain, to subcutaneous tissue, and to the anterior chamber of the eye." Br J Exp Pathol **29**(1): 58-69.

Medzhitov, R. and C. A. Janeway, Jr. (1997). "Innate immunity: the virtues of a nonclonal system of recognition." Cell **91**(3): 295-8.

Melenhorst, J. J., M. D. Lay, et al. (2008). "Contribution of TCR-beta locus and HLA to the shape of the mature human Vbeta repertoire." J Immunol **180**(10): 6484-9.

Mellman, I. and R. M. Steinman (2001). "Dendritic cells: specialized and regulated antigen processing machines." Cell **106**(3): 255-8.

Michaelsson, E., V. Malmstrom, et al. (1994). "T cell recognition of carbohydrates on type II collagen." J Exp Med **180**(2): 745-9.

Miossec, P., T. Korn, et al. (2009). "Interleukin-17 and type 17 helper T cells." N Engl J Med **361**(9): 888-98.

Mosmann, T. R., H. Cherwinski, et al. (1986). "Two types of murine helper T cell clone. I. Definition according to profiles of lymphokine activities and secreted proteins." J Immunol **136**(7): 2348-57.

Mosser, D. M. and J. P. Edwards (2008). "Exploring the full spectrum of macrophage activation." Nat Rev Immunol **8**(12): 958-69.

Muller, G. A., J. Markovic-Lipkovski, et al. (1992). "The role of interstitial cells in the progression of renal diseases." J Am Soc Nephrol **2**(10 Suppl): S198-205.

Murata, H., Y. Kita, et al. (1995). "Limited TCR repertoire of infiltrating T cells in the kidneys of Sjogren's syndrome patients with interstitial nephritis." J Immunol **155**(8): 4084-9.

Myllymaki, J. M., T. T. Honkanen, et al. (2007). "Severity of tubulointerstitial inflammation and prognosis in immunoglobulin A nephropathy." Kidney Int **71**(4): 343-8.

Nakamura, K., A. Kitani, et al. (2004). "TGF-beta 1 plays an important role in the mechanism of CD4+CD25+ regulatory T cell activity in both humans and mice." J Immunol **172**(2): 834-42.

Nath, K. A. (1992). "Tubulointerstitial changes as a major determinant in the progression of renal damage." Am J Kidney Dis **20**(1): 1-17.

Ng, W. F., P. J. Duggan, et al. (2001). "Human CD4(+)CD25(+) cells: a naturally occurring population of regulatory T cells." Blood **98**(9): 2736-44.

Niedermeier, M., B. Reich, et al. (2009). "CD4+ T cells control the differentiation of Gr1+ monocytes into fibrocytes." Proc Natl Acad Sci U S A **106**(42): 17892-7.

Nishida, M. and K. Hamaoka (2008). "Macrophage phenotype and renal fibrosis in obstructive nephropathy." Nephron Exp Nephrol **110**(1): e31-6.

Novobrantseva, T. I., G. R. Majeau, et al. (2005). "Attenuated liver fibrosis in the absence of B cells." J Clin Invest **115**(11): 3072-82.

Oldroyd, S. D., G. L. Thomas, et al. (1999). "Interferon-gamma inhibits experimental renal fibrosis." Kidney Int **56**(6): 2116-27.

Park, H., Z. Li, et al. (2005). "A distinct lineage of CD4 T cells regulates tissue inflammation by producing interleukin 17." Nat Immunol **6**(11): 1133-41.

Park, M. H., V. D'Agati, et al. (1986). "Tubulointerstitial disease in lupus nephritis: relationship to immune deposits, interstitial inflammation, glomerular changes, renal function, and prognosis." Nephron **44**(4): 309-19.

Parra, G., Y. Quiroz, et al. (2008). "Experimental induction of salt-sensitive hypertension is associated with lymphocyte proliferative response to HSP70." Kidney Int Suppl(111): S55-9.

Pedersen, A. E. (2007). "The potential for induction of autoimmune disease by a randomly-mutated self-antigen." Med Hypotheses **68**(6): 1240-6.

Peng, S. L., M. P. Madaio, et al. (1996). "Murine lupus in the absence of alpha beta T cells." J Immunol **156**(10): 4041-9.

Picard, N., O. Baum, et al. (2008). "Origin of renal myofibroblasts in the model of unilateral ureter obstruction in the rat." Histochem Cell Biol **130**(1): 141-55.

Puri, T. S., M. I. Shakaib, et al. (2010). "Chronic kidney disease induced in mice by reversible unilateral ureteral obstruction is dependent on genetic background." Am J Physiol Renal Physiol **298**(4): F1024-32.

Quiroz, Y., H. Pons, et al. (2001). "Mycophenolate mofetil prevents salt-sensitive hypertension resulting from nitric oxide synthesis inhibition." Am J Physiol Renal Physiol **281**(1): F38-47.

Rabb, H., F. Daniels, et al. (2000). "Pathophysiological role of T lymphocytes in renal ischemia-reperfusion injury in mice." Am J Physiol Renal Physiol **279**(3): F525-31.

Robertson, H., S. Ali, et al. (2004). "Chronic renal allograft dysfunction: the role of T cell-mediated tubular epithelial to mesenchymal cell transition." J Am Soc Nephrol **15**(2): 390-7.

Rodriguez-Iturbe, B., H. Pons, et al. (2001). "Role of immunocompetent cells in nonimmune renal diseases." Kidney Int **59**(5): 1626-40.

Rodriguez, A., A. Regnault, et al. (1999). "Selective transport of internalized antigens to the cytosol for MHC class I presentation in dendritic cells." Nat Cell Biol **1**(6): 362-8.

Romagnoli, P., D. Hudrisier, et al. (2002). "Preferential recognition of self antigens despite normal thymic deletion of CD4(+)CD25(+) regulatory T cells." J Immunol **168**(4): 1644-8.

Sanger, F., S. Nicklen, et al. (1977). "DNA sequencing with chain-terminating inhibitors." Proc Natl Acad Sci U S A **74**(12): 5463-7.

Santis, A. G., M. Lopez-Cabrera, et al. (1995). "Expression of the early lymphocyte activation antigen CD69, a C-type lectin, is regulated by mRNA degradation associated with AU-rich sequence motifs." Eur J Immunol **25**(8): 2142-6.

Satpute, S. R., J. M. Park, et al. (2009). "The role for T cell repertoire/antigen-specific interactions in experimental kidney ischemia reperfusion injury." J Immunol **183**(2): 984-92.

Schreiner, G. F., K. P. Harris, et al. (1988). "Immunological aspects of acute ureteral obstruction: immune cell infiltrate in the kidney." Kidney Int **34**(4): 487-93.

Shao, D. D., R. Suresh, et al. (2008). "Pivotal Advance: Th-1 cytokines inhibit, and Th-2 cytokines promote fibrocyte differentiation." J Leukoc Biol **83**(6): 1323-33.

Shappell, S. B., T. Gurpinar, et al. (1998). "Chronic obstructive uropathy in severe combined immunodeficient (SCID) mice: lymphocyte infiltration is not required for progressive tubulointerstitial injury." J Am Soc Nephrol **9**(6): 1008-17.

Shuman, S. (1994). "Novel approach to molecular cloning and polynucleotide synthesis using vaccinia DNA topoisomerase." J Biol Chem **269**(51): 32678-84.

Strutz, F. and E. G. Neilson (1994). "The role of lymphocytes in the progression of interstitial disease." Kidney Int Suppl **45**: S106-10.

Sung, S. A., S. K. Jo, et al. (2007). "Reduction of renal fibrosis as a result of liposome encapsulated clodronate induced macrophage depletion after unilateral ureteral obstruction in rats." Nephron Exp Nephrol **105**(1): e1-9.

Surh, C. D. and J. Sprent (2008). "Homeostasis of naive and memory T cells." Immunity **29**(6): 848-62.

Takada, M., A. Chandraker, et al. (1997). "The role of the B7 costimulatory pathway in experimental cold ischemia/reperfusion injury." J Clin Invest **100**(5): 1199-203.

Takahashi, T., Y. Kuniyasu, et al. (1998). "Immunologic self-tolerance maintained by CD25+CD4+ naturally anergic and suppressive T cells: induction of autoimmune disease by breaking their anergic/suppressive state." Int Immunol **10**(12): 1969-80.

Tapmeier, T. T., K. L. Brown, et al. (2008). "Reimplantation of the ureter after unilateral ureteral obstruction provides a model that allows functional evaluation." Kidney Int **73**(7): 885-9.

Tapmeier, T. T., A. Fearn, et al. (2010). "Pivotal role of CD4+ T cells in renal fibrosis following ureteric obstruction." Kidney Int **78**(4): 351-62.

Thornton, A. M. and E. M. Shevach (2000). "Suppressor effector function of CD4+CD25+ immunoregulatory T cells is antigen nonspecific." J Immunol **164**(1): 183-90.

Thorstenson, K. M. and A. Khoruts (2001). "Generation of anergic and potentially immunoregulatory CD25+CD4 T cells in vivo after induction of peripheral tolerance with intravenous or oral antigen." J Immunol **167**(1): 188-95.

Truong, L. D., A. Farhood, et al. (1992). "Experimental chronic renal ischemia: morphologic and immunologic studies." Kidney Int **41**(6): 1676-89.

Unutmaz, D., P. Pileri, et al. (1994). "Antigen-independent activation of naive and memory resting T cells by a cytokine combination." J Exp Med **180**(3): 1159-64.

Urban, J. L., V. Kumar, et al. (1988). "Restricted use of T cell receptor V genes in murine autoimmune encephalomyelitis raises possibilities for antibody therapy." Cell **54**(4): 577-92.

van Boekel, M. A. and W. J. van Venrooij (2003). "Modifications of arginines and their role in autoimmunity." Autoimmun Rev **2**(2): 57-62.

van den Berg, T. K. and G. Kraal (2005). "A function for the macrophage F4/80 molecule in tolerance induction." Trends Immunol **26**(10): 506-9.

van der Vliet, H. J. and E. E. Nieuwenhuis (2007). "IPEX as a result of mutations in FOXP3." Clin Dev Immunol **2007**: 89017.

van Es, L. A., E. de Heer, et al. (2008). "GMP-17-positive T-lymphocytes in renal tubules predict progression in early stages of IgA nephropathy." Kidney Int **73**(12): 1426-33.

van Stipdonk, M. J., A. A. Willems, et al. (1998). "T cells discriminate between differentially phosphorylated forms of alphaB-crystallin, a major central nervous system myelin antigen." Int Immunol **10**(7): 943-50.

Veldhoen, M., R. J. Hocking, et al. (2006). "TGFbeta in the context of an inflammatory cytokine milieu supports de novo differentiation of IL-17-producing T cells." Immunity **24**(2): 179-89.

Vielhauer, V., H. J. Anders, et al. (2001). "Obstructive nephropathy in the mouse: progressive fibrosis correlates with tubulointerstitial chemokine expression and accumulation of CC chemokine receptor 2- and 5-positive leukocytes." J Am Soc Nephrol **12**(6): 1173-87.

Vielhauer, V., V. Eis, et al. (2004). "Identifying chemokines as therapeutic targets in renal disease: lessons from antagonist studies and knockout mice." Kidney Blood Press Res **27**(4): 226-38.

Vincent, A., O. Lily, et al. (1999). "Pathogenic autoantibodies to neuronal proteins in neurological disorders." J Neuroimmunol **100**(1-2): 169-80.

Wada, T., N. Sakai, et al. (2007). "Fibrocytes: a new insight into kidney fibrosis." Kidney Int **72**(3): 269-73.

Walters, G. and S. I. Alexander (2004). "T cell receptor BV repertoires using real time PCR: a comparison of SYBR green and a dual-labelled HuTrec fluorescent probe." J Immunol Methods **294**(1-2): 43-52.

Wang, Y., D. Mahajan, et al. (2005). "Partial depletion of macrophages by ED7 reduces renal injury in Adriamycin nephropathy." Nephrology (Carlton) **10**(5): 470-7.

Wang, Y., Y. Wang, et al. (2008). "By homing to the kidney, activated macrophages potently exacerbate renal injury." Am J Pathol **172**(6): 1491-9.

Wang, Y., Y. Wang, et al. (2001). "Depletion of CD4(+) T cells aggravates glomerular and interstitial injury in murine adriamycin nephropathy." Kidney Int **59**(3): 975-84.

Wang, Y., Y. P. Wang, et al. (2001). "Role of CD8(+) cells in the progression of murine adriamycin nephropathy." Kidney Int **59**(3): 941-9.

Wang, Y., Y. P. Wang, et al. (2007). "Ex vivo programmed macrophages ameliorate experimental chronic inflammatory renal disease." Kidney Int **72**(3): 290-9.

Wang, Y. M., G. Y. Zhang, et al. (2006). "Foxp3-transduced polyclonal regulatory T cells protect against chronic renal injury from adriamycin." J Am Soc Nephrol **17**(3): 697-706.

Watanabe, T., J. Masuyama, et al. (2006). "CD52 is a novel costimulatory molecule for induction of CD4+ regulatory T cells." Clin Immunol **120**(3): 247-59.

Watson, D., G. Zheng, et al. (2009). "CCL2 DNA vaccine to treat renal disease." Int J Biochem Cell Biol **41**(4): 729-32.

Wilson, A., C. Marechal, et al. (2001). "Biased V beta usage in immature thymocytes is independent of DJ beta proximity and pT alpha pairing." J Immunol **166**(1): 51-7.

Wu, L., C. L. Gabriel, et al. (2009). "Invariant natural killer T cells: innate-like T cells with potent immunomodulatory activities." Tissue Antigens **73**(6): 535-45.

Wu, L., P. W. Kincade, et al. (1993). "The CD44 expressed on the earliest intrathymic precursor population functions as a thymus homing molecule but does not bind to hyaluronate." Immunol Lett **38**(1): 69-75.

Wu, M. J., M. C. Wen, et al. (2006). "Rapamycin attenuates unilateral ureteral obstruction-induced renal fibrosis." Kidney Int **69**(11): 2029-36.

Wynn, T. A. (2004). "Fibrotic disease and the T(H)1/T(H)2 paradigm." Nat Rev Immunol **4**(8): 583-94.

Yamagishi, H., T. Yokoo, et al. (2001). "Genetically modified bone marrow-derived vehicle cells site specifically deliver an anti-inflammatory cytokine to inflamed interstitium of obstructive nephropathy." J Immunol **166**(1): 609-16.

Yang, X. O., R. Nurieva, et al. (2008). "Molecular antagonism and plasticity of regulatory and inflammatory T cell programs." Immunity **29**(1): 44-56.

Yokota, N., F. Daniels, et al. (2002). "Protective effect of T cell depletion in murine renal ischemia-reperfusion injury." Transplantation **74**(6): 759-63.

Zamvil, S., P. Nelson, et al. (1985). "T-cell clones specific for myelin basic protein induce chronic relapsing paralysis and demyelination." Nature **317**(6035): 355-8.